

**“Characterisation of mouse and human dental pulp cells
for auditory regeneration”**

Oscar Omar Solis Castro

Thesis submitted for the degree of Doctor of Philosophy

Supervisors:

Professor Marcelo N. Rivolta

Professor Fiona M. Boissonade

Department of Biomedical Science

The University of Sheffield

August 2018

Acknowledgments

I would like to acknowledge everyone that directly or indirectly helped me to develop my PhD research project. Particularly, the students and staff of the BMS department, the centre for stem cell biology and the Charles Clifford dental hospital of The University of Sheffield. To the past and present members of the Rivolta lab for the training and advice. I would also like to thank my PhD Supervisors Prof. Marcelo Rivolta and Prof. Fiona Boissonade as well as my advisors Dr. Bazbek Davletov and Dr. Matthew Towers for their guidance and feedback. Thanks to CONACYT for granting me a full scholarship for undertaking my PhD studies.

Personally, I would like to thank and show my appreciation to the following people:

A mis padres y hermanos: Por su apoyo incondicional, ejemplo y el amor que me han brindado, los logros no significan nada si no hay con quien compartirlos.

A mi esposa Yutzil: Por estar a mi lado, aprender conmigo y por motivarme a ser mejor cada día. Gracias por los viajes, experiencias y por compartir conmigo lo mejor de ti.

To my supervisors, Professor Marcelo Rivolta and Professor Fiona Boissonade: My sincere thanks for trusting in me, for allowing me to develop professionally and for your guidance and advise.

To my lab friends: Time flies, and I am thankful to have spent it around you. Thanks for teaching me, for the advice, the talks, the sweets and the coffee, and overall, thanks for the smiles and the good times.

To my friends: I've been blessed to have people who care about me without even deserving it, thanks for your support.

"The strength of the team is each individual member. The strength of each member is the team." -

-Phil Jackson

Abstract

Modern-day regenerative medicine is constantly exploring the development and application of stem cells for cell-based therapies in many conditions and diseases. One of such conditions is deafness, which affects over 360 million people worldwide, frequently caused by an irreversible damage to the sensory cells. Therapies which could replace dead or damaged spiral ganglion neurons in deafness are sought as alternatives to the currently limited approaches. In this regard, stem cells from human dental pulp cells (hDPCs) are proposed to be intrinsically neurogenic due to their neural crest origin. Nevertheless, hDPCs have been poorly investigated in the context of auditory nerve regeneration. In the present work, we aimed to obtain a neurogenic population from hDPCs which could be differentiated into auditory neurons. We included mouse incisor dental pulp cells in our experiments, which allowed us to identify conditions that promote a neurogenic phenotype. We established hDPC cultures in serum-free, defined media as a basal condition for growth and propagation, providing pre-clinical advantages to the standard condition containing foetal bovine serum. The specific activity in an auditory regeneration system was tested co-culturing the hDPCs together with denervated cochlear explants *ex-vivo*. Our results have shown that dental pulp cells cultures can be established in serum-free neurogenic conditions; expressing basal levels of markers related to neural progenitor-, neural- and neural crest cells. Particularly, growing hDPCs as sphere aggregates showed and enhanced neural crest molecular signature and showed differentiation into spiral ganglion-like neurons when co-cultured with cochlear explants. Therefore, we present a comprehensive characterisation of human dental pulp cells under standard and defined culture conditions, their ability to express a neural crest stem signature and provided evidence, for the first time, of their potential to differentiate into spiral ganglion-like neurons in an *ex-vivo* model of auditory nerve regeneration.

Table of contents.

| | |
|--|-----------|
| CHAPTER 1..... | 1 |
| 1. Introduction..... | 3 |
| 1.1. Introduction..... | 3 |
| 1.2. The ear..... | 4 |
| 1.3. Inner ear development..... | 6 |
| 1.4. Stem cell approaches for auditory sensory cell replacement | 8 |
| 1.4.1. Pluripotent stem cells (PSC) | 8 |
| 1.4.2. Mesenchymal stromal cells (MSC) | 9 |
| 1.5. The neural crest and their adult stem cell derivatives..... | 11 |
| 1.6. The study of NCSCs | 12 |
| 1.7. Dental-related sources of human neural crest-derived stem cells..... | 13 |
| 1.7.1. Gingival-derived neural crest stem cells (GSC-NCSC): | 14 |
| 1.7.2. NCSCs derived from Periodontal ligament (PDLSC). | 15 |
| 1.7.3. Exfoliated deciduous teeth | 16 |
| 1.7.4. Stem cells from apical pulp cells (SCAP): | 16 |
| 1.7.5. Dental pulp stem cells (DPSC) | 17 |
| 1.8. Current limitations of dental-related NCSCs | 20 |
| 1.9. Tooth development | 20 |
| 1.10. Dental pulp cells <i>in vitro</i>. | 22 |
| 1.11. Advantages of hDPSCs for auditory cell replacement therapies | 23 |
| 1.12. Research statement:..... | 24 |
| 1.13. Aims and objective | 24 |

| | |
|--|-----------|
| 1.13.1. Overall aim | 24 |
| 1.13.2. Specific objectives: | 24 |
| CHAPTER 2..... | 25 |
| 2. Materials and Methods | 27 |
| 2.1. Establishment of human dental pulp cell (hDPCs) cultures | 27 |
| 2.2. Establishment of mouse dental pulp cell (mDPCs) cultures..... | 28 |
| 2.3. Cryopreservation of mouse and human dental pulp stem cells..... | 29 |
| 2.4. Neural differentiation of mDPCs and hDPCs by Sonic Hedgehog induction. | 29 |
| 2.5. Neural differentiation of hDPC neurospheres by dcAMP induction..... | 30 |
| 2.6. Schwann cell differentiation of hDPCs by Forskolin induction..... | 31 |
| 2.7. Schwann cell differentiation of hDPCs by dcAMP induction..... | 32 |
| 2.8. Generation of neural progenitors from mouse and human dental pulp cells. | 33 |
| 2.9. Gerbil Cochlear explants co-culture..... | 34 |
| 2.10. Human dental pulp tissue sectioning | 35 |
| 2.11. Immunocytochemistry (ICC) and immunohistochemistry (IHC). | 35 |
| 2.11.1. Fixing..... | 35 |
| 2.11.2. Labelling | 35 |
| 2.12. Direct reprogramming of human dental pulp cells with EGFP, NeuroD1 and ASCL1: Plasmid Isolation..... | 37 |
| 2.13. Direct reprogramming of human dental pulp cells with EGFP, NeuroD1 and ASCL1: Human dental pulp cells transfection | 37 |
| 2.14. Fluorescence activated cell sorting (FACS) | 38 |
| 2.15. Live cell tracking in ex-vivo assays using Boron-dipyrromethene (Bodipy) staining. 38 | |

| | | |
|--------|--|----|
| 2.16. | Microscopy | 38 |
| 2.17. | RNA Extraction | 39 |
| 2.18. | cDNA Synthesis..... | 39 |
| 2.19. | End point polymerase chain reaction (PCR)..... | 39 |
| 2.20. | Quantitative polymerase chain reaction (RT-qPCR)..... | 40 |
| 2.21. | Statistical analysis | 41 |
| | RESULTS | 43 |
| | CHAPTER 3..... | 45 |
| 3. | Characterisation of dental pulp cell cultures from mice for auditory nerve regeneration..... | 47 |
| 3.1. | Establishment of dental pulp cell culture conditions | 47 |
| 3.2. | Morphological characterisation of mouse dental pulp cells. | 49 |
| 3.3. | Mouse dental pulp cultures molecular characterisation. | 50 |
| 3.4. | Spontaneous neurogenic potential of mouse dental pulp cells | 55 |
| 3.5. | Neural induction of mouse dental pulp cultures | 56 |
| 3.6. | Evaluation of Pax7 as a marker of neural progenitor/NCSCs..... | 62 |
| 3.7. | Characterisation of mDPCs and mDPPSCs after exposure to inductive cues | 67 |
| 3.1. | Neural differentiation of mDPCs and mDPPSCs after inductive treatments | 69 |
| 3.2. | Discussion | 72 |
| 3.2.1. | Establishment of dental pulp cultures from mouse teeth..... | 72 |
| 3.2.2. | Characterisation of mDPC and mDPPSCs..... | 73 |
| 3.2.3. | Neuralisation potential of mDPC and mDPPSC..... | 74 |
| 3.3. | Summary | 75 |

| | |
|---|------------|
| CHAPTER 4..... | 77 |
| 4. Human dental pulp culture, characterisation and evaluation as neural progenitors. | 79 |
| 4.1. Human dental pulp can be extracted and cultured from a variety of patients..... | 79 |
| 4.2. Immunohistochemistry (IHC) characterisation of human dental pulp. | 82 |
| 4.3. Human dental pulp cell cultures can be established in different growth conditions. | 85 |
| 4.4. Expression of basal markers in human dental pulp cultures. | 91 |
| 4.5. Differentiation of Human dental pulp cells into auditory neurons. | 99 |
| 4.6. Differentiation of Human dental pulp cells into Schwann Cells..... | 101 |
| 4.7. hDPC cultures can provide trophic support to otic neural progenitors..... | 108 |
| 4.8. Human dental pulp cells can be driven into sensory-like neurons by transfection with the transcription factors ASCL1 and NEUROD1 (NEUD). | 109 |
| 4.9. Discussion | 115 |
| 4.9.1. Human dental pulp samples | 115 |
| 4.9.2. In situ characterisation of human dental pulp..... | 116 |
| 4.9.3. Culture of human dental pulp cells | 118 |
| 4.9.4. Characterisation of human dental pulp cells | 120 |
| 4.9.5. Differentiation potential of human dental pulp cells..... | 123 |
| 4.10. Summary | 126 |
| CHAPTER 5..... | 127 |
| 5. Evaluating otic neural progenitor obtainment from human dental pulp cells grown in FBS medium. | 129 |

| | |
|---|-----|
| 5.1. Generation and neuralisation of otic neural progenitors from hDPC-FBS cultures by inductive treatments. | 129 |
| 5.2. Evaluation of human Foetal auditory stem cells (hFASCs)-conditioned media on hDPC-FBS cultures. | 144 |
| 5.3. Evaluation of P75 ^{+ve} FACS sorted hDPCs for auditory nerve differentiation. | 152 |
| 5.4. Characterisation of hDPC-FBS transferred to pluripotent stem cell medium. | 167 |
| 5.5. Discussion | 171 |
| 5.5.1. Otic neural progenitor obtainment from hDPC-FBS..... | 171 |
| 5.5.2. Evaluation of P75 as a neurogenic marker in hDPC-FBS cultures. | 172 |
| 5.5.3. Pluripotent stem cell medium for hDPC-FBS growth | 174 |
| 5.6. Summary | 174 |
| CHAPTER 6..... | 175 |
| 6. Derivation of neural crest-derived stem cell neurospheres from human dental pulp and their potential for auditory nerve regeneration. | 177 |
| 6.1. Human dental pulp cells can be grown as spheres in low-attachment conditions. | 177 |
| 6.2. hDPC-spheres present a neural crest-derived stem cell molecular signature and differentiate into neural –like cells by chemically induced cues. | 180 |
| 6.3. hDPC-NCSCs grown as spheres can differentiate into neural-like cells under chemical inductive cues..... | 186 |
| 6.4. hDPC-NCSCs can differentiate into neural-like cells in a model of auditory nerve regeneration..... | 193 |
| 6.5. Schwann cell differentiation of hDPC-NCSC spheres | 201 |
| 6.6. Characterisation of hDPC in a Neural Crest Stem Cell medium (NCSCm). | 205 |
| 6.7. Discussion | 208 |
| 6.7.1. Sphere aggregation as a method to obtain NCSCs | 208 |

| | | |
|----------------|---|-----|
| 6.7.2. | Neural differentiation of hDPC-NCSCs..... | 209 |
| 6.7.3. | hDPCs-NCSCs in a model of auditory nerve regeneration | 211 |
| 6.7.4. | Glial differentiation of hDPC-NCSCs | 212 |
| 6.7.5. | Effect of neural crest stem cell medium on hDPC-FBS | 212 |
| 6.8. | Summary | 213 |
| CHAPTER 7..... | | 215 |
| 7. | General discussion and future directions..... | 217 |
| CHAPTER 8..... | | 221 |
| 8. | Conclusions..... | 223 |
| 9. | References | 225 |
| 10. | Supplementary information. | 239 |

Table of Figures.

| | |
|--|----|
| FIGURE 1.1 THE EAR..... | 5 |
| FIGURE 1.2 COCHLEA AND ORGAN OF CORTI..... | 5 |
| FIGURE 1.3 SUMMARY OF THE INNER EAR DEVELOPMENT..... | 7 |
| FIGURE 1.4 NEURAL CREST CELLS..... | 12 |
| FIGURE 1.5 SOURCES OF STEM CELLS IN DENTAL TISSUES..... | 14 |
| TABLE 1.1. SUMMARY OF DENTAL RELATED-NCSCs..... | 19 |
| FIGURE 1.6. DEVELOPMENTAL STAGES OF TOOTH DEVELOPMENT..... | 21 |
| TABLE 2.1. BASAL CONDITIONS OF MOUSE AND HUMAN DENTAL PULP CELLS..... | 28 |
| TABLE 2.2. MOUSE DENTAL PULP CELL BASAL CONDITIONS..... | 29 |
| FIGURE 2.1 NEURALISATION PROTOCOL WITH SONIC HEDGEHOG (SHH) FLOW CHART..... | 30 |
| TABLE 2.3. NEURALISATION PROTOCOL WITH SONIC HEDGEHOG, MEDIA CONDITIONS..... | 30 |
| FIGURE 2.2 NEURAL DIFFERENTIATION AFTER NEUROSPHERE FORMATION..... | 31 |
| TABLE 2.4. NEURALISATION PROTOCOL AFTER NEUROSPHERE FORMATION..... | 31 |
| FIGURE 2.3 SCHWANN CELL (SC) DIFFERENTIATION WITH DEZAWA'S PROTOCOL FLOW CHART..... | 31 |
| TABLE 2.5. SCHWANN CELL DIFFERENTIATION WITH DEZAWA'S PROTOCOL..... | 32 |
| FIG 2.4. SCHWANN CELL DIFFERENTIATION WITH STUDER'S PROTOCOL FLOW CHART..... | 32 |
| TABLE 2.6. SCHWANN CELL DIFFERENTIATION WITH STUDER'S PROTOCOL..... | 32 |
| TABLE 2.7. TREATMENTS USED TO GENERATE OTIC NEURAL PROGENITORS FROM HDPC..... | 33 |
| TABLE 2.8. TREATMENTS TO GENERATE NEURAL PROGENITORS FROM MOUSE DENTAL PULP CELLS..... | 34 |
| FIGURE 2.5 OVERALL WORK FLOW OF CULTURE ESTABLISHMENT, NEUROSPHERE FORMATION AND CO-CULTURE SETUP..... | 34 |
| TABLE 2.9. EX-VIVO ASSAY MEDIA..... | 35 |
| TABLE 2.10. LIST OF PRIMARY AND SECONDARY ANTIBODIES..... | 37 |
| TABLE 2.11. LIST OF MOUSE PRIMERS..... | 39 |
| TABLE 2.12. LIST OF HUMAN PRIMERS..... | 40 |
| TABLE 2.13. LIST OF TAQMAN ASSAYS..... | 41 |
| FIGURE 3.1. MOUSE PRIMARY CULTURES..... | 49 |
| FIGURE 3.2. MOUSE DENTAL PULP CULTURES AND PASSAGING..... | 50 |
| FIGURE 3.3. GENE EXPRESSION OF NP/NCSC GENES IN MDPCs AND MDPPSCs..... | 51 |
| FIGURE 3.4. MDPC CHARACTERISATION..... | 53 |
| FIGURE 3.5. MDPPSC CHARACTERISATION..... | 54 |
| FIGURE 3.6. QUANTIFICATION OF POSITIVE CELLS BY ICC..... | 55 |
| FIGURE 3.7. SPONTANEOUS DIFFERENTIATION..... | 56 |
| DIAGRAM 3.1. WORKFLOW OF MDPC/MDPPSC NEURALISATION (SHH) AND TABLE REMINDER..... | 57 |

| | |
|--|-----|
| FIGURE 3.8. MDPC AND MDPPSC NEURAL INDUCTION WITH SONIC HEDGEHOG..... | 59 |
| FIGURE 3.10. QUANTIFICATION OF POSITIVE CELLS AFTER NEURAL INDUCTION..... | 61 |
| FIGURE 3.11. GENE EXPRESSION ANALYSIS OF NEURALISATIONS BY RT-QPCR..... | 62 |
| DIAGRAM 3.2. MDPC/MDPPSCS UNDER INDUCTIVE CONDITIONS AND COMPONENTS REMINDER..... | 64 |
| FIGURE 3.12. PAX7-EGFP MDPC AND MDPPSC CULTURES..... | 65 |
| FIGURE 3.13. INDUCTIVE CULTURE CONDITIONS..... | 66 |
| FIGURE 3.14. FLOW CYTOMETRY ANALYSIS OF MDPC IN TREATMENT CONDITIONS..... | 67 |
| FIGURE 3.15. RT-PCR OF NEURAL PROGENITOR AND NEURAL CREST MARKERS AFTER INDUCTIVE CONDITIONS..... | 69 |
| DIAGRAM 3.3. MDPC/MDPPSC NEURALISATION AFTER INDUCTIVE TREATMENTS..... | 70 |
| FIGURE 3.16. INDUCTIVE CONDITIONS + NEURAL DIFFERENTIATION..... | 71 |
| FIGURE 4.1. DENTAL PULP COLLECTION..... | 82 |
| FIGURE 4.2. IN SITU CHARACTERISATION OF HUMAN DENTAL PULP TISSUE..... | 84 |
| FIGURE 4.3. EFFICIENCY OF CULTURE ESTABLISHMENT..... | 86 |
| FIGURE 4.4. MORPHOLOGY OF PRIMARY CULTURES (PASSAGE 0) GROWING IN THE DIFFERENT CULTURE MEDIA..... | 88 |
| FIGURE 4.5. NEURAL MORPHOLOGY IN PASSAGED 0 PRIMARY CULTURES..... | 88 |
| FIGURE 4.6. HUMAN DENTAL PULP CELLS' MORPHOLOGY AND CHANGES..... | 89 |
| FIGURE 4.7. HDPC CULTURE PROLIFERATION..... | 90 |
| FIGURE 4.8. CHARACTERISATION OF HDPC-FBS CULTURES BY ICC..... | 93 |
| FIGURE 4.9. CHARACTERISATION OF HDPC-OSCFM CULTURES BY ICC..... | 94 |
| FIGURE 4.10. CHARACTERISATION OF HDPC-BMP4 CULTURES BY ICC..... | 95 |
| FIGURE 4.11. NO PRIMARY CONTROLS..... | 96 |
| FIGURE 4.12. STRO AND P75 IMMUNOCYTOCHEMISTRY (ICC) QUANTIFICATION..... | 96 |
| FIGURE 4.13. HDPC RT-QPCR CHARACTERISATION-AVERAGES..... | 98 |
| DIAGRAM 4.1 HDPC NEURALISATION WITH SONIC HEDGEHOG (SHH) PROTOCOL..... | 100 |
| FIGURE 4.14. HDPC AFTER NEURAL INDUCTION..... | 100 |
| DIAGRAM 4.2. HDPC-SCHWANN CELL DIFFERENTIATION..... | 101 |
| FIGURE 4.15 HDPCs SCHWANN CELL DIFFERENTIATION..... | 102 |
| FIGURE 4.17. HDPC-FBS SCHWANN CELL DIFFERENTIATION..... | 104 |
| FIG 4.18. HDPC-OSCFM SCHWANN CELL DIFFERENTIATION..... | 105 |
| FIGURE 4.19. HDPCs SCHWANN CELL DIFFERENTIATION (NEURAL MARKERS)..... | 107 |
| FIGURE 4.20. ONPs AFTER GROWING IN HDPC-CONDITIONED MEDIUM (CM)..... | 109 |
| FIGURE 4.21. OPTIMISATION OF TRANSFECTION IN HDPC-FBS CELLS..... | 110 |
| TABLE 4.3. SUMMARY OF HDPC TRANSFECTION ICC..... | 110 |
| FIGURE 4.22. HDPC5 FBS TRANSFECTION (ASCL1/NEUD)..... | 112 |
| FIGURE 4.23. HDPC20 OSCFM TRANSFECTION (ASCL1/NEUD)..... | 113 |

| | |
|---|-----|
| DIAGRAM 5.1. WORKFLOW OF HDPC-FBS TREATMENTS AND NEURAL DIFFERENTIATION USING SONIC HEDGEHOG (SHH) INDUCTION AND MEDIA REMINDER. | 130 |
| FIGURE 5.1. HDPC-FBS TREATED WITH DIFFERENT CONDITIONS | 131 |
| FIGURE 5.2. HDPC-FBS CULTURES TREATED FOR NEURAL PROGENITOR INDUCTION IMMUNOCYTOCHEMISTRY (SOX9 AND NESTIN). | 134 |
| FIGURE 5.3. HDPC-FBS CULTURES TREATED FOR NEURAL PROGENITOR INDUCTION - IMMUNOCYTOCHEMISTRY (PO AND NEUD). | 135 |
| FIGURE 5.4. HDPC-FBS CULTURES TREATED FOR NEURAL PROGENITOR INDUCTION - IMMUNOCYTOCHEMISTRY (GLI1 AND SOX10). | 136 |
| FIGURE 5.5. HDPC-FBS CULTURES TREATED FOR NEURAL PROGENITOR INDUCTION - IMMUNOCYTOCHEMISTRY (SOX2 AND SOXP75). | 137 |
| FIGURE 5.6 NO PRIMARY ANTIBODY (AB) CONTROLS. | 138 |
| FIGURE 5.7. HDPC NEURALISATION AFTER TREATMENTS (PHASE 2)..... | 139 |
| FIGURE 5.8 NEURALISED HDPCs AFTER TREATMENTS - IMMUNOCYTOCHEMISTRY (TUJ1 AND NF200)..... | 141 |
| FIGURE 5.9. NEURALISED HDPCs AFTER TREATMENTS - IMMUNOCYTOCHEMISTRY (NEUD AND GFAP). | 142 |
| FIGURE 5.10. NEURALISED HDPCs AFTER TREATMENTS - IMMUNOCYTOCHEMISTRY (NESTIN AND PERIPHERIN)..... | 143 |
| FIGURE 5.11 HDPC INDUCTIVE TREATMENTS + DIFFERENTIATION NO PRIMARY ANTIBODY (AB) CONTROLS. | 144 |
| FIGURE 5.10. EFFECT OF hFASC CONDITIONED MEDIA ON HDPC-FBS | 146 |
| FIGURE 5.11. EFFECT OF hFASC CONDITIONED MEDIA ON HDPC-FBS..... | 147 |
| FIGURE 5.12. EFFECT OF hFASC CONDITIONED MEDIA ON HDPC-FBS..... | 148 |
| FIGURE 5.13. EFFECT OF hFASC CONDITIONED MEDIA ON HDPC-FBS..... | 149 |
| FIGURE 5.14. EFFECT OF hFASC CONDITIONED MEDIA ON HDPC-FBS..... | 150 |
| FIGURE 5.15. EFFECT OF hFASC CONDITIONED MEDIA ON HDPC-FBS..... | 151 |
| FIGURE 5.16. hFASC-CM NO PRIMARY CONTROL. | 152 |
| DIAGRAM 5.2. WORK FLOW OF P75 FACS AND NEURAL INDUCTION. | 153 |
| FIGURE 5.17 FLOW CYTOMETRY ANALYSIS OF P75 IN HDPCs..... | 156 |
| FIGURE 5.18. NEURALISATION OF HDPC-FBS SORTED FRACTIONS. | 157 |
| FIGURE 5.20. HDPC5 FBS P75 CELL SORTING AND NEURALISATION. | 159 |
| FIGURE 5.21. HDPC5 FBS P75 CELL SORTING AND NEURALISATION. | 160 |
| FIGURE 5.22. HDPC5 FBS P75 CELL SORTING AND NEURALISATION. | 161 |
| FIGURE 5.23. HDPC5 FBS P75 CELL SORTING AND NEURALISATION. | 162 |
| FIGURE 5.24. HDPC5 FBS P75 CELL SORTING AND NEURALISATION WITH ALTERNATIVE PROTOCOL (dcAMP)..... | 164 |
| FIGURE 5.25. HDPC5 FBS P75 CELL SORTING AND NEURALISATION WITH ALTERNATIVE PROTOCOL (dcAMP)..... | 165 |
| FIGURE 5.26. HDPC5 FBS P75 CELL SORTING AND NEURALISATION WITH ALTERNATIVE PROTOCOL (dcAMP)..... | 166 |
| DIAGRAM 5.3. HDPC-FBS TRANSFERRED TO THE “PLURIPOTENT STEM CELL MEDIUM” (PSCM) AND MEDIA REMINDER. | 167 |

| | |
|--|-----|
| FIGURE 5.27. HDPC-PSCM CHARACTERISATION. | 169 |
| FIGURE 5.28. CHARACTERISATION OF HDPC-PSCM. | 170 |
| DIAGRAM 6.1. WORKFLOW OF NEUROSPHERE FORMATION, CHARACTERIZATION AND EVALUATION OF HDPC CULTURES. | 178 |
| FIGURE 6.1. HDPCs CAN BE GROWN AS SPHERE AGGREGATES. | 179 |
| FIGURE 6.2. HDPC-NCSCs FROM FBS CULTURES. | 181 |
| FIGURE 6.3. HDPC-NCSCs FROM OSCFM CULTURES. | 182 |
| FIGURE 6.4. HDPC-NCSCs FROM BMP4 CULTURES. | 183 |
| FIGURE 6.5. HDPC-NCSCs RELATIVE EXPRESSION ANALYSIS. | 184 |
| TABLE 6.1. SUMMARY OF NCSC CHARACTERIZATION BY IMMUNOCYTOCHEMISTRY AND RT-qPCR. | 186 |
| DIAGRAM 6.2. WORKFLOW OF HDPC NEUROSPHERES FOR AUDITORY NEURAL DIFFERENTIATION. | 187 |
| FIGURE 6.6. BRIGHT FIELD IMAGES OF NEURALISED HDPC-NCSCs. | 187 |
| FIGURE 6.7. FBS-DERIVED NEURAL-LIKE CELLS, IMMUNOCYTOCHEMISTRY (ICC). | 189 |
| FIGURE 6.8. OSCFM-DERIVED NEURAL-LIKE CELLS, IMMUNOCYTOCHEMISTRY (ICC). | 191 |
| FIGURE 6.9. BMP4-DERIVED NEURAL-LIKE CELLS, IMMUNOCYTOCHEMISTRY (ICC). | 192 |
| FIGURE 6.10. HDPC-NCSCs AND COCHLEAR EXPLANTS CO-CULTURES. | 194 |
| FIGURE 6.11. COCHLEAR EXPLANTS AND FBS-DERIVED SPHERES. | 195 |
| FIGURE 6.12. COCHLEAR EXPLANTS AND OSCFM-DERIVED SPHERES. | 197 |
| FIGURE 6.13. COCHLEAR EXPLANTS AND BMP4-DERIVED SPHERES. | 199 |
| FIGURE 6.14. COCHLEAR EXPLANTS AND ONPs. | 200 |
| FIGURE 6.15. SCHWANN CELL DIFFERENTIATION OF HDPC-NCSCs FROM FBS CULTURES. | 202 |
| FIGURE 6.16. SCHWANN CELL DIFFERENTIATION OF HDPC-NCSCs FROM OSCFM CULTURES. | 203 |
| FIGURE 6.17. SCHWANN CELL DIFFERENTIATION OF HDPC-NCSCs FROM BMP4 CULTURES. | 204 |
| DIAGRAM 6.3. WORKFLOW OF HDPC-FBS TRANSFERRED TO NEURAL CREST STEM CELL MEDIUM (NCSCM). | 205 |
| FIGURE 6.18. HDPC7 FBS IN NCSCM. | 206 |
| FIGURE 6.19. HDPC7 FBS IN NCSCM, IMMUNOCYTOCHEMISTRY (ICC). | 207 |
| FIGURE S1. TRANSFECTION OF EGFP PLASMID. | 239 |
| FIGURE S2. NO PLASMID CONTROLS. | 240 |
| FIGURE S3. NEURALISATION OF HDPC-FBS CULTURES. | 241 |
| FIGURE S4. NEURALISATION OF HDPC-BMP4 CULTURES. | 242 |
| FIGURE S5. NEURALISATION OF HDPC AFTER P75 SORTING. | 242 |
| FIGURE S6 HDPC16 FBS P75 CELL SORTING AND NEURALISATION. | 243 |
| FIGURE S7. HDPC16 FBS P75 CELL SORTING AND NEURALISATION. | 244 |
| FIGURE S8. HDPC16 FBS P75 CELL SORTING AND NEURALISATION. | 245 |
| FIGURE S9. HDPC16 FBS P75 CELL SORTING AND NEURALISATION. | 246 |

Abbreviations

| | |
|-----------|--|
| ASC | Auditory sensory cells |
| BDNF | Brain Derived Nerve Factor |
| bFGF | Basic Fibroblast Growth Factor |
| BMP4 | Bone Morphogenetic Protein 4 |
| CNC | Cranial Neural Crest |
| CNTF | Ciliary Neurotrophic Factor |
| dcAMP | Dibutyryl-Cyclic Adenosine Monophosphate |
| DMSO | Dimethyl Sulfoxide |
| DP | Dental Pulp |
| DPC | Dental pulp cells |
| DPSCs | Dental pulp stem cells |
| EGF | Epithelial Growth Factor |
| EMT | Epithelial to Mesenchymal Transition |
| ESC | Embryonic stem cells |
| FACS | Fluorescence activated cell sorting |
| FBS | Foetal Bovine Serum |
| FC | Flow cytometry |
| GCP | Good Clinical Practice |
| GDNF | Glial cell line-derived Neurotrophic Factor |
| GMP | Good Manufacturing Practice |
| GSC | Gingival Stem Cells |
| hDPC | Human Dental Pulp Cells |
| ICC | Immunocytochemistry |
| IGF | Insulin Growth Factor |
| iPSCs | Induced pluripotent stem cells |
| mDPC | Mouse Dental pulp cells |
| mDPPSC | Mouse Dental pulp pluripotent stem cells. |
| MET | Mesenchymal to Epithelial Transition |
| MMSC | Multipotent mesenchymal stromal cells. |
| MSC | Mesenchymal stem cells/Mesenchymal stromal cells |
| NCSC | Neural Crest Derived Stem Cells |
| NGF | Nerve Growth Factor |
| NSR | Neurosensory region |
| NT3 | Neurotrophin 3 |
| OCT | Optimal Cutting Temperature |
| OEPD | Otic-epibranchial domain |
| ONP | Otic neural progenitor |
| OSCFM | Otic Stem Cell Full Medium |
| PDGFAA/BB | Platelet Derived Growth Factor AA/BB |
| PDL | Periodontal ligament |

| | |
|------|------------------------------|
| PSCM | Pluripotent Stem Cell Medium |
| PSCs | Pluripotent stem cells |
| RA | Retinoic Acid |
| SCAP | Stem Cell from Apical Pulp |
| Shh | Sonic Hedgehog |
| TE | Trypsin EDTA |

CHAPTER 1

“Introduction”

1. Introduction.

1.1. Introduction.

According to the World Health Organization (WHO), 360 million people suffer from disabling hearing loss (WHO, 2017). Although there is a strong correlation of deafness and aging, other leading causes of hearing loss include ototoxic medications, congenital abnormalities, viral or bacterial infections, and the constant exposure to loud noises ^{1,2}. This condition is accompanied by deficiencies of speech, as well as difficulties in the work environment and social interaction, leading to social segregation ¹.

Auditory sensory cells (ASC) arise from the first trimester of embryonic development in humans. In mammals, these cells cannot be replaced when lost, causing an irreversible damage ^{1,2}. Current therapies for the treatment of deafness include the use of hearing aids, which are efficient when the degree of hearing impairment is low; nevertheless, accessibility to such devices is far from optimal. Although cochlea implants are commonly used in patients with severe deafness, the degree of success is variable and suboptimal ³.

Therefore, alternative strategies for audition recovery are needed. Some examples could include the use of cell therapies to replace the lost cells with functional ones ^{1,2,4}. In this context, a promising field of study is the use of stem cells in regenerative medicine. The principle of the latter lies in the potential of undifferentiated cells being driven into phenotypes of interest. In this case, stem cells could replace the ASC lost in deafness ³.

Nevertheless, major obstacles have to be solved for the therapeutic use of stem cells. For instance, finding an appropriate source of cells with stem cell properties that could be used in autologous cell therapy would create an advantage for this purpose. In this regard, adult stem cells and in particular dental pulp stem cells have been identified as a viable and accessible source that needs to be explored further ^{5,6}.

Herby, I present initial evidence of the use of human dental pulp cells for auditory nerve regeneration.

1.2. The ear

The ear is a sensory organ required for balance and hearing ⁷. The ear can be divided in the outer, middle and inner sections. The outer and middle ear work as sound amplifiers that drive and transmit the sound vibrations into the sensory region of the ear: the inner ear⁸ (Fig. 1.1).

The inner ear consists of the vestibular apparatus and the cochlea. The vestibular apparatus allows the balance by means of mechanoreceptor cells and the cochlea is a spiral-shaped structure that contains the auditory sensory cells (ASC) ⁸.

The cochlea is divided in the scala vestibule (superior), scala media and scala tympani (inferior). The scala vestibule and scala tympani are filled with perilymph while the scala media contains endolymph. The scala media contains the spiral organ also called organ of Corti, which is composed of the inner hair cells (IHC), the outer hair cells (OHC), the basilar membrane and the tectorial membrane (Fig. 1.2) ^{8,9}.

The ASC that make possible the reception and transduction of sound stimuli are the IHC, the OHC and the spiral ganglion neurons (SGN) from the Vestibulo-cochlear (VIII) cranial nerve. ^{1,10}.

The sense of hearing is therefore dependent on the correct functioning of the auditory sensory cells. When sound vibrations are conducted through the perilymph they cause the basilar membrane to move and mechanically stimulate IHCs depolarizing them and creating an action potential that is transmitted to the adjacent spiral ganglion neurons (Reviewed in Dallos 1992; Fettiplace and Carole 2006^{9,10}).

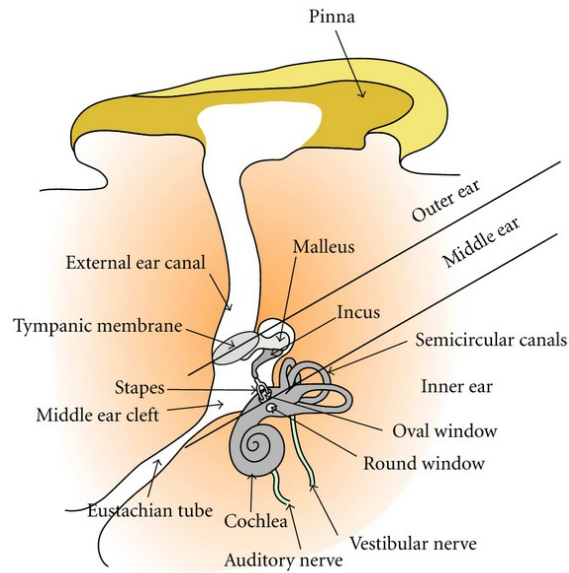


Figure 1.1 The ear. The ear is divided in the outer, middle and inner ear. The outer and middle inner ear directs the sound vibrations into the inner ear, which contains the sensory organs that transduce the sound into the central nervous system (Copyright © under the terms of the creative commons attribution license¹¹).

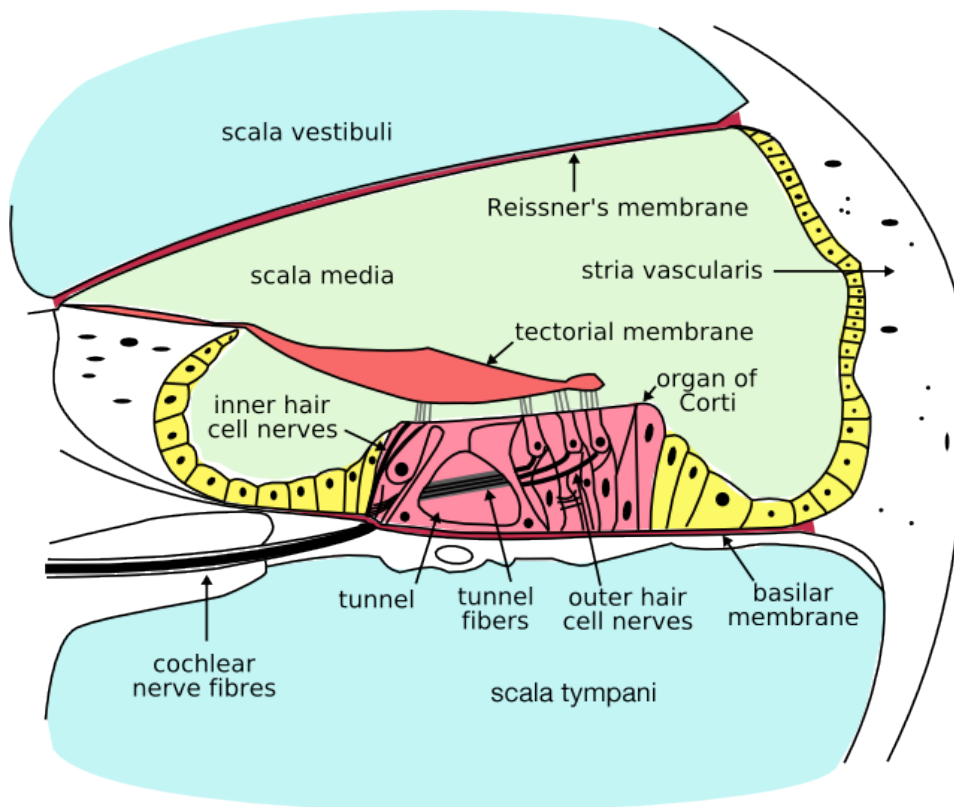


Figure 1.2 Cochlea and organ of Corti. The auditory sensory cells reside in the cochlea which is divided in scala vestibule, scala media and scala tympani; and innervated by the cochlear nerve. The organ of Corti is located in the scala media and contain the inner and outer hair cells, that together with the spiral ganglion neurons permit the sense of hearing. (Copyright © Oarih /Wikimedia Commons/GFDL).

In humans, both hair cell types and SGN within the inner ear are only developed during embryogenesis and are unable to be restored after birth. Each cochlea contains a limited number of hair cells, ranging from 11,000 to 13,000 OHCs and 3,500 IHCs. The limited cell number and the inability of cells to be replaced is an evidence of the delicacy of the ear system, where damaging of a significant number of sensory cells would cause an irreversible damage to the hearing sense, leading to deafness ^{1,8-10}.

1.3. Inner ear development

Soon after the zygote formation, multiple cell divisions give rise to a structure named the morula, consisting of identical cells. Soon after that, the cells begin to acquire distinct fates, that will differentiate them and bound them to specific lineages. This stage is called gastrulation, and by the end of it, three different layers are formed: the ectoderm, the mesoderm and the endoderm. Each of the layers will derive further lineages. From the ectoderm, the process of neurulation occurs. Within neurulation, the neural tube closes, and cells between the epidermal and neural ectoderm located in the neural plate's anterior border diverges into two important progenitor populations: the neural crest cells and the cranial ectodermal placodes. The latter begin to thicken and form the craniofacial sensory system including the otic cells, including the ASCs ^{12,13}.

Early inner ear development is summarised in figure 1.3, and consist of the specification of the pre-placodal region, the formation of the otic epibranchial (OEPD) domain, followed by the separation of the OEPD and formation of the otic placodes and then the otic vesicles.

In order to drive cell determination, different molecular domains need to be set to establish neural crest and placode cell fate. For instance, it has been shown that initial determination of cranial ectodermal placodes requires FGF signaling and the expression of *Six* and *Eya* genes to establish a pre-placodal region. Also, inhibition of Wnt and BMP signaling is required for proper ectodermal cranial placode establishment ¹⁴.

Further lineage commitment at the placodes takes place soon after cranial placode induction. Briefly, the otic placode first originates from the pax2-expressing otic-epibranchial progenitor domain (OEPD) at 4 somite stage (ss) in chicken. Consistent

evidence suggests that OEPD induction depends on FGF signaling, in particular *fgf3* and *fgf10*^{15,16}. However, at 13ss downregulation of FGF signaling and upregulation of canonical WNT signaling is necessary to diverge from the epibranchial domain and commit cells into the otic placode¹⁷ and further continues with the formation of otic vesicles expressing *Dlx5*, *Pax 2*, *Pax 8*, *Sox9* and *Lfng*^{15,16} (Fig 1.3).

In terms of spatial patterning, it is known that retinoic acid (RA) and Sonic Hedgehog (Shh) promotes posterior to anterior and ventral to dorsal specification. The neurosensory region (NSR) is where cell fate specification from otic progenitors at the otic placode happens. In particular, the Shh and RA defined NSR will acquire a neurogenic phenotype expressing *Ngn1* and *NeuroD1*, promoting neuroblast formation and delamination to form the neurons of the auditory vestibular ganglion or spiral ganglion neurons¹⁸⁻²¹.

This brief summary of inner ear development illustrates the key factors involved in cell fate patterning and identification of the otic progenitor lineage, and development of the auditory neurons. This process has helped elucidating developmental causes of deafness, but also, to design *in vitro* models of ear development.

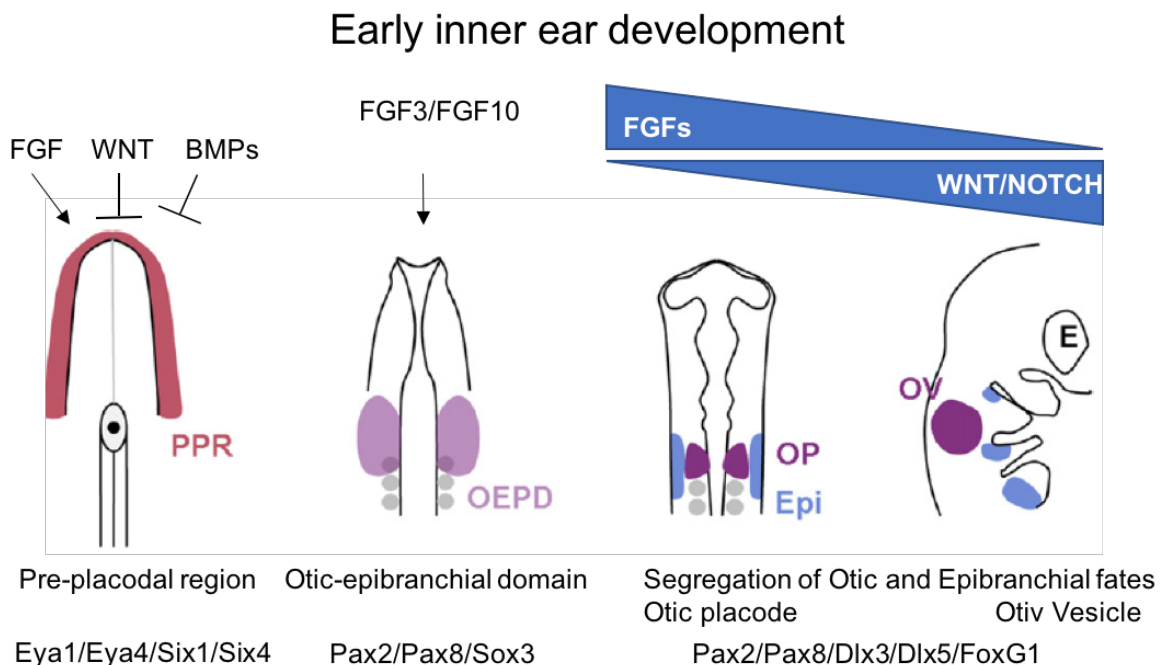


Figure 1.3 Summary of the inner ear development. Molecular signature and cues during early inner ear development. Adapted from Chen and Streit, 2013²² Copyright©, reused with permission (Elsevier).

1.4. Stem cell approaches for auditory sensory cell replacement

The use of stem cells in regenerative medicine has opened a major field in research for their therapeutic potential²³. Stem cells have the ability of differentiation and self-renewal, hallmarks that allow them to commit to many cell lineages²⁴, thus targeting them as powerful tools in tissue engineering and cell therapy. These advantages have also been explored in relation to auditory regeneration with ground breaking discoveries, but also major implications for their use in clinic.

1.4.1. Pluripotent stem cells (PSC)

Pluripotent stem cells (PSCs) are cells capable of differentiating into cell fates from the three developmental germ layers (Ectoderm, mesoderm and endoderm). A PSC source is the inner cell mass of the blastocyst shortly after fertilisation, called embryonic stem cells (ESCs)^{25,26}. Because of their differentiation potential, these cells can virtually become any cell type from the human body, upon proper molecular cues. Furthermore, the implications of being able to maintain and manipulate ESC cultures lead to the discovery of techniques to induce pluripotency from somatic cells, called induced pluripotent stem cells (iPSCs). Besides their differentiation potential, both ESC and iPSC are commonly characterised by the expression of the transcription factors OCT4, SOX2, KLF4, c-MYC and NANOG, but also by their ability to form teratomas²⁷⁻²⁹.

In relation to auditory regeneration, ESC and iPSCs have been used to derive otic progenitors by trying to imitate the developmental signals for ear development. For instance, by inhibiting Dkk1 and SMAD3 in combination with bFGF supplementation, both ESC and iPSC were able to acquire an otic progenitor phenotype, co-expressing Pax2/Pax8 or Pax2/Dlx5. Nevertheless, further differentiation of otic progenitor into morphological and physiological hair-like cells was only possible when co-culturing otic progenitors with inactivated chicken utricle stromal cells³⁰ (Oshima, 2010).

Another example developed in our research group, provided a protocol for the differentiation of ESC into otic progenitors with the use of the factors FGF3 and FGF10 and their further differentiation into the hair-like cells and auditory neurons. Otic neural progenitors (ONP) expressing Pax8, Pax2 and Sox2 derived from the mentioned protocol,

were driven into auditory neurons expressing BRN3a-Tubulin III or BRN3a-NF200 after a maturation protocol including Sonic Hedgehog pathway (Shh) activation plus NT3 and BDNF supplementation. Furthermore, ONPs-derived neurons prove not only to be morphologically, electrophysiological and phenotypically similar to auditory neurons, but remarkably, were also capable of restoring hearing capacity *in vivo*^{31,32}. This research has provided ground breaking evidence of the use of stem cells for auditory nerve regeneration. Recent research has developed more complex protocols with PSCs, where not only the developmental signaling is followed, but also an inclusion of the spatial interaction provided by 3D organoids. In this case, human PSC driven to an otic lineage through manipulation of FGF-2, BMP4 and WNT pathways were driven to hair cell maturation and innervation in a prolonged protocol of cell differentiation by modulating WNT signaling (75 days)³³. This level of complexity has proven to be necessary to obtain relevant hair-like cells from stem cells³⁴.

Although great discoveries have been made from ESCs for deafness therapies, the need of clinical grade culture protocols and safety tests to take them to a clinical grade level is still under development. This opens the door to other stem cell sources to be used for auditory regeneration.

1.4.2. Mesenchymal stromal cells (MSC)

Stem cells can also be isolated from the adult body, these adult stem cells also possess differentiation potential and self-renewal. Their role in the adult body is to allow cell turnover of old, damage or death cells to keep the tissue viable. Therefore, their differentiation potential can be limited to tissue specific lineages. In terms of the nomenclature, many adult stem cells are referred as mesenchymal stem cells (MSCs). However, due to reasons including the diversity of MSCs sources, their actual biological role and clear phenotypic differences compared to their *in vitro* cultures, the current consensus -as proposed by the international society for cellular therapy- is to refer to them as “(multipotent) mesenchymal stromal cells (also MSCs)”^{35,36}. Therefore, MSCs are defined *in vitro* by their ability to adhere to plastic, express/lack of an array of surface antigens (Positive: CD90, CD73, CD105; Negative:CD34, CD45, CD11b), and have adipogenic,

osteogenic and chondrogenic potential²⁶. Besides their mesodermal lineage potential, MSCs have also been shown to differentiate into ectodermal fates including neurons and glial cells^{37,38}. In relation to their source, MSCs have been extracted from several tissues such as bone marrow, adipose, cartilage, tendon, gut, cord blood, salivary glands and dental pulp^{5,39-42}.

MSC arise as an ideal source of cells with therapeutic potential because of their multipotent differentiation, as well as the advantage of being harvest from adult individuals, which makes possible to use cells from the same person (autologous therapy) and avoid immunogenicity. In fact, MSCs are already been used in therapies for hematopoietic diseases and are under clinical trials for several types of illnesses²⁶.

Several attempts to differentiate MSC into auditory cells have been made with important considerations. Jeon et al. (2006⁴³) obtained otic progenitors using the growth factors IGF, EGF and FGF and differentiate them into hair-like cells by Math1 transfection or by successful insertion into developing chicken otocysts.

In addition, our research group has also focused on MSCs for auditory cell regeneration. The evidence obtained revealed that MSC-derived otic progenitors expressing Pax2, Pax8, Sox2 could be obtained if MSCs were cultured in media conditioned with factors from human foetal auditory stem cells (hFASCs). This effect was not possible when treated with FGF3/10 as previously done with ESCs. When MSC-derived otic progenitors were exposed to hair-cell or neural conditions, a small fraction of the cells (<10%) expressed ATOH1/BRN3C/MYO7 and NF200/NGN1/Tubulin III respectively ⁴⁴.

Despite these efforts to support the potential of MSCs to be used in auditory regeneration, very little evidence of *in vivo* functional reports has been provided. Bone marrow-derived MSCs driven to functional neurons have been transplanted into deafened Guinea Pigs and their integration *in vivo* analysed. Although these bone marrow-derived MSCs were able to engraft, differentiate and survive for at least 8 weeks, a definite functional recovery was not shown⁴⁵. The ability of MSCs to integrate and retain the neural phenotype takes relevance because much of their regenerative potential is conferred to a trophic effect, rather than cell replacement as the main mechanism of action⁴⁶. Additionally, adipose

derived-MSCs have also been tested in transplanted Guinea Pigs, evaluating the feasibility of implantation and cell survival⁴⁷. A separate study using adipose derived-MSCs in Guinea Pigs was able to provide evidence suggesting a functional recovery by showing an improved auditory brain response (ABR) in transplanted deafened animals⁴⁸.

The above evidence gives hope for promising future stem cell therapies in the auditory field. However, the now large number of options of stem cell sources raises the question of whether there is a particular stem cell source that could provide advantages for auditory nerve regeneration. In this regard, other commonly described sources of multipotent stem cells are the neural-crest derived stem cells (NCSCs). Due to their ectodermal origin, these cells are also called ectomesenchymal stem cells, and are proposed as cells with greater ectodermal cell fate potential, as it will be described shortly.

1.5. The neural crest and their adult stem cell derivatives

The neural crest (NC) is a transient cell population which begins its formation at the interface between the neural and non-neural ectoderm (neural plate border). Towards the closure of the dorsal tube, the NC cells (NCCs) begin to migrate by triggering the epithelial to mesenchymal transition (EMT), colonizing and differentiating into a variety of organs and tissues. The NC is said to be the fourth germ layer because of its ability to form cell fates from all three germ layers, such as neurons, glia, cardiac muscle, osteoblast, chondrocytes, melanocytes, among others (Fig. 1.4; reviewed in Craine and Trainor 2006⁴⁹). The pluripotent nature of embryonic NCC is evidenced in the different tissues that derive from it during development. In adults, it's possible to find stem cell niches with subpopulations of neural crest origin. These neural crest-derived stem cells (NCSCs) have been the focus of several studies for both basic and applied science due to the proposed advantages of isolating a multipotent cell population.

Neural crest cells

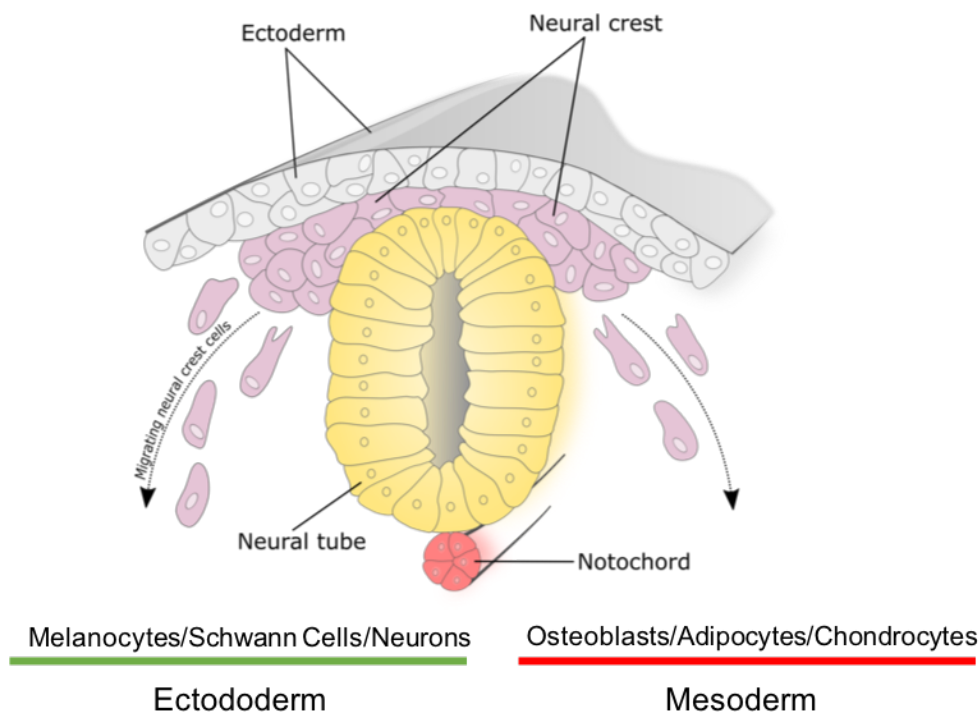


Figure 1.4 Neural Crest Cells. Model of neural crest development and neural crest-derived tissues.

1.6. The study of NCSCs

Recombinant technologies available in animal models have helped to elucidate several niches of neural crest-derived cells in adults. Indeed, the Cre-lox system driven by the expression of WNT1 and P0 has allowed tracing of NCCs into several adult niches such as bone marrow, dorsal root ganglia, whisker pads, iris stroma⁵⁰⁻⁵². Furthermore, *in vitro* culture of NCSCs have shown⁵²⁻⁵⁶ the expression of neural crest-related markers (i.e. Nestin, Sox9, p75, Slug, Snail, Sox10, Pax3, Twist1) and multipotent differentiation into endoderm, mesoderm and ectoderm lineages. The great input that NCCs have in the development of the peripheral nervous system highlights the potential of NCSCs in adult tissues to be used in neurodegenerative disorders. In fact, neuroglial differentiation from animal tissue has been shown for palatal cells, bulge follicle cells and iris stroma, among others. Nevertheless,

it is important to translate those results into cells derived from human tissue to be able to progress in their proposed clinical applications.

It results complicated to trace human NCCs as done in animal models. Nevertheless, assumptions of the neural crest origin of some adult stem cells are supported by the expression *in situ* of neural crest markers, and the ability of growing cells *in vitro*, with neural crest characteristics. Current work has begun to characterize NCSCs derived from human tissues including the palate, inferior turbinate, bulge hair follicle, and from dental related tissues⁵⁶⁻⁵⁹.

Relevant to the current interest in stem cells for regenerative medicine, it would be appropriate to identify NCSCs niches in accessible sites, that could also provide advantages for autologous cell therapies.

In particular for NCSCs in auditory regeneration, only one recent report was found regarding the use of mouse bulge hair follicle-NCSCs, which were able to integrate into inner ear tissue *ex-vivo*. This report provides evidence that NCSCs can be used for auditory nerve regeneration⁶⁰. Nevertheless, it is clear that further investigation is needed to support their use in future therapeutic applications. In particular, evidence supporting a direct application of human NCSCs for auditory nerve regeneration is required.

1.7. Dental-related sources of human neural crest-derived stem cells

There are a number of advantages associated with using dental tissues as a potential source of stem cells. Dental-related stem cells are accessible through routine dental practice procedures where samples and/or biopsies could be taken from surplus tissue, commonly discarded after the procedures. However, it would be necessary to extend the current knowledge of dental tissues as a potential source of human NCSCs to be used in regenerative medicine and in particular for auditory regeneration. A summary of the described NCSCs from dental-related sources and their use is presented in the next section and summarized in Figure 1.5 and Table 1.1.

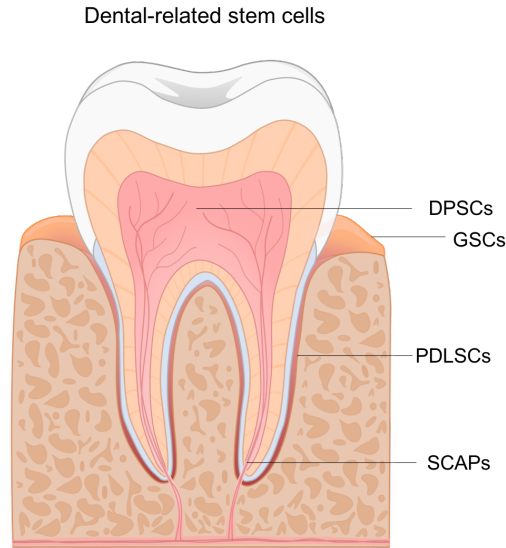


Figure 1.5 sources of stem cells in dental tissues. Stem cells can be found and isolated from dental tissues including: Dental pulp stem cells (DPSCs), Gingiva stem cells (GSCs), Periodontal ligament stem cells (PDLSCs) and Stem cells from apical pulp (SCAPs).

1.7.1. Gingival-derived neural crest stem cells (GSC-NCSC):

The gingiva (gum), is a soft tissue and a visible part of the periodontium, in which a tooth is invested⁶¹⁻⁶³. Human gingiva fibroblastic cultures (GF) and GF-derived clone cultures (referred as Gingival stem cells-GSC), showed expression of Snai1, Twist1, Sox9, Nestin, FoxD3 and Pax3, commonly associated to neural crest cells by qPCR. Further growth of GFs as neurospheres resulted in the presence of CONNEXIN 43, TUBIII, COL1 VIMENTIN and FIBRONECTIN by immunocytochemistry (ICC). Interestingly, GF neurospheres presented higher levels of nestin, tenascin-C and Sox9 than their GF monolayer counterpart⁶⁴.

Recently, Zhang et al. (2018)⁶⁵, described neural crest-derived GSCs from human tissue obtained by a number of different approaches: 1) Spontaneously detached spheres formed from monolayer cultures growing in medium containing EGF and bFGF, 2) 3D spheroids grown in ultra-low attachment plates again with EGF and bFGF and 3) by activating WNT while inhibiting TGF- β signaling. The latter condition resulted in cells with epithelial morphology and an enhanced expression of NCSCs genes. Additionally, to the culture and characterization of NCSCs from gingiva, the authors provided relevant evidence for their

regenerative application in a rat model of facial nerve regeneration. By inserting the cells in nerve conduits, NCSCs demonstrated a higher expression of S100 β , TUBIII, Neurofilament and GAP-43 in regenerated nerves as well as greater myelination and stronger compound action potentials than their GSC counterpart⁶⁵. This evidence is one of very few physiologically results reported for an oral-derived NCSCs.

1.7.2. NCSCs derived from Periodontal ligament (PDLSC).

The periodontal ligament, a connective tissue that allows tight and strong connection between the teeth and the jaw, also contains cells with mesenchymal stem cell features⁶⁶. Early evidence of NCSCs from PDLSCs was obtained by culturing the cells in inductive medium containing chicken embryo extract, EGF and FGF2. This condition yielded cells expressing Nestin, Protein 0, TUBIII, NFM and α -SMO at the RNA level, representing markers belonging or derived from NCSC. Additionally, immunocytochemistry (ICC) for HNK-1 and P75 showed their expression in <10% of the cells in culture. Thus, HNK-1 and P75 expressing cells represented a putative undifferentiated population of NSCSs⁶⁷. Another strategy for isolating NCSCs from adult tissues has been through direct isolation of a particular population identified with a specific marker. Indeed, Pelaez et al. (2013)⁶⁸, isolated CX43^{+ve} cells from PDLSC by magnetic bean sorting. A higher gene expression of OCT4, NANOG, and SOX2 was found in comparison to that found in the unsorted PDLSC culture and mesenchymal stromal cells. Importantly, the presence of SOX10 and P75 as key molecules for NCSCs phenotype was identified in the positive fraction. The detection of pluripotent markers as well as the ability of CX43^{+ve} cells to form teratomas suggested a degree of pluripotency in NCSCs and highlights the importance of NCSC selection from heterogeneous cultures. Recently, Ramirez-Garcia et al. (2017)⁶⁹, provided a deeper analysis of the effect of WNT activation and TGF- β inhibition in PDLSC cells. Flow cytometry analysis showed a larger population of P75 and HNK-1 positive cells when these pathways were modified. Importantly, this phenotype was found to be dynamic and affected by the presence of serum in the culture. The authors argue that the dynamism can be partially attributed to the cells capacity to undergo Epithelial to Mesenchymal Transition/Mesenchymal to Epithelial Transition (EMT/MET), evidence of a NCSC phenotype⁷⁰. However, PDLSC-derived

NCSCs are mainly defined by the expression of neural crest-related markers and further functional/behavioral evidence is needed.

1.7.3. Exfoliated deciduous teeth

Stem cells from human exfoliated deciduous teeth (SHEDs) have been recently investigated for the expression of neural crest markers modified by the culture conditions. Indeed, in an additional study to their previous work on PDLSC derived NCSCs⁶⁹, Gazarian et al. (2017)⁷⁰ tested the effect of Wnt pathway activation and TGF- β blockade as a growth condition for neural crest-like stem cells. These pathway modifications provided a deeper insight of neural crest and mesenchymal marker dynamics. Flow cytometry data showed an increased population of cells expressing the neural crest markers P75^{+ve} and HNK-1^{+ve}, and a decrease of the mesenchymal marker CD90^{+ve} bearing cells in the neural crest medium.

1.7.4. Stem cells from apical pulp cells (SCAP):

The soft tissue located at the apex of a developing teeth, such as third molars extracted for orthodontic reasons, has proven to be a source of another source of stem cells: SCAPs. Early research characterized a population of cells with a migratory capacity to outgrow from tissue explants *in vitro*. These motile cells analyzed by flow cytometry still presented typical MSC markers such as CD90, CD73 and CD166. Nevertheless, these migratory cells also expressed Snai1, Snai2, Sox9 and Twist1⁷¹. Neurosphere formation has also been used to derive NCSCs from SCAPs. Western blot and ICC revealed the expression of MUSHASHI, P75 and NESTIN in the neurospheres while endpoint PCR showed Mushashi, Slug, Snai and p75 RNA expression. Furthermore, neurospheres presented a lower signal of the mesenchymal markers CD166 and CD105 compared to the monolayer parental cultures⁷², supporting the idea proposed by Gazarian and Ramirez-Garcia^{69,70} that neural crest phenotype in adult derived neural crest stem cells correlates with an epithelial phenotype. In terms of their differentiation potential, NCSC from SCAPs showed classical differentiation potential into adipogenic, myogenic, chondrogenic and neurogenic fates, but haven't been tested in a relevant model of regeneration.

1.7.5. Dental pulp stem cells (DPSC)

A well-documented source of adult stem cells is the dental pulp of permanent teeth, which consists of the soft tissue within a tooth, containing a variety of cells including vascular cells, fibroblast and odontoblasts^{5,73}. Despite their proposed potential and interest for applications in neurodegenerative diseases, the culture and growth of NCSCs from DPSCs has not been widely described. A report from Al-Zer et al., (2015)⁷⁴ presented evidence for the growth and expansion of cells migrating from dental pulp explants in defined medium containing EGF and FGF2. The migratory cells expressed P75, Nestin, Sox10 by ICC and were able to form spheres and be induced to osteogenic, glial and melanocytic differentiation. However, this unique report should be further complemented with an extensive phenotypic characterization and functional assays.

Dental-related sources of human neural crest-derived stem cells

| Source | Description | Condition components | Markers | Functional assay. | Author |
|---------|--|--|---|--|---------------------|
| Gingiva | Self-Induced Spheres and sphere-derived monolayer cultures. Spontaneously detached cells from Lam/PLO coated dishes. | -DMEM/F12 (1:1) -Neurobasal medium -Human bFGF (20ng/mL) -Human EGF (20ng/mL) -βMe (55μM) -N2 (1%) -B27 (1%) -Pen/Strep (100U/100μg/mL) | <i>ICC:</i> P75, Nestin, SOX9, SNAIL1. <i>qPCR:</i> Sox9, FoxD3, Slug, Snail1. | Nerve conduits in rats: functional recovery. | Zhang et al., 2018. |
| | Enhanced NCSCs Passaged NCSCs with WNT activation and TGFβ inhibition. | NCSCs medium + CHIR99021 (2.5μM) SB43152 (5μM) | Loss of MSC: CD29, CD44, CD73, CD90. -Gain of NCSC: P75. | N/A | |

| | | | | | |
|----------------------|--|--|---|---|--------------------------------------|
| | <p>Neurospheres</p> <p>From monolayer cultures grown in standard FBS-containing medium.</p> | <p>-DMEM/F12 (1:1)</p> <p>-L-Glut (2mM)</p> <p>-EGF (20ng/mL)</p> <p>-FGF2 (40ng/mL)</p> <p>-B27 (2%)</p> | <p>Monolayer and neurospheres (qPCR):</p> <p>Nestin, Pax3, Twist1, Snai1, FoxD3, Sox9.</p> <p>Neurospheres (ICC):</p> <p>VIMENTIN, NESTIN, COL1, FIBRONECTIN.</p> | <p>Neural differentiation <i>in vitro</i>.</p> | <p>Fournier et al., 2016.</p> |
| Periodontal ligament | <p>Monolayer</p> <p>From monolayer cultures grown in standard FBS-containing medium. For NCSCs conditions: low density (100 cells per 24 well plate).</p> | <p>-a-MEM</p> <p>-FBS (10%)</p> <p>-Chicken embryo extract (2%)</p> <p>-Transferrin (10mg/mL)</p> <p>-Hydrocortisone (0.1mg/mL)</p> <p>-Glucagon (0.01ng/mL)</p> <p>-Insulin (1ng/mL)</p> <p>-Triiodonrironine (0.4ng/mL)</p> <p>-EGF (0.1ng/mL)</p> <p>-FGF2 (1ng/mL)</p> <p>-Pen/Strep (100U/100µg/mL)</p> | <p>NCSCs conditions:</p> <p><i>ICC:</i> P75, HNK-1, NESTIN.</p> <p><i>RT-PCR:</i> Nestin, βTubIII, Nfm, Map2, Peripherin, P0, GFAP, aSma.</p> | <p>None</p> | <p>Coura et al., 2008.</p> |
| | <p>Monolayer</p> <p>Sorting from monolayer cultures grown in standard FBS-containing medium.</p> | <p>Connexin 43⁺ cell sorting from monolayer cultures.</p> | <p>CX43⁺ population (ICC):</p> <p>NANOG, SOX2, SOX10, OCT4, NESTIN, p75.</p> | <p>Teratoma formation as pluripotency test.</p> | <p>Pelaez et al. 2013</p> |
| | <p>Monolayer</p> <p>From monolayer cultures grown in a defined MSC medium and changed to a NCSCm.</p> | <p>MESENDEM (FN-coating):</p> <p>-Optimem,</p> <p>-ITS (1X)</p> <p>-βME (50µM)</p> <p>-Glutamax (2mM)</p> <p>-FGF2 (5ng/mL)</p> <p>-EGF (10ng/mL)</p> <p>-Anti Anti (1X)</p> <p>-0.5, 1, 2, 10% FBS.</p> <p>NCSCm (FN-Coating):</p> <p>-DMEM/F12</p> <p>-N2 (1X)</p> <p>-B27 (1X)</p> <p>-FGF2 (10ng/mL)</p> <p>-EGF (10ng/mL)</p> | <p>NCSCs medium:</p> <p><i>FC:</i> increase in P75 and HNK1, E-CAD.</p> <p><i>RT-PCR:</i> Oct4, Sox2, Myc, Cdh1, Zeb and Sox10.</p> | <p>None</p> | <p>Ramirez et al., 2017</p> |

| | | | | | |
|--|---|---|---|---|----------------------------------|
| | | -BIO (2µM) -REPSOX (1µM) | | | |
| Human exfoliated deciduous teeth. | Monolayer From monolayer cultures grown in a defined MSC medium and changed to a NCSCm. | DentEpiMesMed (FN-Coating): -DMEM/F12 -N2 (1%) -Ascorbic Acid (100µg/mL) -βME (50µM) -Glutamax (2mM) -FGF2 (2.5ng/mL) -EGF (10ng/mL) -IGF (10ng/mL) -Anti Anti (1X) -MEM AA (1X) -Anti Anti (1X) -1 or 2% FBS NCSCm (FN-Coating): -DentEpiMesMed + -BIO (1µM) -REPSOX (5µM) | NCSC medium: FC: Upregulation of P75 and E-cad, downregulation of CD73. ICC: Upregulation of SOX10 qPCR: upregulation of SOX10, ZO-1, E-cadherin. | In vitro neural differentiation (From defined MSC culture, but not from NCSCm cultures) | Gazarian and Ramirez 2017 |
| Apical pulp cells | Monolayer: Standard 10%FBS medium. | Characterised in standard FBS medium. | Snai1, Snai2, Sox9, Twst1, Msx2 and Dlx6. STRO-1 Negative. | In vitro neural differentiation. | Degistirici et al., 2008 |
| | Neurospheres: Initial growth in Standard 10%FBS medium and induced neurosphere formation. | -DMEM/F12 -20ng/ml FGF2 -20ng/ml EGF -N2 | Neurospheres: ICC: Nestin, Mushashi-1, P75. RT-PCR: Nestin, Mushashi-1, Slug, Snail, P75. | In vitro neural differentiation | Abe et al., 2012 |
| Dental Pulp Stem Cells | Monolayer: Dental pulp cells outgrown from explants. | -Neurobasal medium -N27 without Vitamin A -20ng/ml FGF2 -20ng/ml EGF -2.5µM Insulin -2mM L-Glut -10nM Neuregulin-β1 | NCSC Explants: ICC: P75, Nestin, Sox10. | Schwann Cell Differentiation. | Al-Zer et al., 2015 |

Table 1.1. Summary of dental related-NCSCs.

1.8. Current limitations of dental-related NCSCs

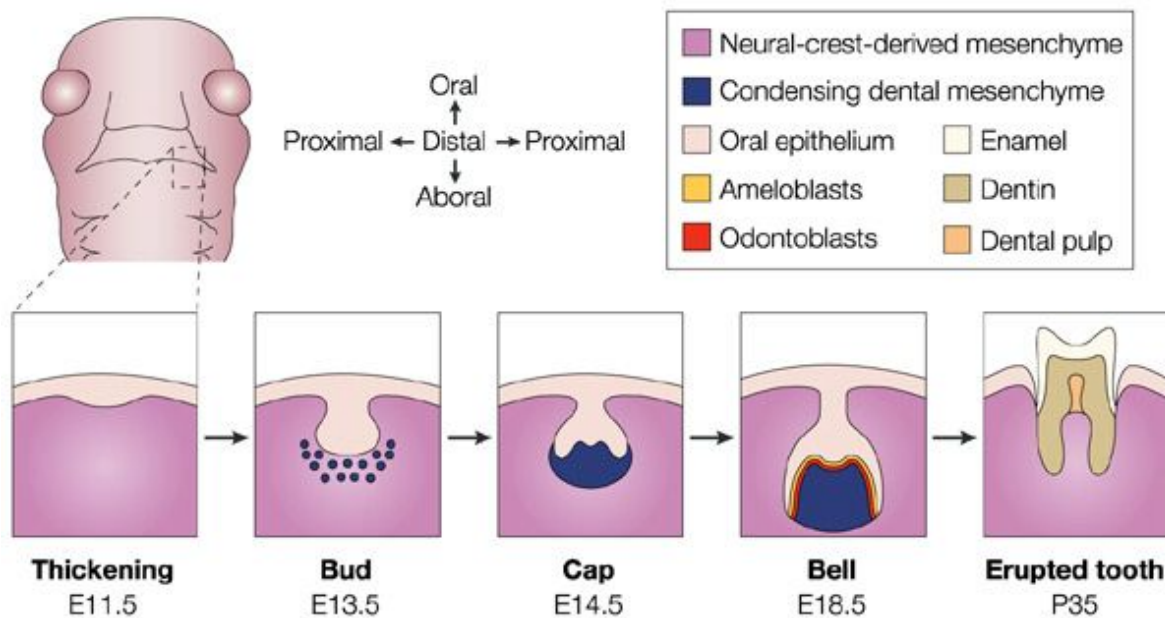
As described, dental related stem cells grown and characterized as NCSCs hold the promise to be used in regenerative medicine. However, current reports are limited to the characterization of the NCSC phenotype, rather than testing their functional behavior. To the best of our knowledge, only gingival-derived NCSCs have been tested in a relevant model of nerve regeneration, and there is no evidence of their particular use in auditory regeneration⁶⁵. Therefore, it is encouraged to investigate the potential of dental related-NCSCs for specific applications. In this regard, our particular interest is to evaluate the use of NCSCs derived from human dental pulp cells for auditory nerve regeneration.

To further understand the biology of human dental pulp cells (hDPCs), a summary of the tooth development process will be described followed by the current knowledge of *in vitro* hDPC cultures.

1.9. Tooth development

Tooth development requires a bilateral interaction between the oral epithelium and the mesenchyme, where the development of both depends each component signaling in a timely fashion⁷⁵. Oral mesenchyme is derived from cranial neural crest cells (CNC) migrating from rhombomeres I, II and III that populate the 1st pharyngeal arch. CNCs are known to become mesenchymal and because they arise from the ectoderm, their derived cells are sometimes called ectomesenchymal cells^{76,77}.

Tooth development is performed in stepwise manner. The developmental progress of tooth formation can be divided into: dental placode formation (thickening), bud, cap and bell stages. In summary, during thickening and bud stage the epithelium migrate and intrude the mesenchyme⁷⁸. The epithelial cells surround the mesenchyme and form a signaling centre named enamel knot. The epithelial cells in the bud structure invaginate forming a cap and by the end of the cap stage the tooth acquires a bell shape. The bell stage is the final stage where cells are finally established and begin their differentiation^{76,79}. Mesenchymal tissue forms the dental papilla that in turn become the dental pulp and odontoblasts, whereas epithelial tissue forms the outer layer of ameloblasts (Fig 1.6; Reviewed by⁷⁸⁻⁸⁰).



Nature Reviews | Genetics

Figure 1.6. Developmental stages of tooth development. Tooth development arise from a bilateral interaction between epithelium and mesenchyme of ectodermic origin. (2004)⁸⁰. Copyright©, reused with permission.

Molecular signaling during tooth development is complex and involves major signaling molecules such as Wnt, Sonic Hedgehog (Shh), FGFs and TGF β super family⁸¹. In particular, the molecular signaling that drives tooth formation is dependent on the TGF- β superfamily member BMP4 (Bone morphogenetic protein 4). For instance, substantial evidence has shown that BMP4 signaling confers the dental potential of oral epithelium that is later transferred to the oral mesenchyme for tooth specification⁸²⁻⁸⁴. Furthermore, FGF factors are also implicated in tooth development in the mesenchyme, and along BMP4 depend on the hox gene *msx1*^{82,83}. Therefore, BMP4 has been consistently proven to be a key player in tooth development.

1.10. Dental pulp cells *in vitro*.

Although we have already described briefly the characteristics and experimental approaches in dental-related NCSCs, it is important to further describe the current knowledge of the particular population of our interest: the dental pulp cells.

As described earlier, the dental pulp (DP) is the soft inner component of the tooth, and it derives from dental papilla. The DP contains different cell types such as fibroblasts, odontoblasts, immune cells, nerves ends, glia and MSCs^{5,85}.

It must be noted that the dental-related stem cells considered above are neural crest-derived by origin. However, the first reports and the current status quo describe them as MSCs, expressing the relevant markers (i.e. CD105, CD90, STRO-1) and able of trilineage differentiation (adipogenic, chondrogenic and osteogenic)^{5,63,66,86}. In addition, Atari et al⁸⁷ characterised a small pluripotent-like population of cells within the dental pulp by culturing DPSCs in a pluripotent growth medium⁸⁷.

Attempts to differentiate dental MSCs into neural lineages have mostly failed to show a mature or functional phenotype when grown from their basal conditions which contains foetal bovine serum (FBS). Indeed, careful analysis of previous reports indicate that mature neural induction is achieved only after multistep differentiation protocols including EGF/FGF2 conditioning, epigenetic modification and neurosphere formation⁸⁸⁻⁹⁰, resembling NCSC culture conditions. This suggests that successful and physiological relevant differentiation can only be achieved when a putative NCSC phenotype is induced or selected in the first steps. By using this multi-step protocols, pre-clinically relevant reports have demonstrated the potential of human dental-derived stem cells for regenerative medicine, where it has been shown that DPSCs can differentiate into functional neurons and Schwann cells^{90,91}. As an example, Fujii et al., (2015)⁹² generated dopaminergic neurons and tested them *in vivo* in a rat Parkinson model, or Martens et al. (2016)⁹¹, differentiating hDPSCs into Schwann cells that when inserted in artificial conduits for nerve regeneration allowed myelin formation and axon guidance in rats. Therefore, providing evidence for neurodegenerative cell therapies. However, it must be noted that these success examples

come from cultures initially treated and characterized as MSCs in standard media supplemented with foetal bovine serum (FBS). Thus, the initial growing conditions would not be allowed in a therapeutic approach due to the presence of factors from animal origin, which go against good clinical practice and good manufacturing practice (GCP/GMP) standards⁹³⁻⁹⁵.

In this regard, an advantage of growing dental related cultures as NCSCs, besides their proposed differentiation potential, is the use of defined culture conditions without animal serum and factors that can be more easily replaced by xeno-free, GMP/GCP standard components⁹⁴. Therefore, future work would benefit from developing approaches using initial derivation and expansion conditions in serum-free or GMP compliant media as well as providing evidence not only of a molecular neural crest signature, but also by functional tests in relevant regenerative models.

1.11. Advantages of hDPSCs for auditory cell replacement therapies

So far, adult stem cell differentiation into auditory neurons has been attempted with adipose and bone marrow's MSCs^{31,43,44,47}. However, their non-ectodermal origin could represent a disadvantage in the potential of acquiring an otic phenotype. This, is evidenced from the low neuron-like cell yield observed by Boddy et al. (2012)⁴⁴ in addition to the requirement of foetal conditioned medium, or by Jeon et al., (2007)⁴³ with the need of transfection of the otic factor Math1 as a condition for a phenotypic change into otic progenitor cells. On the other hand, neural crest-derived stem cells are proposed to be intrinsically neurogenic and are therefore hypothesised as a better source of readily available adult stem cells for auditory nerve regeneration. Furthermore, hDPSCs have the advantage over other sources as their collection, culture and banking can be performed from routine and relatively non-invasive standard procedures⁹⁶. Collection and banking are already being undertaken by bio-companies around the world. Also, children and adults have potentially the same opportunities to benefit from autologous stem cell therapies by means of their dental pulp.

1.12. Research statement:

The need of alternative therapies in deafness to replace the lost or damage sensory neurons, pose this condition as a perfect candidate for stem cell replacement therapies. The current reports already mentioned, provide evidence of the feasibility of such therapeutic approach. In this regard, it would be beneficial to seek additional candidate sources with a proposed enhanced neurogenic potential, such as neural crest-derived stem cells. In particular, dental pulp cells of neural crest origin should be investigated to validate their neural crest resemblance, and to provide concise evidence of their use in particular models of regeneration, rather than just implying their therapeutic potential.

1.13. Aims and objective

1.13.1. Overall aim

Evaluate the use of dental pulp cells (DPCs) for auditory nerve regeneration.

1.13.2. Specific objectives:

- 1) Evaluate and characterise mouse dental pulp cells for auditory nerve differentiation.
- 2) Evaluate and characterise human dental pulp cells in defined monolayer culture conditions for neural crest-derived stem cell growth.
- 3) Evaluate human dental pulp cells potential for otic progenitor and auditory nerve differentiation.
- 4) Characterise human dental pulp cells grown as neural crest-derived stem cells in 3D cultures (hDPC-NCSCs).
- 5) Evaluate hDPC-NCSCs in a relevant model of auditory regeneration.
- 6) Evaluate hDPCs glial-like potential.

CHAPTER 2

“Materials and Methods”

2. Materials and Methods

2.1. Establishment of human dental pulp cell (hDPCs) cultures

The ethical approval for collecting human teeth and extracting dental pulp for research purposes was granted by the NRES committee, protocol number: STH19019.

After obtaining informed consent, teeth were extracted and immediately placed into a container with ice cold PBS and 100I.U/mL-100µg/mL of penicillin-streptomycin (GIBCO, UK- hereby referred as 1X P/S) and rapidly transferred to the laboratory.

In the laboratory and inside a fume hood, the procedure for extracting the dental pulp was performed. Dental pulp extraction was achieved by making a longitudinal groove on the tooth using an electric drill with a diamond disc, cooled under running water. The groove should not reach the chamber completely to avoid overheating the pulp and damage to living cells. Once the groove was in place, the tooth chamber and dental pulp were exposed by positioning a 5mm osteotome in the groove and hitting with a mallet to fracture the tooth and expose the pulp.

Once the chamber was exposed, the pulp was extracted with fine forceps and transferred to a vial containing Duplecco's modified eagle media (DMEM, SIGMA, UK) with 1x P/S and left on ice until digestion. All the instruments in contact with the dental pulp was sterilised prior to use in 70% ethanol.

The extracted dental pulp was then digested by incubating with collagenase IV (3mg/mL, GIBCO, UK) at 37C for 1h. The tissue was manually dissociated by pipetting every 30 minutes. Once the digestion was finished, the dissociated tissue was passed through a 100µm cell strainer into a falcon tube. Then, the cells were centrifuged for 5 minutes at 400g. After discarding the supernatant, cells were washed with PBS and centrifuged again 5 minutes at 400g. After the wash, the supernatant was removed, and the cell pellet was re-suspended in culture medium and seeded into well plates into either 20% FBS, OSCFM or BMP4 media (details in table 2.1).

| Medium | Basal Conditions |
|--|--|
| 20% Fetal bovine serum (FBS) ⁵ | DMEM, 1x P/S, 2nM Glutamax (GIBCO), 100µM Ascorbic Acid (Sigma), 20% foetal bovine serum (FBS; GIBCO). No coating. |
| OSCFM (Otic stem cell full medium) ³² : | DFNB (DMEM:F12 (GIBCO), 1% N2 (GIBCO), 2% B27 (GIBCO)), 1x P/S (SIGMA), 20ng/mL bFGF (R&D Systems), 50ng/mL IGF (R&D Systems), 20ng/mL EGF (R&D Systems). Coated with mouse laminin (2.5ug/cm ² ; Cultrex). |
| OSCFM+BMP4 (BMP4): | OSCFM supplemented with 10ng/mL BMP4 (R&D Systems). Coated with mouse laminin (2.5ug/cm ² ; Cultrex). |

Table 2.1. Basal conditions of mouse and human dental pulp cells.

For the primary culture establishment, the cultures remained undisturbed for the first 4 days. At day 4, half a volume of the respective medium was added. From day 7, half of the culture medium was replaced every other day, until day 12. From day 12, the medium was completely replaced every 2-3 days. The primary cultures that were able to reach at least 60% confluence at week 4, were passaged and maintained as successful cultures.

Passaging of 20% FBS culture was done using 1:10 trypsin EDTA (TE 1:10; Sigma), whereas OSCFM and BMP4 cultures were passaged using TE 1:80. Optimal seeding density was 5,000-10,000 cells/cm².

2.2. Establishment of mouse dental pulp cell (mDPCs) cultures

To collect dental pulp cells from mice it was necessary to collect and pool tissue from 5 different individuals. Mice were treated in accordance with the schedule 1 procedures of the animal (scientific procedures) act 1986. The lower mandible was removed, and the incisors were dissected. The Skin and muscles were removed. To expose the incisor's chamber a 25G fine needle was inserted longitudinally from the posterior region of the tooth, this is from the cervical loop. The needle was then moved to break the hard tissue and expose the dental pulp. Dental pulp tissue was then collected and processed as

described above for human dental pulp cells. The cultures were established directly into either FBS-containing medium or Pluripotent stem cell medium (PSCM; Table 2.2).

| Medium | Basal Conditions |
|--|--|
| <i>Fetal bovine serum (FBS)</i> ⁵ | DMEM, 1x P/S, 2mM Glutamax (GIBCO), 100µM Ascorbic Acid (Sigma), 10%, 15% or 20% foetal bovine serum (FBS; GIBCO). No coating. |
| <i>Pluripotent stem cell medium</i> ^{52,87} | 60% DMEM-Low Glucose (SIGMA), 40% MCDB-201 (Sigma), 1X Insulin-transferrin-selenium (ITS, Sigma), 1X linoleic acid-bovine serum albumin (LA-BSA; Sigma), 1nM Dexamethasone (Sigma), 100µM Ascorbic Acid, 100 I.U./mL Penicillin/100µg/mL Streptomycin, 2% FBS (HyClone, Fisher Scientific), 10ng/mL hPDGF-BB (R&D Systems), 10ng/mL EGF (R&D Systems). Coated with 100ng/mL Fibronectin (Sigma). |

Table 2.2. Mouse dental pulp cell basal conditions.

2.3. Cryopreservation of mouse and human dental pulp stem cells.

Cell cultures were trypsinised with TE 1:10 or TE1:80 accordingly. After one wash with PBS and centrifugation at 400g for 5 minutes, the pellets were re-suspended in freezing medium consisting of foetal bovine serum (FBS) with 10% Dimethyl Sulfoxide (DMSO, SIGMA). Samples were inserted in a freezing container with isopropanol and frozen at -80°C.

To recover frozen cell cultures, the cryovials were fast thawed in hot water and slowly pipetted into their respective media. The cells were pelleted by centrifugation at 400g for 5 minutes, the supernatant discarded and the pellet re-suspended in their respective media. The cells were seeded into appropriate culture vessels.

2.4. Neural differentiation of mDPCs and hDPCs by Sonic Hedgehog induction.

Neuralisation of DPCs was attempted using the protocol described for human otic neural progenitor differentiation (Chen et al. 2012^{31,32}). Confluent mouse and human cultures from their basal conditions were detached using trypsin 1:10 (T 1:10; Sigma) and seeded in laminin coated plates (2.5ug/cm²) at 8,000 cells/cm² (unless otherwise stated) according to the protocol (Fig 2.1 and Table 2.3).

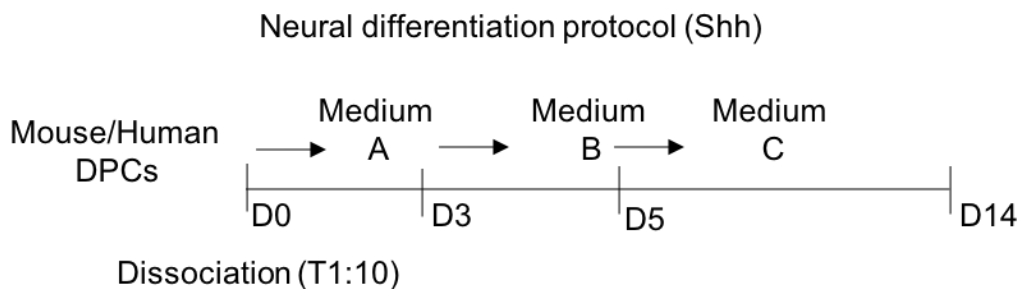


Figure 2.1 Neuralisation protocol with Sonic Hedgehog (Shh) flow chart. Cells were dissociated from their basal conditions (FBS, OSCFM or BMP4) using Trypsin and initially seeded with neuralising medium A for 3 days (D0-D3), followed by media changes. First to medium B for 2 days (D3-D5), and then changed to medium C for 9 days (D5-D14); medium C was replaced every second day to fresh medium.

| Medium | Conditions |
|-------------------------------|---|
| Neuralising medium A (D0-D3) | DFNB (DMEM:F12 (GIBCO), 1% N2 (GIBCO), 2% B27 (GIBCO)), bFGF (20ng/mL; R&D Systems), Shh (500ng/mL; R&D Systems). |
| Neuralising medium B (D3-D5) | DFNB, bFGF (20ng/mL; R&D Systems), Shh (500ng/mL; R&D Systems), NT3 (10ng/mL; Peprotech) and BDNF (10ng/mL; Peprotech). |
| Neuralising medium C (D5-D14) | DFNB, bFGF (20ng/mL; R&D Systems), NT3 (10ng/mL; Peprotech) and BDNF (10ng/mL; Peprotech). |

Table 2.3. Neuralisation protocol with Sonic hedgehog, media conditions.

2.5. Neural differentiation of hDPC neurospheres by dcAMP induction.

Neuralisation of DPCs was induced using the protocol established for hDPSCs (Gervois et al., 2015). Confluent cultures were detached with either TE 1:10 (20% FBS) or TE 1:80 (OSCFM and BMP4). Cells were then re-suspended in sphere medium at 5,000-10,000 cells per 100uL in low attachment culture plates (Costar). At day 6-8 neurospheres were transferred to a Poly-ornithine (0.01%; Sigma)/Laminin (2.5µg/cm²) coated plate in neuralising medium. The medium was replaced every 2-3 days for 1 week (s) according to the protocol (Fig. 2.2 and Table 2.4).

Neural differentiation protocol from neurospheres

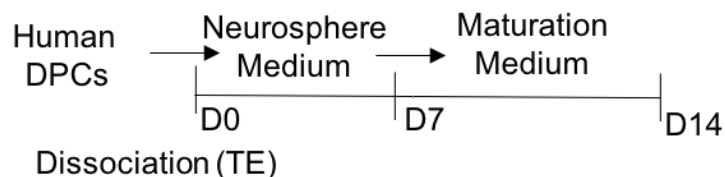


Figure 2.2 Neural differentiation after neurosphere formation. hDPCs were dissociated from their basal conditions (FBS, OSCFM or BMP4) using Trypsin-EDTA (TE) and grown in low-attachment conditions in neurosphere medium for 7 days (D0-D7) and then transferred to appropriate vessels with maturation medium for 7 days (D7-D14).

| | |
|--------------------|--|
| Medium | Basal Conditions |
| Sphere medium | DNFB, 1x P/S (SIGMA), 20ng/mL bFGF (R&D Systems), 20ng/mL EGF (R&D Systems). |
| Neuralising medium | DNFB, NT3 30ng/mL (Prepotech), 1mM dcAMP (Tocris). |

Table 2.4. Neuralisation protocol after neurosphere formation.

2.6. Schwann cell differentiation of hDPCs by Forskolin induction.

Schwann cell differentiation was attempted using a protocol by Dezawa et al., (2009)³⁸ which was slightly modified by Martens et al., 2012⁹¹ for hDPSC. The cultures were detached by TE 1:10 (20% FBS) or TE 1:80 (OSCFM and BMP4) and seeded at 8000 cells/cm² and allowed to settle and attach for 2 days. Cultures were then treated by replacing the medium according to the protocol (Fig. 2.3 and Table 2.5).

Schwann cell differentiation protocol (Dezawa)

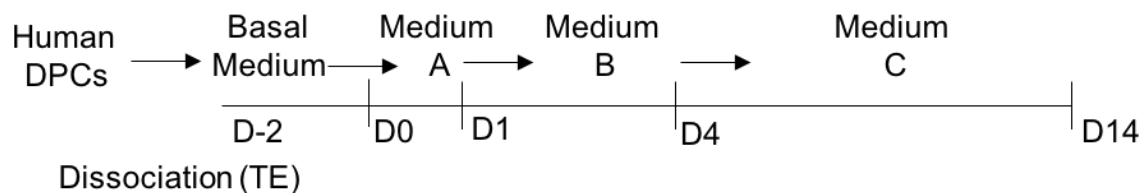


Figure 2.3 Schwann cell (SC) differentiation with Dezawa's protocol flow chart. Human dental pulp cells were grown in their basal conditions (FBS, OSCFM or BMP4) for 2 days after dissociation with trypsin-EDTA (D-2). Schwann cell differentiation was induced by replacing the medium with medium A for one day (D0-D1), then medium B for 3 days (D1-D4) and finalising with medium C for 10 days (D4-D14).

| Medium | Conditions |
|----------------------|--|
| SC-Medium A (D0-D1) | DMEM (Sigma), 1X P/S (Sigma), 2mM Glutamax (GIBCO), 1mM B-Mercaptoethanol (GIBCO). |
| SC-Medium B (D1-4) | DMEM (Sigma), 1X P/S (Gibco), 2mM Glutamax, 10% FBS, 35ng/mL Retinoic Acid. |
| SC-Medium C (D4-D14) | DMEM (Sigma), 1X P/S (GIBCO), 2mM Glutamax (GIBCO), 10% FBS, Forskolin (5uM; LKT), bFGF (10ng/mL; R&D Systems), PDGF-AA (5ng/mL; Millipore, UK), Her-β1 (200ng/mL; Biolegend). |

Table 2.5. Schwann cell differentiation with Dezawa's protocol.

2.7. Schwann cell differentiation of hDPCs by dcAMP induction.

Schwann cell differentiation was attempted using a protocol by Studer's group (2007⁹⁷) which induces the cAMP cascade by addition of dcAMP. The cultures were detached by TE 1:10 (20% FBS) or TE 1:80 (OSCFM and BMP4) and seeded at 8000 cells/cm² in the Schwann cell differentiation medium for 2 weeks (Fig. 2.4 and table 2.6):

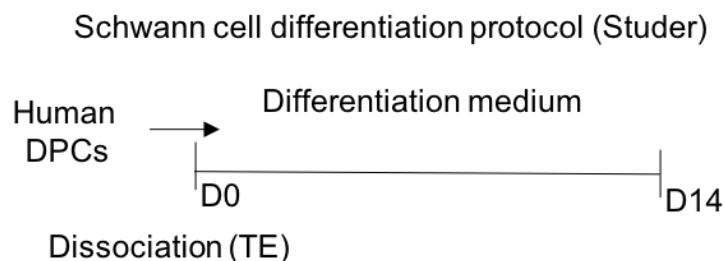


Fig 2.4. Schwann cell differentiation with Studer's protocol flow chart. Human dental pulp cells in their basal conditions (FBS, OSCFM or BMP4) were dissociated with trypsin-EDTA (TE) and treated with Schwann cell differentiation medium (Studer) for 14 days (D0-D14).

| Medium | Basal Conditions |
|-------------------------------------|---|
| Schwann cell medium (Studer) D0-D14 | DFNB, 1X P/S, NGF (10ng/mL; R&D Systems), GDNF (10ng/mL; R&D Systems), dcAMP (1mM; Trocis), CNTF (10ng/mL; R&D Systems), Neuregulin (20ng/mL; R&D Systems). |

Table 2.6. Schwann cell differentiation with Studer's protocol.

2.8. Generation of neural progenitors from mouse and human dental pulp cells.

Human dental pulp cells and mouse dental pulp cells were detached by TE1:10 (hDPC-FBS and mDPC/mDPPSCs) and TE 1:80 (hDPC-OSCFM and hDPC-BMP4) and seeded at high density 10,000-20,000 cells/cm² in 2.5µg/cm² laminin coated dishes in the respective inductive medium (details below). The cells were transferred to laminin (Cultrex) coated dishes (2.5µg/cm²) in the respective media treatment:

Treatments for human dental pulp otic neural progenitors:

Untreated control (CTL) 20% FBS, basal medium control (DFNB), DFNB + 6-bromoindirubin-3'-oxime (BIO) + BMP4 (DFNB BB), FGF3/FGF10, OSCFM, OSCFM + BIO + BMP4 (OSCFM BB; table 2.7).

| Medium | Conditions |
|--------------|--|
| 20% FBS | DMEM, 1x P/S, 2mM Glutamax (GIBCO), 100µM Ascorbic Acid (Sigma), 10%, 15% or 20% foetal bovine serum (FBS; GIBCO). No coating. |
| DFNB | DMEM:F12 (GIBCO), 1% N2 (GIBCO), 2% B27 (GIBCO), 1x P/S. |
| OSCFM | DFNB (DMEM:F12 (GIBCO), 1% N2 (GIBCO), 2% B27 (GIBCO)), 1x P/S (SIGMA), 20ng/mL bFGF (R&D Systems), 50ng/mL IGF (R&D Systems), 20ng/mL EGF (R&D Systems). Coated with mouse laminin (2.5ug/cm ² ; Cultrex). |
| OSCFM BB | OSCFM + 10ng/mL BMP4 (R&D) + BIO 0.75µM (Sigma), 1x P/S |
| FGF 3/ FGF10 | DFNB + 10ng/mL FGF3 (R&D) + FGF10 (R&D). |
| DFNB BB | DFNB + 10ng/mL BMP4 (R&D) + BIO 0.75µM (Sigma), 1x P/S |

Table 2.7. Treatments used to generate otic neural progenitors from hDPC.

Treatments for mouse dental pulp neural progenitors

-Untreated controls (20FBS/PSCM), OSCFM, OSCFM + Valproic Acid (VPA), OSCFM + BIO (6-bromoindirubin-3'-oxime; BIO; Sigma), OSCFM + BIO+BMP4 (B+B; Table 2.8).

| Medium | Conditions |
|--------|--|
| DFNB | DMEM:F12 (GIBCO), 1% N2 (GIBCO), 2% B27 (GIBCO), 1x P/S. |

| | |
|----------|--|
| OSCFM | DFNB (DMEM:F12 (GIBCO), 1% N2 (GIBCO), 2% B27 (GIBCO)), 1x P/S (SIGMA), 20ng/mL bFGF (R&D Systems), 50ng/mL IGF (R&D Systems), 20ng/mL EGF (R&D Systems). Coated with mouse laminin (2.5ug/cm ² ; Cultrex). |
| VPA | OSCFM + valproic Acid 1mM (Tocris), 1x P/S. |
| BIO | OSCFM, BIO 0.75μm (Sigma), 1X P/S. |
| BIO+BMP4 | OSCFM + 10ng/mL BMP4 (R&D) + BIO 0.75μm (Sigma), 1x P/S. |

Table 2.8. Treatments to generate neural progenitors from mouse dental pulp cells.

2.9. Gerbil Cochlear explants co-culture.

Gerbil pups, aged 3-10 days (P4-10) were treated in accordance with the schedule 1 procedures of the animal (scientific procedures) act 1986. Cochlear explants were dissected as described by Parker et al. (2010⁹⁸). Cochlea were removed from the ear and dissected in DMEM-P/S. The cochlea was firmly grabbed from the basal region while the organ was uncoiled from the apical region using fine tweezers. Once uncoiled, further dissection was done by removing the spiral ligament and nerves along the Organ of Corti. The remaining hair cell layers were then transferred in 150uL of explant medium to a glass-bottom 35mm (Ibidi) dish previously coated with 0.1% Poly-L-ornithine (Room temperature, >8H; Sigma), 2.5μg/cm² Laminin (37C, >8H). The following day the explant medium was removed and the neurospheres grown for 6-8 days were added together with 200uL of co-culture medium. 1mL of co-culture medium was added every second day until day 7 or 10 (Table 2.9 for media specification).

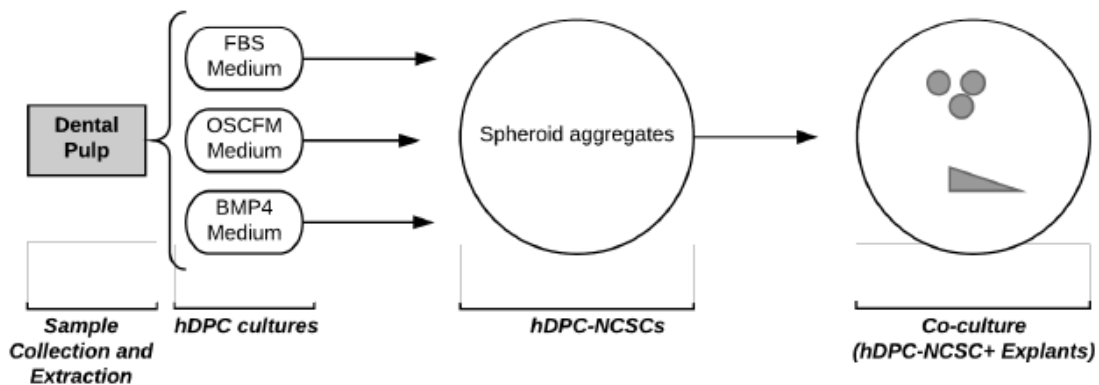


Figure 2.5 Overall work flow of culture establishment, neurosphere formation and co-culture setup. hDPC: Human dental pulp cells, NCSCs: Neural crest-derived stem cells.

| Medium | Basal Conditions |
|-------------------|--|
| Explant medium | DFNB, 10%FBS, 100µg/mL Ampicillin. |
| Co-culture medium | DFNB, 100µg/mL Ampicillin, 50ng/mL NT3 (Peprotech) and 50ng/mL BDNF (Peprotech). |

Table 2.9. Ex-vivo assay media.

2.10. Human dental pulp tissue sectioning

Teeth were collected, and dental pulp was exposed as described in section 2.1. After mechanically exposing the dental pulp using the mallet, the split teeth were then submerged in Zamboni's fixative as described below. After fixing, the dental pulp was carefully removed from the chamber and transferred to a sucrose gradient of 7.5%, 15%, 22%, 30% and Optimal Cutting Temperature solution (OCT) for 12H-24H each at 4C. The tissue was then positioned in OCT and fast frozen on a dry ice/methyl-butane bath. Cryosectioning was then performed in a Bright OTF5000 cryostat. Sections of 10-15µm thickness were collected on gelatin-coated slides.

2.11. Immunocytochemistry (ICC) and immunohistochemistry (IHC).

2.11.1. Fixing

Cell cultures and monoculture experiments were grown on either flasks or well plates. For culture characterisation and sphere aggregates, the medium was removed, and the cells washed two times with PBS. Paraformaldehyde (PFA) 4% was added for 10-15 minutes. For differentiated cells (neural or glial) and co-cultures, Methanol-free PFA 16% (Alfa Aestar) was added directly to the medium to a 4% final concentration and left for 10-15 minutes. For human dental pulp tissue, fixation was achieved by using Zamboni's fixative (4%PFA, 0.2% Picric Acid in 0.1M phosphate buffer, pH 7.4) for 24H. The fixative was washed thoroughly with PBS and processed as described above.

2.11.2. Labelling

After fixation, PFA was then removed and the cells washed with PBS before labelling. Cells were washed two times with PBS + 0.1% Triton (PBST) for 10 minutes and blocked for 1 hour with 5% donkey serum-PBST (Blocking solution). After blocking, washing was done two

times with PBST for 10 minutes each. Primary antibodies diluted in blocking solution were then added according to the table 2.10 and left overnight at 4C.

The following day cells were washed two times for 10 minutes each with PBST and the secondary antibodies, diluted in blocking solutions added for 1 hour. After secondary antibody incubation, cells were washed two times for 10 minutes each using PBST before being incubated in 4', 6-Diamidino-2Phenylindole, Digydrochloride (DAPI; 1:100 in PBS) for 10 minutes. Finally, cells were washed two times in PBST for 10 minutes and two PBS washes for ten minutes. For sections, slides were cover-slipped using fluoroshield (Sigma) and sealed with nail polish. The labelled samples (dishes or slides) were stored in the dark at 4C in PBS and imaged within 4 weeks of staining.

| Type | Antibody | Manufacturer | Dilution |
|---------------------------|--|---------------------------|----------|
| Neural markers | aRBT-NF200 (Neurofilament 200) | Sigma N4142 | 1:100 |
| | aRBT-PER (Peripherin) | Millipore AB1530 | 1:100 |
| | aMSE-SYP (Synaptophysin) | Santa Cruz (D-4) SC17750 | 1:100 |
| | MSE-TUJ1 (Neuron-specific Class III β Tubulin) | Biologend 801202 | 1:100 |
| | aRBT-Tau | Santa Cruz (H-150) 5587 | 1:100 |
| | aGoat-NaKATPase α 3 (NKA α 3) | Santa Cruz 16052 | 1:75 |
| | aRBT-GLUTR2 (Glutamate receptor 2) | PA1598 Boster biological | 1:100 |
| Neural progenitor markers | aMSE-TLX3 (T-cell leukaemia Homeobox 3) | Santa Cruz SC514691 | 1:100 |
| | aMSE-Brn3a (Brain specific homeobox domain protein 3a) | Santa Cruz SC6429 | 1:100 |
| | aMSE-ASCL1 (Achaete-scute homolog 1) | Santa Cruz (G-7) 390794 | 1:100 |
| | aGoat-NeuroD1 (Neuronal differentiation 1) | Santa Cruz SC1084 | 1:100 |
| | aRBT-SOX2 (sex determining region Y-box2) | Millipore AB5603 | 1:100 |
| | aRBT-GLI1 (Glioma associated oncogene homolog) | Novus NBP2-78259 | 1:100 |
| Neural crest Markers | aMSE-AP2a (activating enhancer binding protein 2 alpha) | Santa Cruz SC12726 | 1:100 |
| | aMSE-NESTIN | Santa Cruz (10c2) 23927 | 1:100 |
| | aMSE-P75 (Nerve growth factor receptor) | CSCB ME 20.4 | 1:10 |
| | aMSE-SLUG (Snail family transcriptional repressor 2) | Santa Cruz (A-7) SC166476 | 1:100 |
| | aMSE- SNAI (SNAIL1)-(Snail family transcriptional repressor 1) | Santa Cruz (G-7) SC271977 | 1:100 |
| | aRBT-P0 (Myelin protein 0) | Millipore ABN363 | 1:100 |
| | aRBT-SOX9 (SRY-BOX9) | Millipore AB5535 | 1:100 |
| | aGoat-SOX10 (SRY-BOX10) | Santa Cruz SC17342 | 1:100 |
| | aMse PAX7 (Pair box 7) | DSHB | 1:10 |
| Glial Markers | aRBT-GFAP (Glial fibrillary acidic protein) | E18320 Spring bioscience | 1:100 |
| | aMSE-MBP (Myelin binding protein) | Millipore AB62631 | 1:100 |
| | aMSE-S100B (S100 calcium-binding protein B) | Sigma 52657 | 1:100 |
| | aMSE-GFAP (Glial fibrillary acidic protein) | Biologend 644701 | 1:100 |
| | aMSE-STRO-1 | R&D MAB1038 | 1:100 |

| | | | |
|------------------------------|---|-----------------------------|-------|
| Mesenchymal stem cell marker | aRBT-CELSR1 (Cadherin family member 9) | Santa Cruz (E-3) SC-514376 | 1:100 |
| Hair cell marker | aRBT-MYO7a (Myosin 7a) | Proteus Biosciences 25-6790 | 1:100 |
| | aMse-CtBp2 (Ribeye-C-terminal binding protein) | Biologend 612044 | 1:100 |
| Human Mitochondria marker | aRBT-CLPP (Caseinolytic protease proteolytic subunit) | Genetex Gtx104656 | 1:100 |
| | aMSE-hMIT (Human mitochondria) | Novus NBP2-32980 | 1:100 |
| Other | aRBT-GFP (green fluorescent protein) | Torrey Pines Biolab TP401 | 1:100 |
| | aMse-EPCAM (Epithelial cell adhesion molecule) | Millipore AB7504 | 1:100 |
| Secondary ab | DNKaMSE-Alexa 488 | Invitrogen A21202 | 1:250 |
| | DNKaRBT-Alexa 568 | Invitrogen A10042 | 1:250 |
| | DNKaGoat-Alexa 568 | Invitrogen A11057 | 1:250 |
| | DNKaMSE-Alexa 568 | Invitrogen A10037 | 1:250 |
| | DNKaGoat-Alexa 488 | Invitrogen A11055 | 1:250 |
| | DNKaRBT-Alexa 488 | Invitrogen A21206 | 1:250 |
| | DNKaGoat-650 | Dylight (101D5) | 1:100 |

Table 2.10. List of primary and secondary antibodies.

2.12. Direct reprogramming of human dental pulp cells with EGFP, NeuroD1 and ASCL1: Plasmid Isolation

Human dental pulp cells growing under basal conditions (FBS, OSCFM or BMP4) were used for transfection and direct reprogramming (Chapter 4). The plasmids containing EGFP, NEUROD1 and ASCL1 were acquired from Addgene (NeuroD1-TetO-FUW, Ascl1-TetO-FUW and TetO-FUW-EGFP; Vierbuchen et al., 2010). Transformed bacteria containing the vectors were grown in liquid LB-Broth (Sigma) medium with Ampicillin overnight at 37C, 200rpm. Plasmid extraction was achieved by using plasmid minikit (Qiagen) according to the manufacturer instructions. To identify proper plasmid isolation, the inserted fragments were digested from the plasmid accordingly to the EcoR1 restriction site flanking the sequence (Biolabs). Digestion was done for 1H 37C and the result was revealed by agarose gel electrophoresis (1.5%; Sigma).

2.13. Direct reprogramming of human dental pulp cells with EGFP, NeuroD1 and ASCL1: Human dental pulp cells transfection

After cell detachment and dissociation with respective Trypsin-EDTA solutions, cells were passed through a 100µm strainer. 200,000 cells were counted and washed with PBS and re-

suspended in 100uL transfection buffer (Mirus). 4mm electroporation cuvettes (VWR) were used for transfection at 150V, 3 pulses. The electroporated cells were re-suspended in the respective medium. Cell viability was calculated using trypan blue and manual or automated cell count.

2.14. Fluorescence activated cell sorting (FACS)

Cell cultures were suspended in 2% FBS-PBS after their respective TE treatment. The primary antibody was added (concentration in Table 2.7) and incubated for an hour at 4C while rocking. The secondary antibody Alexa Fluor 488 was added and incubated for another hour. The cells were then washed once with PBS to remove the excess of antibody. The negative control was incubated only with the secondary antibody. The FACS was performed in The BD FACSJazz™ by the facility manager Dr. Mark Jones or the postdoctoral researcher Dr. Ae-Ri Ji. More details in the following chapters.

2.15. Live cell tracking in ex-vivo assays using Boron-dipyrromethene (Bodipy) staining.

Sphere aggregates were washed once with PBS and then re-suspended in sphere medium with 20µM of Bodipy green cell tracker (Thermo Fisher Scientific) for 30 minutes and left in incubator (37°C). The cells were washed twice with PBS and seeded in the experiment.

2.16. Microscopy

For fluorescence microscopy, the EVOS cell imaging system and the InCell Analyser microscopes were used. Confocal imaging was performed at the Wolfson Light Microscopy facility, using the Nikon A1 confocal microscope. For proper comparison, the same intensity and exposure were used in groups directly compared (i.e. same antibody across different treatments).

2.17. RNA Extraction

Extraction of RNA was done using the Qiagen microkit or minikit depending on cell yields. The protocol was followed according to the manufacturer instructions. RNA quantification was performed using the Nanodrop™ Spectrophotometer.

2.18. cDNA Synthesis

cDNA synthesis from RNA was performed with the ThermoFisher Superscript IV retro transcriptase. Briefly, 500ng of RNA were taken and cDNA synthesis was carried out using OligoDT primers and Random primers (Promega) according to the manufacturer instructions. The synthesis was carried out in an automated thermal cycler (Eppendorf).

2.19. End point polymerase chain reaction (PCR)

PCR was done following the GoTaq® G2 flexi DNA polymerase (Promega, UK) according to the manufacturer instructions. The PCR reaction was carried out in the Eppendorf MasterCycler thermal cycler with the following program: Initial denaturation for 2 minutes at 94°C, followed by 40 cycles of 94°C-15 seconds/ annealing temperature-30 seconds / 72°C-30 seconds, and a final extension phase for 5 minutes at 72°C. The specific annealing temperatures for each primer are specified in table 2.11 and 2.12.

| Gene | Forward 5'-3' | Reverse 5'-3' | Tm |
|-----------------|---------------------------|-----------------------------|------|
| <i>Gapdh</i> | GGGAAGCCATCACCATCT | GCCTCACCCATTGATGTT | 60°C |
| <i>Sox2</i> | ggcagctacagcatgatgcaggagc | ctggtcatggagttgtactgcagg | 67°C |
| <i>Sox10</i> | CAGCCACGAGGTAATGTCCAA | GTGTAGGCGATCTGGGAAGG | 60°C |
| <i>Gli1</i> | GAAGGAATTCGTGTGCCATT | GCAACCTTCTTGCTCACACA | 57°C |
| <i>p75</i> | GAGGCACCGTGACAACCT | CAGGCCTCGTGGGTAAAGG | 61°C |
| <i>Gata3</i> | CGAGATGGTACCGGGCACTA | GACAGTTCGCGCAGGATGT | 60°C |
| <i>Gap43</i> | ACCACCATGCTGTGCTGTATGA | CCTTATGAGCCTATCCTCCGG | 60°C |
| <i>Nfn</i> | CGTAAACACGCGTCTAAAACTG | GAGTACACCTGGCGTGTT | 60°C |
| <i>Brn3a</i> | AGGCCTATTTGCCGTACAACC | CTCCTCAGTAAGTGGCAGAGAATTCAT | 62°C |
| <i>TubIII</i> | ACGCATCTCGGAGCAGTT | CGGACACCAGGTCATTCA | 61°C |
| <i>Pax7</i> | ACCTACAGCACCCTGGCTA | TTGGCCAGGTAATCAACAGCA | 60°C |
| <i>eGFP</i> | AAGCTGACCCTGAAGTTCATCTGC | CTTGTAGTTGCCGTCGTCCTTGAA | 60°C |
| <i>Synapsin</i> | AGCTCAACAAATCCCAGTCTCT | CGGATGGTCTCAGCTTTCAC | 59°C |
| <i>Vglut1</i> | GTGCAATGACCAAGCACAAG | AGATGACACCGCCGTAGTG | 59°C |

Table 2.11. List of mouse primers.

| Gene | Forward 5'-3' | Reverse 5'-3' | Tm |
|---------------|---------------------------|------------------------|-------|
| <i>RPLPO</i> | GAAGGCTGTGGTGTGATGG | CCGGATATGAGGCAGCAGTT | 58°C |
| <i>SOX10</i> | ACCGCACACCTTGGGACACG | CAACGCCACCTCCTCGGAC | 58 °C |
| <i>OCT4</i> | AGCGAACCAGTATCGAGAAC | TTACAGAACCACACTCGGAC | 55 °C |
| <i>NESTIN</i> | TCCAGGAACGGAAAATCAAG | GCCTCCTCATCCCCTACTTC | 57 °C |
| <i>SOX9</i> | GACGCTGGGCAAGCTCTGGAGACTT | TTCTTCACCGACTTCTCCGCCG | 64 °C |
| <i>P75</i> | TCATCCCTGTCTATTGCTCCA | TGTTCTGCTTGCAGCTGTTC | 58°C |

Table 2.12. List of human primers.

2.20. Quantitative polymerase chain reaction (RT-qPCR)

Real time PCR was performed with Taqman probes (Table 2.13). The master-mix, assays and water volumes were used according to the manufacturer concentrations in a final volume of 7.5µL per reaction. All reactions were carried out in four technical replicates in 384 well plates (Alpha laboratories). The Thermofishers QuantStudio™ 12k Flex Real time PCR system was used for detection and quantification.

| Gene | Expression Assay |
|---------------------|------------------|
| Sox2 | Hs00602736_s1 |
| Oct4 | Hs04260367_gH |
| Nanog | Hs02387400_g1 |
| Ecadherin (ECAD) | Hs01023895_m1 |
| Sox10 | Hs00366918_m1 |
| p75 | Hs00609976_m1 |
| Brn3a | Hs00366711_m1 |
| Vglut1 | Hs00220404_m1 |
| Gata3 | Hs00231122_m1 |
| Synaptophysin (SYP) | Hs00300531_m1 |

| | |
|----------------|---------------|
| Synapsin (SYN) | Hs00199577_m1 |
| Rlplo | Hs00420895_gH |
| Pax8 | Hs01015257_g1 |
| FoxG1 | Hs01850784_s1 |
| GFAP | Hs00902901_m1 |
| S100B | Hs00902901_m1 |
| MBP | Hs00921945_m1 |
| p0 | Hs00559329_m1 |
| Sox9 | Hs01001343_g1 |
| Nestin | Hs04187831_g1 |
| Ascl1 | Hs00269932_m1 |
| GFP | Mr03989638_m1 |
| NeuroD1 | Hs01922995_m1 |
| Snai1 | Hs00195591_m1 |
| B3GAT1 (HNK-1) | Hs00218629_m1 |
| TFAP2A (AP2a) | Hs01029413_m1 |

Table 2.13. List of Taqman assays.

2.21. Statistical analysis

Statistical analysis utilised was One-way-ANOVA followed by Tukey test or Sidaks test for pair-wise comparison. For comparison between two groups a Student T-Test. All the analysis was performed using GraphPad Prism 7. N number in the figures can refer to independent cultures (cultures established from different patients) or technical replicates (calculations obtained from the same experiment) as described in figure legends.

RESULTS

CHAPTER 3

“Characterisation of dental pulp cell cultures from mice for auditory nerve regeneration”

3. Characterisation of dental pulp cell cultures from mice for auditory nerve regeneration.

Stem cells are located in specific niches in many of organs and allow to maintain tissue homeostasis by replenishing old or death cells during aging and repair. In the mouse incisors, stem cells play a constant role in repair and regeneration due to the continuous tooth growth present in these animals throughout their life spans⁹⁹⁻¹⁰². *In vitro*, some studies have characterised the mouse dental pulp cells and identified neurogenic properties, proposing their use in nerve regeneration^{52,103}. Thus, we decided to test the potential of using mouse dental pulp stem cells to regenerate the auditory neurons that are lost during deafness. In this chapter, we aimed to establish mouse dental pulp cultures and to test their differentiation into auditory-like cell progenitors and neurons.

3.1. Establishment of dental pulp cell culture conditions

Mouse's dental pulp cell cultures are not commonly used in literature in comparison to human dental pulp cells. Therefore, few culture establishment protocols were described at the beginning of this research project. As a consequence, we first explored different conditions to establish mouse dental pulp cell cultures. We tested culture different media (FBS vs PSCM, see below and methods), two age ranges (8-10d and 4-6w) and different types of teeth (Incisors and molars). A summary of the different dental pulp cell cultures is depicted in table 3.1.

| Culture label | Age | Medium | Max Passage | # of Mice used per culture |
|----------------|-----|--------|-------------|----------------------------|
| mDPC B Incisor | --- | 10FBS | 1 | 1 |
| mDPC C Incisor | 2m | 10FBS | 1 | 2 |
| mDPC D Incisor | 5m | 10FBS | 1 | 1 |
| mDPC E Incisor | 5m | 10FBS | 2 | 1 |
| mDPC F Incisor | -- | 10FBS | 1 | 1 |
| mDPC F Incisor | --- | 15FBS | 3 | 1 |
| mDPC G Incisor | 4w | 20FBS | 6 | 4 |
| mDPC H Incisor | 10d | 20FBS | 11 | 4 |
| mDPC I Molar | 10d | 20FBS | 6 | 4 |
| mDPC 3 Incisor | 4w | 20FBS | 4 | 5 |
| mDPC 3 Molar | 4w | 20FBS | 1 | 5 |
| mDPC2 Incisor | 9d | 20FBS | 5 | 5 |

| | | | | |
|-----------------|----|-------|----|---|
| mDPC2 Molar | 9d | 20FBS | 1 | 5 |
| mDPPSC1 Incisor | 6w | PSCM | 8 | 5 |
| mDPPSC1 Molar | 6w | PSCM | 2 | 5 |
| mDPPSC2 Incisor | 8d | PSCM | 6 | 4 |
| mDPPSC2 Molar | 8d | PSCM | 6 | 4 |
| mDPPSC3 Incisor | 5w | PSCM | 10 | 3 |
| mDPPSC4 Incisor | 9d | PSCM | 3 | 5 |
| mDPPSC4 Molar | 9d | PSCM | 1 | 5 |
| mDPPSC5 Incisor | 4w | PSCM | 4 | 5 |
| mDPPSC5 Molar | 4w | PSCM | 3 | 5 |

Table 3.1. Summary of dental pulp cultures. mDPC: cultures containing FBS (10%, 15% or 20%). mDPPSC: cultures established in "pluripotent stem cell medium" (PSCM). Animal age in days (d), weeks (w) or months (m).

We asked if sufficient cells for mouse cultures could be obtained from only one animal or from pooling cells from several animals. Hence, we compared obtaining cells from the incisors of one animal growing in 10% FBS-DMEM (10FBS) or from 3 to 5 animals growing in 20% FBS-DMEM (20FBS). None of the 5 culture attempts from 10FBS worked to establish proliferating dental pulp cell cultures, not being able to survive continuous passaging. In contrast, 20FBS cultures reached confluence easier and survive passaging better, as suggested by the maximum passage number reached by the independent cultures (Table 3.1). Therefore, using 20% FBS and 3-5 animals resulted in yielding high cell numbers consistently.

We also tested different mice age (8-10d or older than 4 weeks) as well as teeth type (molars or incisors). The final decision of using incisors from older animals (>4 weeks) was based on the practicality of extracting the tissue from older mice with larger sized teeth.

As a parallel condition, we tested a "pluripotent stem cell medium" (PSCM; Atari, et al., 2012⁸⁷). It was theorised that the use of this medium could result in the selection of a pluripotent-like cell population (details below). In terms of maximum passage reached, PSCM was similar to the use of 20FBS (Table 3.1). Therefore, we selected the cells grown in PSCM (hereby termed dental pulp pluripotent stem cells or "mDPPSCs", by convention) and in 20FBS (hereby termed dental pulp cells or "mDPCs") for further experiments.

3.2. Morphological characterisation of mouse dental pulp cells.

Once culture conditions were defined, the morphological and molecular traits of cultured cells were investigated. Dental pulp cultures showed a very heterogeneous composition. Initially, cells recently established (passage 0) presented colony-like aggregates surrounded by other cell types; this feature was shown regardless of the culture type (i.e. molar vs incisor, P10 vs 6w teeth or 20FBS vs PSCM) as seen in figure 3.1.

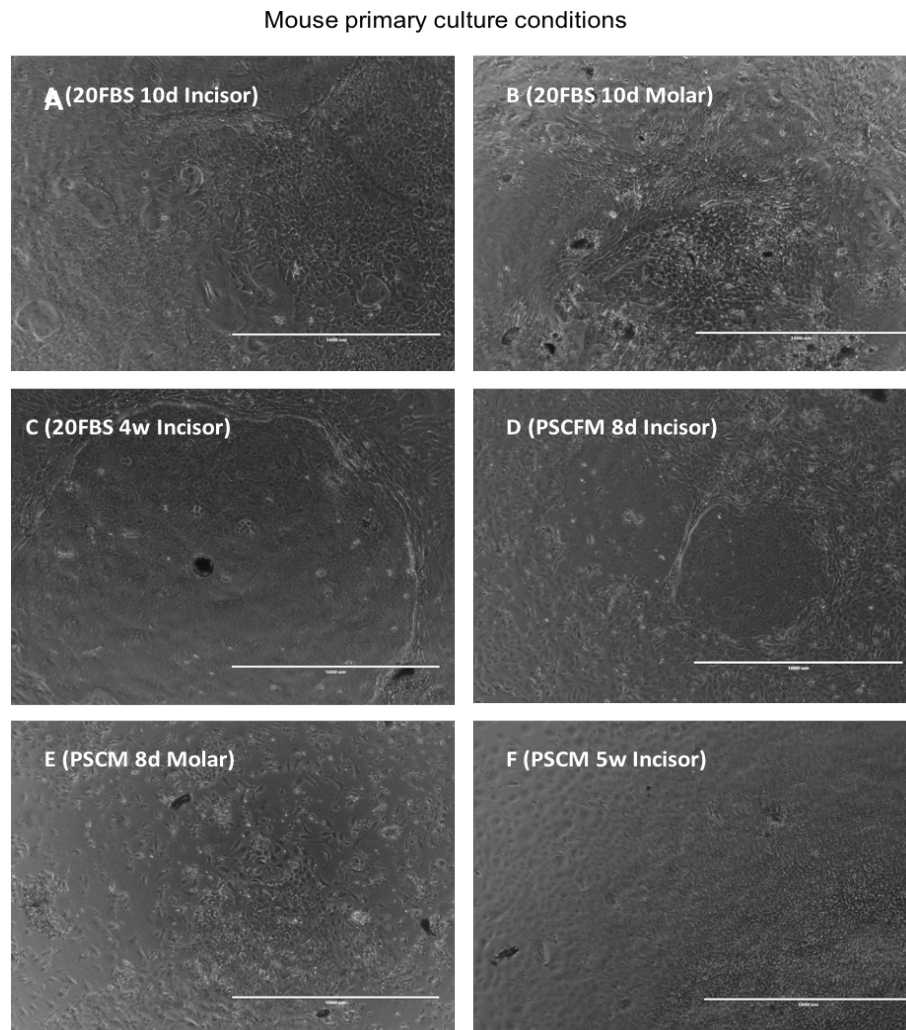


Figure 3.1. Mouse primary cultures. Different cell morphology, growth pattern or colonies observed in newly established primary cultures (Passage 0). Dental pulp tissue from mice molars and incisors were cultured in medium containing 20% FBS (20FBS; mDPC) or in “Pluripotent stem cell medium” (PSCM; mDPPSCs). Samples were taken from young mice (8-10-day-old) or older mice (>4 weeks). A) 20FBS P10 Incisor, B) 20FBS P10 Molar, C) 20FBS 4W Incisor, D) PSCM P8 Incisor, E) PSCM P8 Molar, F) PSCM 5W Incisor. Scale bar: 1000 μ m.

Cells were passaged at a density of between 10,000 and 15,000 cells/cm² during culture maintenance, commonly reaching confluence within a week in early passages (P1-4).

Passaging influenced the composition of the cultures, changing in morphology and the defined colonies observed at passage 0 disappeared (Fig. 3.2).

Aspect of mouse dental pulp cultures

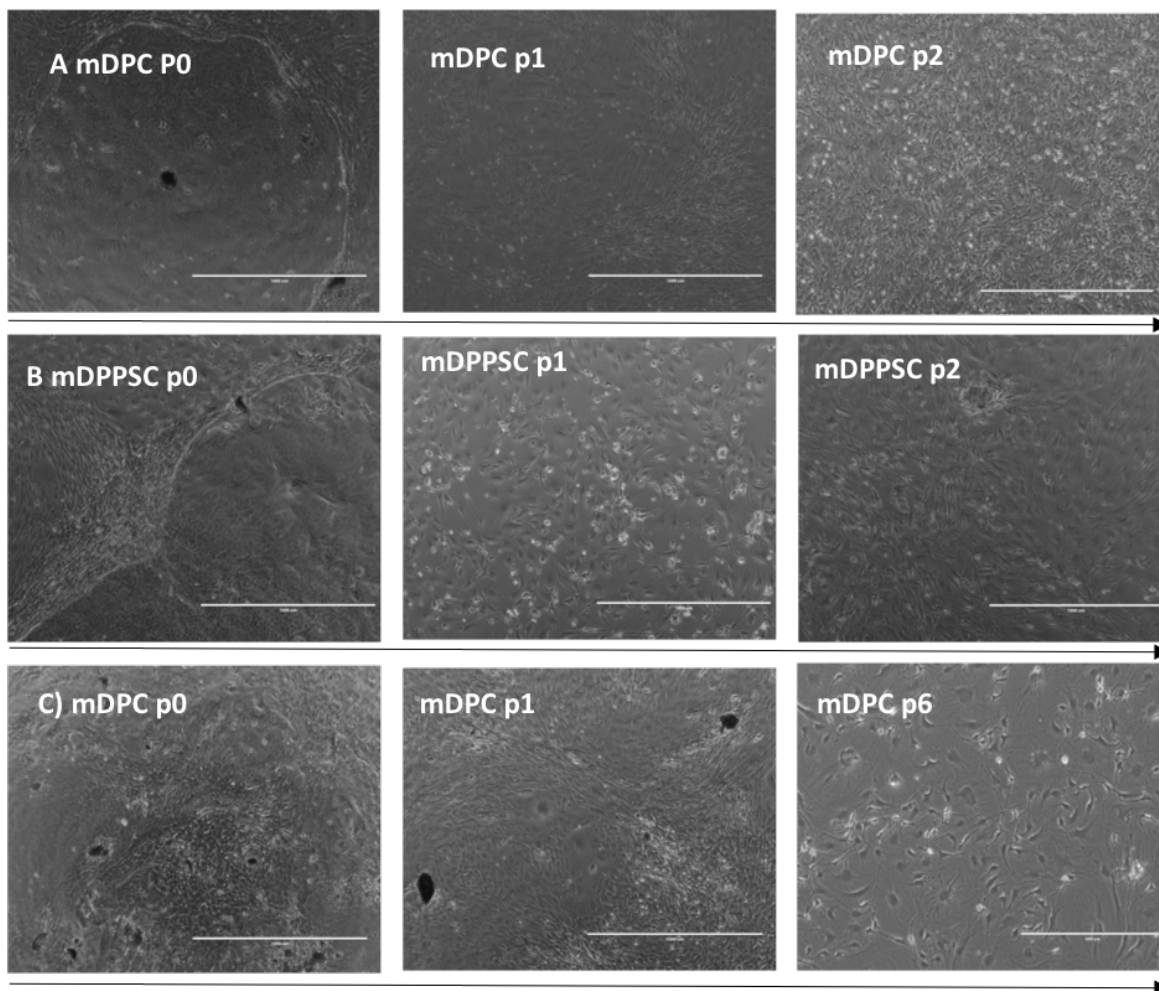


Figure 3.2. Mouse dental pulp cultures and passaging. The morphology of cultures established in 20FBS (mDPCs) and PSCM (mDPPSCs) is shown at different passage number (p; ascendant from left to right) from: A) mDPC incisors at P0, P1 and P2, B) mDPPSC incisors at P0, P1, and P2, and C) mDPC molars at p0, p1 and p6. Scale bar: 1000 μ m.

3.3. Mouse dental pulp cultures molecular characterisation.

Next, we wanted to establish the molecular profile of these mouse dental pulp cultures. We evaluated the expression of neural crest/neural progenitor (NC/NP) related genes

by conventional RT-PCR on different mouse dental pulp cultures. The analysis revealed that mDPCs and mDPPSC expressed *Gli1*, *Gata3*, *Sox2* (Neural progenitor-related), *Sox10* and *p75* (Neural crest-related-Fig. 3.3). The consistent expression of *Sox10* and *p75* suggests the presence of a putative cell population within the culture with neural crest-like resemblance, regardless of the initial medium condition (20FBS vs PSCM). The presence of these markers by RT-PCR was also present in the dental pulp tissue. The neuralised mouse neuroblastoma N2a cell line was used as a control of positive expression.

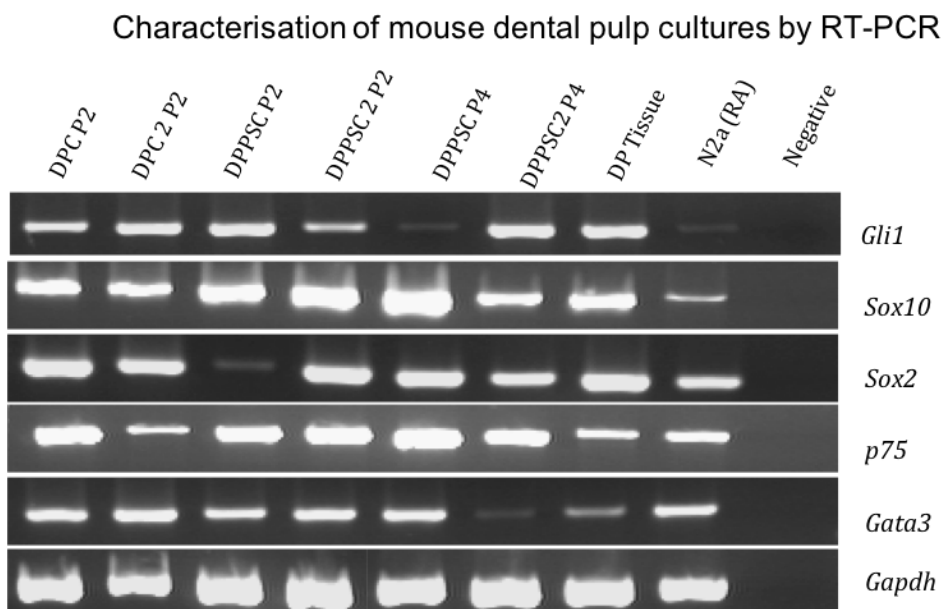


Figure 3.3. Gene expression of NP/NCSC genes in mDPCs and mDPPSCs. Electrophoresis gel of RT-PCR products of relevant markers expressed in Dental pulp cells in 20FBS (mDPCs) and Dental pulp pluripotent stem cell (mDPPSCs).

Characterisation of other neural crest- or neural progenitor-related markers was done by immunocytochemistry (ICC). Characterization of the different cultures was performed for GLI1, SOX10, SOX2 and PAX2 was also included as a neural progenitor marker. Both mDPC and mDPPSC cultures were highly positive for these markers (Fig. 3.4 and Fig. 3.5). The quantification of marker-positive cells for both culture conditions revealed that over 90% of the cells within the culture were positive for all markers, except for SOX10 (Fig. 3.6). SOX10 expression among our cultures presented the greatest variation and usually had the

weakest fluorescent signal, which affected counting. Nevertheless, morphologically the cultures were heterogeneous, manifested also by the different sized nuclei, visible in the DAPI staining. There were no significant differences ($p>0.05$) in the total percentage of positive cells between the mDPC and mDPPSC cultures. However, the pattern of GLI1 staining appeared slightly different in some cases. In particular, GLI1 was restricted to the nuclei in mDPC, whereas in mDPPSC it was also present adjacent to the nucleus. OCT4 was not present in either mDPC or mDPPSC by RT-PCR and ICC, suggesting a lack of truly pluripotent cells within cultures.

Overall, the molecular characterisation showed that the cultures presented markers that are related to neural crest and neural progenitor cells, suggesting the presence of these population(s) in the cultures.

Mouse Dental Pulp Cells (mDPC) characterisation by ICC

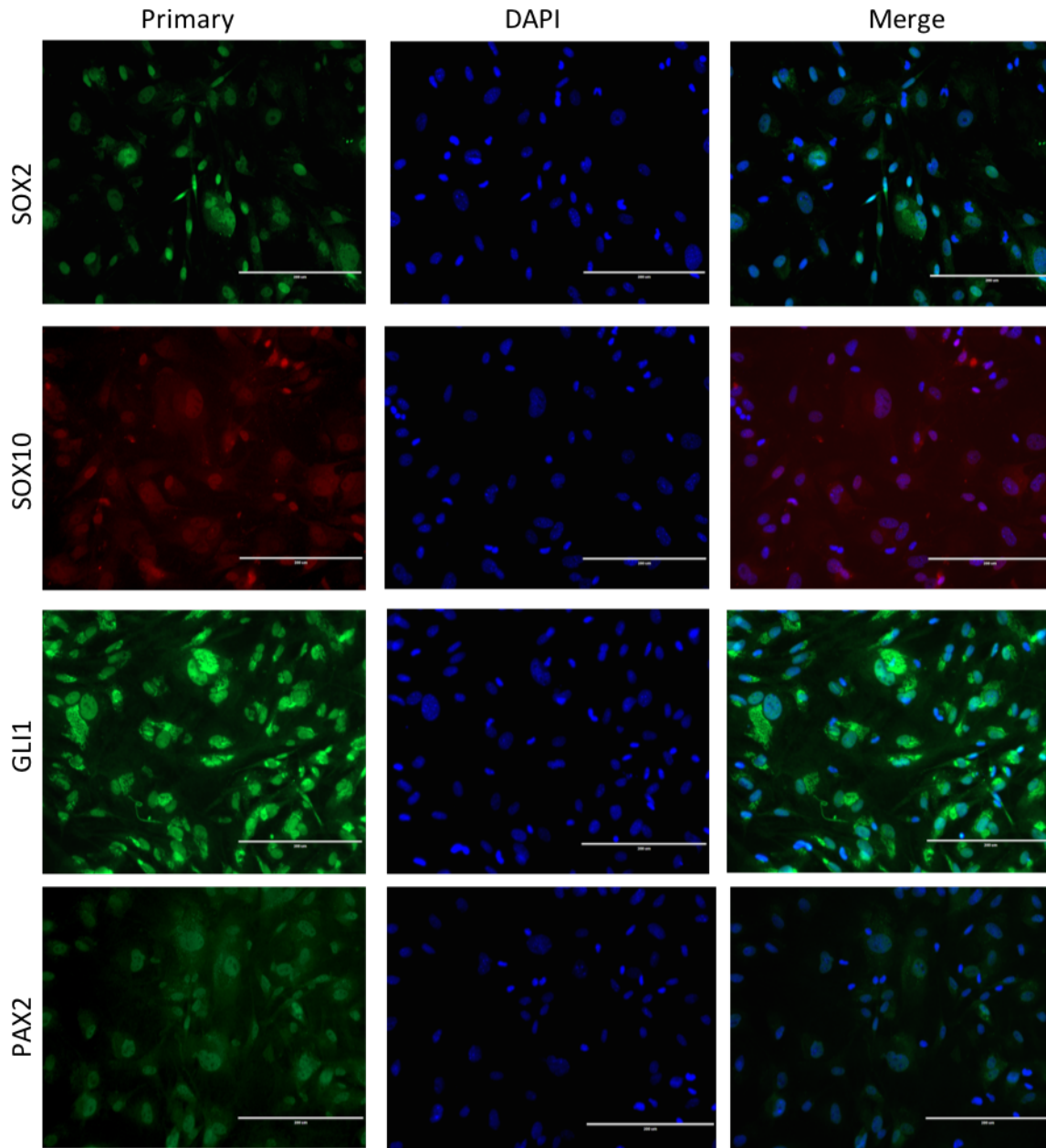


Figure 3.4. mDPC characterisation. Immunocytochemistry (ICC) of markers expressed in dental pulp cells from incisors grown in 20% FBS (mDPC). Scale bar: 200 μ m.

Mouse Dental Pulp Pluripotent Cells (mDPPC) characterisation by ICC

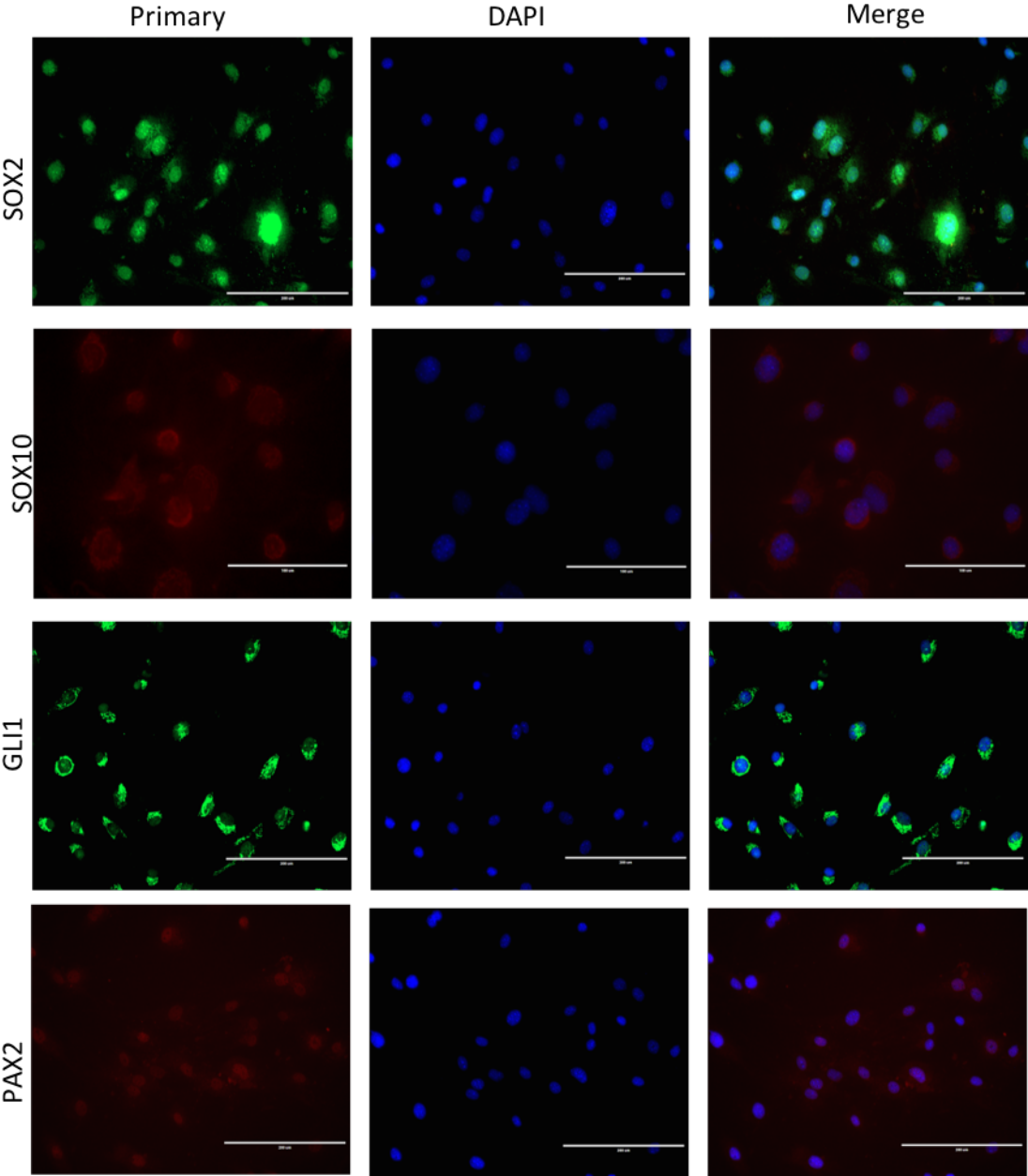


Figure 3.5. mDPPSC characterisation. ICC of markers expressed in dental pulp cells from incisors grown in PSCM (mDPPSCs). Scale bar: 200µm; SOX10 Scale bar: 100µm.

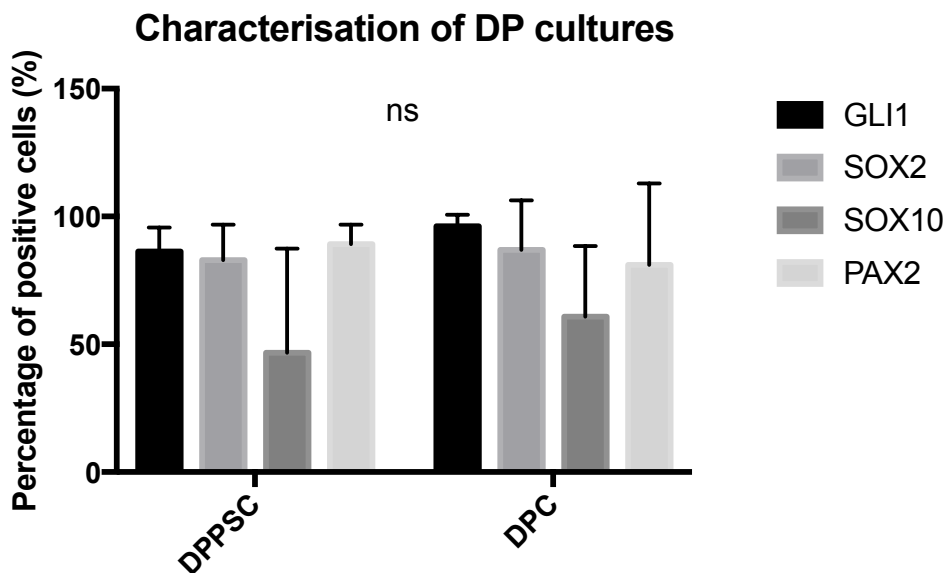


Figure 3.6. Quantification of positive cells by ICC. Cultures positive for a fluorescent signal were counted from at least 5 fields each. The percentage of positive cells for a given marker was determined from the total cell count. Non-significant differences were found ($p>0.05$). $n= 3$ independent experiments.

3.4. Spontaneous neurogenic potential of mouse dental pulp cells

After careful examination of the molecular signature of both DP cultures, a profile that resembled a neural progenitor or neural crest stem cell population was identified. Thus, it was necessary to examine the potential to differentiate into neural-like cells.

A phenomenon of spontaneous neural-like differentiation was observed in 2 independent mDPC cultures and one mDPPSC culture that were maintained for more than 35d without passaging. This further supports the neurogenic nature of the cultures as indicated by their neural progenitor or neural crest stem cell phenotype. The spontaneously differentiated cells formed long, thin cell projections and formed networks (Fig. 3.7A and 3.7B). Furthermore, ICC revealed the expression of the neural markers TUJ1 and NFH (Fig. 3.7C). We also observed some cells that remained undifferentiated within the same culture with neuralised cells. (figure 3.7 A and B, Arrows). Thus, suggesting that there is in fact a cell population more capable of neurogenesis and supporting the heterogeneous nature of mouse dental pulp cultures (mDPCs and mDPPSCs).

Spontaneous neural differentiation of mouse dental pulp cultures

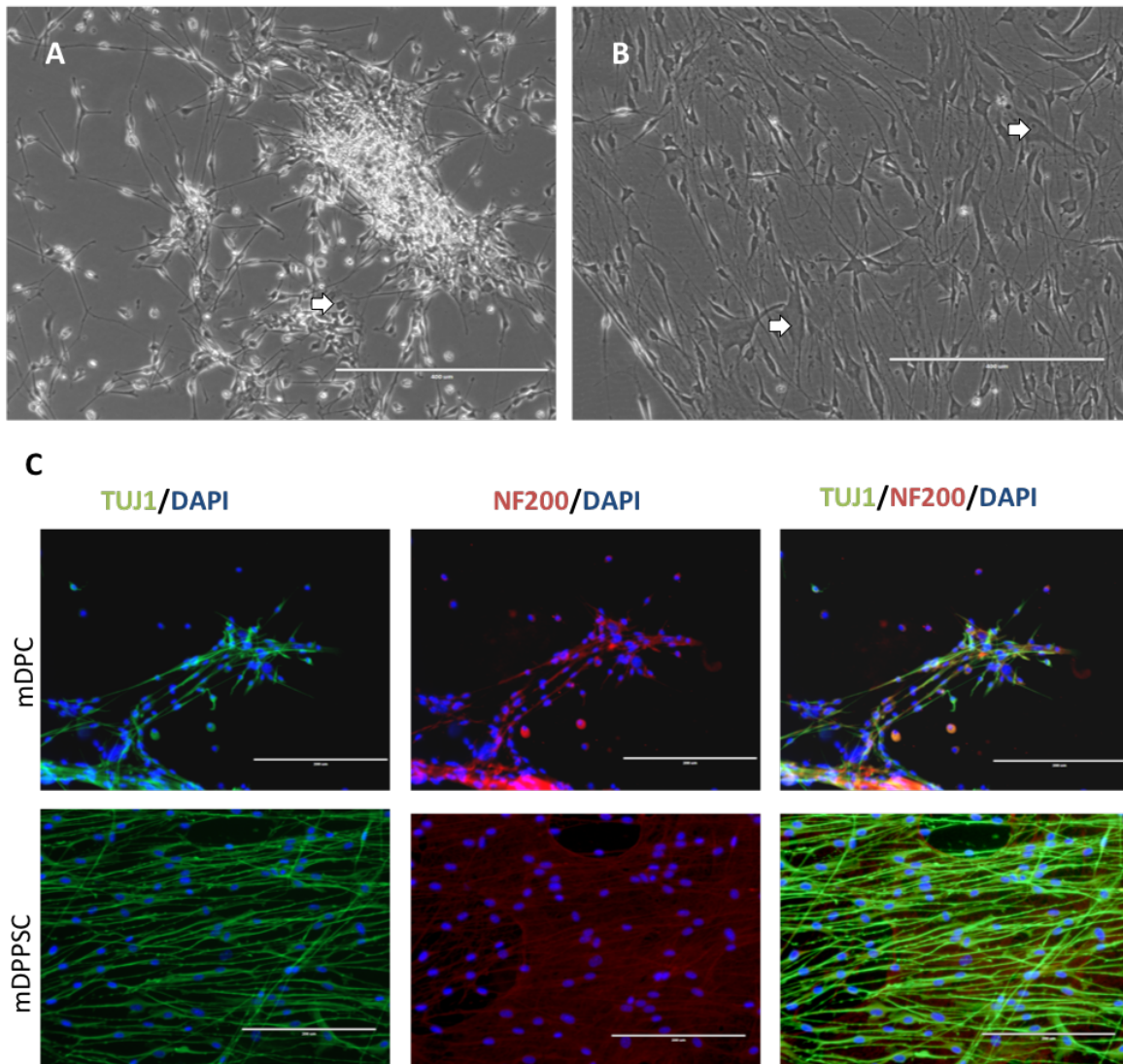
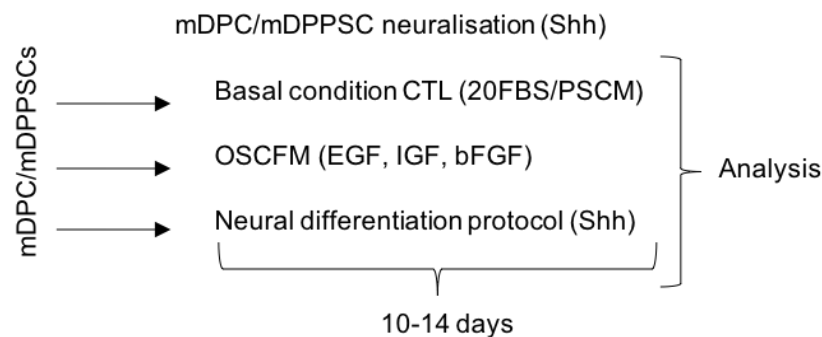


Figure 3.7. Spontaneous differentiation. cells cultured over a long period spontaneously showed a change in morphology into long, thin cells with projections. Other undifferentiated cells can be seen as well (Arrows). A) Cells from 20FBS cultures (mDPC), B) Cells from PSCM cultures (mDPPSC). C) Immunocytochemistry showing the expression of TUJ1 and NF200 in mDPC (Upper panel) and mDPPSCs (Lower panel) after long culturing conditions (>35 days). Scale bar: A, B, C) 400 μ m.

3.5. Neural induction of mouse dental pulp cultures

The expression of neural progenitor-related markers, combined with the intrinsic capacity of the cultures to acquire a neural-like phenotype, supported the idea of a resident population within the dental pulp that could be used for direct differentiation into neurons (neuralisation). We aimed to obtain sensory neurons that could resemble spiral ganglion

neurons found in the cochlea. Therefore, we tested the neuralising protocol developed by our research group to obtain auditory neurons from otic neural progenitors (ONPs)^{31,32}. The mDPCs and mDPPSCs were directly induced to neuralise at least on two occasions each. Sonic Hedgehog induction protocol was used as described in materials and methods. The neuralised cultures (Neu) were compared to cultures in their basal condition (20FBS or PSCM) and to cultures growing in OSCFM (see materials and methods) as a non-inductive medium (Diagram 3.1).



| Medium | Basal Conditions |
|--|--|
| 20% Fetal bovine serum (FBS) ⁵ | DMEM, 1x P/S, 2nM Glutamax (GIBCO), 100µM Ascorbic Acid (Sigma), 20% foetal bovine serum (FBS; GIBCO). No coating. |
| Pluripotent stem cell medium ^{52,87} | 60% DMEM-Low Glucose (SIGMA), 40% MCDB-201 (Sigma), 1X Insulin-transferrin-selenium (ITS, Sigma), 1X linoleic acid-bovine serum albumin (LA-BSA; Sigma), 1nM Dexamethasone (Sigma), 100µM Ascorbic Acid, 100 I.U./mL Penicillin/100µg/mL Streptomycin, 2% FBS (HyClone, Fisher Scientific), 10ng/mL hPDGF-BB (R&D Systems), 10ng/mL EGF (R&D Systems). Coated with 100ng/mL Fibronectin (Sigma). |
| OSCFM (Otic stem cell full medium) ³² : | DFNB (DMEM:F12 (GIBCO), 1% N2 (GIBCO), 2% B27 (GIBCO)), 1x P/S (SIGMA), 20ng/mL bFGF (R&D Systems), 50ng/mL IGF (R&D Systems), 20ng/mL EGF (R&D Systems). Coated with mouse laminin (2.5ug/cm ² ; Cultrex). |
| Neuralisation (Shh) Table 2.3 Methods | Sonic Hedgehog, bFGF, NT3, BDNF, N2 and B27 as described in methods. |

Diagram 3.1. Workflow of mDPC/mDPPSC neuralisation (Shh) and table reminder. mDPC and mDPPSCs in culture where dissociated and transferred to either a basal control condition, a non-inductive condition (Otic Stem Cell Full Medium: OSCFM) and a neuralising condition using the Sonic Hedgehog neuralisation protocol (Shh) for 10-14 days.

mDPCs and mDPPSCs had variable responses to the treatment. For instance, morphologically, cultures from 20FBS and PSCM still presented different cell types, including neural-like cells. OSCFM medium also induced changes to the cultures, especially in mDPPSCs. mDPPSCs under neuralising conditions with Sonic Hedgehog presented cells with elongated projections (Fig. 3.8).

The expression of neural markers TUJ1, NF200 and NEUROD1 was identified by ICC, and quantified by counting positive cells (Fig 3.9). Differences in percentage of positive cells between the conditions (Neu, OSCFM and 20FBS/PSCM) were analysed statistically using a one-way ANOVA. For mDPCs, the percentage of TUJ1 positive cells was consistent throughout the conditions tested (Neu, OSCFM and 20FBS), remaining below 6% and showing no significant difference. The neural marker NF200 was present in a higher percentage in both OSCFM (51.15 ± 19.6) and Neu (64.27 ± 17.47) compared to the 20FBS group (21.97 ± 11.32) however, no statistical significance was observed. The percentage of NEUROD1 positive cells varied between the 20FBS (19.77 ± 8.46), OSCFM (46.87 ± 9.73) and Neu (38.92 ± 9.38) conditions, however, no significant difference was found (Fig. 3.9A, Fig 3.10).

Similarly, in mDPPSCs, the percentage of TUJ1 positive cells was similar across groups. The markers NF200 and NEUROD1 were also not different among the different medium conditions. Overall, no statistical differences, in terms of the percentage of positive cells were seen after neural induction with Sonic Hedgehog (Fig. 3.9B, Fig 3.10). Importantly, it can be noted a high variability within the experimental groups, where heterogeneity could be affecting the overall differentiation.

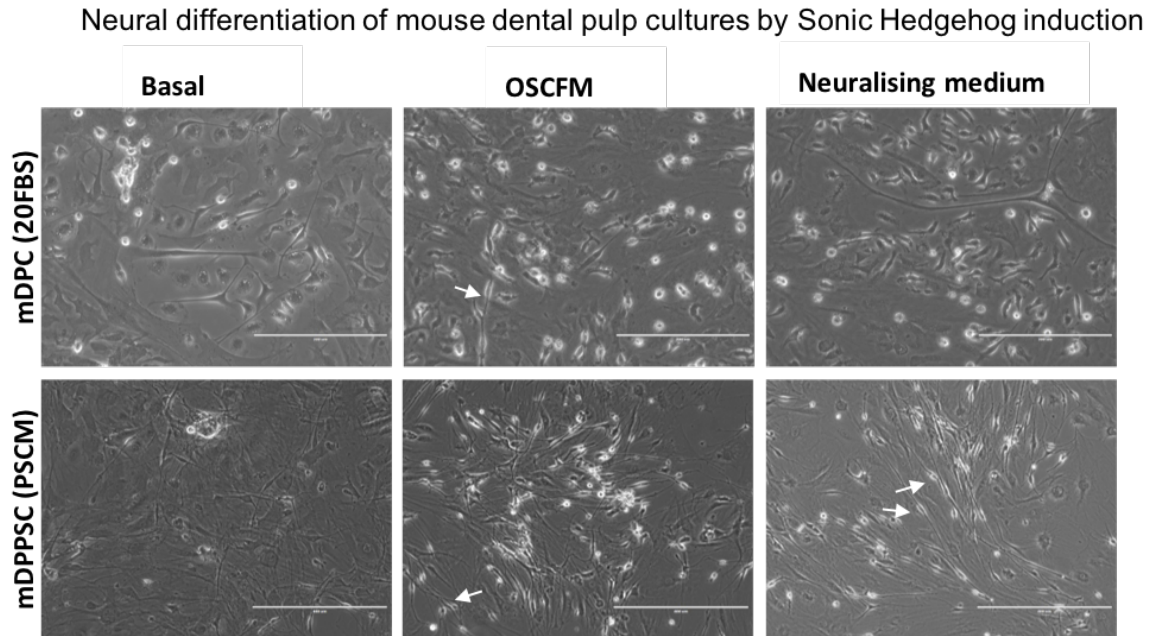


Figure 3.8. mDPC and mDPPSC neural induction with Sonic Hedgehog. Appearance of cultures in control conditions (Basal: 20FBS or PSCM accordingly) compared to cultures in OSCFM and Neuralising medium. Cultures in OSCFM and Neuralising medium present bipolar cells with elongated cells bodies (Arrows). Scale bar: 200 μ m.

Neural induction was also assessed using RT-qPCR to measure the expression for the neural markers: *Gap43*, *Nfh*, *TubIII* and *Brn3a* between the basal (20FBS or PSCM) and the neuralised (Neu) conditions. A student t-test was used to determine if a statistically significance could be observed. mDPCs showed a decreased expression level of all the markers tested in three independent experiments (Fig. 3.11A). Whereas, mDPPSCs showed a tendency to upregulate *Gap43*, but with no statistical significance was seen. In addition, *Nfh* and *Brn3a* showed no relative difference with the PSCM condition. *TubIII* was the only marker that appeared upregulated in the neuralised group (Fig. 3.11B).

Neuralisation of mouse dental pulp cultures by Sonic Hedgehog induction

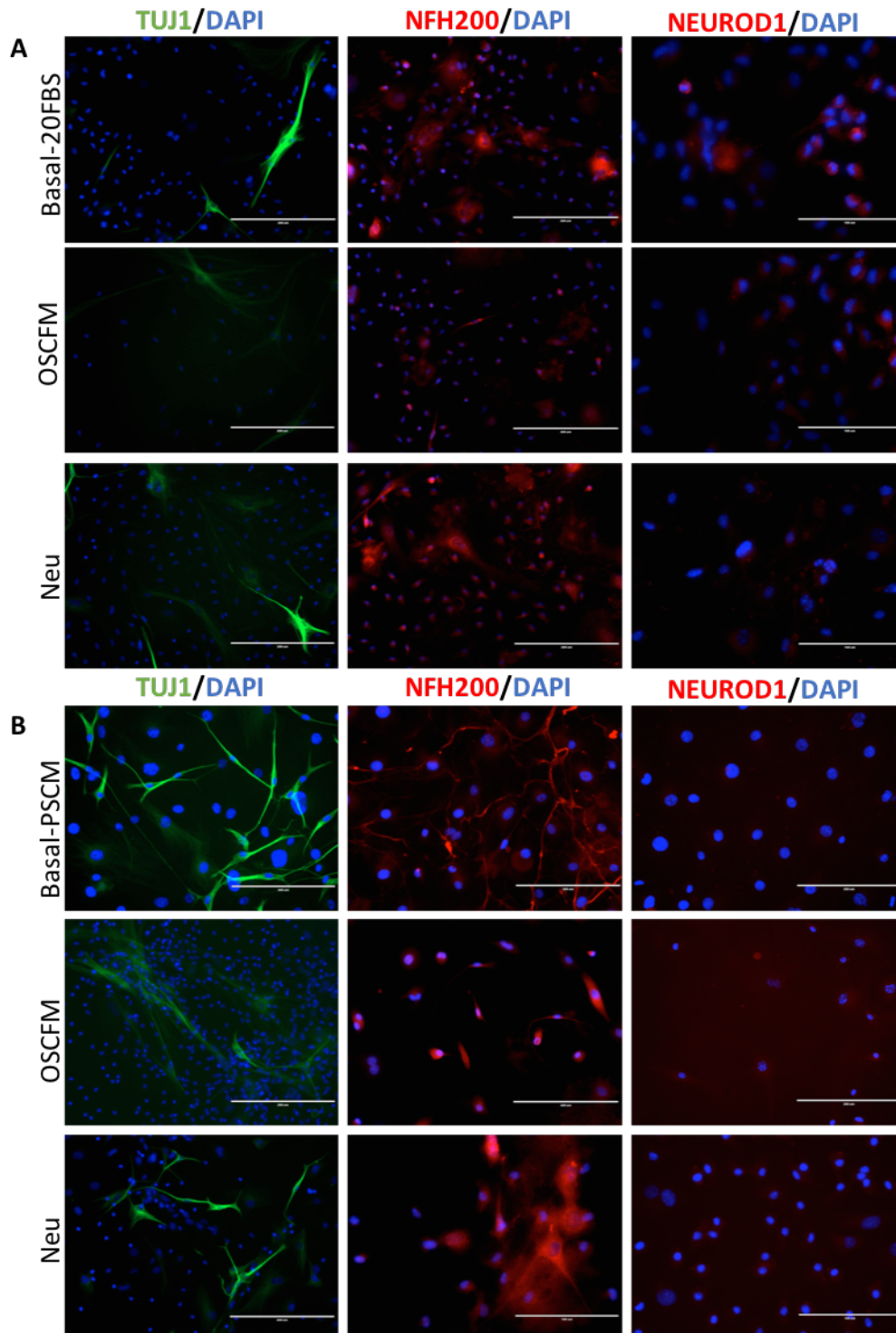


Figure 3.9. Immunocytochemistry (ICC) of neuralised mDPC and mDPPSC. Fluorescence microscopy of TUJ1, NF200 and NEUROD1 positive cells in basal, OSCFM and neuralising medium (Neu) in A) mDPC (20FBS) and B) mDPPSCs (PSCM). TUJ1, NF200 positive cells can be seen in all groups. NEUROD1 is weak or null. Scale bar: 200µm.

Quantification of positive cells after neural differentiation (ICC)

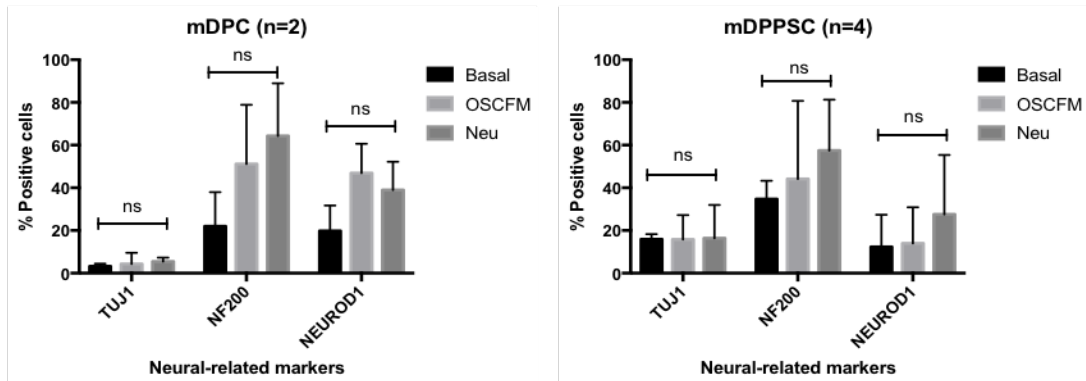


Figure 3.10. Quantification of positive cells after neural induction. Cultures labelled by immunocytochemistry (ICC) were counted to calculate the percentage of cells positive for TUJ1, NF200 and NEUROD1. Cultures from 20FBS (mDPCs) and PSCM (mDPPSCs) in their respective treatments (Basal, OSCFM and Neuralisation (neu) were compared. ns: $P > 0.05$. n=independent samples (cultures established from different animals). Hundreds of cells were counted per condition.

Together, the observation at protein and mRNA levels by ICC and RT-qPCR respectively, didn't show a clear upregulation of neural genes after the neural induction. Although some trends can be observed, the differentiation efficiency is highly variable. The suggested explanations for the effect observed could be: the inability of the cultures to respond to Sonic Hedgehog signaling for neural differentiation and/or inefficiency to differentiate due to heterogeneity. Therefore, we proposed to test a method for enriching or isolating a neural progenitor or a neural crest-like (NCSC) population from dental pulp cultures.

Gene expression analysis after neuralisation with Sonic Hedgehog

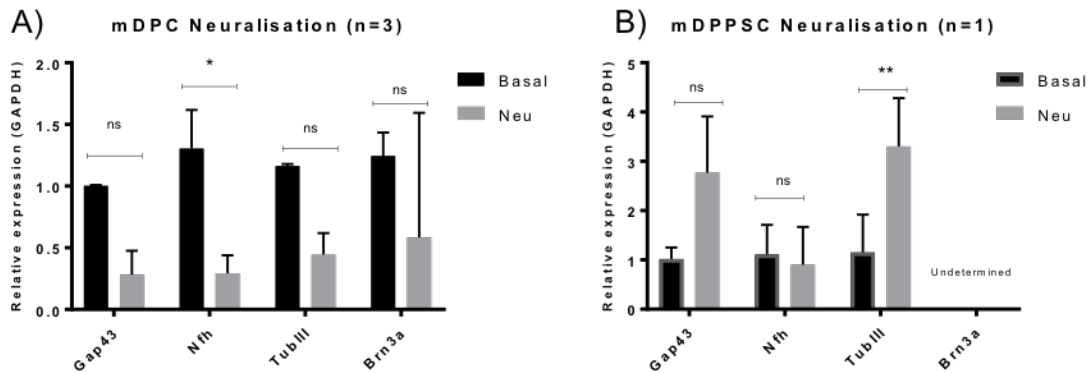


Figure 3.11. Gene expression analysis of neuralisations by RT-qPCR. Relative expression analysis of neural-related genes after neuralisation using Sonic Hedgehog induction in A) mDPCs (Basal: 20FBS) and B) mDPPSCs (basal: PSCM). A student T-test was done. * $P \leq 0.05$, ** ≤ 0.01 . n= independent experiments. In “B” Error bars represent technical replicates.

3.6. Evaluation of Pax7 as a marker of neural progenitor/NCSCs.

Neuralisation varied in both DPCs and DPPSCs. Nevertheless, the fact that some individual experiments yielded a higher fraction of neural-like cells compared to control groups, motivated us to find strategies to isolate or enrich the proposed subpopulation responding to the neural induction.

Pax7 is a transcription factor present in cranial neural crest cells during development. Additionally, it is usually co-expressed with Pax3, a marker commonly associated with neural crest cells¹⁰⁴. Therefore, we hypothesised that Pax7 could serve as a marker of neural crest cells in mouse dental pulp cells. To test this hypothesis, we used a mutant mouse strain with a Pax7-eGFP reporter. The reporter was designed by recombination of the nuclear EGFP sequence in the first exon of *Pax7*¹⁰⁵. The transgenic mice were kindly provided to us by Dr. Shahragim Tajbakhsh, Institut Pasteur.

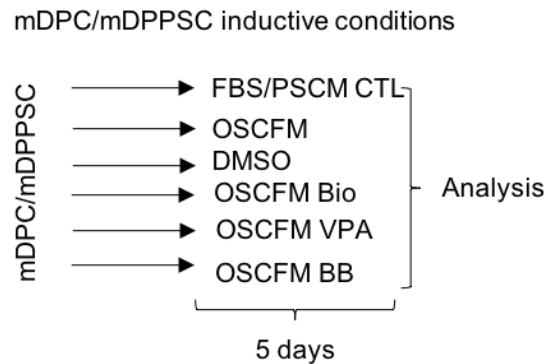
We sought to evaluate if the expression of PAX7 correlated with eGFP. First, we observed that the intrinsic eGFP signal given by the reporter was weak, and evident only in a few cells from mDPC and mDPPSCs (Fig. 2.12A). Seemingly, the eGFP signal was amplified by the use of an α -GFP antibody for immunocytochemistry, resulting in cells clearly positive to Pax7-GFP in mDPC and mDPPSCs (Fig. 2.12B). At mRNA levels, the RT-PCR revealed discrepancies

in *Pax7* and *eGfp* co-expression. Theoretically, the *eGfp* expression should correlate with *Pax7* expression, therefore both should be present if *Pax7* is active. However, results from mDPCs and mDPPSCs presented a mixed expression pattern, even within the same cultures grown in different vessels (sister-flasks) (i.e. mDPPSC4 and mDPPSC5; Fig. 3.12C). In particular, cultures grown in 20FBS (mDPCs) only expressed *Pax7*, but no eGFP. At the same time, two mDPPSCs growing in PSCM showed the expression of *Pax7* and eGfp together, but only in one of the three sister flasks in each culture (mDPPSC4 and mDPPSC5). Oddly, we also observed the expression of eGfp alone in one mDPPSC and in the dental pulp tissue (Fig. 3.12C).

Following detection of *Pax7*-eGFP signal in culture by ICC and RT-QPCR, we evaluated *Pax7*-eGFP cultures by flow cytometry (FC). Flow cytometry allows the detection and quantification of cell populations when they are fluorescent for a target of interest (i.e. *Pax7*-eGfp). The flow cytometry analysis revealed a very low percentage of GFP positive cells in mDPC and mDPPSC cultures. mDPC cultures had 0.21% of *Pax7*-eGFP positive cells while mDPPSC cultures had 0.02-0.18%.

As a secondary effort to increase *Pax7*-eGFP positive cells, we attempted to culture the cells under inductive conditions that were hypothesized to favour or select the growth of NCSC-like cells, allowing the expression of *Pax7* and in turn, the detection of the GFP signal. These conditions were chosen based on the role that specific factors have been shown to have on neural crest or neural progenitor cell induction¹⁰⁶⁻¹⁰⁸. The selected conditions were: OSCFM medium, OSCFM + DMSO, OSCFM + 6-Bromoindirubin-3'-oxime (BIO; 0.75 μ M), OSCFM + Valproic Acid (VPA 1mM) or OSCFM + BIO (0.75 μ M)/BMP4 (10ng/mL) (Diagram 3.2). mDPCs and mDPPSCs were exposed to these conditions for 5 days (Fig. 3.13). Flow cytometry analysis of the treatment conditions was performed on mDPC. The percentage of positive cells detected was small, being BIO+BMP4 (B+B) the highest with 2.55% of positive cells (Fig. 3.14).

As the starting cell numbers from such cultures are small, the use of Pax7 as a tool for sorting putative neural crest-like cells was unviable. As suggested by our results, the signal can be amplified by ICC. However, the latter approach requires the cells to be fixed, stopping us to use them in posterior experiments.



| Medium | Conditions |
|------------------------------------|--|
| DFNB | DMEM:F12 (GIBCO), 1% N2 (GIBCO), 2% B27 (GIBCO), 1x P/S. |
| OSCFM (Otic Stem Cell Full Medium) | DFNB (DMEM:F12 (GIBCO), 1% N2 (GIBCO), 2% B27 (GIBCO)), 1x P/S (SIGMA), 20ng/mL bFGF (R&D Systems), 50ng/mL IGF (R&D Systems), 20ng/mL EGF (R&D Systems). Coated with mouse laminin (2.5ug/cm ² ; Cultrex). |
| VPA (Valproic Acid) | OSCFM + valproic Acid 1mM (Tocris), 1x P/S. |
| BIO | OSCFM, BIO 0.75μm (Sigma), 1X P/S. |
| BIO+BMP4 | OSCFM + 10ng/mL BMP4 (R&D) + BIO 0.75μm (Sigma), 1x P/S. |

Diagram 3.2. mDPC/mDPPSCs under inductive conditions and components reminder. mDPCs and mDPPSCs were transferred to different treatment conditions for 5 days.

Pax7-eGFP reporter in mouse dental pulp cultures

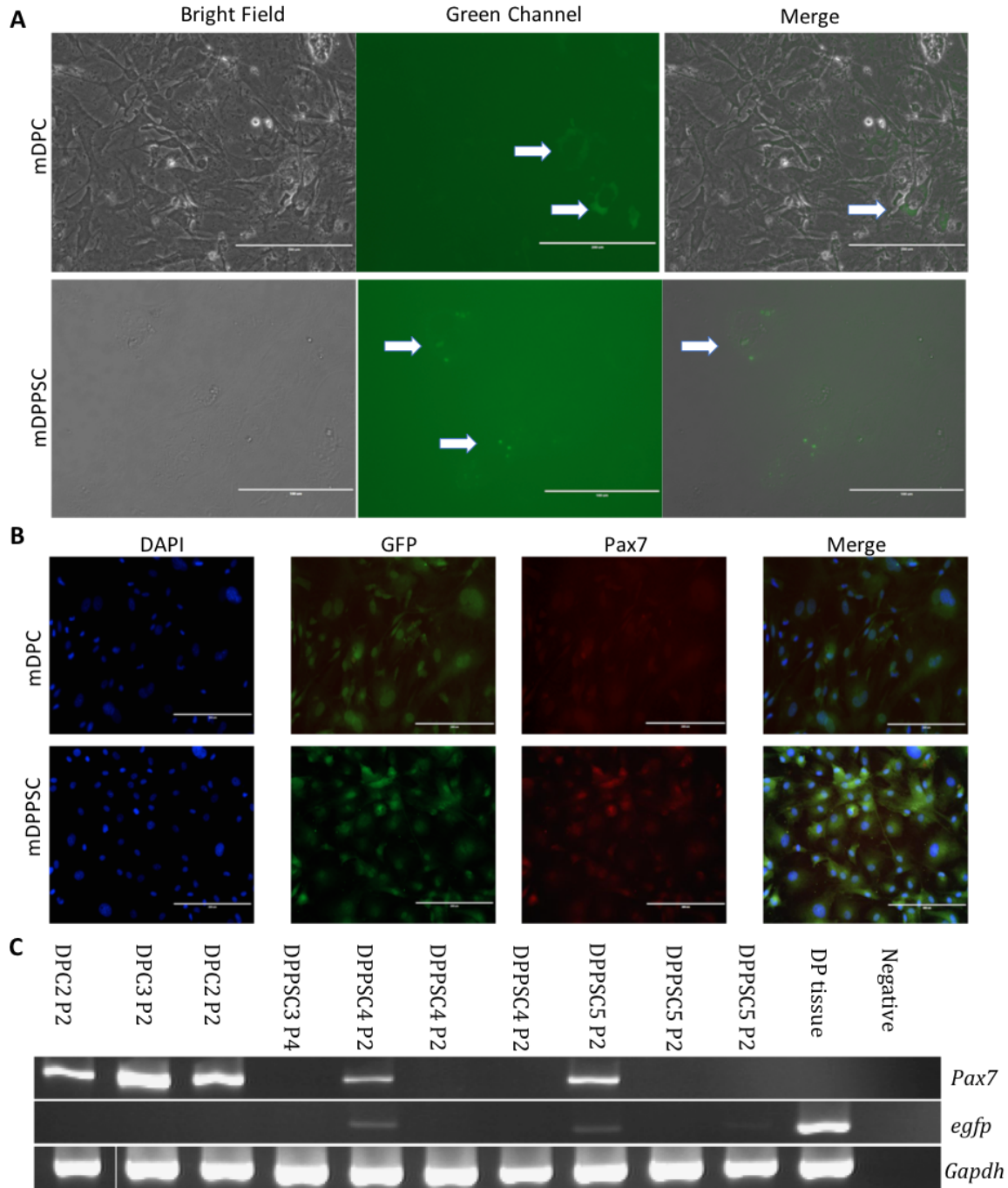


Figure 3.12. Pax7-eGFP mDPC and mDPPSC Cultures. A) Intrinsic eGFP signal (arrows) from mDPCs and mDPPSCs in culture can be detected by fluorescent microscopy. B) GFP and Pax7 can be detected by Immunocytochemistry on mDPCs and mDPPSCs. C) RNA expression by RT-PCR of *Pax7* and *Gfp* in mDPC and mDPPSC cultures. Wells with the same name correspond to cultures grown in different flasks (sister flasks). mDPC2 P2 *Gapdh* was done in a separate gel. Scale bars: A) 100µm, B) 200µm.

mDPC and mDPPSC under Inductive conditions

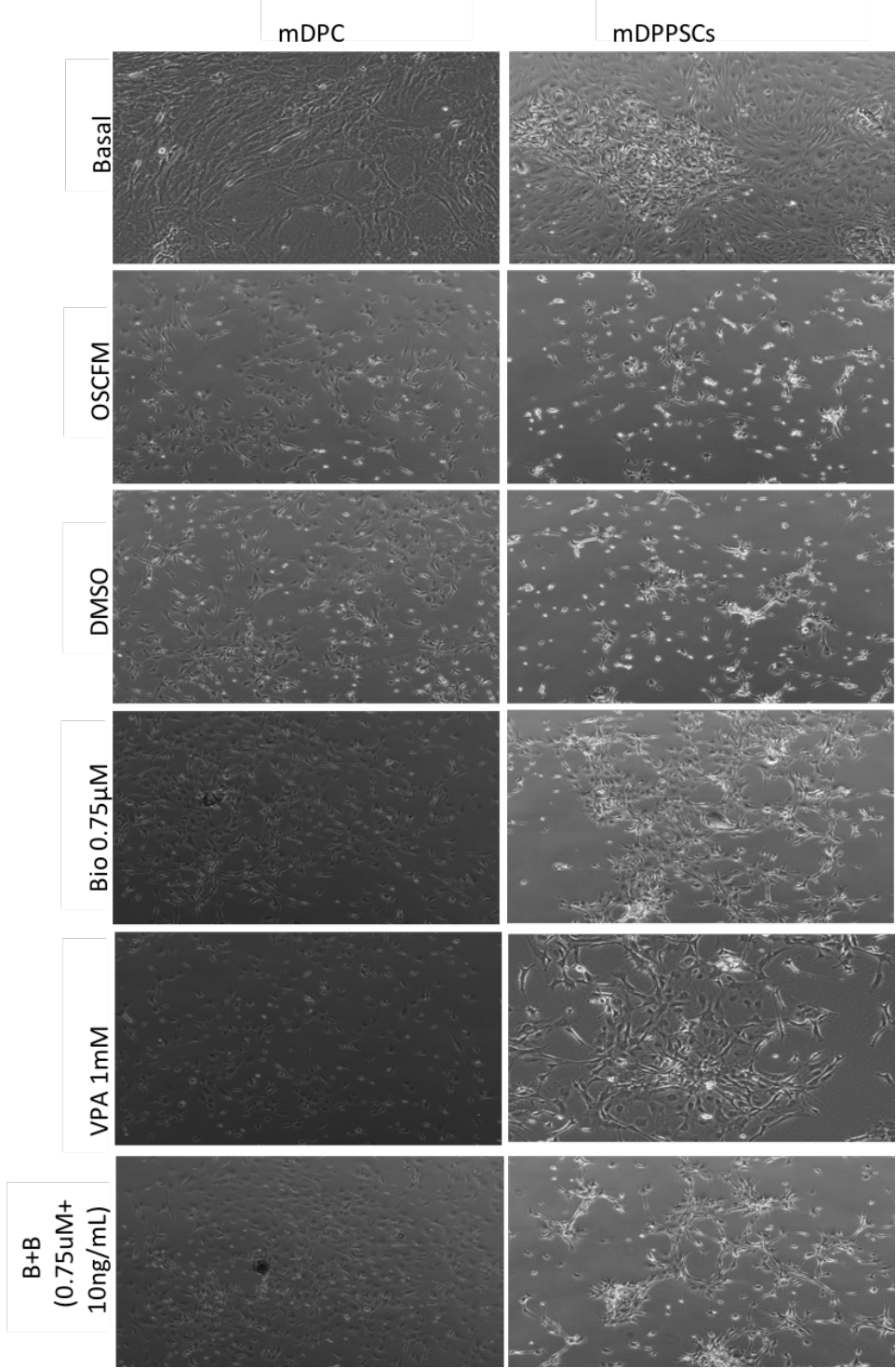


Figure 3.13. Inductive culture conditions. mDPC (Left) and mDPPSC (Right) were grown under conditions proposed to induce neural crest or neural progenitor phenotype, as a method to also induce Pax7-eGFP expression. 20FBS/PSCM (basal condition), OSCFM medium (OSCFM), OSCFM + DMSO (DMSO), OSCFM + BIO (BIO), OSCFM + VPA (VPA) and OSCFM + BIO + BMP4 (B+B).

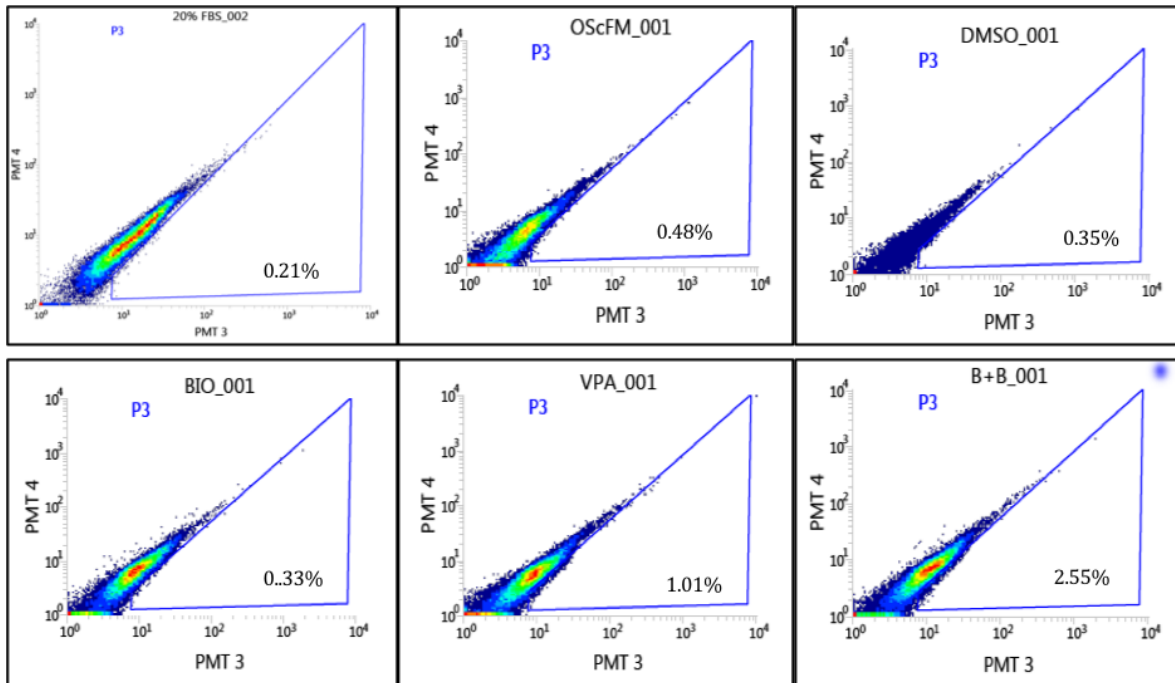


Figure 3.14. Flow cytometry analysis of mDPC in treatment conditions. Intrinsic eGFP signal of Pax7-mDPCs from 20FBS was analysed after cells were cultured in the alternative inductive conditions. 20FBS (basal condition), OSCFM medium (OSCFM_001), OSCFM + DMSO (DMSO_001), OSCFM + BIO (BIO_001), OSCFM + VPA (VPA_001) and OSCFM + BIO + BMP4 (B+B_001). Gating was performed by establishing a non-fluorescent baseline from cells not coming from the Pax7-eGfp strain. Fluorescence detected above that baseline (P3-blue rectangle) was taken as coming from the eGFP signal.

3.7. Characterisation of mDPCs and mDPPSCs after exposure to inductive cues

Although the mentioned culture conditions did not allow exploring Pax7 as a tool for NCSC selection, the cultures presented morphological changes that invited to further explore them at the molecular level.

To determine if any induction of Neural progenitor (NP) markers was evident, we used RT-qPCR to determine the relative expression of markers such as *Brn3a*, *Gata3*, *Sox2* and *Sox10*. The relative expression levels were analysed using Two-way ANOVA to determine statistical significance, followed by a Tukey test for pair wise comparisons.

Neural progenitor-related genes were evaluated after treatment with OSCFM, DMSO, BIO, VPA and B+B for 5 days. For these experiments, two independent cultures of mDPCs (mDPC6 and mDPC9) and mDPPSCs (mDPPSC7 and mDPPSC10) each were tested. In the

case of mDPC6, the treatment with B+B resulted in statistically significantly higher levels of *Gata3*, *Sox2* and *Sox10* than the rest of the treatments. VPA treatment resulted only higher expression levels of *Gata3* (Fig. 3.15A). On the other hand, mDPC9 line presented a higher level of *Brn3a* expression only after B+B induction, but no changes were detected in *Gata3* and *Sox10* expression in any other condition tested (Fig. 3.15B).

Regarding mDPPSCs, mDPPSC7 presented an increased relative expression only of *Gata3* and *p75* when treated with B+B, but no changes in *Sox10* in any of the conditions tested (Fig 3.15C). The culture mDPPSC10 expressed significantly higher levels of *Brn3a* and *Gata3* when treated with B+B. Interestingly, OSCFM was also able to induce *Gata3* and *Sox10* expression in this culture (Fig. 3.15D).

Although the expression of specific genes was somehow variable, there was a consistent pattern of neural progenitor markers supported by culture in OSCFM, and largely enhanced when in B+B conditions. Nevertheless, it would be necessary to include more cultures to validate this trend.

Gene expression after inductive treatments

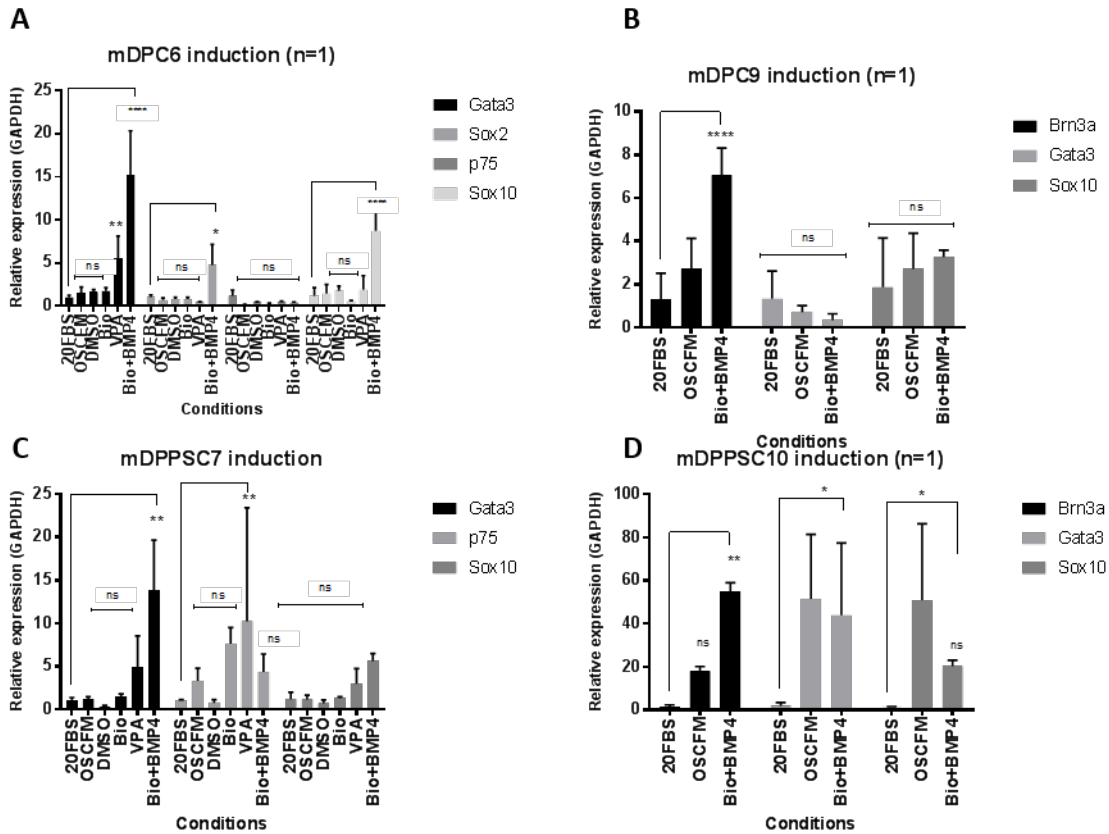


Figure 3.15. RT-PCR of neural progenitor and neural crest markers after inductive conditions. mDPC cultures and mDPPSCs were transfer from 20FBS and PSCM (Respectively) to neural crest/progenitor inductive media and their gene (RNA) expression profile evaluated by RT-qPCR. *P ≤0.05, **P≤0.01, ****P≤0.0001. Error bars represent technical replicates.

3.1. Neural differentiation of mDPCs and mDPPSCs after inductive treatments

It was proposed that if the upregulation trend of neural progenitor markers was real, then the OSCFM and B+B-treated cultures would be more responsive to neural differentiation with Sonic hedgehog induction (Diagram 3.3).

Neural induction with Sonic Hedgehog was performed as described earlier on the inductive treated cells (20FBS, OSCFM and B+B). Cultures reached different levels of confluency and heterogeneity. The mDPC control group (20FBS) looked very confluent and displayed an

array of morphologically different cells, which was expected from the results presented above on mDPCs. The OSCFM and B+B treated cells after Shh induction (OSCFM-Neu and B+B-Neu, respectively) were less confluent, and still presented some distinct types of cells within the culture. However, the remaining cells looked elongated, and some extended neurite-like projections (Fig 3.16A). A relative expression analysis was conducted and revealed that after neural induction on OSCFM and B+B-treated cells, mDPCs expressed significantly higher levels of the neural markers *Nfh* and *Brn3a*. Additionally, an increase of *Vglut* and *Syn* mRNA was detected, although the higher expression levels was not statistically significant (3.16B). The upregulation of neural markers after OSCFM and B+B induction plus neuralisation suggests an improvement of their neurogenic capacity from the basal 20FBS condition.

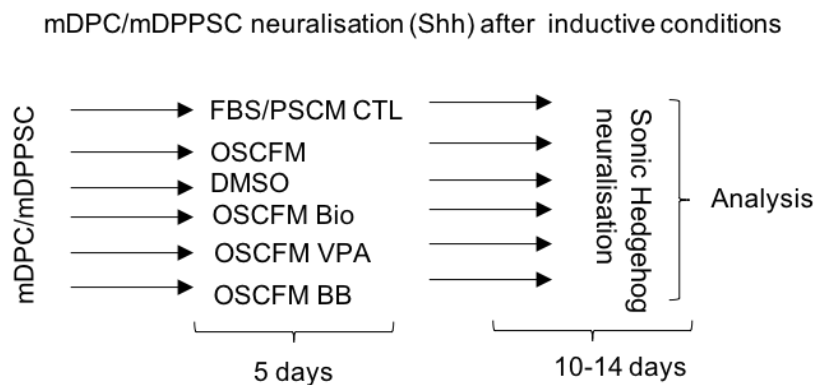


Diagram 3.3. mDPC/mDPPSC neuralisation after inductive treatments. mDPCs and mDPPSCs were transferred to the different inductive conditions for 5 days, and then treated with the Sonic Hedgehog (Shh) neuralisation protocol for 10-14 days.

3.2. Discussion

3.2.1. Establishment of dental pulp cultures from mouse teeth

The study of dental pulp stem cells has been widely focused on cells from human origin. However, the reports of mouse dental pulp cultures showed interesting neurogenic features *in vitro*. Nevertheless, at the beginning of this thesis only a few of those reports disclosed in detail how to establish cell cultures from mouse dental pulp. Therefore, we were in the necessity to establish the ideal culture conditions to grow mouse dental pulp cells *in vitro*.

Using at least 3 animals and mainly the incisors to establish the cultures, rather than fewer animals and the molars, allowed us to get enough cell numbers to continue with the experiments. Also, we preferred the use of 20% FBS instead of a lower percentage (i.e. 10% and 15% FBS) to establish and maintain our cell cultures. Thus, the decision of using these conditions was based on practicality, rather than a biological justification. In this regard, at the time of experimentation (2014-15) the reported examples of mouse incisor-DPCs *in vitro* used adult animals (5-8-weeks-old) and grown the cells in 10% FBS supplemented medium¹⁰⁹⁻¹¹¹. However, they don't state if the cultures were established from one single animal or by pooling tissue from several animals, like our work did. In the case of DPCs from molars, there is evidence of progenitor cells isolated from early postnatal mouse molars (P5-P7) grown in 20% FBS, similar to our work¹¹². However, such reference also didn't specify if the cultures belonged to a single animal or a group of them. We also succeeded in culturing DPCs from molars, we preferred to continue the research on incisors based not only on practicality, but also as an effort to further the knowledge on incisors, given that molars have been explored elsewhere⁵².

Similar to human dental pulp cells (hDPCs), murine DPCs (mDPC) are described as mesenchymal stromal cells (MSCs), able to differentiate into the classical osteoblast, adipocyte and chondrocyte lineages and to express MSCs antigens¹⁰⁹⁻¹¹². However, the published evidence by Atari et al., (2012) suggesting that a population human dental pulp cells could display a pluripotent phenotype when grown under specific conditions, invited us to test their "Pluripotent stem cell medium (PSCM)" in our cells, and evaluate the culture

behaviour⁸⁷. Furthermore, Breyer et al., (2006) presented evidence of mouse bone marrow-MSCs cultured in this PSCM medium, and reported an upregulation of pluripotent stem cell markers and differentiation into ectodermal, mesodermal and endodermal cell fates¹¹³. Therefore, we decided to test the PSCM and established mDPC cultures directly into PSCM, and only by convention, termed the cells mouse dental pulp pluripotent stem cells (mDPPSCs).

3.2.2. Characterisation of mDPC and mDPPSCs

Little was known about the neural differentiation potential and the neurogenic nature of mouse dental pulp cells. In the present chapter, we identified neural crest and neural progenitor markers in mDPC and mDPPSC cultures. The profile that we found provides further evidence of their neural crest origin, and neurogenic nature. In this regard, a key report by Janebodin et al., (2011⁵²) used cell tracing experiment with a Wnt1-Cre reporter transgene, provided developmental evidence of the neural crest origin of the dental pulp in mice. In the same report, mDPC primary cultures from molars expressed P75, Twist1, Slug, Snail, among others, justifying their description as neural crest-derived stem cells (NCSCs). Importantly, they used the same growing conditions used by us (named PSCM in our thesis) in their cultures⁵². Together with our results from incisors, these allow us to suggest that NCSCs can be obtained from mDPCs and mDPPSCs from both teeth types: incisors and molars.

In terms of their neurogenic potential, our cultures showed spontaneous differentiation of a subset of cells when grown over long periods of time. This spontaneous ability suggests an intrinsic neurogenic nature, which could be resulting from the NCSC phenotype. We hypothesized that a subset of mDPCs and mDPPSCs could be responding to paracrine or autocrine signals in the culture that induce neural fate lineage. There is evidence in the literature, of neurotrophic factors produced in rat DPCs such as NGN, BDNF and GDNF that support the possibility of a neural inductive signaling within the culture^{114,115}. Based on the expression of markers and the intrinsic neurogenic potential observed by us, our results provide further evidence of a neural crest-derived stem cell phenotype *in vitro* in both mDPCs and mDPPSCs.

3.2.3. Neuralisation potential of mDPC and mDPPSC

By using the neuralisation protocol designed for otic neural progenitors (ONPs) of ESC origin (using Sonic Hedgehog as an inductive factor)^{31,32}, we explored if mDPC and mDPPSC were competent to differentiate into an auditory neural lineage. This protocol was not able to induce a generalised differentiation in the culture, and only some cells showed signals of neural differentiation. This result, could be related to the heterogeneity found in the cultures, as seen in the bright field images. In support of this notion, Young et al., (2016) described the clonal heterogeneity and differential neurogenic potential in clones from the same culture¹¹⁶. Noteworthy, evidence of functional neural maturation using mouse dental pulp cells has been reported. In this regard, Ellis et al., (2014¹¹¹) were able to neuralise mDPC cultures by a multi-step protocol requiring epigenetic modifiers. This protocol, as well as other protocols used for neuralisation of other adult NCSCs, required the generation of a homogeneous population or a severe reprogramming step to achieve neural maturation as an intermediate step^{54,117}. Therefore, it's evident that the basal culture conditions are not neurogenic enough and require intermediate steps for neural maturation.

In this regard, we attempted to include in our protocol a method for isolating or enriching a more homogeneous population with a neurogenic potential. We first tried to use Pax7 as a proposed marker of neural crest-derived cells in mDPCs. By using a Pax7 driven eGFP reporter mouse strain, we evaluated the presence of a Pax7 population within mDPCs and mDPPSCs. Unfortunately, flow cytometry data showed a very small population, technically challenging to isolate. Pax7 has been described as an early cranial neural crest marker, preceding the expression of other important markers such as Sox10¹⁰⁴. Thus, Pax7 expression could be mainly restricted to early developmental stages, resulting in its small presence in the adult dental pulp-derived cell cultures, as shown by us.

An additional strategy for NCSCs induction or enrichment, was to treat the cells with culture conditions hypothesised to induce or expand the NCSC phenotype. By testing different conditions (i.e. OSCFM, VPA, BIO+BMP4), we were able to identify that the activation of WNT pathway together with the addition of BMP4 (termed: BIO+BMP4 condition) resulted in an apparent induction to express neural progenitor markers. Furthermore, after neural

induction with Sonic Hedgehog, an apparent upregulation of sensory neural markers was also evident. The BIO+BMP4 treatment also expanded the Pax7-eGFP population. Thus, the BIO+BMP4 condition may be selecting the neurogenic population within the dental pulp cultures, which agrees with reports that support neural crest cell induction and sensory neural differentiation by using WNT activation and BMP4 addition^{108,118}. We propose to validate these preliminary results further.

3.3. Summary

In summary, our results presented here suggest that some cells within mDPCs and mDPPSCs cultures responded to Shh neural induction, as seen by the TUJ1^{+ve} immunofluorescence cell counts. However, RT-qPCR analysis did not detect a significant increase in the relative expression of more specific sensory neural related genes. This agrees with the concept that only a small cell population in these heterogeneous cultures is capable to produce neural phenotypes. On the other hand, mDPCs were able to significantly increase *Nfh* and *Brn3a* relative expression levels, as well as seemingly presented higher levels of *Vglut1* and *Syn* if coming from the OSCFM and BIO+BMP4 conditions. Therefore, it is concluded that an initial treatment with BIO and BMP4 could allow to enrich or induce a pro-neural phenotype that responds better to Shh neural differentiation.

Altogether, the results suggest that a NCSCs population can be found within mDPC and mDPPSCs, and the enrichment or induction with a combination of BIO and BMP4 can make it more responsive to neural differentiation, compared to their basal, heterogeneous state.

CHAPTER 4

**“Human dental pulp culture, characterisation and
evaluation as neural progenitors”**

4. Human dental pulp culture, characterisation and evaluation as neural progenitors.

Almost three decades have passed since the first recognised characterisation of human dental pulp stem cells (hDPSCs) by Gronthos et al., (2000). Currently, there is an increasing recognition that the hDPSC's neural crest origin and neurogenic capacity could be ideal for neurodegenerative disorders (commented on Luo et al., 2018¹¹⁹). However, the effect of the diversity between patients, teeth type and teeth condition are not always described, limiting the scope of their potential use in regenerative medicine. Furthermore, the media solutions commonly used in the literature contain serum, which immediately discard them for clinical translation.

Therefore, we aimed to describe the clinical conditions of the collected teeth in relation to their capacity to grow *in vitro*. Also, we characterised the cultures in serum and serum-free media conditions and determined if their neurogenic and gliogenic potential could change in the different growing solutions.

4.1. Human dental pulp can be extracted and cultured from a variety of patients.

In this study we collected 60 teeth samples with informed consent at the Charles Clifford Dental Hospital, the ethical approval was granted by the Leeds East Research Ethics Committee of the National Research Ethics Service (NRES). Patient data collected was minimal and consisted of age, sex and reason for tooth extraction. The age varied from 15 to 61-year-old patients, with a mean of 27 years (± 8.9), a median of 26 years and a mode of 27 years. Most of them were molars (Position 6, 8), but we also collected incisors (Position 2), canines (Position 3) and premolars (Position 5). A mixture of intact and carious teeth was collected. We considered to use carious teeth when the caries did not extend beyond the dentin (Fig. 4.1; Table 4.1). The reason for extraction varied from impacted third molars, orthodontic reasons or loose/diseased teeth.

| Sample Number | Age | Sex | Remarks (#position) | Medium/End point use | Successful |
|---------------|-----|-----|--------------------------|----------------------|------------|
| 1 | 61 | f | Periodontal disease | FBS | No |
| 2 | 52 | f | Pulpitis (5) | FBS | No |
| 3 | 19 | f | Intact - Unerupted (8) | FBS | Yes |
| 4 | 23 | f | Intact (8) | FBS | Yes |
| 5 | 22 | f | Intact (8) | FBS | Yes |
| 6 | 20 | f | Fragmented (8) | FBS | Yes |
| 7 | 27 | f | Caries (8) | FBS | Yes |
| 8 | 23 | m | Intact (8) | IHC | N/A |
| 9 | 28 | f | Fragmented (8) | N/A | N/A |
| 10 | 28 | f | Intact (8) | IHC | N/A |
| 11 | 26 | f | Fragmented (8) | RNA | N/A |
| 12 | 23 | f | Intact (8) | RNA | N/A |
| 13 | 26 | f | Intact (8) | IHC | N/A |
| 14 | 26 | f | Caries - Slight (8) | IHC | N/A |
| 16 | 16 | f | Intact (8) | FBS | Yes |
| 16 | 16 | f | Intact (8) | OSCFM | Yes |
| 17 | 22 | m | Fragmented (8) | FBS | Yes |
| 18 | 30 | f | Intact (8) | FBS | Yes |
| 19 | 27 | f | Intact (8) (Facial Pain) | FBS | Yes |
| 19 | 27 | f | Intact (8) (Facial Pain) | OSCFM | Yes |
| 20 | 27 | f | Intact (8) (Facial Pain) | FBS | Yes |
| 20 | 27 | f | Intact (8) (Facial Pain) | OSCFM | Yes |
| 21 | 21 | m | Intact (8) | OSCFM | Yes |
| 22 | 24 | f | Intact (8) | FBS | Yes |
| 23 | 24 | f | Caries (8) | FBS | Yes |
| 24 | 26 | f | Intact (8) | OSCFM | Yes |
| 25 | 33 | f | Intact (8) | BMP4 | Yes |
| 26 | 15 | f | Caries - Slight (7) | IHC | N/A |
| 26 | 15 | f | Caries - Slight (7) | OSCFM | No |
| 27 | 20 | f | Non-specified (8) | OSCFM | No |
| 28 | 36 | f | Caries - Slight (8) | Non-specified | No |
| 29 | 36 | f | Intact (8) | BMP4 | Yes |

| | | | | | |
|----|---------------|---------------|--------------------------|-------|-----|
| 32 | 35 | m | Fragmented (?) | OSCFM | No |
| 34 | 24 | f | Intact (8) | BMP4 | No |
| 34 | 24 | f | Intact (8) | OSCFM | Yes |
| 35 | 24 | m | Caries - Slight (8) | IHC | N/A |
| 36 | 34 | f | Non-specified (8) | IHC | N/A |
| 37 | 38 | f | Non-specified-Mobile (8) | BMP4 | No |
| 38 | 38 | f | Periodontal disease (?) | OSCFM | No |
| 39 | 17 | m | Intact (3) | BMP4 | No |
| 39 | 17 | m | Intact (3) | OSCFM | Yes |
| 40 | 17 | m | Intact (3) | BMP4 | Yes |
| 41 | 17 | m | Intact (3) | BMP4 | Yes |
| 42 | 20 | f | Intact (8) | BMP4 | No |
| 43 | 22 | f | Intact (8) | BMP4 | Yes |
| 44 | 29 | m | Intact (8) | FBS | Yes |
| 45 | 29 | m | Non-specified (8) | OSCFM | Yes |
| 46 | Non-specified | Non-specified | Non-specified | OSCFM | Yes |
| 47 | 27 | m | Caries (8) | BMP4 | No |
| 48 | 27 | m | Caries (6) | FBS | Yes |
| 49 | 39 | m | Fragmented (8) | OSCFM | No |
| 50 | 28 | m | Caries (6) | BMP4 | No |
| 51 | 31 | m | Fragmented (8) | FBS | No |
| 52 | 45 | m | Fragmented (8) | BMP4 | No |
| 53 | 21 | f | Intact (8) | BMP4 | No |
| 53 | 21 | f | Intact (8) | OSCFM | Yes |
| 54 | 17 | f | Intact (2) | FBS | No |
| 54 | 17 | f | Intact (2) | OSCFM | No |
| 55 | 17 | f | Intact (5) | BMP4 | No |
| 56 | 37 | F | Non-specified | BMP4 | No |
| 56 | 37 | F | Non-specified | OSCFM | No |
| 57 | 37 | F | Caries - Slight (?) | FBS | Yes |
| 57 | 37 | F | Caries - Slight (?) | OSCFM | Yes |
| 58 | 37 | F | Caries - Slight (?) | BMP4 | No |
| 58 | 37 | F | Caries - Slight (?) | FBS | Yes |

| | | | | | |
|----|---------------|---------------|------------|------|-----|
| 59 | Non-specified | Non-specified | Intact (?) | FBS | Yes |
| 60 | 47 | M | Caries (8) | BMP4 | No |

Table 4.1. Human sample collection log. Human dental pulp tissue was collected from the Charles Clifford dental hospital, University of Sheffield. The samples that were used or attempted to be used were recorded with age and sex. Clinical remarks were made by the clinical team by describing the tooth state during dental pulp extraction (i.e. if caries was evident, fragmented tooth). In cases, tooth description was not recorded (Non-specified). Carious teeth were described as caries or slight caries by the clinical staff. The samples were either used for culture (FBS, OSCFM or BMP4), Immunohistochemistry (IHC), or RNA extraction. In cases, the same sample digest (see methods) was splat in two different conditions (i.e. samples: 19, 20, 54, 56, 57, 58). Some other samples were used for other conditions unsuccessfully, and not described in this thesis.

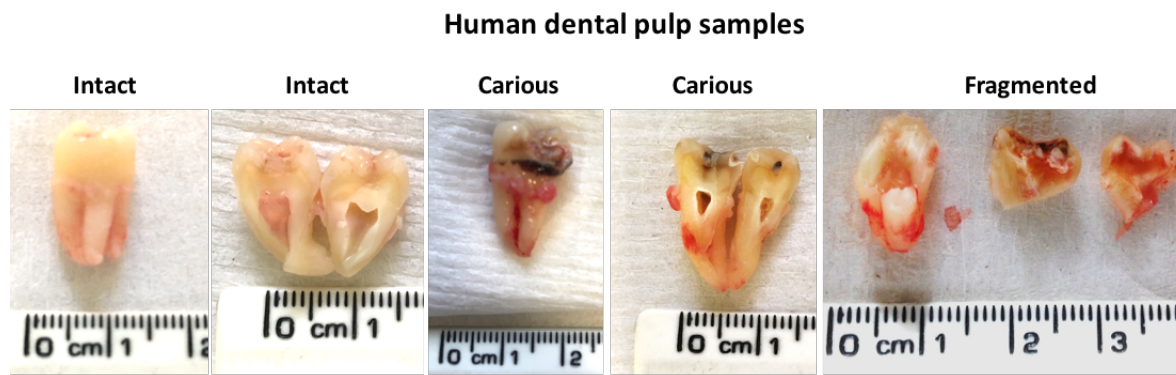


Figure 4.1. Dental pulp collection. Human tooth samples were collected and the dental pulp was extracted from dental pieces. The conditions of the samples varied from intact to carious and some others were fragmented during extraction.

4.2. Immunohistochemistry (IHC) characterisation of human dental pulp.

The samples were first characterised by immunohistochemistry (IHC) to identify markers related to the innervation and stem cell niches identified or proposed elsewhere (As discussed below).

Once the samples were collected, 9 were processed for immunohistochemistry. We aimed to characterise the *in-situ* state of the human dental pulp tissue. We determine the expression of the neural progenitor/ neural crest marker NESTIN (n=3) and the neural markers labelled by Tubulin β III (TUJ1) (n=2), Neurofilament heavy chain (NF200) (n=4) and neurotrophin receptor (P75) (n=4; Fig 4.2A). The presence of the glioma-associated oncogene homolog 1 (GLI1) as a proposed stem cell marker¹⁰² was also evaluated and found

to be expressed in 4 of 6 samples throughout the whole pulp. GLI1 colocalised with the nerve bundles labelled by TUJ1 (Fig 4.2B) and also with NESTIN (Fig 4.2C). A rare appearance was observed for SYR-Box10 in 1 out of 6 samples. SOX10 is a glial marker also associated to neural crest cells and was observed at the perivascular niche marked by STRO-1⁷³, which was found in 5 of 7 samples tested (Fig. 4.2D). In a similar frequency, Cadherin family member 9 (CELSR1)¹²⁰, a proposed cell quiescence marker co-labelled with GLI1 at the putative nerve bundles (Fig. 4.2E).

Human dental pulp tissue characterisation

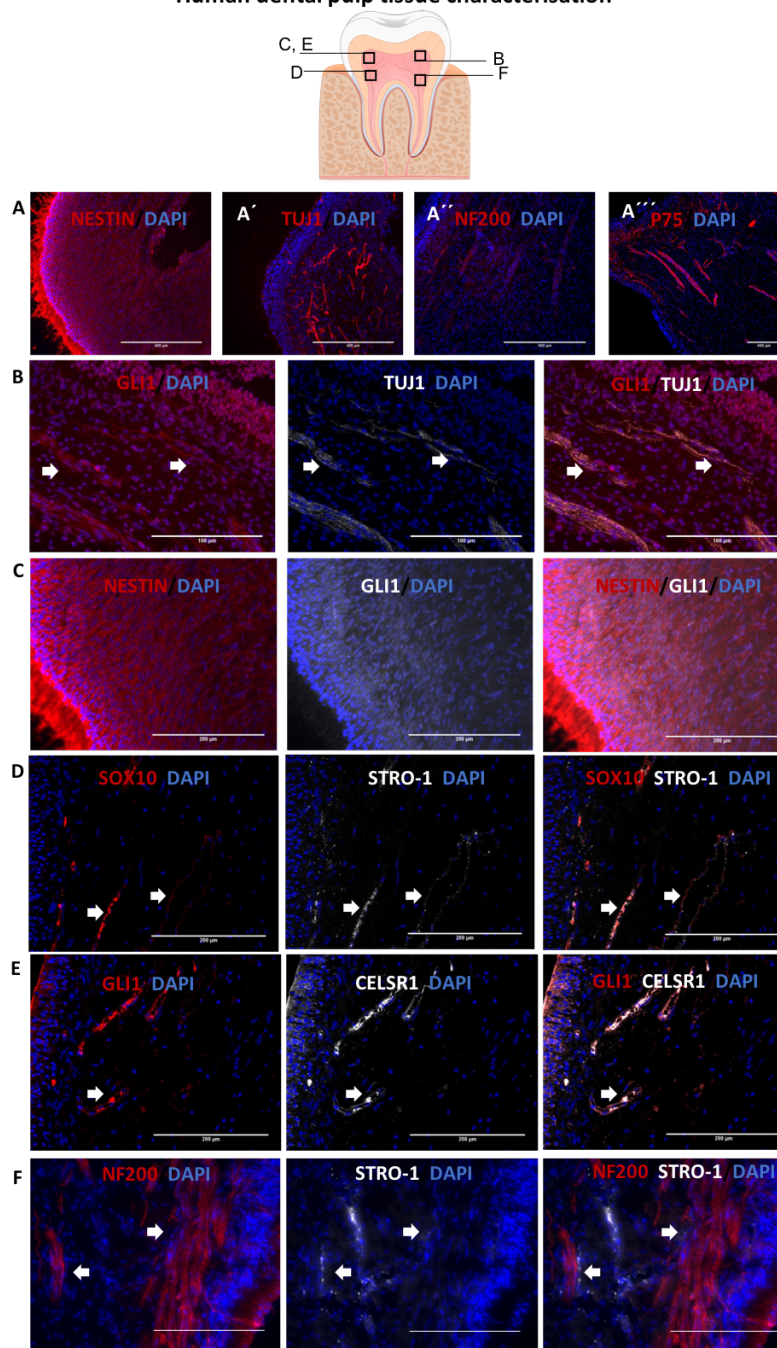


Figure 4.2. In situ characterisation of human dental pulp tissue. Sections of human dental pulp tissue labelled for relevant markers. On top an approximate reference of section position. A) General pulp overview of the neural crest marker NESTIN, and the innervation labelled by TUJ1 (A'), NF200 (A'') and P75 (A'''). B) Colocalization of GLI1 and TUJ1 is observed in the nerve bundles, GLI1 expression also present throughout the pulp. C) Colocalization and permanent expression of NESTIN and GLI1. D) Rare SOX10 expression colocalizing with STRO-1 in the putative perivascular niche. E) GLI1 also found co-localising with CELSR1 marker in putative nerve bundles. F) Nerve bundles positive for NF200 co-localising with STRO-1. Arrows show dual labelling in all cases. Scale bar: A) 400µm, B, F) 100µm, C, D, E) 200µm.

4.3. Human dental pulp cell cultures can be established in different growth conditions.

We establish *in vitro* cultures to investigate the potential of human dental pulp cells (hDPCs) in deafness therapies. Three basal conditions were selected to culture hDPCs directly from tissue. First, the standard serum-containing medium (FBS), widely used in the literature containing 20% FBS. The second medium was the Otic Stem Cell Full Medium (OSCFM), which can maintain the proliferation of neural progenitor cells *in vitro* and contains EGF, bFGF and IGF³². Finally, OSCFM supplemented with Bone Morphogenic Protein 4 (BMP4), which has been identified as a key factor for sensory neural differentiation and neural crest formation¹²¹ (See methods for further information).

The *in vitro* efficiency of each culture system was determined by recording the number of cultures that managed to survive, proliferate and be passaged in each group for more than 4 passages. The highest success rate of surviving cultures was FBS, followed by OSCFM and BMP4 with 80.95% (n=21), 61.11% (n=18) and 29.41% (n=17) respectively (Fig. 4.3A). As mentioned above, the conditions of the samples varied from patient and were categorised as intact, caries and fragmented (broken) during extraction. Dental pulp culture establishment from intact teeth had 76.66% of efficiency (n=30) caries had a small impact in efficiency with 54.54% (n=11) of the cultures surviving and stablishing in culture conditions. On the other hand, fragmented teeth did not allow a quality extraction and processing, which was reflected in only 33.33% (n=6) of efficiency to stablish cultures (Fig 4.3B). Due to the low efficiency of the fragmented teeth, those samples were excluded from the calculations (Exclusion Criteria-EC). Also, two samples from a 52-year-old and a 61-year-old patient were excluded due to the lack of pulp within the teeth. Another exclusion criteria was when the sample information obtained was incomplete (i.e. age/condition not written during the collection). Considering the EC, efficiencies elevated to 93.75% (n=16) in FBS cultures, whereas OSCFM had 81.81 (n=11) and BMP4 35.71% (n=14). Age was another variable in our samples, efficiency was calculated based on three main age gaps: Young: 15-20 Yrs, Middle: 21-30 Yrs and Old > 30 Yrs. The young gap had 50% (n=12) efficiency rate, while the highest efficiency was achieved from samples in the middle gap with 80.95%

(n=21). Samples taken from patients older than 30 Yrs were successful in 66% (n=9) of the attempts (Fig 4.3D). However, consideration should be made to the specific conditions. FBS Cultures were highly successful throughout, with the lowest at the young aged samples with 66% of success (Fig. 4.3E). OSCFM cultures were established with greater frequency from samples in the middle age gap (100%; n=7), followed by the youngest (n=4) and oldest (n=2) both with 50% success rate (Fig. 4.3F). On the other hand, BMP4 cultures had the lowest efficiency rate overall and success increased with age from the young (40%; n=5), to the middle (20%; n=5) and the highest efficiency from cultures derived from older patients (50%; n=4; Fig. 4.3G).

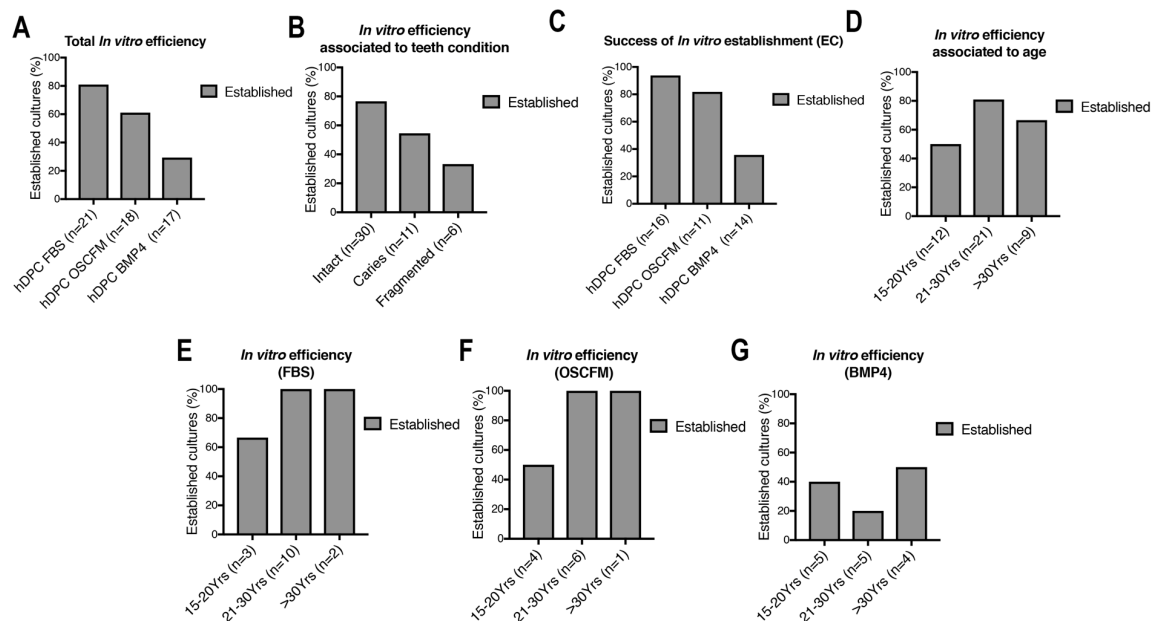


Figure 4.3. Efficiency of culture establishment. The percentage of success of individual samples to grow *in vitro* calculated from the samples under the following criteria: A) Total samples collected for culture establishment, B) Teeth condition, C) with exclusion criteria (refer to text), D) associated to age, E) grown in FBS medium (refer to text), F) grown in OSCFM medium (refer to text) and G) grown in BMP4 medium. FBS: 20% foetal bovine serum-DMEM. OSCFM: Otic stem cell full medium. BMP4: OSCFM + Bone morphogenic protein 4.

Once in culture, successful *in vitro* establishment was more evident after 3 to 4 weeks. By this time, the proliferating cells expanded more rapidly usually within a colony, by the end of this period cells were passaged. Established cultures *in vitro* showed a variety of composition containing cells with different morphology. The cultures emerged from tight

colonies or from more spread-out cell groups. Also, fibroblastic and epithelial-like cells were observed in all culture conditions. This heterogeneity was observed even in cultures within the same culture condition (Fig. 4.4). A neural-like morphology was also evident in cultures derived in OSCFM and BMP4, providing another cell type in our conditions (Fig. 4.5). After 4 weeks, the cultures were passaged for further expansion. The effect of passaging in cell culture was monitored in all our conditions. Bright field images were taken at early passage and followed until later passages. Cultures grown in FBS remained similar to their younger versions until late passages, where the cells proliferated slower and took longer to reach confluence (Fig 4.6A-hDPC16). hDPC in OSCFM had a similar pattern, but the cell morphology was evidently more variant at later passages. As an example, hDPC 20 and 24 in OSCFM at passage P9 and P10 respectively, changed to a flat morphology with expanded cytoplasm (Fig 4.6B). Finally, BMP4 cultures initially presented a fibroblastic morphology, which continued through cell passaging. Interestingly, BMP4 cultures began to change earlier in passaging (P5-P6), and aggregated leaving empty spaces in the surface, rather than expanding on the whole area (Fig 4.6C). The neural-like cells disappeared after passage 1 in both OSCFM and BMP4 cultures.

Human dental pulp primary cultures (p0)

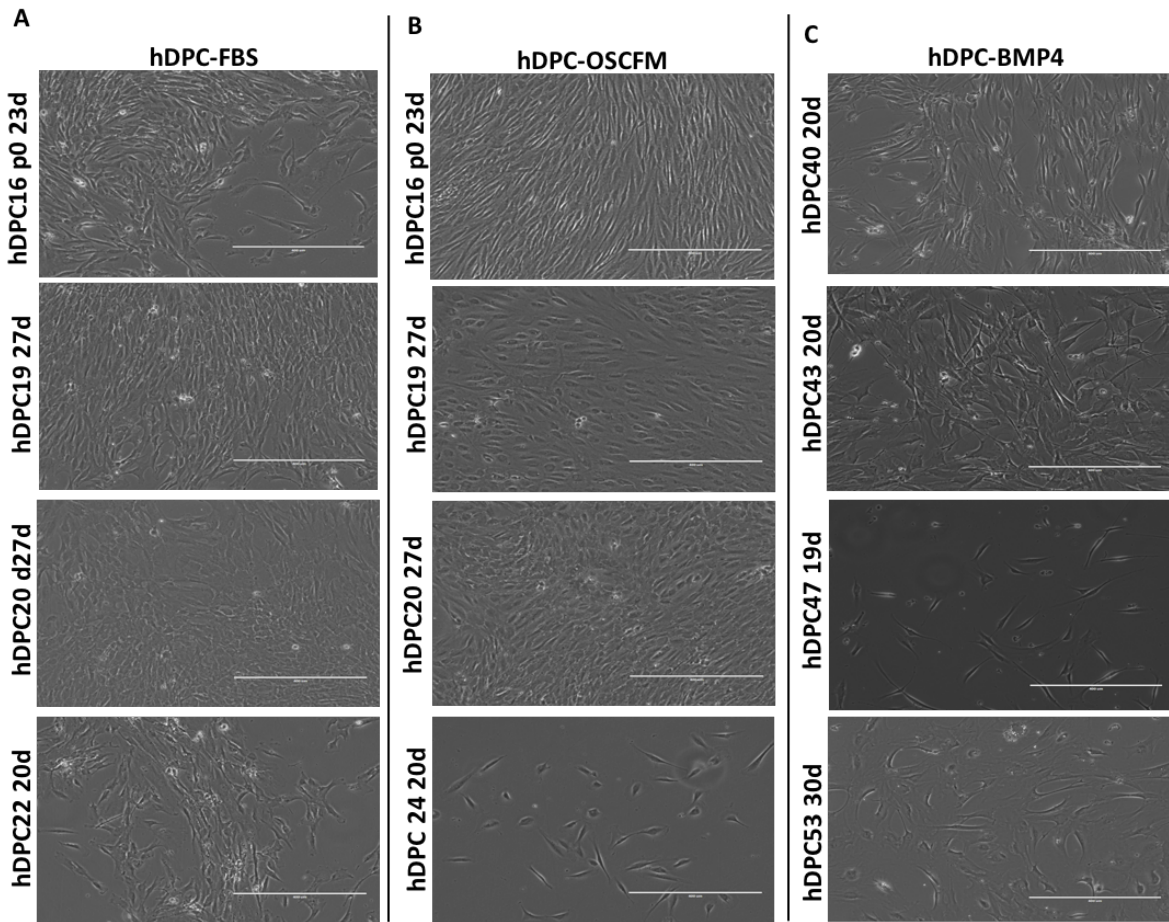


Figure 4.4. Morphology of primary cultures (Passage 0) growing in the different culture media. Each image represents a culture established from a different subject at passage 0 (p0) in either FBS, OSCFM or BMP4. The very tight or close together cells with epithelial-like morphology usually represented growing colonies: A) FBS-hDPC19 and hDPC20, B) OSCFM-hDPC 16, 19 and 20. Spread out cell groups were seen with fibroblastic, polymorphic shape: A) FBS-hDPC16 and hDPC22, B) OSCFM-hDPC24, C) BMP4-hDPC47 and hDPC53. Scale bar: 400 μ m. FBS: 20% foetal bovine serum-DMEM. OSCFM: Otic stem cell full medium. BMP4: OSCFM + Bone morphogenic protein 4.

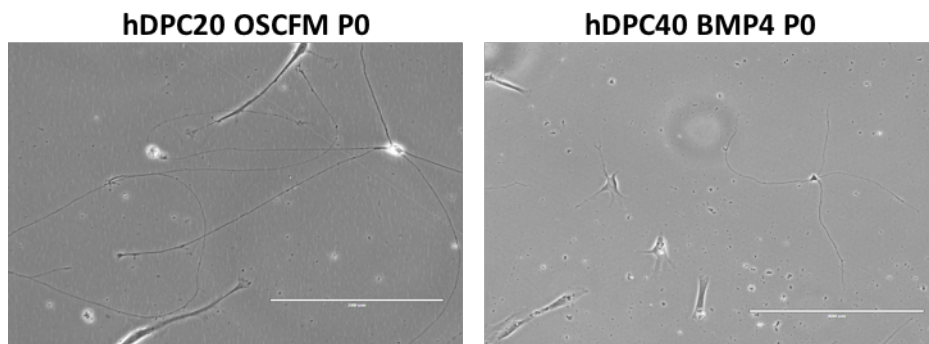


Figure 4.5. Neural Morphology in passaged 0 primary cultures. Cell with thin and long projections were evident among the other cell types in culture. OSCFM and BMP4 cultures commonly contain this cell type at

P0. Scale bar: 200µm (OSCFM), 400µm (BMP4). OSCFM: Otic stem cell full medium. BMP4: OSCFM + Bone morphogenic protein 4.

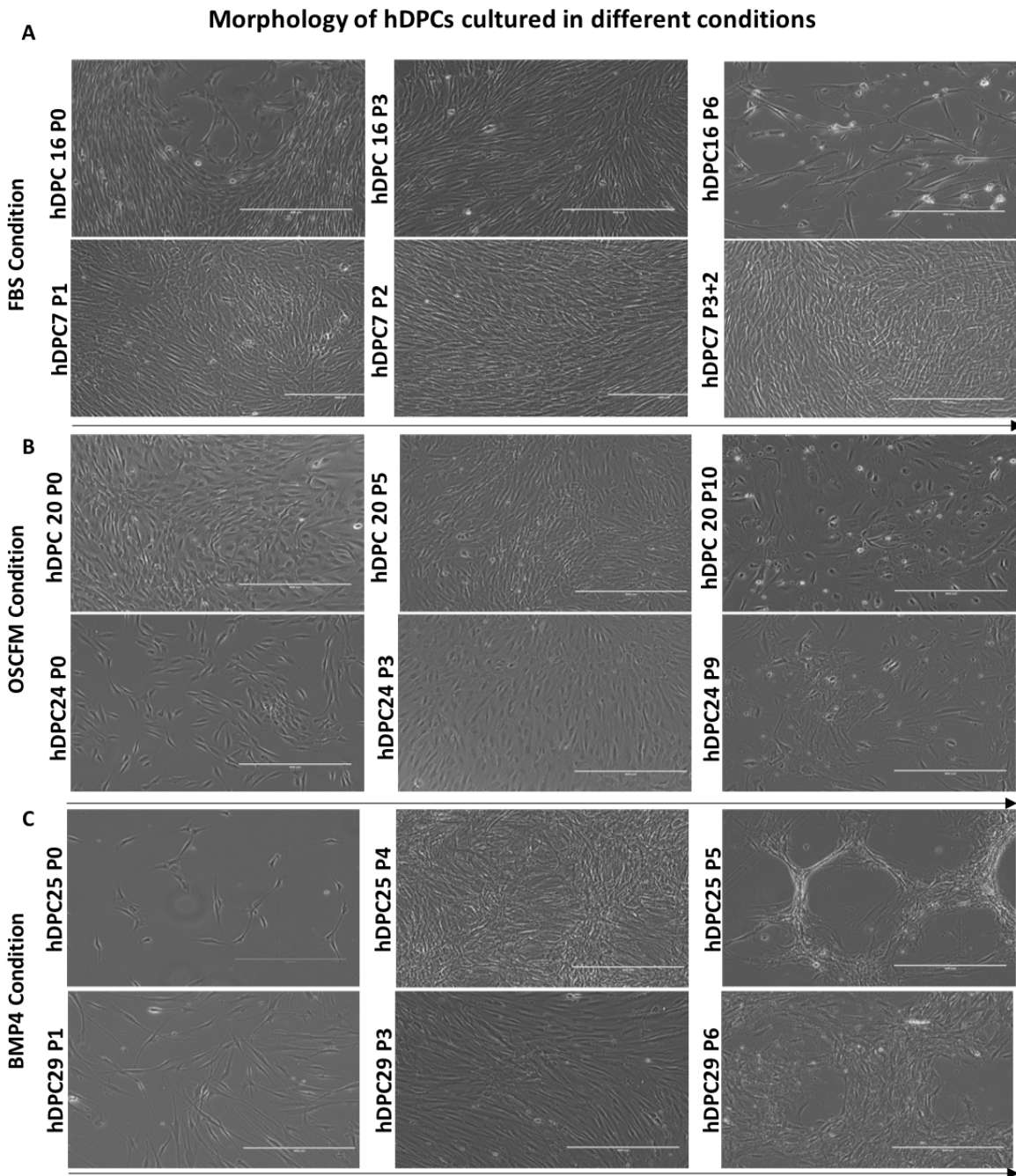


Figure 4.6. Human dental pulp cells' morphology and changes. Comparison of independent cultures grown in different conditions (FBS, OSCFM and BMP4) and changes in relation to their passage number (Indicated by P0-P10). Passaging in the cultures is arranged from left to right in ascending order Two separate cultures from each condition are shown as example at early and later passages. A) FBS cultures, B) OSCFM cultures, C) BMP4 cultures. Scale bar: 400µm. FBS: 20% foetal bovine serum-DMEM. OSCFM: Otic stem cell full medium. BMP4: OSCFM + Bone morphogenic protein 4.

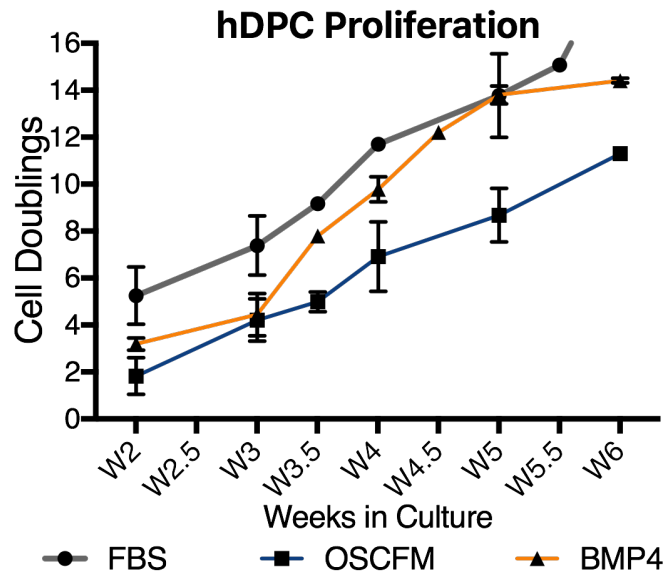


Figure 4.7. hDPC culture proliferation. A) Cell doublings per week (W) were calculated for the three different culture conditions. Averages from 2-6 different cultures from each condition were taken when possible. Data points with no error bars represent a single cell culture. B) Average cell doublings per passage. Passages 2 to 6 from 5-6 independent cell cultures were averaged per condition. FBS: 20% foetal bovine serum-DMEM. OSCFM: Otic stem cell full medium. BMP4: OSCFM + Bone morphogenic protein 4.

We continued to investigate the *in vitro* behaviour, hDPCs were counted at every passage to calculate the cell doublings per week. To calculate the total number of cell doublings during the first 6 weeks, the counts were added to the previous counts each week (cell doubling = $3.32(\text{Log UCY} - \text{Log I}) + X$), where UCY is the final cell count, I is the initial cell number seeded and X the previous cell doubling number (American type culture collection-ATCC). The proliferation curve suggested a larger cell growth in FBS cells, followed by BMP4 cultures. Seemingly, OSCFM cultures presented the lowest proliferation (Fig. 4.7). Proliferating cultures usually reached confluence at day 7, and were the ones used for downstream experiments. It must be mentioned that slow-proliferating cultures were also observed in cultures from all conditions but did not reach more than 4 passages. The

experiments performed on the slow proliferating cultures were limited due to the low cell count and reached confluence later than 7 days.

4.4. Expression of basal markers in human dental pulp cultures.

Once culture establishment was optimised, we aimed to characterise, at the molecular level, the expression of relevant markers for neural progenitor, neural crest and a mesenchymal stem cell marker. We used immunocytochemistry (ICC) to obtain a qualitative description of the cultures. A summary of the expression of relevant markers is located in table 4.2.

Overall, hDPC cultures from all conditions clearly expressed the neural crest associated markers NESTIN, Snail family transcriptional repressor 2 (SLUG), Myelin protein 0 (P0) and Glioma-associated oncogene homolog 1 (GLI1), the last three in a very defined nuclear localisation, while NESTIN was cytoplasmic. SNAIL1 was weakly expressed in FBS and OSCFM media, and seemingly slightly stronger in BMP4 cultures. The transcription factors SRY BOX2 (SOX2), SRY BOX9 (SOX9) and SRY BOX10 (SOX10) presented a cytoplasmic pattern, not completely nuclear (Figure 4.8-4.10).

Cultures were particularly heterogeneous for Nerve grow factor receptor (P75) and STRO-1. These markers have special relevance, since p75 will primarily label a neurogenic population of Neural Crest cells, while STRO-1 has been associated with the more mesenchymal derivatives of the Neural Crest^{122,123}. This prompted us to quantify the number of positive cells in each condition and their changes through passaging. The number of cells expressing the mesenchymal marker STRO-1 increased during passaging regardless of the culture condition (Fig. 4.12A). Contrastingly, P75 was not identified by fluorescence microscopy in cultures after passage 1, and when present, it was only occasionally detected in a few cells. (Fig. 4.12B).

| | Neural progenitor | | | Neural Crest | | | | | | | MSC |
|---------------|-------------------|-----------------|----------------|----------------|---------------|-----------------|-------------------|----------------|---------------|----------------|-------|
| | GLI1 | SOX2 | NESTIN | NESTIN | SLUG | SNAIL1 | SOX9 | SOX10 | P0 | P75* | STRO1 |
| hDPC FBS | ++ N n=8 | + CN n=11 | ++ C n=6 | ++ N n=2 | + N n=2 | ++ CN n=7 | + CN n=7/11 | ++ N n=6 | + C n=3 | ++ C n=6 | |
| hDPC OSCFM | ++ N n=3 | + CN n=3 | ++ C n=6 | ++ N n=2 | + N n=2 | ++ CN n=7 | + CN n=3 | ++ N n=4 | + C n=3 | ++ C n=6 | |
| hDPC BMP4 | ++ N n=2 | + CN n=2 | ++ C n=2 | ++ N n=2 | + N n=2 | ++ CN n=1 | + CN n=1 | ++ N n=1 | + C n=4 | ++ C n=6 | |

Table 4.2. hDPC characterisation by ICC. The expression of neural progenitor, neural crest and a mesenchymal stromal marker (MSC) was evaluated in our culture conditions from different passage number (P0-P4). High signal (++), Medium signal (+-), very low signal (+--). N= Nuclear, C= Cytoplasmic, CN= Nuclear and cytoplasmic. n=number of independent cultures. *P75 was mainly present at passage 0. FBS: 20% foetal bovine serum-DMEM. OSCFM: Otic stem cell full medium. BMP4: OSCFM + Bone morphogenic protein 4.

hDPC Characterisation by ICC (FBS n=2-6)

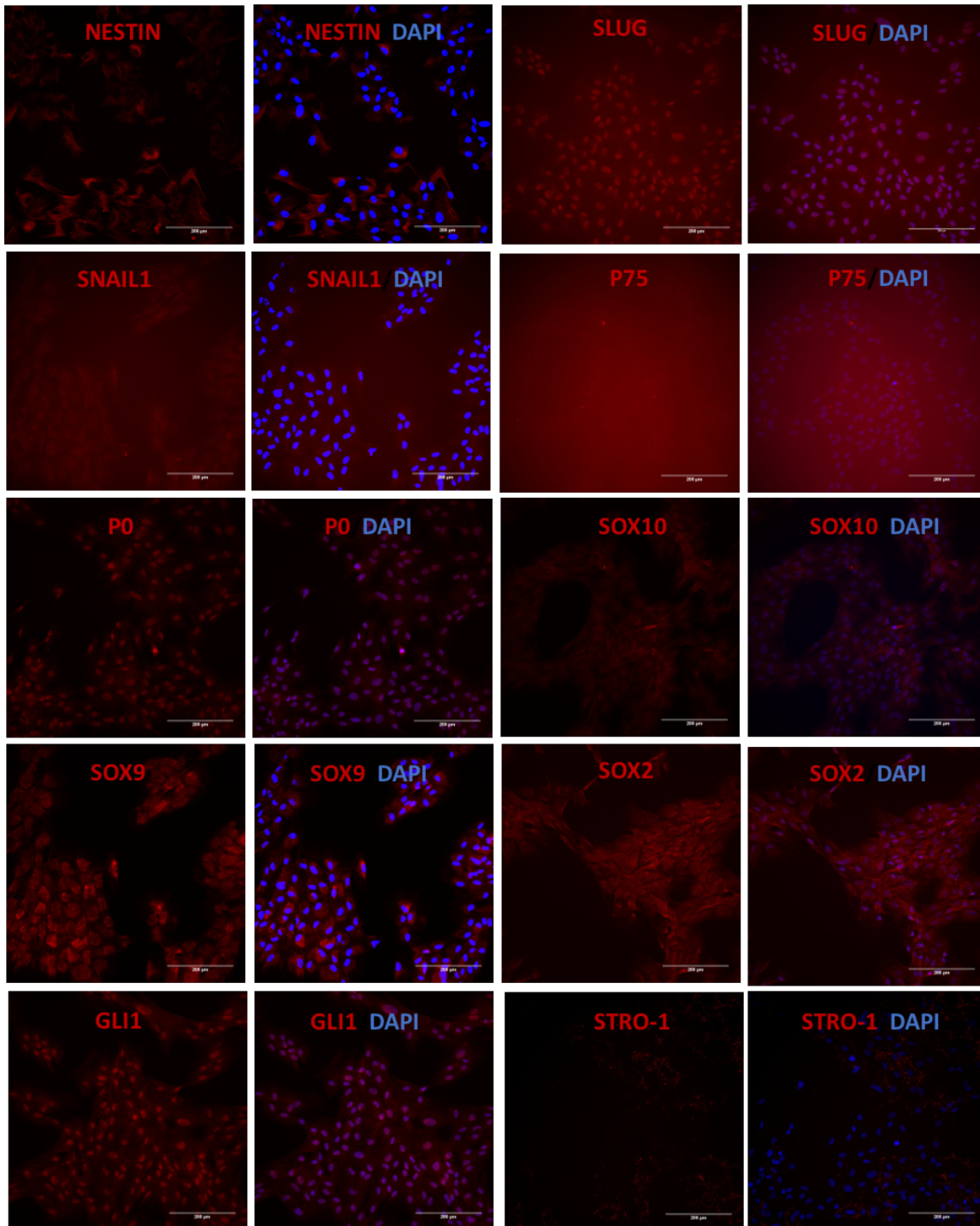


Figure 4.8. Characterisation of hDPC-FBS cultures by ICC. The expression of relevant markers was evaluated in hDPC derived in FBS medium by ICC. The presence of NESTIN, SLUG, GLI1, STRO-1 and cytoplasmic presence of SNAIL1, SOX2, SOX9 and SOX10 can be seen. Poor or null P75 signal is also evident. Scale bar= 200µm. For each marker, the image was taken with the same configuration among treatments to allow comparison.

hDPC Characterisation by ICC (OSCFM n=2-6)

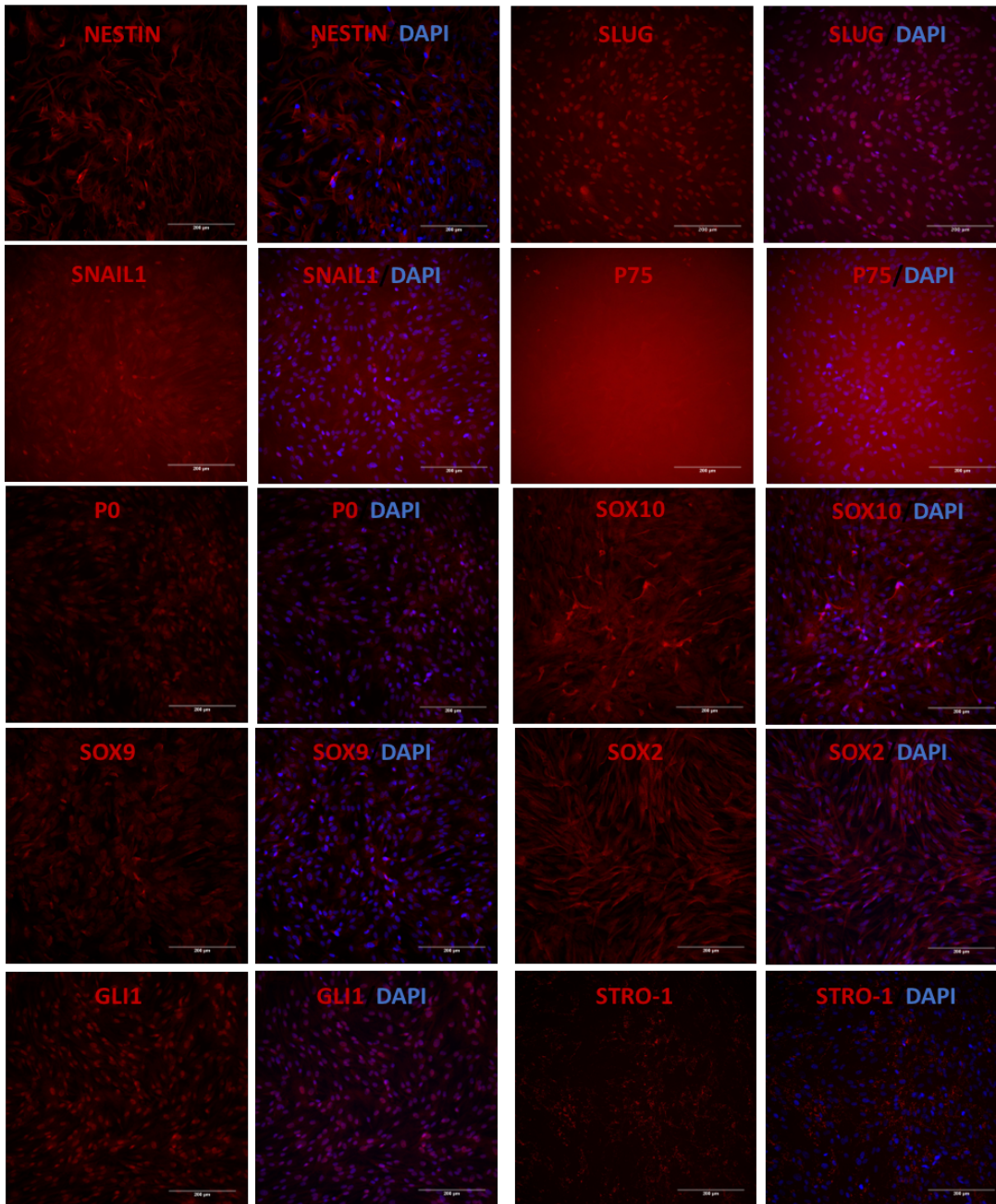


Figure 4.9. Characterisation of hDPC-OSCFM cultures by ICC. The expression of relevant markers was evaluated in hDPC derived in Otic stem cell full medium (OSCFM) by ICC. The presence of NESTIN, SLUG, GLI1, STRO-1 and cytoplasmic presence of SNAIL1, SOX2, SOX9 and SOX10 can be seen. Poor or null P75 signal is also evident. Scale bar= 200µm. For each marker, the image was taken with the same configuration among treatments to allow comparison.

hDPC Characterisation by ICC (BMP4 n=2-6)

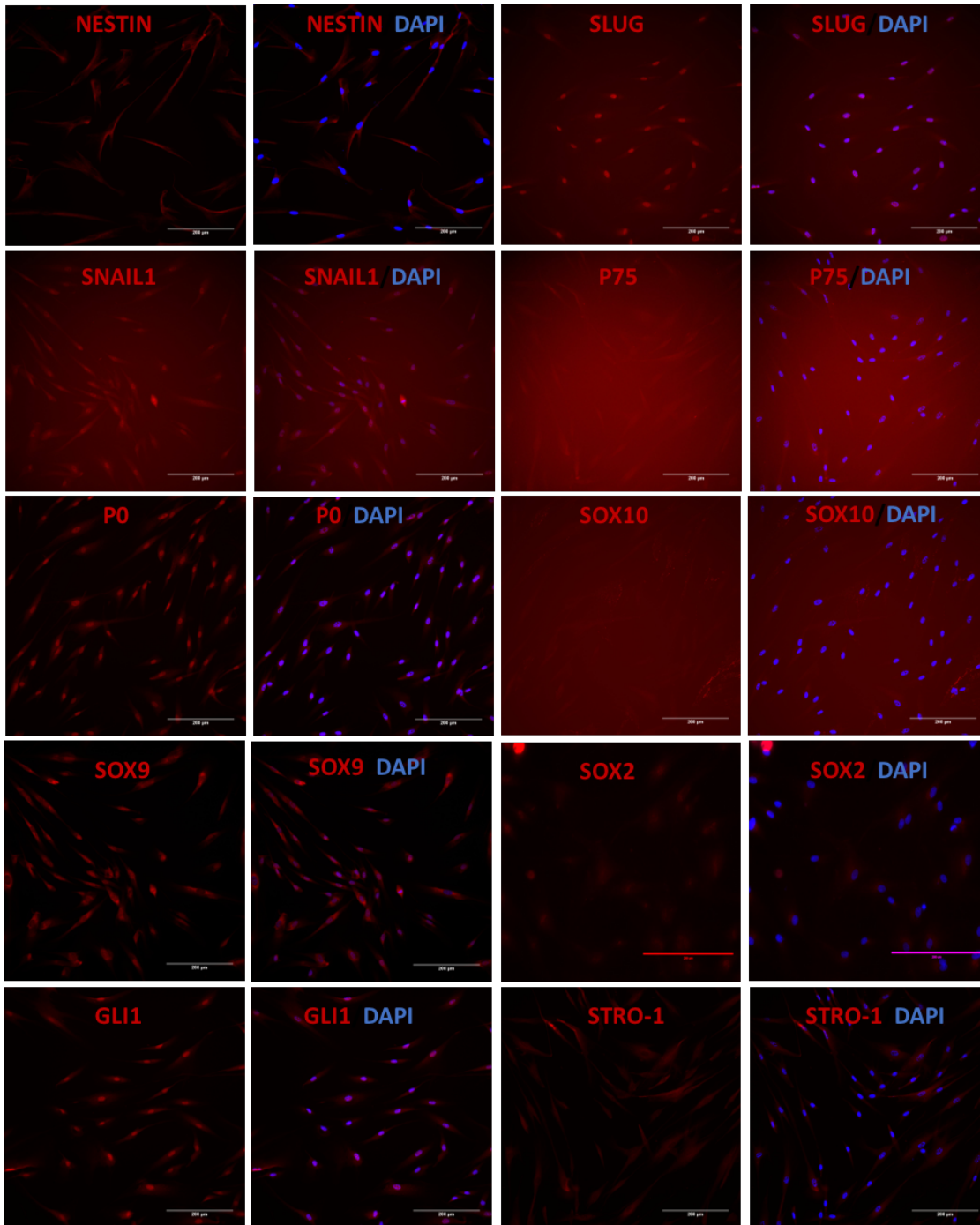


Figure 4.10. Characterisation of hDPC-BMP4 cultures by ICC. The expression of relevant markers was evaluated in hDPC derived in BMP4 medium (OSCFM + BMP4) by ICC. The presence of NESTIN, SLUG, SNAIL1, GLI1, SOX2 and STRO-1 and cytoplasmic presence of SOX9 and SOX10 can be seen. Poor or null P75 signal is also evident. Scale bar= 200µm. For each marker, the image was taken with the same configuration among treatments to allow comparison.

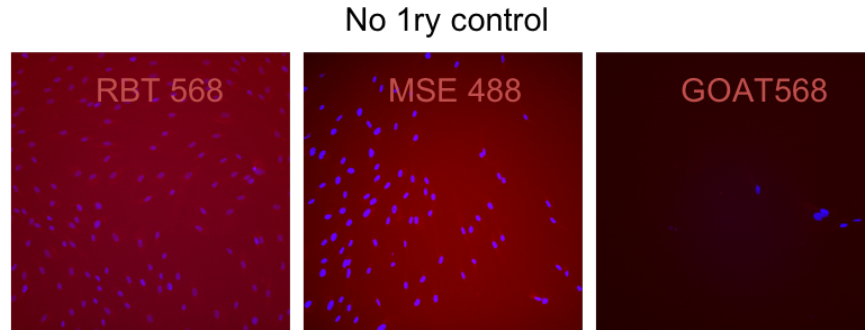


Figure 4.11. No primary controls. No primary antibody controls are shown for Goat-568, Rabbit 568 and Mouse 488 Alexa Fluor secondary antibodies.

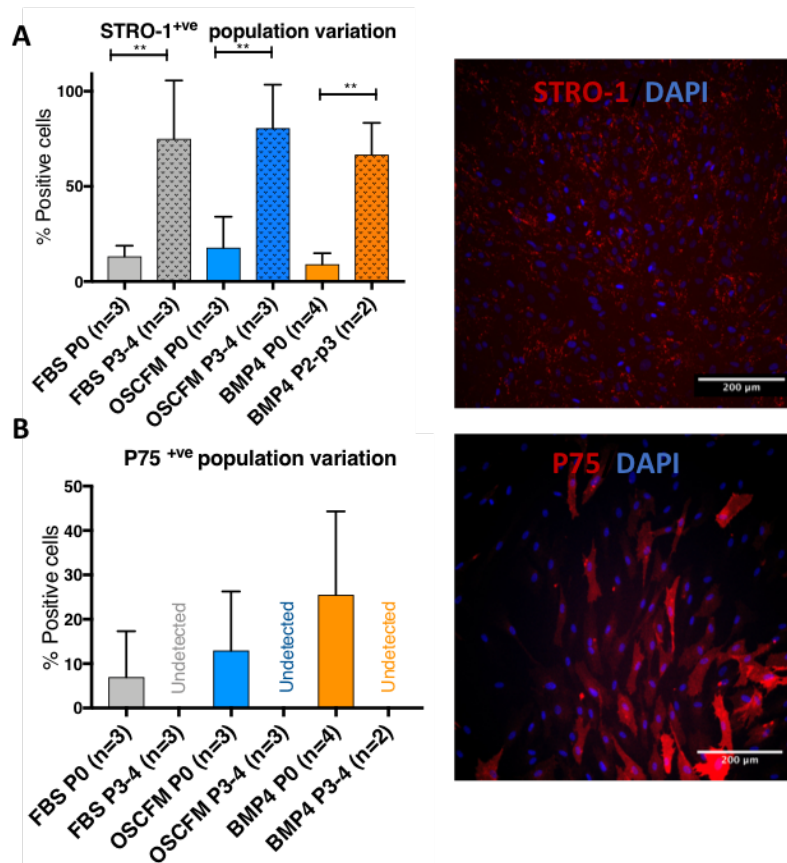


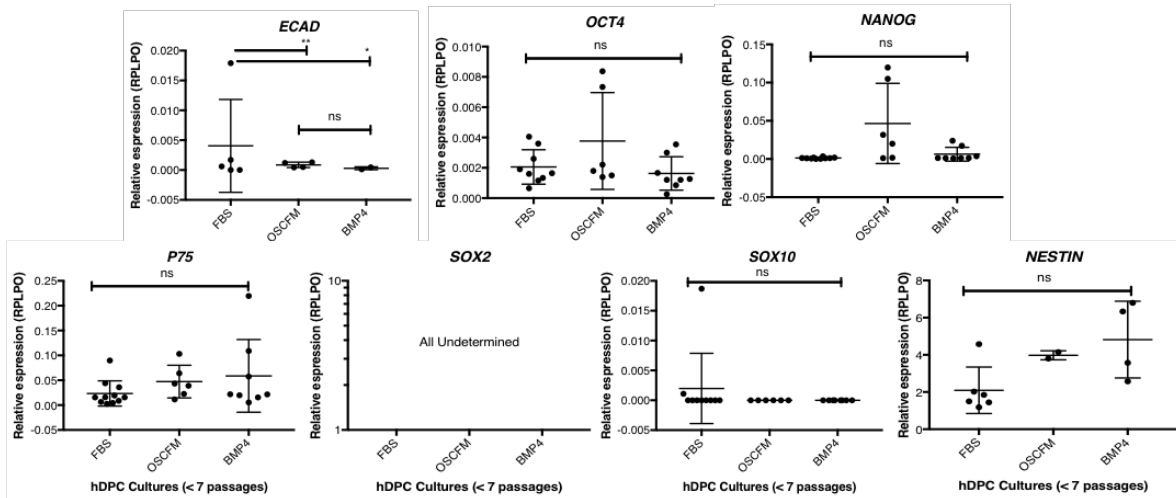
Figure 4.12. STRO and P75 Immunocytochemistry (ICC) quantification. A) hDPC cultures presented an increase in STRO-1 positive cells with passage number (Left). Representative image of STRO-1 by ICC (Right). B) hDPC cultures presented a decrease in P75 positive cells with passage number (Left). Representative image of P75 by ICC (Right). Scale bar: 200µm. One way-ANOVA followed by Sidak's pairwise comparison test. **P<0.01. FBS: 20% foetal bovine serum-DMEM. OSCFM: Otic stem cell full medium. BMP4: OSCFM + Bone morphogenic protein 4.

The molecular signature of human dental pulp cell culture was also evaluated at the mRNA level by relative expression analysis using quantitative PCR (RT-qPCR). To normalise the

data, all hDPC cultures were compared to the pluripotent embryonic stem cell line H14 S9. The pluripotent stem cell markers *OCT4*, *NANOG* and *SOX2* were evaluated together with the neural crest markers *SOX10*, *P75* and the epithelial marker *ECAD* in young cultures (<P7). *OCT4*, *NANOG*, *P75* and *ECAD* were present in individual cultures at variable levels while *SOX2* and *SOX10* mRNAs were not detected. (Fig. 4.13A).

The average for each hDPC condition was calculated and a One-way-ANOVA was performed, followed by a Tukey test. Only *ECAD* in FBS appeared statistically different from the other conditions. Variance from patient to patient within the same conditions evidenced the heterogeneity of human dental pulp cells, regardless of the initial media condition in which the primary cultures were established (Fig. 4.13A). We also analysed the basal expression of the neural markers *NFH*, *VGLUT1*, *TUBIII*, *SYN* and *SYP*, relative to ESC-derived ONPs, a well-characterised population of otic neural progenitors. The results showed a basal expression of the neural markers with an overall average higher in hDPC-OSCFM cultures, but not statistically significant across the hDPC cultures (Fig. 4.13B).

A) hDPC Basal Characterisation (qPCR)



B)

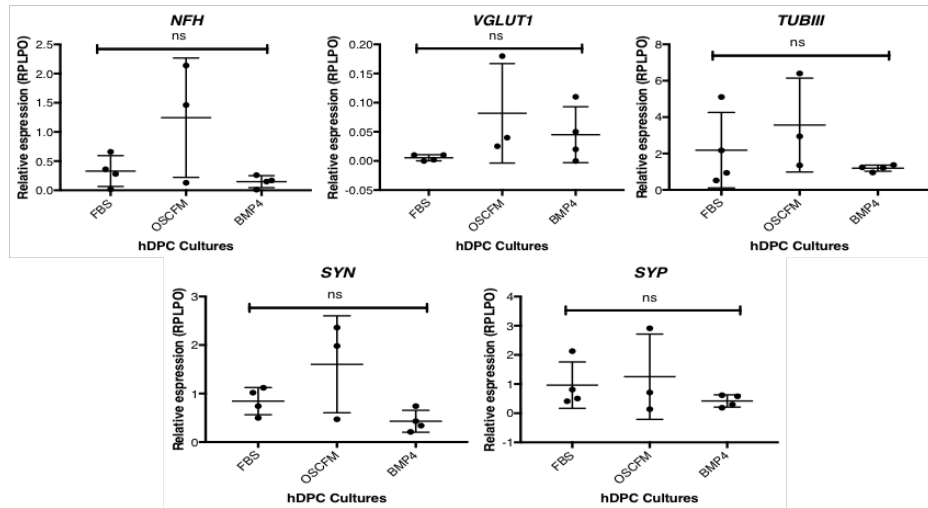


Figure 4.13. hDPC RT-qPCR characterisation-Averages. Cultures grown in the basal conditions (FBS, OSCFM and BMP4) were subjected to a relative gene expression analysis. The graph shows the expression of A) Pluripotent and neural crest-related markers compared to the embryonic stem cell line H14 S9 and B) the expression of neural-related markers compared to otic neural progenitors (ONPs) in basal conditions. *P<0.05, **P<0.01. FBS: 20% foetal bovine serum-DMEM. OSCFM: Otic stem cell full medium. BMP4: OSCFM + Bone morphogenic protein 4.

4.5. Differentiation of Human dental pulp cells into auditory neurons.

After characterising the hDPC cultures we were interested in looking at their potential to differentiate into auditory neurons that could be used in deafness therapies. Based on the marker expression, we hypothesised that the cultures could differentiate further into inner ear neurons. The protocol that was followed was chosen based on the reported generation of spiral ganglion neurons from human foetal auditory stem cells (hFASC) and ESC-derived ONPs after an initial induction phase with Sonic Hedgehog, followed by neurotrophin supplementation.^{31,32} We analysed results from at least 3 independent experiments for hDPC-FBS and hDPC-BMP4 cultures and one OSCFM culture.

The cultures presented only minor morphologically changes after inducing the cells with media containing Sonic Hedgehog, NT3 and BDNF for 12-14 days (Refer to methods, diagram 4.1). hDPC-FBS cultures presented a more elongated cell body after induction. The hDPC-OSCFM cultures presented some elongated cells but remained largely unchanged. The hDPC-BMP4 cells behaved similar to cultures in OSCFM, with no particular change. Overall, a definitive neural morphology was not apparent in any hDPC culture (Fig. 4.14A). We then looked at the expression of neural markers after neural induction, the data was analyzed by One-way-ANOVA followed by Sidak's Multiple comparisons test. The results largely confirmed a lack of upregulation of neural genes. hDPC-FBS cultures presented an upregulation of the pan-neural markers *NFH* and *TUBIII* in one of the cultures analyzed but did not present an upregulation of the sensory-related markers *SYN*, *SYP* and *VGLUT*. hDPC cultures from OSCFM and BMP4 didn't present an upregulation in any of the observed genes, but rather significantly downregulated some of them (*TUBIII* in OSCFM and *SYN*, *VGLUT1* in BMP4; Fig. 4.14B and Fig S3, S4).

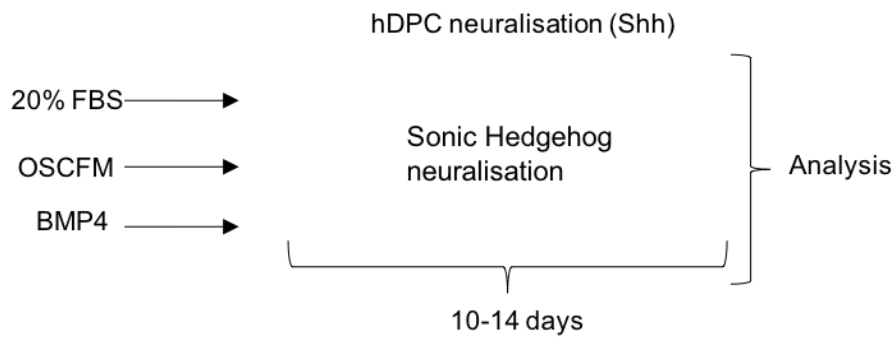


Diagram 4.1 hDPC neuralisation with Sonic hedgehog (Shh) protocol. Human dental pulp cells from our 3 basal conditions were treated with the Sonic hedgehog neural differentiation protocol for 10-14 days. OSCFM: Otic Stem Cell Full Medium; BMP4: OSCFM + Bone Morphogenic protein 4. Sonic Hedgehog protocol contained bFGF, Sonic Hedgehog, NT3, BDNF (refer to material and methods for further details).

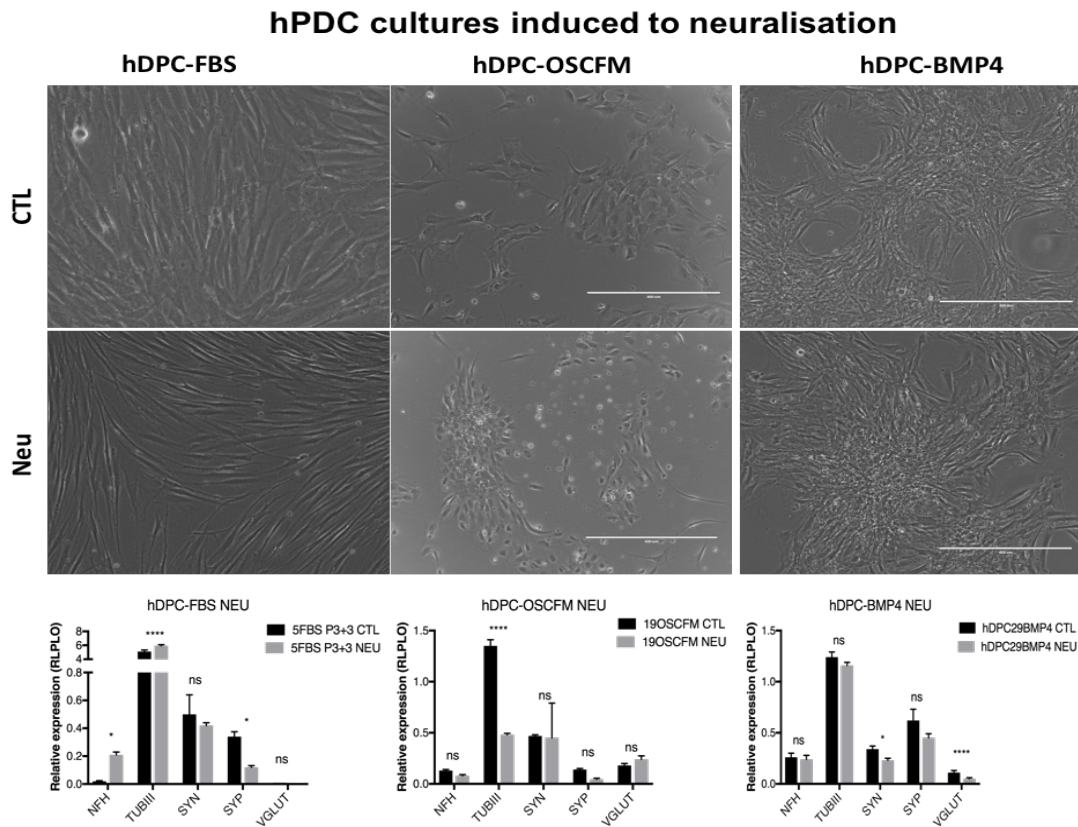


Figure 4.14. hDPC after neural induction. hDPC from different conditions after 12-14 days of otic neural induction. A) Bright field images showing the morphology of cell cultures in the control (CTL) basal conditions (FBS, OSCFM or BMP4) and after neural induction (Neu). B) Relative expression analysis normalised to otic neural progenitor cells (ONPs). * $p < 0.05$, *** $p < 0.001$, **** $p < 0.0001$. Error bars represent technical replicates. Scale bar: 400 μ m. CTL: Undifferentiated, Neu: Neural induced. Similar results were observed in at least 2 other independent experiments for FBS and BMP4 cultures. OSCFM was only analysed once by RT-qPCR. FBS: 20% foetal bovine serum-DMEM. OSCFM: Otic stem cell full medium. BMP4: OSCFM + Bone morphogenic protein 4.

4.6. Differentiation of Human dental pulp cells into Schwann Cells.

To further evaluate the potential of human dental pulp cells, we attempted to differentiate them into Schwann cells. Because glial cells play key roles in peripheral nerve regeneration, and hDPCs have been shown to differentiate into a glial fate, we tried to replicate two protocols for Schwann cell differentiation on our hDPCs grown under defined conditions. We tested a protocol that has been tested on mesenchymal stem cells and a protocol that has been used on neural crest cell derived from embryonic stem cells. The former is referred as “Dezawa’s” while the latter as “Studer’s”, based on the publishing authors (Diagram 4.2)^{38,97}.

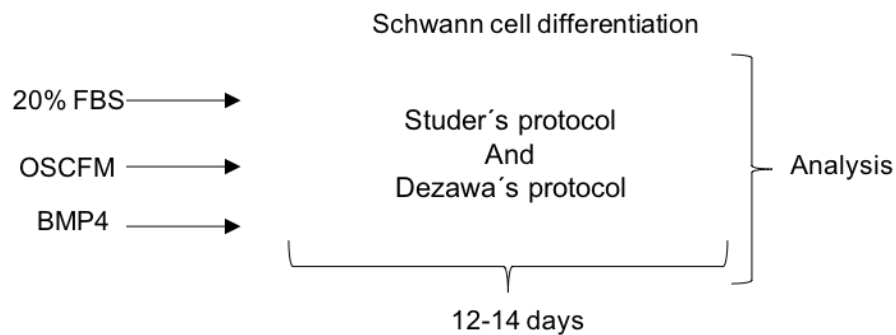


Diagram 4.2. hDPC-Schwann cell differentiation. Human dental pulp cells from our 3 basal conditions were treated in two independent Schwann cell differentiation protocols: Studer’s and Dezawa’s for 12-14 days. Studer’s protocol contained dbcAMP, bFGF, CNTF, Neuregulin. Dezawa’s protocol contained β -ME, Retinoic Acid, PDGF-AA, HER- β 1, Forskolin, bFGF (Refer to materials and methods for further details). OSCFM: Otic Stem Cell Full Medium; BMP4: OSCFM + Bone Morphogenic protein 4.

After the treatment for Schwann cell differentiation, hDPC cultures presented evident changes in morphology. After 12-14 days in culture, all the control groups growing in their respective basal media (FBS, OSCFM and BMP4) were very confluent. Cell morphology after Dezawa’s protocol presented some similarities among the hDPC groups. Cultures presented an organised swirling pattern and also a distinctive cell type with round and small cell body. On the other hand, the Studer’s protocol gave rise to a similar morphology pattern, but also to more of these round and small cells, in some cultures more abundant than others. In a first glance, these particular cell types looked more neuron-like (Fig. 4.15).

To determine if the cultures presented features of a Schwann cell phenotype, a relative expression analysis was done for the glial-related genes: *SOX10*, *GFAP*, *MBP*, *P75* and *S100 β* .

From the 3 independent cultures for hDPC-FBS and hDPC-OSCFM and a single culture for hDPC-BMP4, it was found that *SOX10* and *GFAP* were largely absent even after the Schwann cell treatments using both protocols. Only one hDPC-OSCFM culture after the Studer's protocol upregulated *SOX10*. Myelin Binding Protein (MBP) presented mixed results. One culture from each condition under the Studer protocol presented an upregulation of this gene. However, one hDPC-OSCFM culture showed a downregulation and the rest of the cultures didn't present a significant change with this protocol. In the case of Dezawa's protocol, there wasn't any important change using this approach. For P75, one hDPC-FBS culture under the Dezawa's protocol and the hDPC-BMP4 culture under the Studer's protocol, presented an upregulation of P75, the rest of the cultures did not change significantly or were downregulated (hDPC19 OSCFM). S100 β expression was clearly induced the Studer's protocol in 2 hDPC-FBS and 2 hDPC-OSCFM cultures. S100 β was also induced in hDPC-FBS under the Dezawa's protocol. Overall, important glial markers such as *SOX10* and *GFAP* are absent, and the variant presence of the observed upregulated markers suggest an incomplete Schwann cell differentiation in both protocols tested (Fig. 4.16).

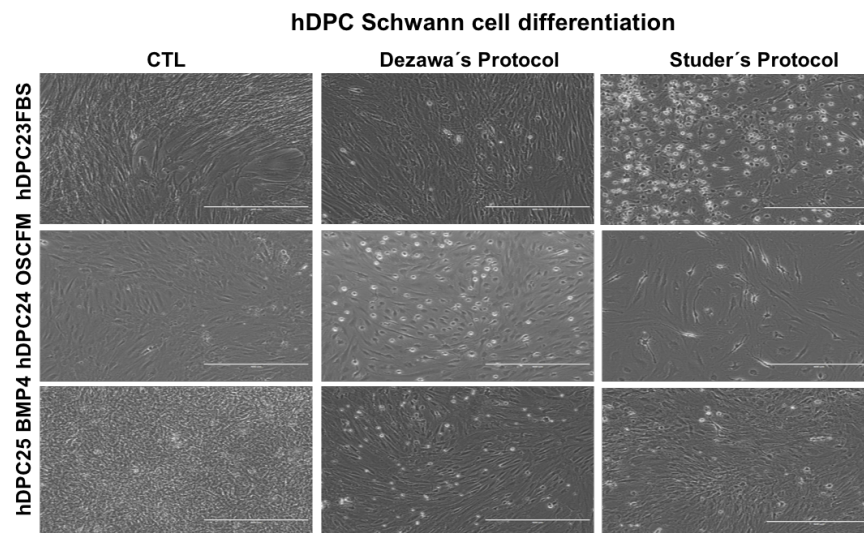


Figure 4.15 hDPCs Schwann cell differentiation. Bright field images of hDPC-FBS, OSCFM and BMP4 after treatments for Schwann cell differentiation. Control (CTL) groups are untreated samples growing in their respective media conditions (FBS, OSCFM or BMP4). Treated cells were induced using protocols described in the literature by Dezawa's³⁸ and Studer's⁹⁷. Scale bar: 400 μ m. FBS: 20% foetal bovine serum-DMEM; OSCFM: Otic Stem Cell Full Medium; BMP4: OSCFM + Bone Morphogenic protein 4.

Schwann Cell Differentiation

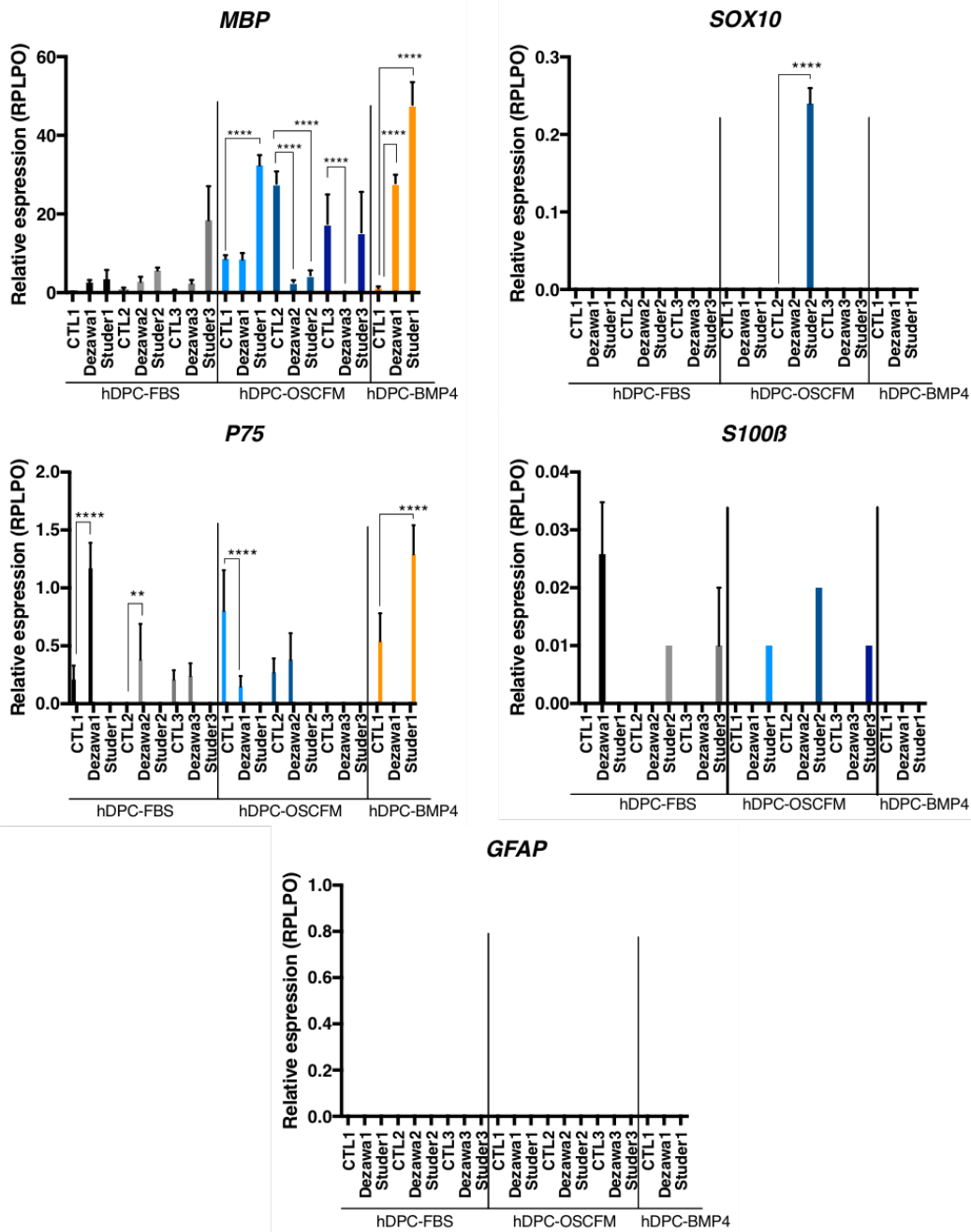


Fig. 4. 16. Relative expression analysis of glial genes after treatments. After Schwann cell induction, untreated controls (CTL) and cultures treated with Dezawa's and Studer's protocols were prepared for a relative expression analysis by RT-qPCR. Three independent cultures were tested for FBS and OSCFM groups (#1-3; also, colour coded), and only one from BMP4cultures (#1). The expression levels were relative to embryonic stem cells. ** $p < 0.01$, **** $p < 0.0001$. Error bars represent technical replicates. FBS: 20% Foetal bovine serum; OSCFM: Otic Stem Cell Full Medium; BMP4: OSCFM + Bone Morphogenic protein 4

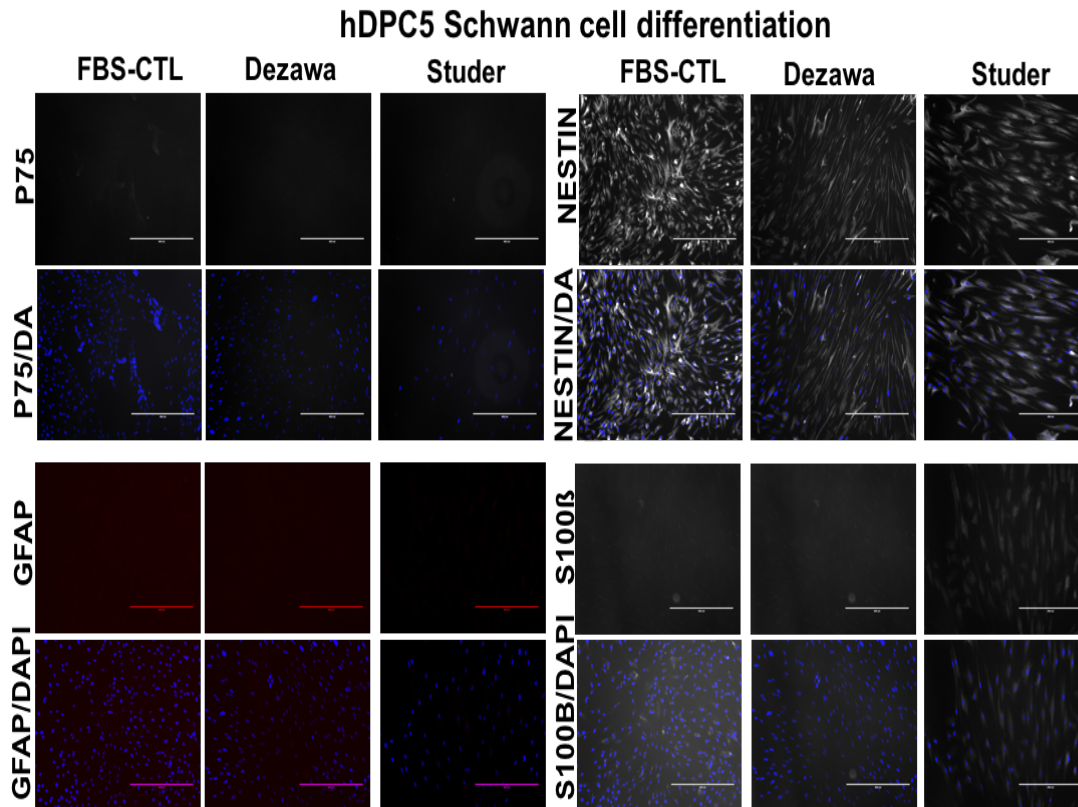


Figure 4.17. hDPC-FBS Schwann cell differentiation. Glial related markers on hDPC-FBS after treatment to obtain Schwann cells. Scale bar: 400µm. For each marker, the image was taken with the same configuration among treatments to allow comparison. No primary control in figure 4.16.

To continue evaluating the Schwann cell differentiation of hDPC cultures, A hDPC-FBS and a hDPC-OSCFM cultures were analysed by ICC. hDPC-FBS cells resulted in a negative expression of P75 and GFAP in both protocols and the undifferentiated control. S100β was seemingly present at a higher level after the Studer’s protocol. NESTIN was also evaluated and was present in all groups (Fig. 4.17).

In the case of the hDPC-OSCFM culture, SOX10 and P75 glial markers were absent in the control and Dezawa’s protocol, but weakly present in the Studer’s protocol group. S100β and MBP were present in all groups. Two neural markers, NF200 and TUJ11 were tested in this case. Both of them appeared present in all groups (4.18).

The limited snapshot of hDPC-FBS and hDPC-OSCFM obtained by ICC supports the observations from the qPCR data. The expression of glial markers is not consistent in any protocol, and Schwann cell differentiation seems partial at best, or more likely null.

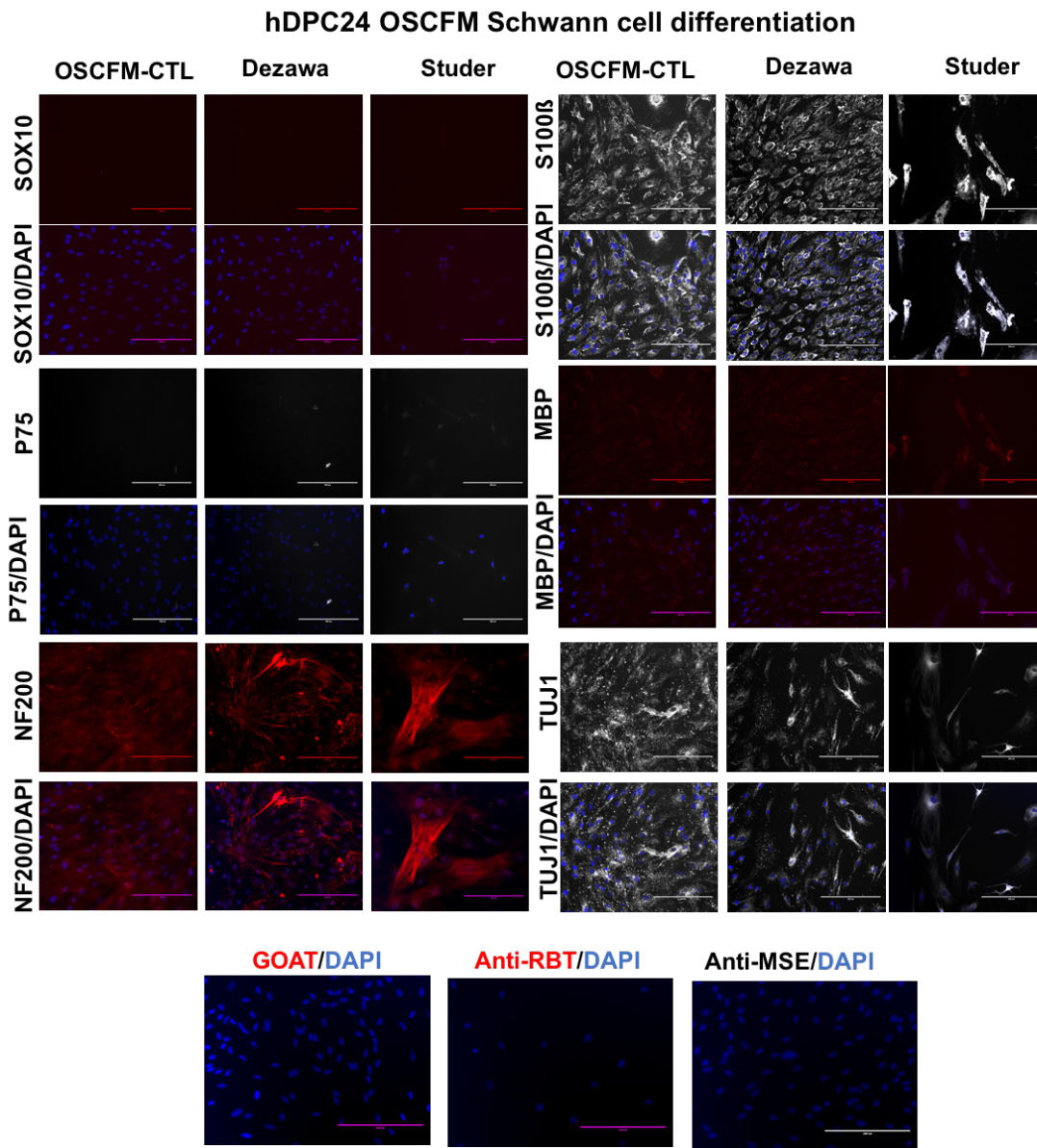


Fig 4.18. hDPC-OSCFM Schwann cell differentiation. Glial related markers on hDPC-OSCFM after treatment to obtain Schwann cells. Scale bar: 200µm. No primary antibody controls are shown for Goat-568, Rabbit 568 and Mouse 488 Alexa Fluor secondary antibodies. OSCFM: Otic Stem Cell Full Medium. For each marker, the image was taken with the same configuration among treatments to allow comparison.

However, the presence of neural-like cells in the cultures after treatment in both protocols (Fig. 4.15), invited us to analyse if we rather had a neural population resulting from the treatments. A relative expression analysis was performed again, but this time for the neural-

related genes: *NFH*, *SYN*, *SYP*, *TUJ1* and *VGLUT1* relative to an ONP line. In this case, again no particular trend could be observed for any of the hDPC-FBS and hDPC-OSCFM cultures. *NFH* was found upregulated in a hDPC-OSCFM culture after the Studer's protocol, *TUJ1* was higher expressed after Dezawa's protocol in two hDPC-FBS cultures, and *SYN* in one hDPC-OSCFM culture after Dezawa's treatment. Interestingly, the hDPC-BMP4 analysed, presented a significant upregulation of *SYN*, *TUBIII* and *VGLUT1* after the Studer's protocol. Overall, similar to the glial differentiation, a clear neural phenotype was not apparent after any of the protocols tested on hDPC-FBS and hDPC-OSCFM. hDPC-BMP4 seemed to acquire a sensory neural phenotype in Studer's protocol (Fig. 4.19).

Schwann Cell Differentiation-Neural Markers

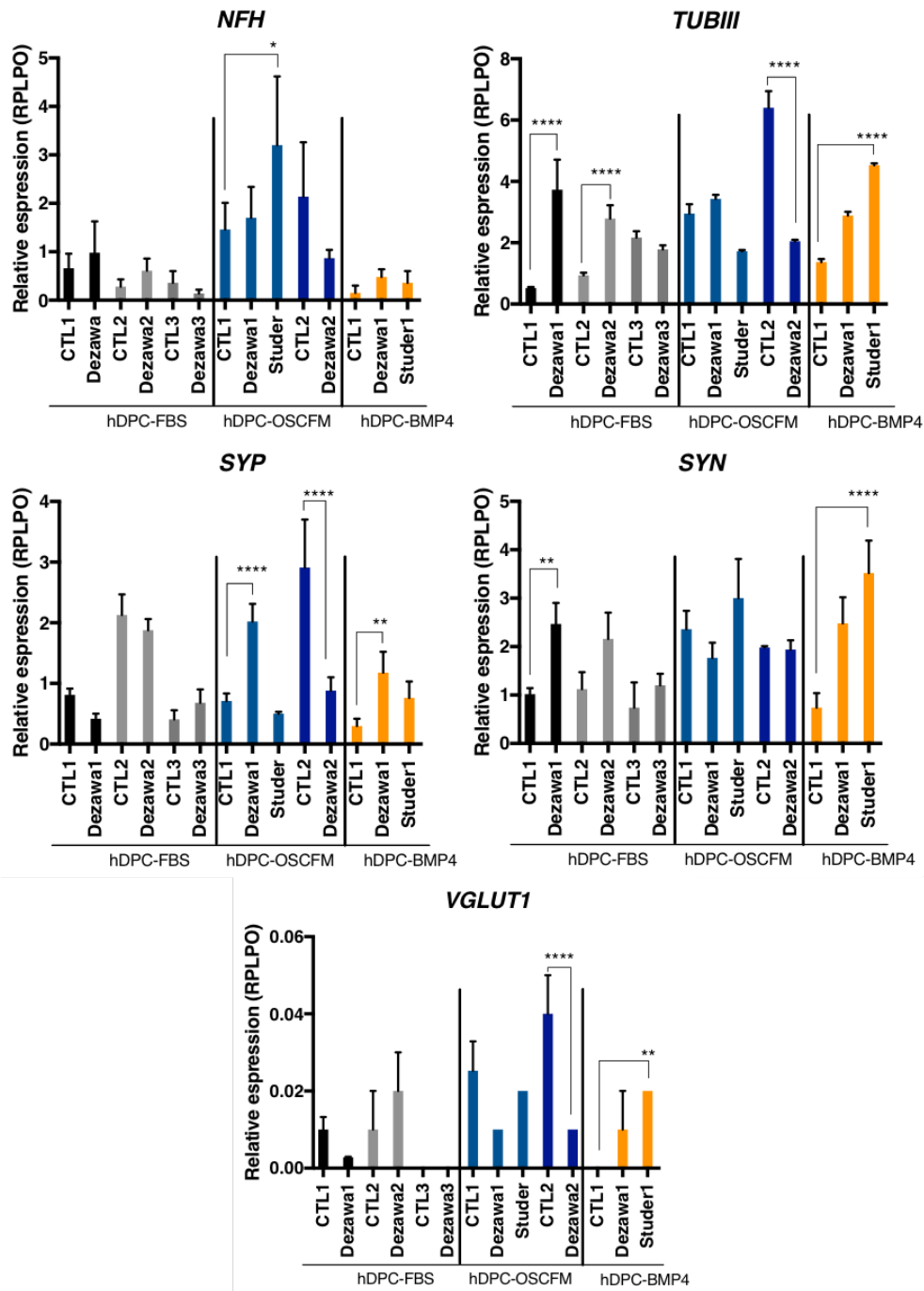


Figure 4.19. hDPCs Schwann cell differentiation (Neural Markers). After Schwann cell induction, untreated controls (CTL) and cultures treated with Dezawa's and Studer's protocols were prepared for a relative expression analysis by RT-qPCR. Independent cultures were tested for FBS and OSCFM groups (#1-3; also, colour coded), and only one from BMP4 cultures (#1). The expression levels were relative to otic neural progenitors (ONPs) derived from hESCs. **p<0.01, ****p<0.0001. Error bars represent technical replicates. FBS: 20% foetal bovine serum-DMEM; OSCFM: Otic Stem Cell Full Medium; BMP4: OSCFM + Bone Morphogenic protein 4

4.7. hDPC cultures can provide trophic support to otic neural progenitors.

As shown previously, hDPCs cultured under the conditions explored presented a very limited capacity to differentiate into Schwann cells. Nevertheless, hDPCs have been shown to secrete neurotrophic factors that could help support neural lineages^{114,115}. Hence, we investigated the effect that medium conditioned by human dental pulp cells could have on otic neural progenitors (ONPs) derived from ESC. To investigate this, we compared ONPs growing under basal conditions against ONPs that were triggered to neuralise by direct dissociation with trypsin, diluted 1:10 (T1:10). Trypsin alone can trigger neural differentiation^{31,32} by activating the PAR1-2 receptors (Objoon Trachoo PhD Thesis). We wanted to observe if a particular advantage could be observed by using conditioned medium from hDPCs when administered to the ONPs after treatment with T1:10. After 10 days of growing ONPs in these media, we quantified the cells positive for the neural marker TUJ1 as an indicative of the neural-like cells obtained from the T1:10 induction and maintained until the end of the experiment.

After quantification, ONPs grown in hDPC-CM resulted in the highest percentage of TUJ1 positive cells, statistically significant than the basal conditions. At the same time, the basal OSCFM-grown ONPs did not differ significantly from ONPs treated with T1:10, although a higher percentage trend could be noted in the latter (Fig. 4.20A). Furthermore, the positive cells observed in the ONPs triggered with T1:10 presented an elongated, neural-like morphology, in contrast to ONPs in basal conditions (Fig 4.20B). This result suggests a trophic effect of human dental pulp cells, and their protective effect on otic neural progenitors.

ONPs grown in hDPCs conditioned medium (OSCFM)

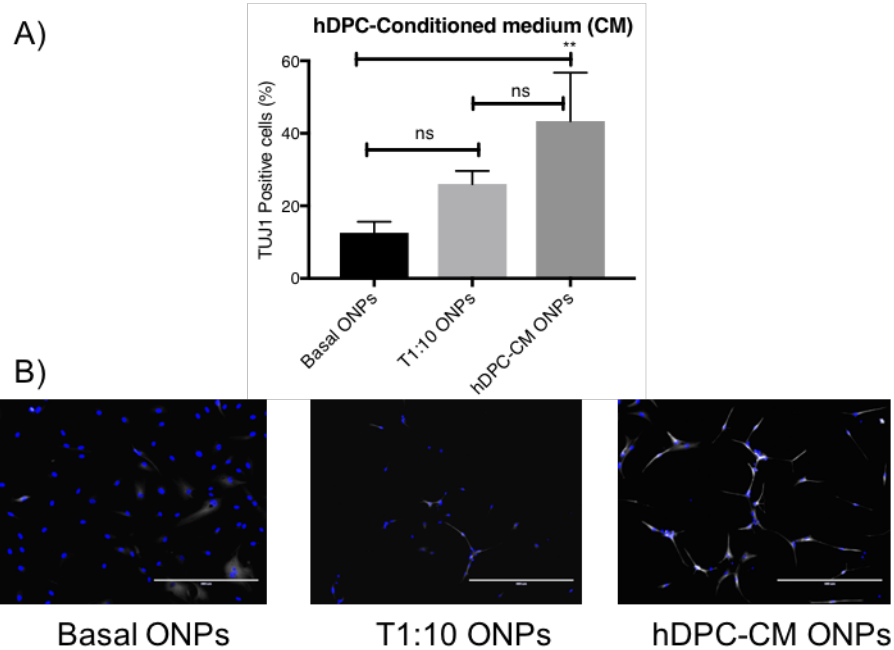


Figure 4.20. ONPs after growing in hDPC-Conditioned Medium (CM). TUJ1 positive cells expressed in otic neural progenitors (ONPs) grown in fresh OSCFM (Basal ONPs), in fresh OSCFM after trypsinisation with T1:10 (T1:10 ONPs), and in OSCFM conditioned by hDPC-OSCFM (hDPC-CM ONPs). A) Quantification of TUJ1 positive cells. B) Fluorescence microscopy of TUJ1 positive cells among conditions. * $P < 0.01$. Scale bar: 400 μ m. OSCFM: Otic stem cell full medium. T1:10: Trypsin diluted 1:10. Basal ONPs: Trypsin EDTA:1:80.

4.8. Human dental pulp cells can be driven into sensory-like neurons by transfection with the transcription factors ASCL1 and NEUROD1 (NEUD).

Given the failure to differentiate into auditory neurons following the protocol designed for otic neural progenitors, we decided to explore the competence of hDPC to produce the desired cell type by direct reprogramming. To do so, we overexpressed the transcription factors ASCL1 and NEUROD1 (NEUD) in our hDPC cultures. These factors were chosen based on their ability to induce neural differentiation of mouse fibroblast, and to drive non-sensory mouse cochlear epithelium into spiral ganglion-like cells¹²⁴.

We first transfected a plasmid containing an eGFP sequence (tetO-FUW-eGFP, Addgene) into hDPC-FBS cultures to optimise the electroporation conditions for plasmid uptake. As

the plasmid should only report the green fluorescent signal, we also intended to use it as a negative control of neural induction. Our main variables for the electroporation were the number of pulses and voltage, and we calculated the transfection efficiency and cell viability in comparison to an untransfected, non-electroporated control. Based on the higher cell viability after electroporation, we choose 150V and 3 pulses as a standard condition for all samples (Fig. 4.21).

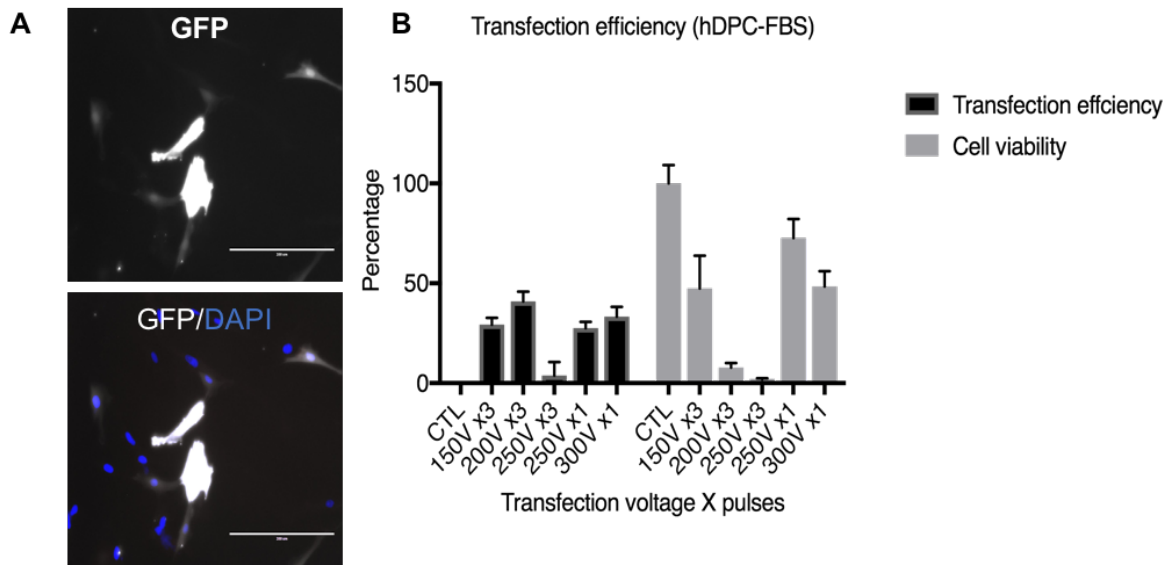


Figure 4.21. Optimisation of transfection in hDPC-FBS cells. Transfection by electroporation was optimised with the plasmid tetO-FUW-eGFP (Addgene) on hDPC-FBS. A) Representative image of EGFP-positive cells after transfection (Top: Green channel, Bottom: Merge with DAPI). B) Efficiency (Black bars) and cell viability (Grey bars) after multiple transfection conditions (X axis). CTL: No electroporation; transfection groups: Voltage (V) multiplied by the number of pulses given. Scale bar: 200µm.

| | ASCL1 | NEUD | TUJ1 | NF200 | BRN3a | PERIPHERIN | SYP | TAU | GFAP | SOX2 | NESTIN | SOX10 |
|--------|-------|------|------|-------|-------|------------|-----|-----|------|------|--------|-------|
| tFBS | ++ | ++ | -- | ++ | +- | -- | +- | +- | +- | +- | ++ | +- |
| tOSCFM | ++ | ++ | ++ | ++ | +- | ++ | +- | -- | ++ | +- | ++ | +- |
| tBMP4 | ++ | -- | ++ | ++ | ++ | ++ | ++ | -- | N/A | N/A | N/A | N/A |

Table 4.3. Summary of hDPC transfection ICC. Qualitative Intensity of fluorescent signal: High (++), Medium (+-), very low (---). tFBS: hDPC-FBS Cultures transfected with ASCL1/NEUROD1; tOSCFM: hDPC-OSCFM Cultures transfected with ASCL1/NEUROD1; tBMP4: hDPC-BMP4 Cultures transfected with ASCL1/NEUROD1. N/A: Were not measured. FBS: 20% foetal bovine serum-DMEM. FBS: 20% Foetal bovine serum-DMEM; OSCFM: Otic stem cell full medium. BMP4: OSCFM + Bone morphogenic protein 4.

We then transfected hDPCs with the plasmids containing ASCL1 (tetO-FUW-ASCL1, Addgene) and NEUROD1 (tetO-FUW-NEUROD1, Addgene) transcription factors¹²⁵. The transfected hDPCs were fixed and stained for relevant neural markers. ASCL1 and NEUROD1 were identified in FBS and OSCFM in some cells, but not frequently, suggesting a low double transfection efficiency. In the case of hDPC-FBS cultures, the cells didn't show a striking change of morphology, but showed signal corresponding to the markers: NF200, BRN3a, SYP, TAU, GFAP, SOX2, NESTIN and SOX10 (Fig. 4.22). OSCFM-hDPCs showed some neural-like morphology but presented a similar marker expression with the exception of TUJ1, PERIPHERIN which appeared positive, and TAU which was not detectable (Fig. 4.23). The most evident change was observed in hDPC-BMP4 cultures, which not only presented a neural-like morphology, but also presented a clear patterns of neural marker expression: TUJ1, NFH, PERIPHERIN, BRN3a and SYP (Fig. 4.24). EGFP-only transfection and No plasmid electroporation were done as controls, the expression of relevant neural markers and the morphological changes observed in ASCL1/NEUD1 double transfection were not evident in the negative controls (Fig. S1 and S2). Summary on table 4.3.

hDPC5 FBS transfected with ASCL1/NEUD1

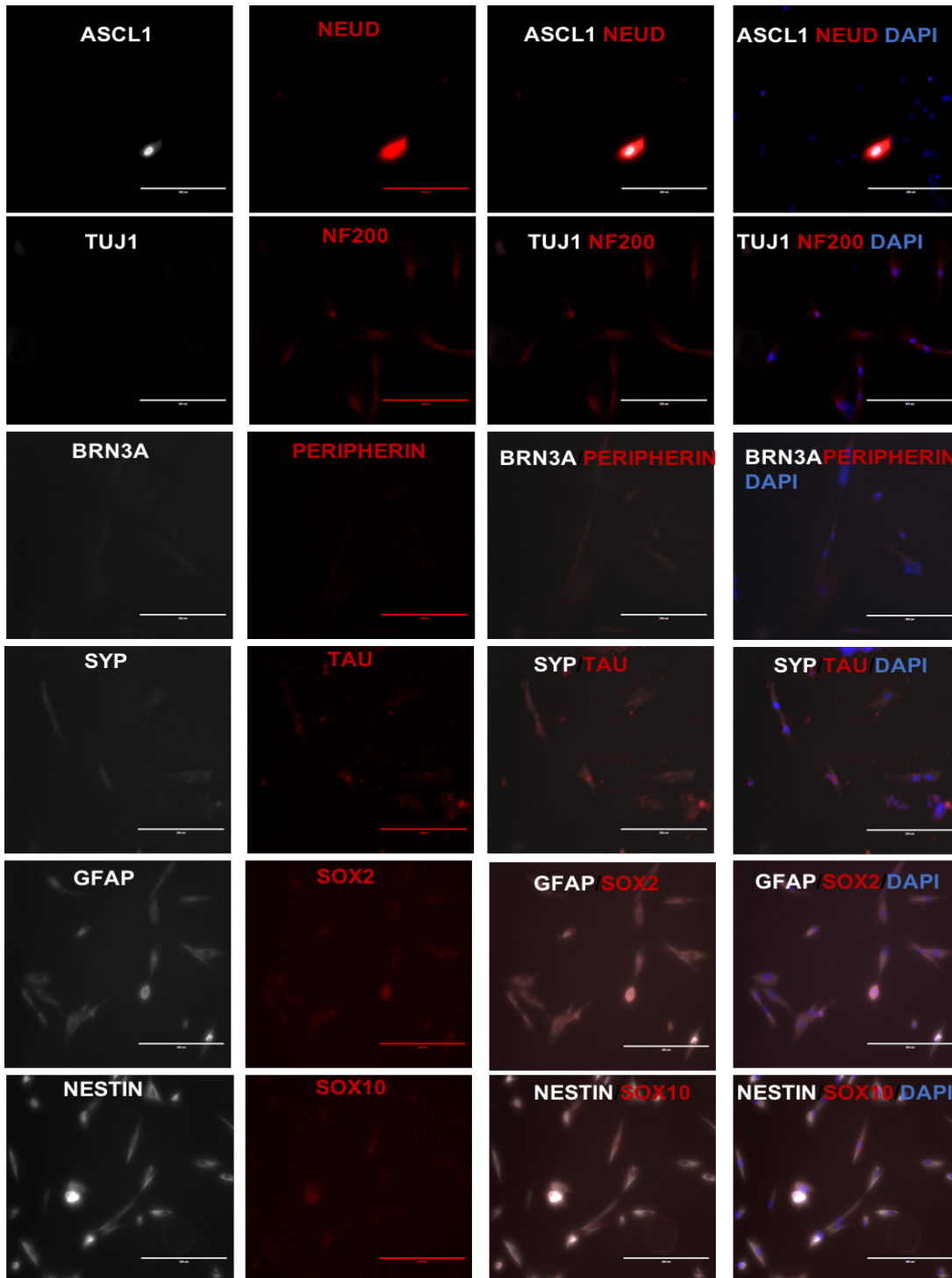


Figure 4.22. hDPC5 FBS transfection (ASCL1/NEUD). hDPC-FBS 7 days post-transfection with the plasmids tetO-FUW-ASCL1 (Addgene) and tetO-FUW-NEUROD1 (Addgene). The expression of neural markers was observed: ASCL-1, NEUD, TUJ1, NF200, TAU, SYP. GFAP, SOX2, Nestin and SOX10 were also observed. BRN3a and Peripherin signal were weak. Scale bar 200 μ m. FBS: 20% Foetal bovine serum-DMEM. For each marker, the image was taken with the same configuration among treatments to allow comparison.

hDPC19 OSCFM transfected with ASCL1/NEUD1

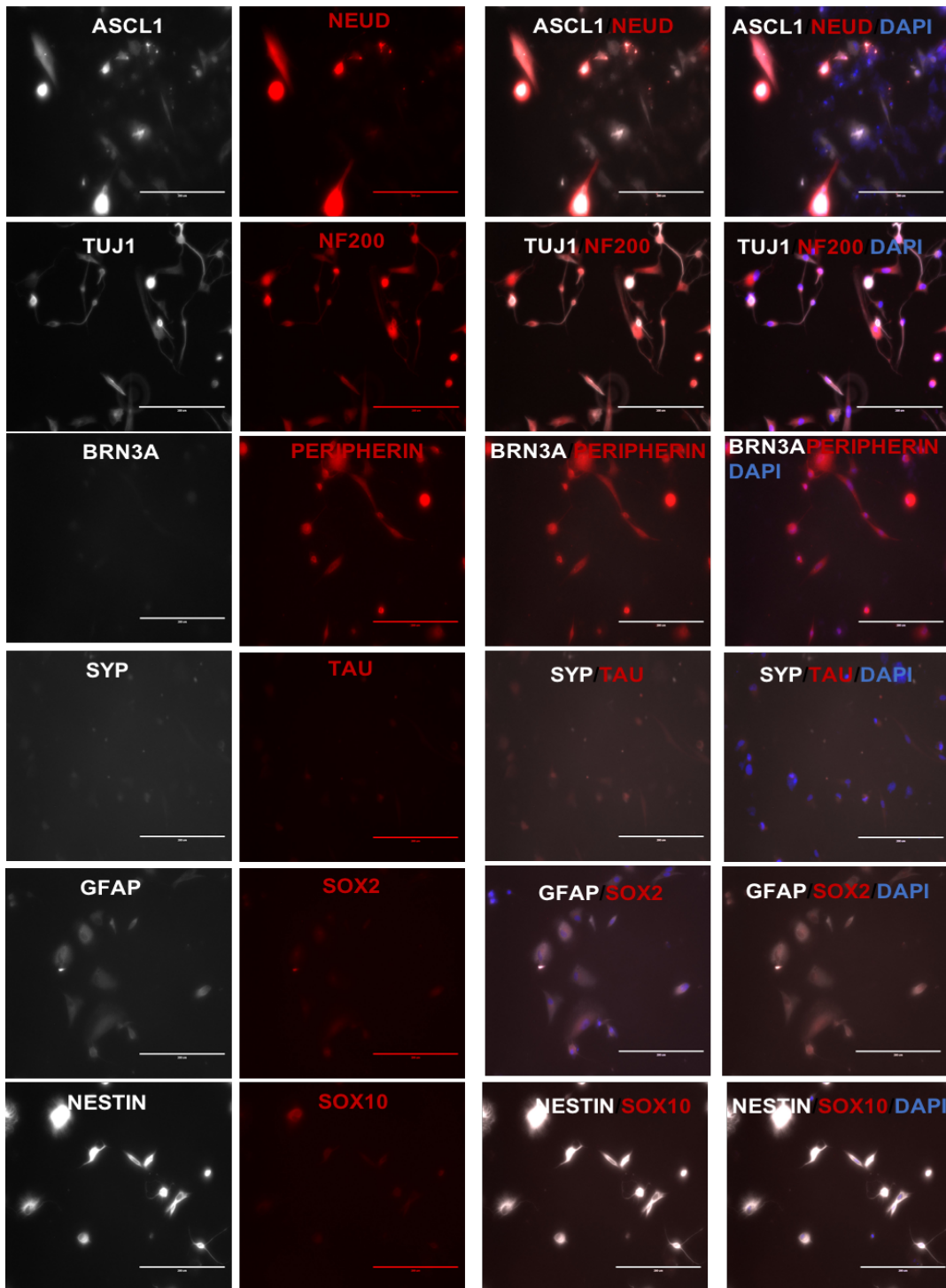


Figure 4.23. hDPC20 OSCFM transfection (ASCL1/NEUD). hDPC-OSCFM 7 days post-transfection with the plasmids tetO-FUW-ASCL1 (Addgene) and tetO-FUW-NEUROD1 (Addgene). The expression of neural markers was observed: ASCL-1, NEUD, TUJ1, NF200 and Peripherin. GFAP, SOX2, Nestin and SOX10 were also observed. BRN3a and SYP and TAU signal were weak. Scale bar 200 μ m. OSCFM: Otic Stem Cell Full Medium. For each marker, the image was taken with the same configuration among treatments to allow comparison.

hDPC29 BMP4 transfected with ASCL1/NEUD1

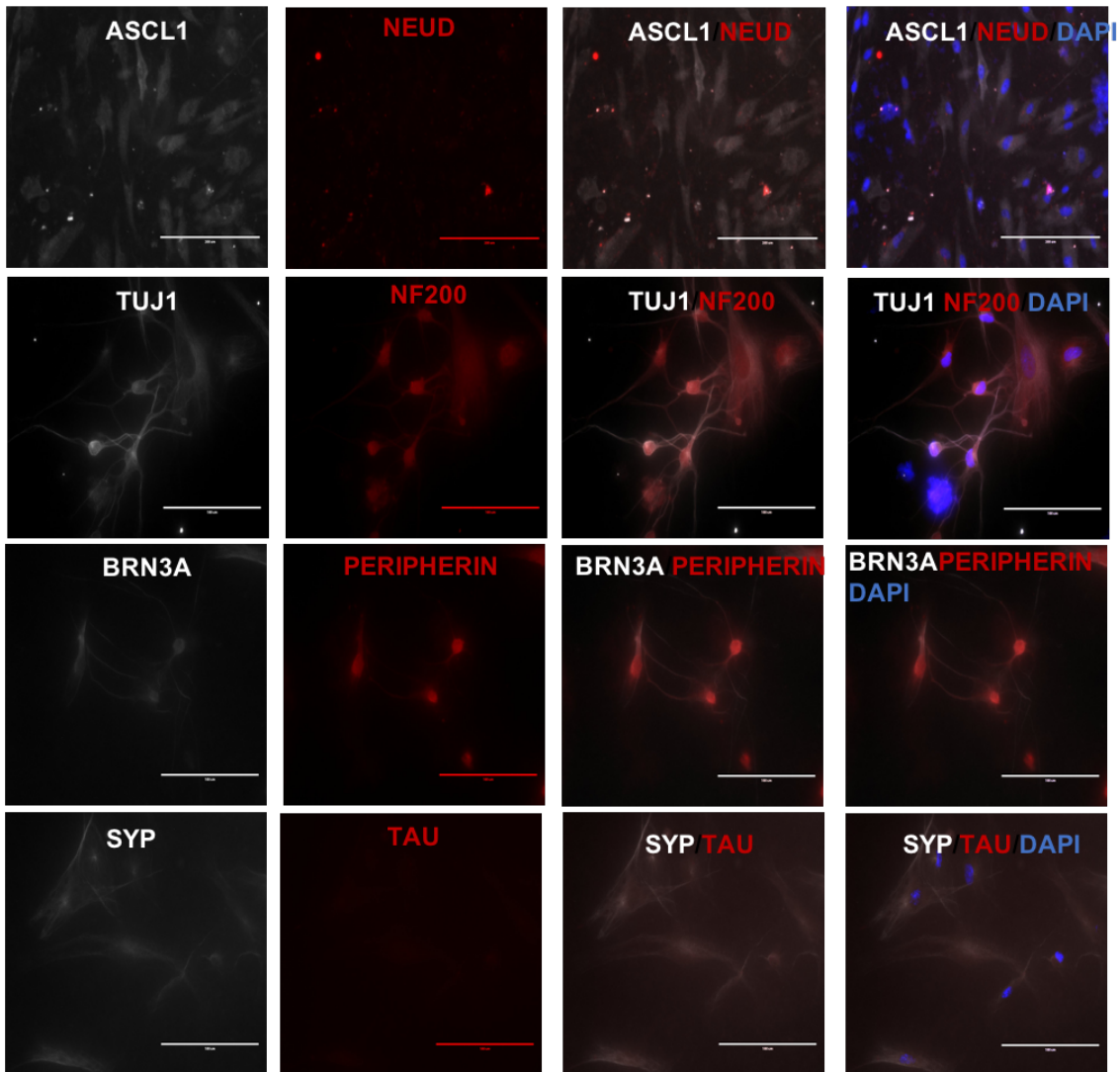


Figure 4.24. hDPC29 BMP4 transfection (ASCL1/NEUD). hDPC-BMP4 7 days post-transfection with the plasmids tetO-FUW-ASCL1 (Addgene) and tetO-FUW-NEUROD1 (Addgene). The expression of neural markers was observed: ASCL-1, TUJ1, NF200, Peripherin, BRN3a and SYP. TAU and NEUD signal were weak. Scale bar 200 μ m. BMP4: OSCFM + Bone Morphogenic protein 4. For each marker, the image was taken with the same configuration among treatments to allow comparison.

4.9. Discussion

4.9.1. Human dental pulp samples

In contrast with mouse dental pulp tissue, human dental pulp tissue has been widely used in cell culture. Many different methods for dental pulp extraction, culture and characterisation have been published since the earliest recognised dental pulp work from Gronthos et al., 2000⁵. In the present work, we have described the establishment of dental pulp cultures from a wide variety of patients, from teenage to adulthood and senior subjects. This range of samples allowed us to present a relevant cohort from which we can extract relevant pre-clinical data in terms of efficiency, patient age and sample condition. Such data would need to be considered for translational research to be taken to a clinical level. Until now, we could have an idea of the samples' nature mostly by gathering the information from several independent reports. Actually, the most complete report from a cohort of 40 samples was from patients aged 18-30 years showing 78% of success rate to grow *in vitro*¹²⁶. The described report does not establish the conditions of the samples; however, they reached a similar overall success percentage than us (76.66% with exclusion criteria). The samples that were not successful in their experiments were contaminated with yeast. Contrary to the present study, they did not use antibiotics and antifungal agents in the transport solution (ours was PBS). However, they did process their samples with a disinfectant step with such reagents. In our hands, the unsuccessful samples were mainly due to the sample being fractioned or broken or unable to grow in the defined culture media, rather than contamination. It must be mentioned, that their culture medium was a commercial growing solution for the growth of MSCs: MesenCult (Stem Cell technologies). In terms of the age, our results provide a larger age span among the samples, from 15 to 61-year-old patients. The youngest successful culture came from a 16-year-old patient, while the oldest from a 37-year-old patient. The oldest samples were from patients aged 61 and 52, and in both cases, there was virtually no pulp present in the sample. It remains to be seen if a healthier tooth from a similar age could be efficiently grown *in vitro* in our defined conditions. The success percentage that was found in our study seemed to be independent of the age and be more affected by the type of media condition that we used.

This can be reflected in cultures in BMP4 medium, where the highest efficiency belongs to the oldest age group. Therefore, we believe that cultures could be established from patients older than 37 years of age. In support of this, independent reports have used dental pulp from 40, 45 and up to 60-year-old patients in standard medium^{87,127-129}.

We have also provided evidence of the possibility to grow DPCs from carious teeth. In our hands, 54% of the carious samples were able to grow. This percentage includes cultures from all three conditions, and samples from young and old patients. The inclusion of all types of samples (i.e. Medium, age) in our 54% of success in carious teeth, could explain the difference with a report describing that 80% of carious samples were able to grow *in vitro*¹³⁰. Additionally, separate studies also supported the use of carious teeth from children younger than 5 years for dopaminergic differentiation and inflamed pulp from young patients^{131,132}. Together with our results, this data provides consistent evidence that dental pulp cells from different group patient age and carious teeth are usable for cell culture growth.

4.9.2. In situ characterisation of human dental pulp

We included in our analysis the characterisation of dental pulp tissues *in situ*. By performing immunohistochemistry, we detected the presence of important markers that have been reported elsewhere. For instance, NESTIN, a neural crest marker was expressed widely in all the samples tested in this study and has also been shown in separate reports in tooth pulp^{133,134}. In animal models, the neural crest origin of the dental pulp has been evidenced by embryonic cell tracing in transgenic models⁵². In humans, the expression of neural crest-related markers, such as NESTIN can support the developmental origin as well. It has been suggested that different stem cell niches can be found within the dental pulp, more specifically in capillaries and nerves marked by STRO-1¹³⁴. Shi and Gronthos (2003)⁷³, identified a STRO-1 MSC niche in dental pulp tissue, which was located in the perivascular CD146⁺ perivascular region. STRO-1 in the mentioned study, was present also in the nerve bundles. This stem cell niche is also supported by two further independent reports, with the additional finding that the stem cell niche in the nerve bundles could be restricted to younger patients^{133,134}. Our results were able to identify STRO-1 in all our samples in putative vascular regions, and in the youngest sample analysed (15-year-old) we were able

to detect it co-labelling with NF200 in a nerve bundle. We also analysed markers that have been identified in the mouse incisors as stem cell niches: GLI1 and SOX10^{100,102}. Zhao et al. (2014) presented a detailed analysis of the GLI1⁺ niche in mouse incisors provided evidence of being conformed of slow cycling cells (quiescent), highly dependent on Sonic hedgehog (Shh) signaling from the nerve bundles. Furthermore, the GLI1⁺ niche was responsible for forming the mesenchyme of the mouse incisor and giving rise to transient amplifying cells. The evidence provided by them, also suggested that MSCs *in vitro* could have their origin from this quiescent niche¹⁰². In molars, the same study showed that GLI1⁺ cells were found in animals (Guinea pig) with a continuous molar teeth growth in the apical region of the tooth¹⁰². In mice molars, a separate report found a GLI1⁺ niche present during dentition development in early postnatal mice, but not in adult or mature molars^{102,135}. Together, the published results strongly suggest a stem cell niche labelled by GLI1 in teeth under constant growth or under development. In our results, GLI1 was observed in nerve bundles co-localised with TUJ1, and also throughout the dental pulp, and therefore was not specific to a particular niche. Thus, the wide expression of GLI1 in human dental pulp tissue found by us, is not likely to mirror the homeostatic events that happen in rodent incisors or developing molars. Therefore, rather than labelling a specific stem cell niche in our human dental pulp tissue, GLI1⁺ cells could be present as part of Shh role in odontoblast differentiation or another aspect of pulp homeostasis. In the present study, GLI1 was also found co-expressed with CELSR1 (also known as flamingo). CELSR1 has been found *in vivo* in quiescent haematopoietic stem cells, as part as the non-canonical WNT pathway¹²⁰. Nevertheless, similar to GLI1 expression, CELSR1 presence in our dental pulp samples cannot be suggested to have the same role as the one observed in rodents. On the other hand, SOX10 appeared as a rare event in our dental pulp tissue. When present, it co-labelled with STRO-1 in the putative perivascular niche. Evidence from Kaukua et al., (2014¹⁰⁰) in mouse incisors, suggested the SOX10⁺ population may be glial cells with the ability of transdifferentiation to yield the mesenchymal stem cells within the tooth after injury¹⁰⁰. The important roles found for GLI1 and SOX10 in mouse incisors have been studied with powerful transgenic tools that are not available in human samples for obvious ethical, legal

and technical reasons. Therefore, the presence of these markers in human dental pulp cannot be considered to exert the same role. At the same time, we cannot rule out the possibility of any homeostatic role from GLI1, SOX10 and/or CELSR1 positive niche. We propose that analysing the expression of these markers in dental pulp tissue in teeth with different degrees of caries (as an insult to trigger a stem cell response) could aid in deciphering a particular role in human homeostasis. In this thesis, we analysed carious and non-carious teeth, however, we would require a higher cohort to get conclusive results. The advantage of animal models is that the experiments can be controlled, the insult or lesions can be induced, and the responses can be measured at consistent time points. Whereas in humans, the time from the start of the insult to the time of measurement can be highly variable from patient to patient. Our results just suggest the presence in human dental pulp of stem cell markers found in mouse incisors, but we cannot attribute any particular role to them. In this regard, the only example of a human *in vivo* stem cell response in wound healing was performed by Yoshida et al., (2012¹³⁶). In the cited report, tooth capping was performed after mechanically exposing the pulp and sealing (capping) the injured site with mineral trioxide aggregate and investigating the presence of SMAa and STRO-1 in different time points. Their results revealed that human dental pulp stem cell markers SMAa and STRO-1 progressively accumulated around the reparative zone in relation to the time for healing¹³⁶. Nevertheless, it's our opinion that the presence of SMAa and STRO-1 could be related to the revascularisation of the damaged zone, rather than a mobilization of stem cells within the tooth.

4.9.3. Culture of human dental pulp cells

In terms of *in vitro* growth, hDPCs cultures were established by using the enzymatic dissociation method. With this method, a disruption of the tissue is made and passed through a cell strainer to then culture the cells. Therefore, all cells in the dental pulp, which we have characterised *in situ*, were plated for *in vitro* culture. A second existing method for establishing primary cultures from dental pulp is the explant method, which allows small explants from dental pulp tissue to outgrow on the plate's surface. A comparative experiment between the two methods performed elsewhere, revealed similarities in the

surface MSC markers CD105, CD90 and CD73. In terms of morphology, two separate studies reported that enzymatic digestion resulted in a more heterogeneous culture based on cell shape and is also what we observed in our cultures regardless of the initial culture media^{127,137}. In terms of differentiation, the results suggested that the enzymatic digestion could favour osteogenic capacity, while the explant method favours adipogenic potential¹²⁷. To the best of our knowledge, no evidence has been found on the effect of the extraction method (Enzymatic vs Explant method) on neural differentiation. Because our aim was to grow and identify a population with resemblance of a neural crest phenotype, we used enzymatic digestion to release all the cellular content from the tissue and potentially grow the cells that could respond positively to the medium growth factors (OSCFM and BMP4). Our worked showed that primary cultures in any of our conditions present heterogeneous cell populations, and under defined conditions (OSCFM and BMP4), we were able to detect neural-like cells with long thin cell projections. Therefore, enzymatic digestion could have allowed the released of neurogenic cells.

In relation to the medium conditions that we used, it was important to evaluate not only the use of a neurogenic cell media, but also conditions that could be easily replaced for xeno-free components and translated to good manufacturing/good tissue practices for clinical grade applications (cGMP)^{126,138}. The use of cGMP media in hDPC culture has been recognized, but scarcely reported¹³⁹, and several authors have described the growth of hDPC in defined serum-free and xeno-free conditions^{93,94,140-142}. Therefore, we took particularly interest using serum-free conditions and also conditions with neurogenic potential. In These neurogenic solutions containing EGF and bFGF are believed to favour the proliferation and neural commitment of progenitor cells⁵⁵, whereas the addition of BMP4 has been shown to promote a sensory neural phenotype¹⁰⁸. Our media conditions OSCFM and BMP4 already contained recombinant human bFGF, IGF, EGF, BMP4, and also with B27 and N2 supplements, which can be replaced for their xeno-free, good manufacturing practice-derived (cGMP) homologs (Termofisher scientific). Enzymatic digestion and surface coating substrate would need to be optimised with cGMP products such as triple select (Gibco) and human laminin (Biolamina). Thus, our results have shown

the viability of hDPCs to grow under serum-free conditions, in support of future xeno-free culture derivation. Therefore, we have provided further evidence of the growth of hDPC to be established under defined conditions, potentially easily translated to cGMP products.

4.9.4. Characterisation of human dental pulp cells

Once established, the morphology of the hDPC cultures was evaluated during passaging. Overall, changes in the cell composition and culture dynamic were evident in the three culture conditions, although only in a minor degree in FBS media. OSCFM and BMP4 media a rapid cell change in a matter of a few passages. We performed a further characterisation of human dental pulp cells under FBS and the defined conditions OSCFM and BMP4 by qPCR. The pluripotent markers *NANOG* and *OCT4* present in our cultures have also been identified elsewhere in hDPCs and other oral-derived NCSCs^{87,129,143,144}. Nevertheless, most of these reports have not analysed them with highly sensitive technologies (Taqman) and/or compared them to a pluripotent stem cell line, as we have done. Thus, our results suggest that the levels of the pluripotent stem cell markers *OCT4* and *NANOG* are not significant to suggest a pluripotent state in any of our conditions.

In terms of ectodermal markers, results revealed a general basal expression of neural crest and neural progenitor molecules at the protein and mRNA level. An initial characterisation of the basal, undifferentiated state of hDPCs was done by Martens et al., (2012)¹³³, showing that cells grown in standard conditions with 10%FBS expressed TUBIII, S100 β , SYP, NESTIN and VIMENTIN. This expression profile in undifferentiated primary culture hDPCs suggest an already neural progenitor state in proliferative conditions¹³³. Our results agree with those observations and included a wider panel of markers for a more comprehensive characterisation of hDPCs in standard and defined conditions. At protein level, ICC revealed qualitative data suggesting a stronger expression of the neural crest markers SLUG, SNAIL1, P0 and a clearer nuclear localisation of SOX2 and SOX9 and SOX10 in hDPC-BMP4 cultures. In addition to the mentioned markers, we also observed the Sonic Hedgehog pathway member GLI1 as a neural progenitor marker. As mentioned before, GLI1 defines an *in vivo* stem cell niche that gives rise to mesenchymal cell in mouse incisors. *In vitro*, GLI1^{+ve} cells disappear and give rise to the multipotent stromal cells when grown with the explant

method (Mouse)¹⁰². In our work, both mouse (Chapter 3) and human DPCs present a generalised expression of *GLI1*, one explanation could be attributed to the digestion method being used to establish the cultures. Thus, releasing all the cellular content from the tissue, instead of only expanding cells with high proliferation capacity. Evidence of Sonic Hedgehog pathway members and activity in dental pulp has been reported elsewhere, showing expression of pathway members such as *GLI1*, *PTCH* and *SMO*^{145,146}.

Quantitative RT-qPCR data also revealed basal expression of *P75* and *NESTIN* also in accordance to Martens et al., (2012)¹³³. We also examined the neural genes *NFH*, *SYN*, *SYP*, *TUBIII* and *VGLUT*, and showed basal levels of these genes. Overall, from this expression profile, our data support that of Martens et al., (2012)¹³³, in the sense that some level of neural markers are detectable in hDPCs at the initial stages, during expansion *in vitro*. In addition, we have provided further evidence of a neural crest-like signature by ICC. However, our results together with other published work, bring important considerations evaluating neural differentiation by the presence of some of the evaluated neural markers. In this sense, when comparing neuralised hDPCs to an undifferentiated, basal state, we suggest to the use of highly sensitive technologies.

Here, we tested defined growth media to evaluate the feasibility of translating hDPC cultures into serum-free, xeno-free conditions in neurogenic solutions. Considering the similar expression profile in OSCFM and BMP4 defined conditions, a few reports have also found the presence of markers such as *NESTIN*, *TUBIII*, *NFM* and *PLP1* in serum-free, FGF2/EGF-containing media^{94,140}. Nevertheless, the report from Jung et al. (2016)⁹⁴, strongly suggest differences between the standard condition with FBS and the neurogenic medium in terms of expression of markers like *MAP2*, *NESTIN*, *NEUROD1*, *OLIG2*, *PAX6*, *SOX1*, *SOX2* and *VIMENTIN*. Our initial hypothesis was that the neurogenic media would allow the grow of cells with an enhanced neurogenic nature. Thus, we did not expect a null difference among our groups by RT-qPCR. The key differences with our work with Jung et al., (2016) are that we use IGF and Laminin coating in our defined conditions. Justification of using IGF was because it has been broadly described as a key factor for neural progenitors¹⁴⁷. However, in dental pulp cells, IGF has been described to allow proliferation

and enhance mesodermal differentiation^{129,148}. Therefore, we can't rule out the possibility of IGF interfering with a neurogenic potential. In addition, two important markers for a neural crest phenotype were not found by RT-qPCR. *SOX10* and *SOX2*, which both showed a weak signal in fluorescent microscopy. *SOX10* RNA was detected only at early passage in two hDPC-FBS evaluated, while *SOX2* was not detected in any hDPCs. Low detection of *SOX2* by Taqman RT-qPCR has been reported previously¹⁴⁹, and the lack of *SOX10* expression argues against a fully neural crest phenotype in our basal conditions.

Furthermore, our cultures were proven to be heterogeneous based on the differential expression of P75 and STRO-1 at different passage number. We observed a dramatic reduction of P75^{+ve} cells after first passaging. However, a more sensitive technique (Flow cytometry) allowed us to identify a small percentage of P75^{+ve} cells in later passages (details in chapter 5) and we were also able to detect basal mRNA levels at later passages. In contrast, STRO-1 marker showed an opposite behaviour, increasing the positive cell population with passage number. In support of the heterogenic nature of hDPCs, Pisciotta et al., (2015)¹⁵⁰ and Pan et al., (2016)¹²² characterised subpopulations of STRO-1^{+ve} and P75^{+ve} cells respectively. It is worth mentioning that STRO-1 positive population reported in literature is significantly less than what we observed in our cultures, with reports of <3% and up to 10% STRO-1^{+ve} cells by flow cytometry and immune-fluorescence, respectively^{123,150,151}. Discrepancies could be related to how cells are gated and how many STRO-1 cells survive trypsinization for passaging, which could affect sensitive cells. This sensitiveness could also be affecting the survival of P75 positive cells after first passage. Thus, our conditions have shown a level of heterogeneity despite of culturing them under defined, serum-free conditions.

Evidence of cell passaging shown elsewhere on hDPCs, have shown no apparent proliferation or mesodermal differentiation potential changes comparing cells at passage 2 (P2) against cells at passage 15 (P15). However, senescence markers p16 and p21 appeared upregulated at P15. Furthermore, the stem cell markers OCT4, NANOG, SSEA4 and SOX2 present at P2 were diminished at P15¹⁵². An analysis of early vs late passaged samples would

allow to further investigate the dynamics of the basal conditions we have presented. We would expect the markers to drop with culture passaging.

Overall, we have provided evidence of hDPC cultures establishment, an extensive basal characterisation of relevant neural-crest, neural progenitor and neural markers, and also presented evidence of culture heterogeneity within standard and defined growing conditions.

4.9.5. Differentiation potential of human dental pulp cells

The presence of neurogenic and neural crest-related markers in our hDPC (P0-7) were surprisingly similar among the media conditions (FBS, OSCFM and BMP4). Therefore, we were interested in testing the ability of the hDPCs to differentiate into auditory neurons and Schwann cells.

By using the protocol established in our research group, hDPCs from all conditions were induced for neural differentiation with no success. With only discrete morphological changes, RT-qPCR analysis did not show any general upregulation of the sensory neural genes tested. Although several reports have been published suggesting the neural differentiation of hDPCs, only a few of them had provided evidence of a functional maturation *in vitro*, under cytokine/chemical cues⁸⁸⁻⁹⁰. These protocols have used different levels of reprogramming and multistep conditions, such as epigenetic modification and neurosphere formation in order to obtain such results from FBS-grown cultures. None of them have characterised the intermediate cell populations, but it can be deduced that a neural progenitor population was sought to respond to the maturation steps. In our work, the use of OSCFM and BMP4 as neurogenic media, was hypothesised to be yield cells more responsive to neural inductive cues *in vitro*. However, all our conditions (FBS, OSCFM and BMP4) failed to respond when induced with Sonic hedgehog for auditory neuron differentiation. Nevertheless, it's possible to suggest that the lack of neural differentiation was because the protocol is more effective on cells with an otic progenitor character, as it was designed to mimic auditory neuron development^{31,32}. Sonic hedgehog activity has also been reported to allow the proliferation and maintenance of neural stem cells¹⁵³, therefore its activity is not always related to neural maturation. The activity of sonic hedgehog has

not been widely studied in dental pulp cultures. However, a recent report has shown that Shh activation can promote cell proliferation and osteogenic/odontoblastic differentiation¹⁴⁵, suggesting a different role than neural induction. We did not look for any particular osteogenic/odontogenic differentiation marker and we do not claim such induction occurred, however, the cited report, together with our results, do reflect that sonic hedgehog activity did not induce a neural phenotype in any of our hDPC culture conditions. In terms of neural maturation in hDPCs, successful reports have induced the cAMP cascade through /cytokine/chemical analogous molecules or activators of cAMP, such as dcAMP and Forskolin⁸⁸⁻⁹⁰. Hence, failure of neural commitment in the present work should be attributed to the inability of Shh to induce a neural phenotype in hDPCs, rather than a lack of ability to become neurons. A recent publication suggests the ability of hDPC to differentiate into ganglion neurons by a two-step protocol following neurosphere formation. Their success was based on the expression of GATA3 and NTRK2 as markers of ganglion neurons and intracellular calcium activity¹⁵⁴. Therefore, the mentioned report supports that differentiation towards an auditory nerve lineage is possible when more appropriate cues are used.

As a strategy to keep testing the possibility of obtaining a sensory-neural differentiation in our hDPC cultures, transfection of plasmids containing the transcription factors *Ascl1* and *NeuroD1* was done in all our hDPC conditions. Both factors were identified from a screen of 19 candidates to differentiate mouse fibroblasts into sensory neurons with high efficiency¹²⁵. Furthermore, the ectopic expression of these markers was evaluated in cochlear non-sensory epithelium in embryonic and postnatal tissue from mice¹²⁴. Our results have found that a neural-like phenotype can be induced by these factors in human cells. Nevertheless, the results are not as conclusive as what has been shown in mouse tissue¹²⁵. A recent report uncovered key regulatory “gatekeepers” for neural maturation in human adult fibroblasts. In this report, in contrast to the neural maturation by transfecting *ASCL1* alone in mouse embryonic fibroblasts¹²⁵, in human fibroblasts it was first required the inhibition of the gatekeeper: RNA binding protein PTB and its paralog PTBP2 for the subsequent activation of *BRN2* and *miR-9* to allow a neural maturation after transfection¹⁵⁵.

In our results, a neural-like phenotype was more evident morphologically and phenotypically in hDPC-OSCFM and specially in hDPC-BMP4 cultures, suggesting that our defined conditions could be more (but not completely) poised for neural maturation. The expression of BRN2, miR-9 and PTB would need to be evaluated to evaluate if a “gatekeeper” mechanism is involved in our hDPC culture conditions. Nevertheless, our results showed qualitatively a better response in our defined condition hDPC-BMP4 in comparison to the standard FBS medium.

As our aim was also to evaluate a neural crest-like phenotype in our hDPC-cultures, we decided to test glial differentiation by a driving Schwann cell phenotype. The differentiation of hDPCs into glial cells and its evaluation in nerve conduits for peripheral nerve regeneration has given promising results^{38,91,156}. The protocol followed by us and the mentioned reports have been modified from Dezawa’s protocol to obtain Schwann Cells from bone marrow MSCs³⁷. We also tested a protocol used in neural crest cells from embryonic stem cells to provide further evidence of a possible neural crest-like phenotype response⁹⁷. However, we did not observe a definitive change into Schwann Cells by the expression of glial markers at protein nor mRNA levels with any protocol. Upregulation of some of the genes was detected, but it wasn’t a general effect. The evaluation of hDPC differentiation by Martens et al., (2014)⁹¹ was done by qualitatively looking at GFAP, P75, NESTIN, VIMENTIN and CD104 by ICC. However, they never performed a quantitative analysis to validate those results, as we have done. Importantly, the *in vivo* testing for hDPC-Schwann cell driven nerve regeneration by implantation of hDPC in artificial conduits did not compare them with hDPC in their basal state (undifferentiated). Comparison with an undifferentiated hDPC is important due to the reported positive effect of basal-hDPCs in nerve regeneration coupled with artificial conduits¹⁵⁷. In our results, we did observe some inconsistent expression of glial markers such as S100 β , P75 and MBP in some conditions and in some protocols. Thus, we cannot rule out a degree of glial differentiation that could enhance their regenerative properties *in vivo*.

In this regard, we have shown than hDPC-OSCFM under basal conditions secreted factors that allowed the prevalence of TUJ1 positive neurons from otic neural progenitors, as

suggested by culture in conditioned medium. In this work, the composition of the factors enriched in hDPC-conditioned medium was not determined. Nevertheless, previous studies from rat DPCs, provided evidence of the presence of NGF, GDNF and BDNF mRNA and their ability to rescue motorneurons after injury in the spinal cord¹⁵⁸. In human dental pulp, it was recently described that dental-related DPCs (SCAP, DPSC and PDLSC) also produced levels of NGF, GDNF and NT3 and promoted neurite outgrowth in a similar experiment to ours.¹⁵⁹ Together, our results provide evidence of a trophic effect exerted by human dental pulp cells and suggest an innate neuroprotective effect, that does not require cells to be differentiated into glial-like phenotype.

4.10. Summary

We were able to grow dental pulp cell cultures under defined serum-free conditions and identified neural crest and neural related markers in a basal state (OSCFM and BMP4). Nevertheless, the cells grown in the basal conditions (FBS, OSCFM or BMP4) do not respond to sonic hedgehog as an inductive factor for auditory neuron differentiation. Schwann cell differentiation was achieved partially and inconsistently. Additionally, it seems that there may be an innate trophic effect within the hDPC culture that may support differentiation of cells into neurons.

CHAPTER 5

**“Evaluating otic neural progenitor obtainment from
human dental pulp cells grown in FBS medium”**

5. Evaluating otic neural progenitor obtainment from human dental pulp cells grown in FBS medium.

Previous work in the research group provided a protocol to generate otic neural progenitors (ONPs) from pluripotent stem cells by treating the cells with FGF3 and FGF10 (FGF3/10)³¹. The same FGF3/10 treatment was followed on bone marrow MSCs with a lack of success. However, growing the cells in human foetal auditory stem cells (hFASC) allowed an ONP-like phenotype from bone marrow MSCs⁴⁴. In our results, we observed a lack of response to Sonic Hedgehog to directly derive auditory neurons from our hDPCs (Chapter 4). Thus, we explored if treating hDPC-FBS cultures with different conditions, could yield otic neuron precursors (ONPs) as an intermediate state before neuron maturation. Additionally, we tried to isolate a proposed neurogenic population by using P75 as a single marker for neurogenic cells¹²².

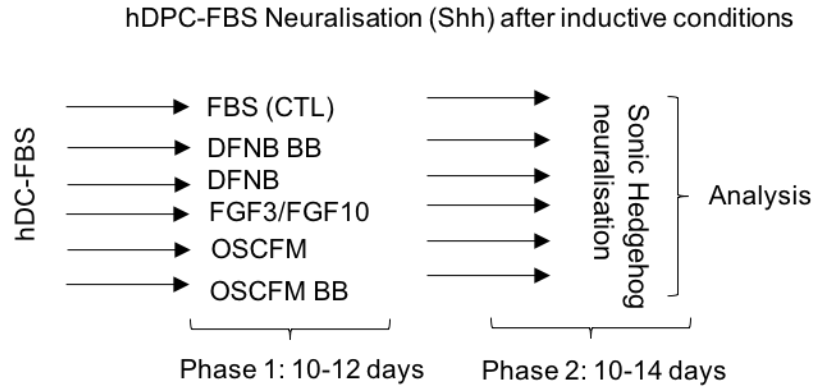
5.1. Generation and neuralisation of otic neural progenitors from hDPC-FBS cultures by inductive treatments.

The observations taken from our studies of mouse DPC work, suggested that treatment with different factors such as 6-Bromindirubin-3'-oxime (BIO) for WNT activation and BMP4 could also be used to generate neural progenitor-like cells. Additionally, the literature suggested the use of FGF3/10 for otic progenitor induction^{32,44}. Therefore, we treated hDPC established only in FBS (hDPC-FBS) with different media combinations and factors (WNT, BMP4, FGF 3, FGF10) to test if their neurogenic potential could be enhanced.

The complete set of treatments used on hDPC-FBS cultures, were the following (Diagram 5.1, phase 1):

- Untreated control (CTL): 20% FBS.
- Basal medium control DFNB: DMEM: F12, 1% N2 supplement and 2% B27 supplement.
- DFNB BB: 1 μ m BIO and 10ng/mL BMP4 in DFNB as neural progenitor inductor.

- FGF3/10: FGF3 and FGF10 (10ng/mL) in DFNB as otic neural progenitor inducer.
- OSCFM: as an additional condition.
- OSCFM BB: OSCFM + 1µm BIO + 10ng/mL BMP4.



| Medium | Conditions |
|--------------|--|
| 20% FBS | DMEM, 1x P/S, 2mM Glutamax (GIBCO), 100µM Ascorbic Acid (Sigma), 10%, 15% or 20% foetal bovine serum (FBS; GIBCO). No coating. |
| DFNB | DMEM:F12 (GIBCO), 1% N2 (GIBCO), 2% B27 (GIBCO), 1x P/S. |
| OSCFM | DFNB (DMEM:F12 (GIBCO), 1% N2 (GIBCO), 2% B27 (GIBCO)), 1x P/S (SIGMA), 20ng/mL bFGF (R&D Systems), 50ng/mL IGF (R&D Systems), 20ng/mL EGF (R&D Systems). Coated with mouse laminin (2.5ug/cm ² ; Cultrex). |
| OSCFM BB | OSCFM + 10ng/mL BMP4 (R&D) + BIO 0.75µm (Sigma), 1x P/S |
| FGF 3/ FGF10 | DFNB + 10ng/mL FGF3 (R&D) + FGF10 (R&D). |
| DFNB BB | DFNB + 10ng/mL BMP4 (R&D) + BIO 0.75µm (Sigma), 1x P/S |

Diagram 5.1. Workflow of hDPC-FBS treatments and neural differentiation using Sonic Hedgehog (Shh) induction and media reminder. hDPC-FBS cultures were transferred to different treatments to generate otic neural progenitors (ONPs; Phase 1). After the phase 1 conditions, the cultures were induced to neuralisation using the Shh protocol (neural induction; phase 2: NT3, BDNF, bFGF, Shh as described in materials and methods) . OSCFM: Otic Stem Cell Full Medium; BMP4: OSCFM + Bone morphogenic protein 4.

After 10-12 days in treatment, cultured cells presented a change in morphology. DFNB and FGF3/10 treated cells presented a flat morphology, with a large cytoplasm. DFNB and OSCFM with the addition of BIO and BMP4 (DFNB BB and OSCFM BB) resulted in cell death and small, round cells. Whereas the cultures transferred to the OSCFM treatment resulted in cells with similar morphology to hDPC-OSCFM established cultures in early passage (Fig. 5.1).

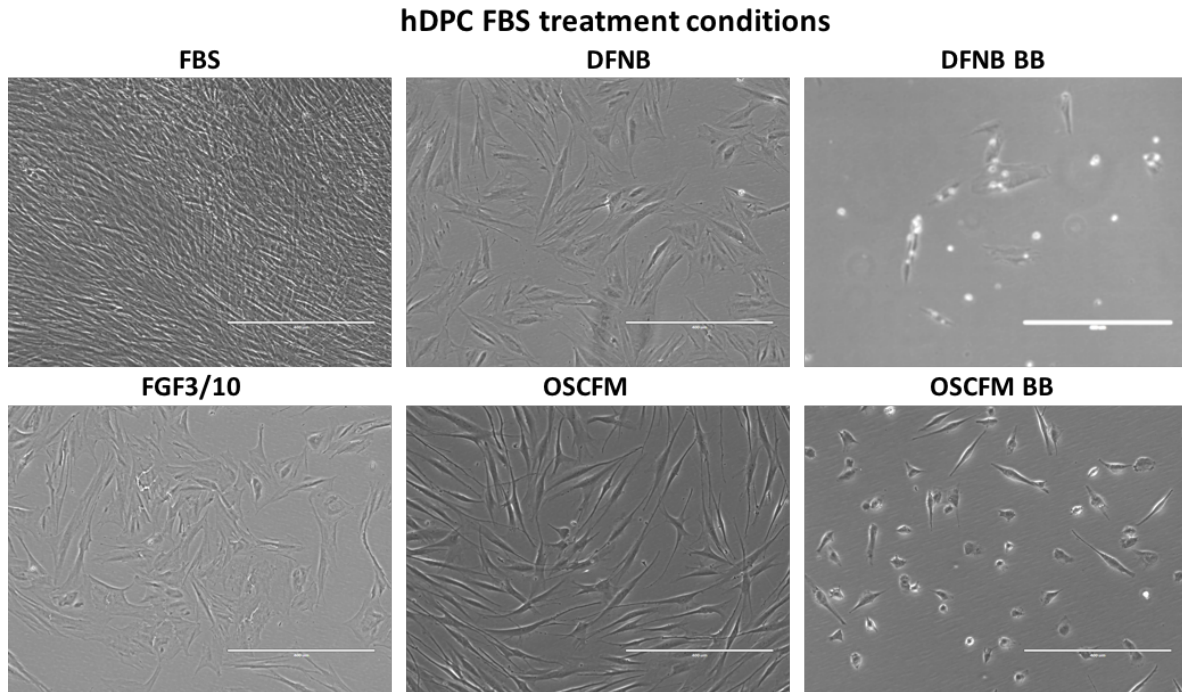


Figure 5.1. hDPC-FBS treated with different conditions. Morphology of hDPC initially grown in FBS medium were transferred to DFNB, DFNB BB, FGF3/10, OSCFM and OSCFM BB. Media details in diagram 5. 1.

Immunocytochemistry (ICC) was performed to look at neural progenitor and neural crest markers after 10-12-days of treatment (summary in table 5.1). The results showed a constant expression of SYR BOX9 (SOX9), NESTIN, Myelin protein 0 (P0), Glioma associated oncogene homolog 1 (GLI1) and SRY BOX2 (SOX2) across all groups (Fig. 5.2-5.6). The marker Neuronal differentiation 1 (NEUD) was not clearly evident in the control group grown in FBS but appeared clearly expressed in the treatments supplemented with BIO and BMP4 (DFNB BB and OSCFM BB; Fig. 5.3). SRY BOX10 (SOX10) was also clearer in the treatments containing BIO and BMP4, and absent from the other groups (Fig. 5.4). Nerve growth factor receptor (P75) showed a very weak signal in all of them (Fig. 5.5), attributable to background noise (Fig. 5.6). Generally speaking, the qualitative data suggest an effect of the treatments on hDPC-FBS cell morphology, and only slight changes in marker expression when exposed to the different treatments.

| | SOX9 | NESTIN | P0 | GLI1 | SOX2 | NEUD | SOX10 | P75 |
|----------|------|--------|----|------|------|------|-------|-----|
| FBS CTL | ++ | ++ | ++ | ++ | ++ | +- | -- | +-- |
| OSCFM | ++ | ++ | ++ | ++ | ++ | ++ | -- | +- |
| FGF3/10 | +- | ++ | ++ | ++ | ++ | +- | -- | +-- |
| OSCFM BB | ++ | ++ | ++ | ++ | ++ | ++ | ++ | +-- |
| DFNB | ++ | ++ | ++ | ++ | ++ | +- | +-- | +-- |
| DFNB BB | ++ | ++ | ++ | ++ | ++ | ++ | +- | +-- |

Table 5.1. Summary of hDPC FBS after treatments - immunocytochemistry (ICC). The expression of neural progenitor (NESTIN, GLI1, SOX2 and NEUD) and neural crest (SOX9, NESTIN, P0, SOX10 and P75) markers was evaluated by ICC after treating hDPC-FBS with different conditions as described in the text. Clear signal (++), Medium signal (+-), very low signal (+--). Refer to figures 5.2 to 5.5. Details of media in diagram 5.1.

After the 10-12 days in treatment, the experimental groups were transferred to the neuralising conditions for sensory auditory neuron generation with the Sonic Hedgehog (Shh) induction protocol used before (Chapter 4-section 4.5; diagram 5.1, phase 2). Differences in the cell's morphology of the Shh induced cultures were observed (FBS-Neu, DFNB-Neu, DFNB BB-Neu, FGF3/10-Neu, OSCFM-Neu and OSCFM BB-Neu). The basal condition induced to neuralise (FBS-Neu), changed to thin and somewhat elongated cells, some of them grouped in small colonies. The remaining treated groups presented cells in low densities and a small, round and thin morphology. OSCFM BB was not included (Fig 5.6A).

Following the differentiation, a relative expression analysis by qPCR was performed. Results from two independent hDPC-FBS cultures showed an overall upregulation of sensory-neural markers after neuralisation on treated cultures compared to the FBS control (Fig. 5.6B). In particular, expression of *NFH* increased in FBS-Neu and the FGF3/10-Neu groups in the hDPC4 FBS culture. *TUBIII* was upregulated in OSCFM-Neu and FGF3/10-Neu treatments in the hDPC4 FBS culture, whereas the hDPC16 FBS culture expressed a higher level in the

FGF3/10-Neu, DFNB-Neu and DFNB BB-Neu. In turn, *SYN* was found upregulated in the neuralised FBS group, FGF3/10-Neu, DFNB BB-Neu in the hDPC4-FBS culture. The hDPC16-FBS culture showed an upregulation of *SYN* after the neuralisation of DFNB (DFNB-Neu) and DFNB BB (DFNB BB-Neu) treatments. Neural induction upregulated *SYP* in the hDPC4 and hDPC16 FBS cultures treated with OSCFM (OSCFM-Neu) and FGF3/10 (FGF3/10-Neu). Finally, *VGLUT1* was found upregulated in FGF3/10 and DFNB BB treated hDPC4 FBS and DFNB treated hDPC16 FBS after neuralisation (Fig. 5.6B).

In other words, FBS-Neu cells after neuralisation generally failed to upregulate sensory neural markers, as shown before (Fig 4.13). The OSCFM group responded similarly, only showing significant upregulation of *NFH* and *SYP* in one of the two independent experiments. The FGF3/10 treatment responded better to the neural induction, upregulating *TUBIII*, *SYN*, *SYP* and *VGLUT1* in at least one of the two hDPC-FBS cultures. The DFNB group was also able to upregulate *TUBIII*, *SYN* and *VGLUT1*, but only in the hDPC16 FBS. Lastly, *TUBII*, *SYN* and *VGLUT1* were found in the neuralised DFNB BB in at least 1 of the hDPC-FBS cultures. Overall, the FGF3/10 upregulation was more consistent for both hDPC-FBS cultures (Fig. 5.7B).

We then evaluated the qualitative expression of the neural markers Tubulin β 3 (TUJ1), NESTIN, Neurofilament Heavy Chain (NF200), Neuronal Differentiation 1 (NEUD), Glial Fibrillary Acidic Protein (GFAP) and PERIPHERIN by ICC. As expected from previous results, TUJ1 and NESTIN were present in all groups, whereas NF200 appeared with a more defined cellular pattern in the neuralised groups of all treatments. NEUD appeared more positive in OSCFM, FGF3/10 and DFNB after neuralisation. GFAP was negative in all groups except for the neuralised DFNB and BB groups, where the expression was stronger. Finally, PERIPHERIN was present in all groups, seemingly weaker in the non-neuralised FBS control (Table 5.2., Fig. 5.8, 5.9 and 5.10). In summary, the treatments allowed a very mild, qualitative neuralisation response, with more clear changes in the expression of NEUD and GFAP for some treatments.

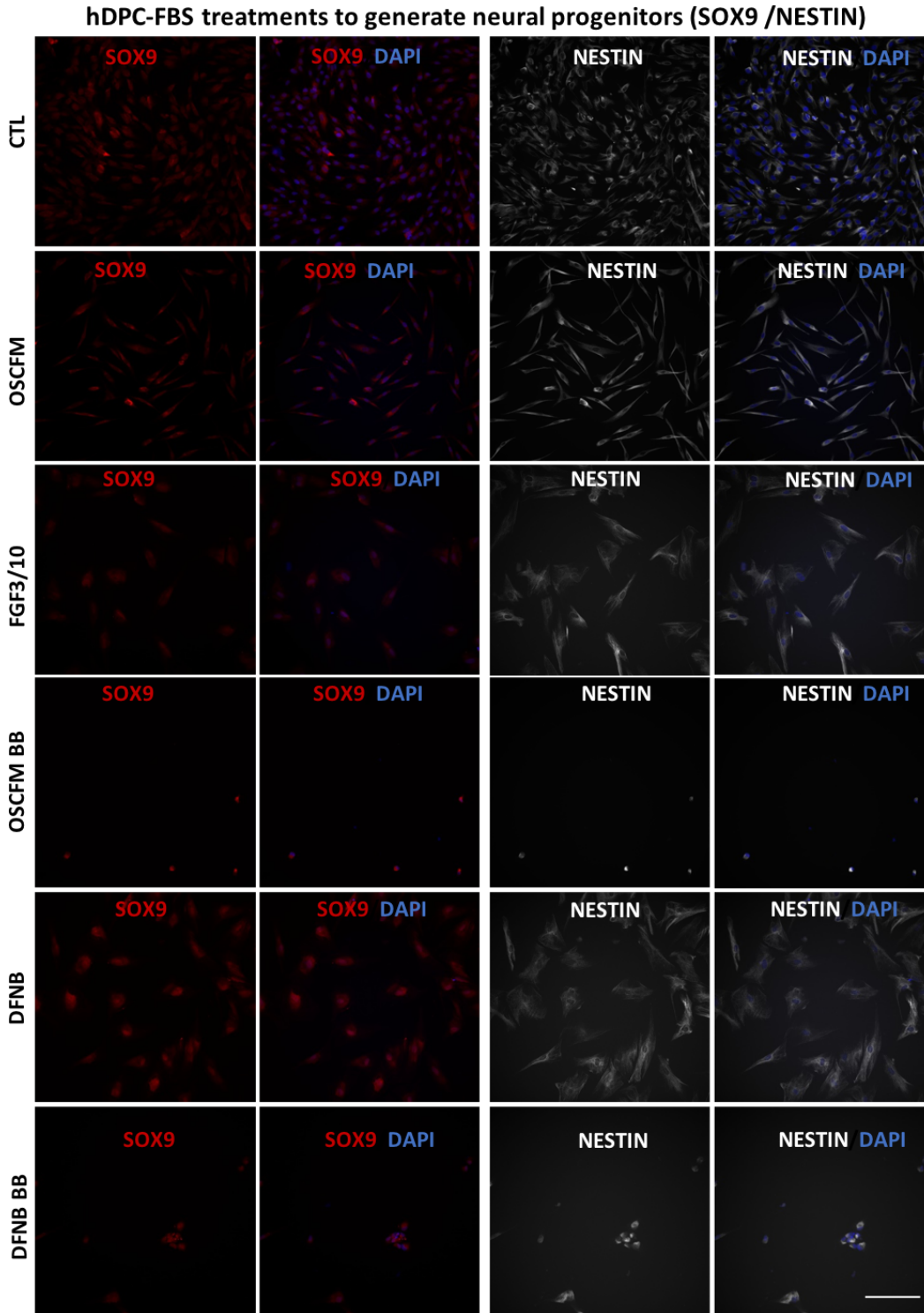


Figure 5.2. hDPC-FBS cultures treated for neural progenitor induction Immunocytochemistry (SOX9 and NESTIN). Immunocytochemistry of hDPCs-FBS treated with different conditions. Nuclear expression of SOX9 is evident after all treatments, except for OSCFM. NESTIN expression is seen in all treatments. Scale Bar: 200µm. Details of media in diagram 5.1. For each marker, the image was taken with the same configuration among treatments to allow comparison.

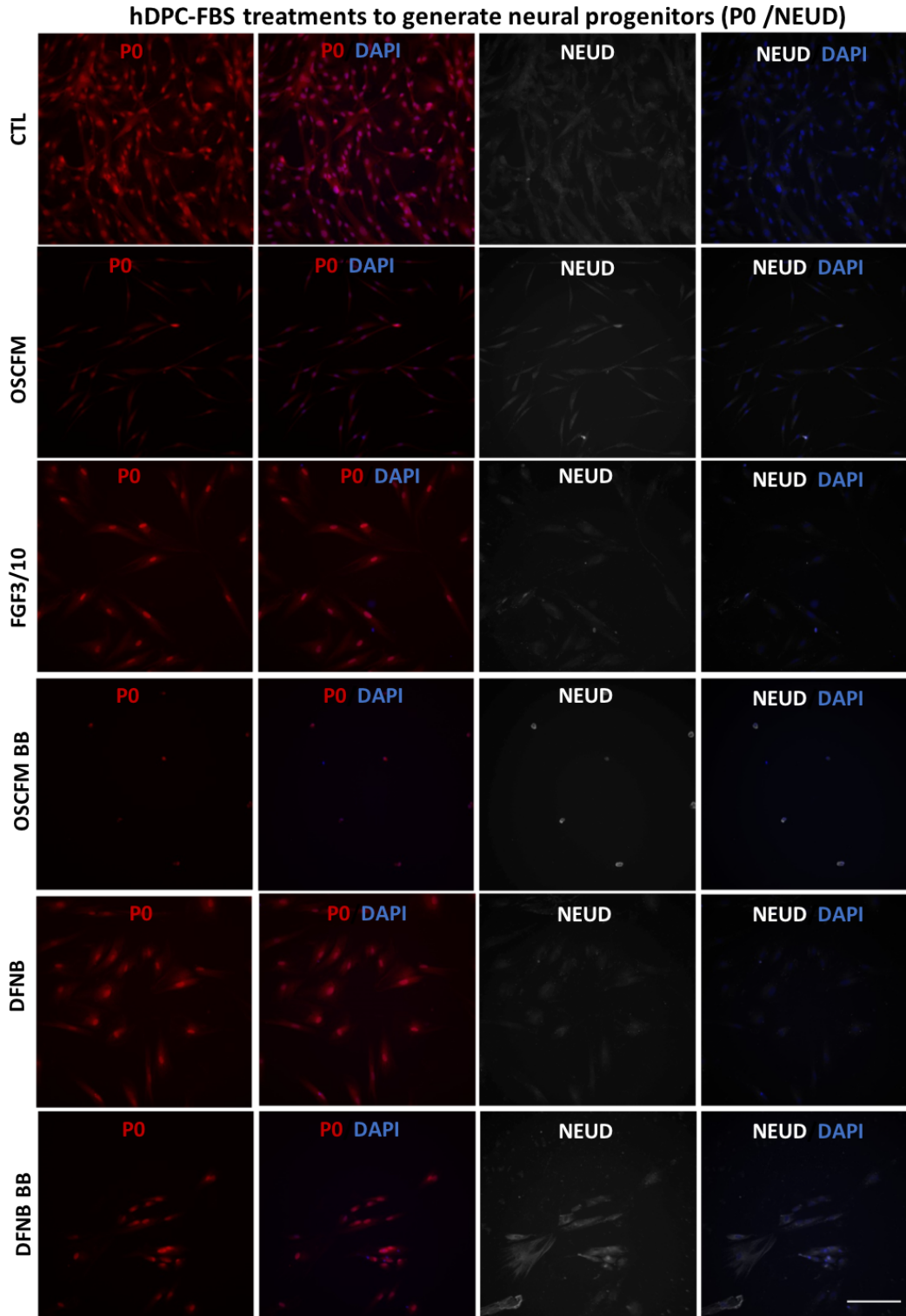


Figure 5.3. hDPC-FBS cultures treated for neural progenitor induction - Immunocytochemistry (P0 and NEUD). Immunocytochemistry of hDPCs-FBS treated with different conditions. Nuclear expression of P0 is evident after all treatments. NEUD expression was detected in all treatments, but in different intensities. Scale Bar: 200 μ m. Details of media in diagram 5.1. For each marker, the image was taken with the same configuration among treatments to allow comparison.

hDPC-FBS treatments to generate neural progenitors (GLI1 /SOX10)

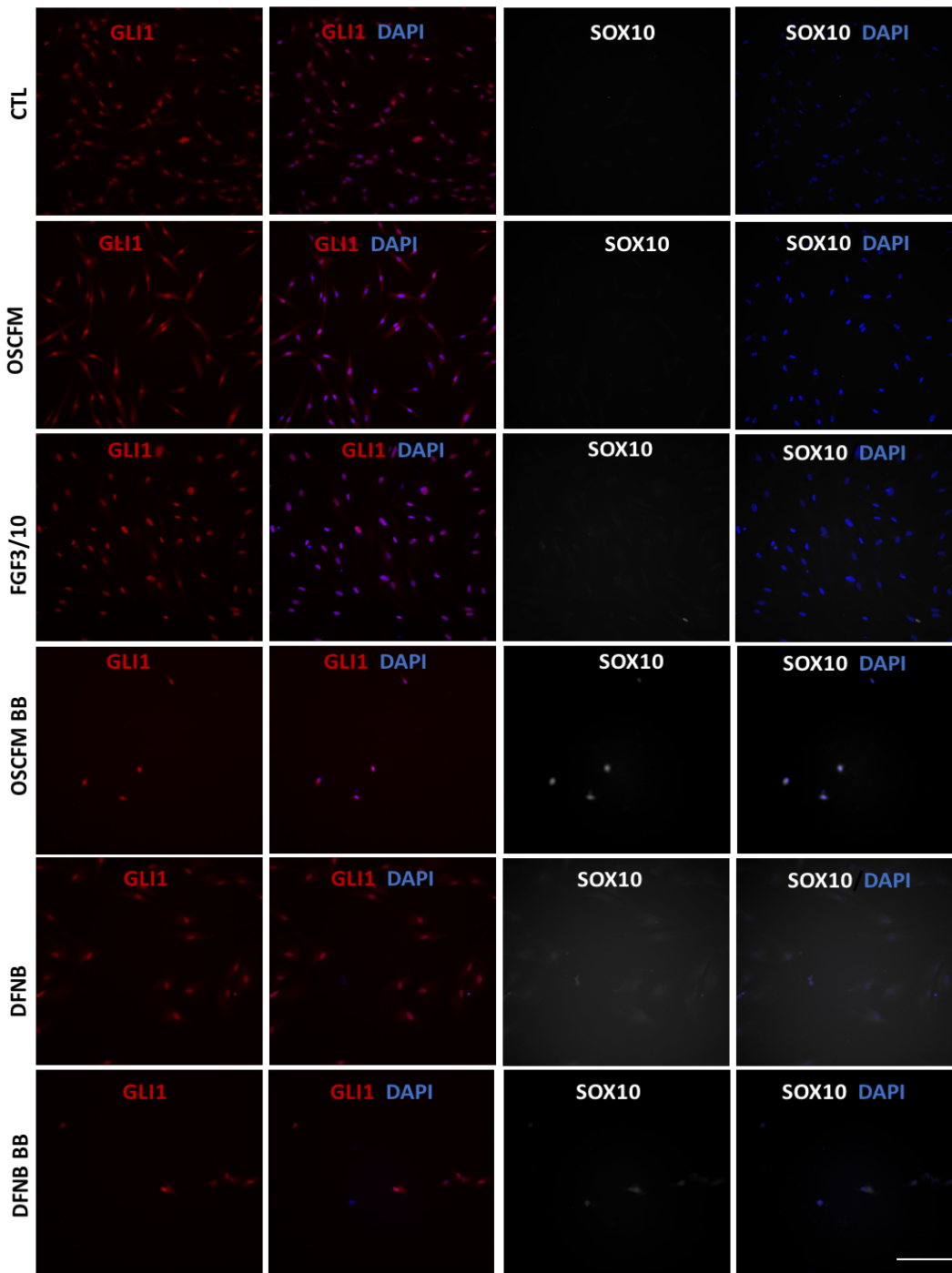


Figure 5.4. hDPC-FBS cultures treated for neural progenitor induction - Immunocytochemistry (GLI1 and SOX10). Immunocytochemistry of hDPCs-FBS treated with different conditions. Nuclear expression of GLI1 is evident after all treatments. SOX10 expression was detected only in OSCFM BB, DFNB and DFNB BB treatments in different intensities. Scale Bar: 200µm. Details of media in diagram 5.1. For each marker, the image was taken with the same configuration among treatments to allow comparison.

hDPC-FBS treatments to generate neural progenitors (SOX2 /P75)

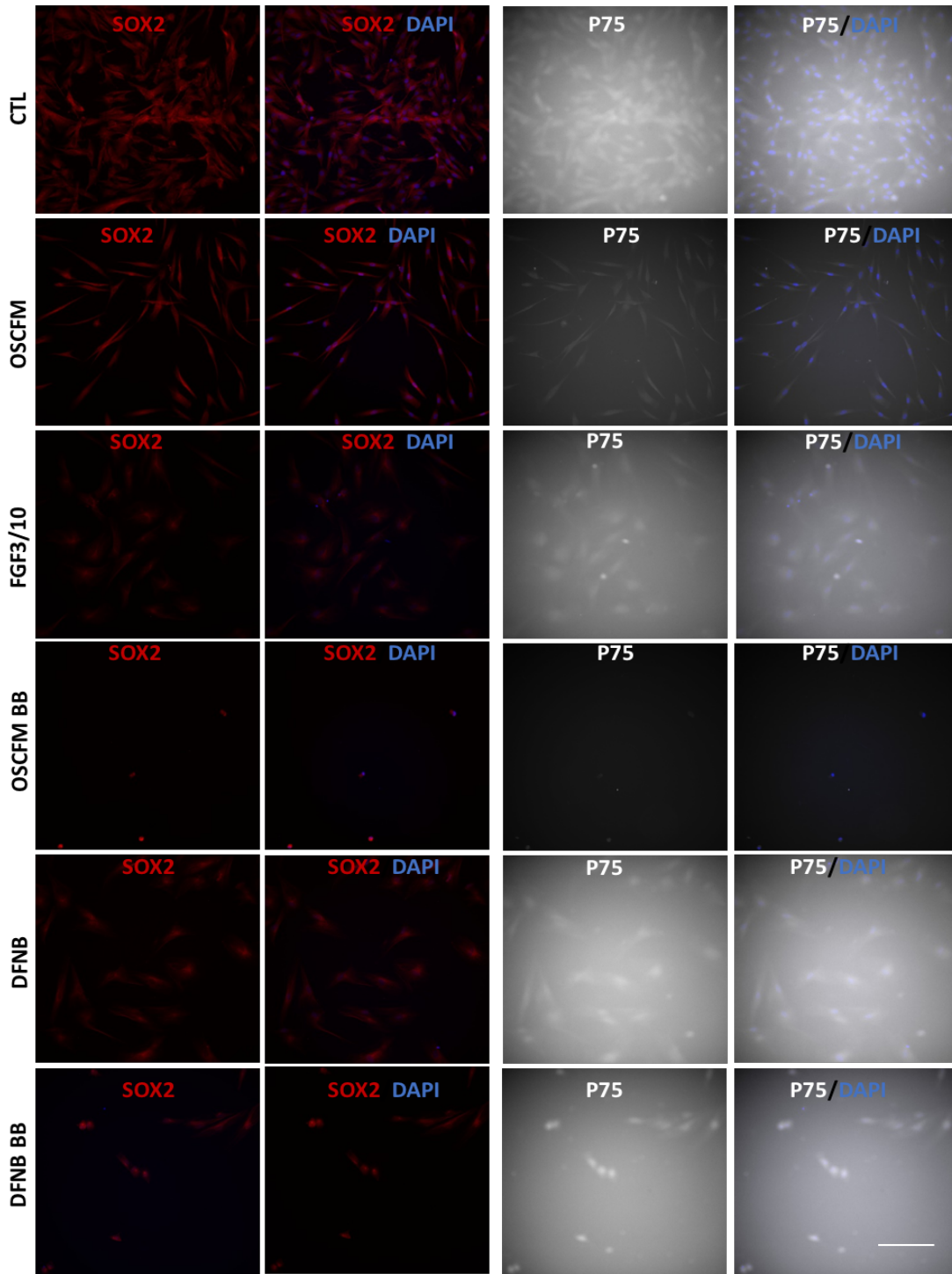


Figure 5.5. hDPC-FBS cultures treated for neural progenitor induction - Immunocytochemistry (SOX2 and SOXP75). Immunocytochemistry of hDPCs-FBS treated with different conditions. Nuclear expression of SOX2 is evident after all treatments. P75 expression was very weak in all treatments, the signal is likely to come from the high exposure, similar to the no primary negative control (See below). Scale Bar: 200µm. Details of media in diagram 5.1. For each marker, the image was taken with the same configuration among treatments to allow comparison.

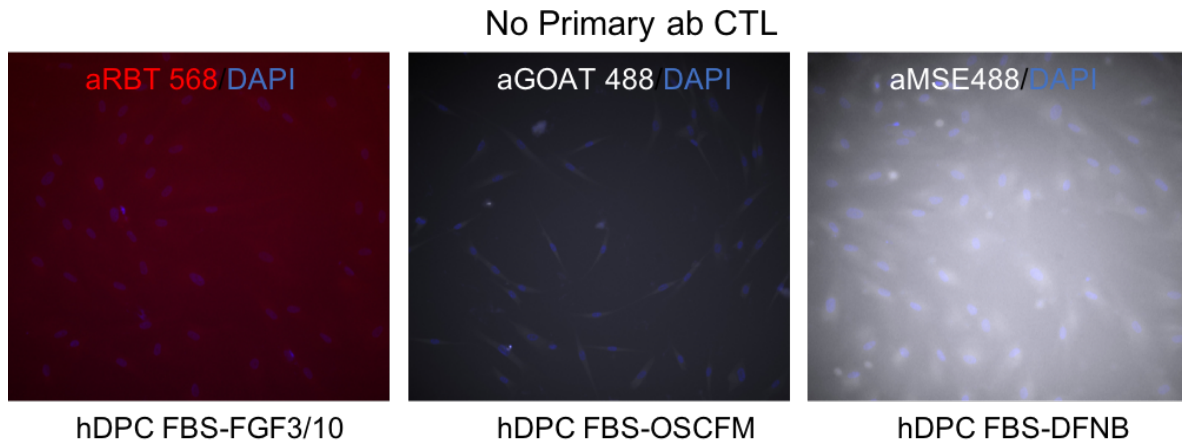


Figure 5.6 No primary antibody (ab) controls. hDPC FBS were treated with different media. A control of negative staining was done by incubating the cultures without the primary antibody to detect any unspecific signal from the secondary antibody. A random group (treatment) was chosen to incubate without primary antibody. aRBT 568 did not present unspecific signal, aGOAT and aMSE 488 presented unspecific signal when over-exposed.

Neuralisation of treated hDPC-FBS.

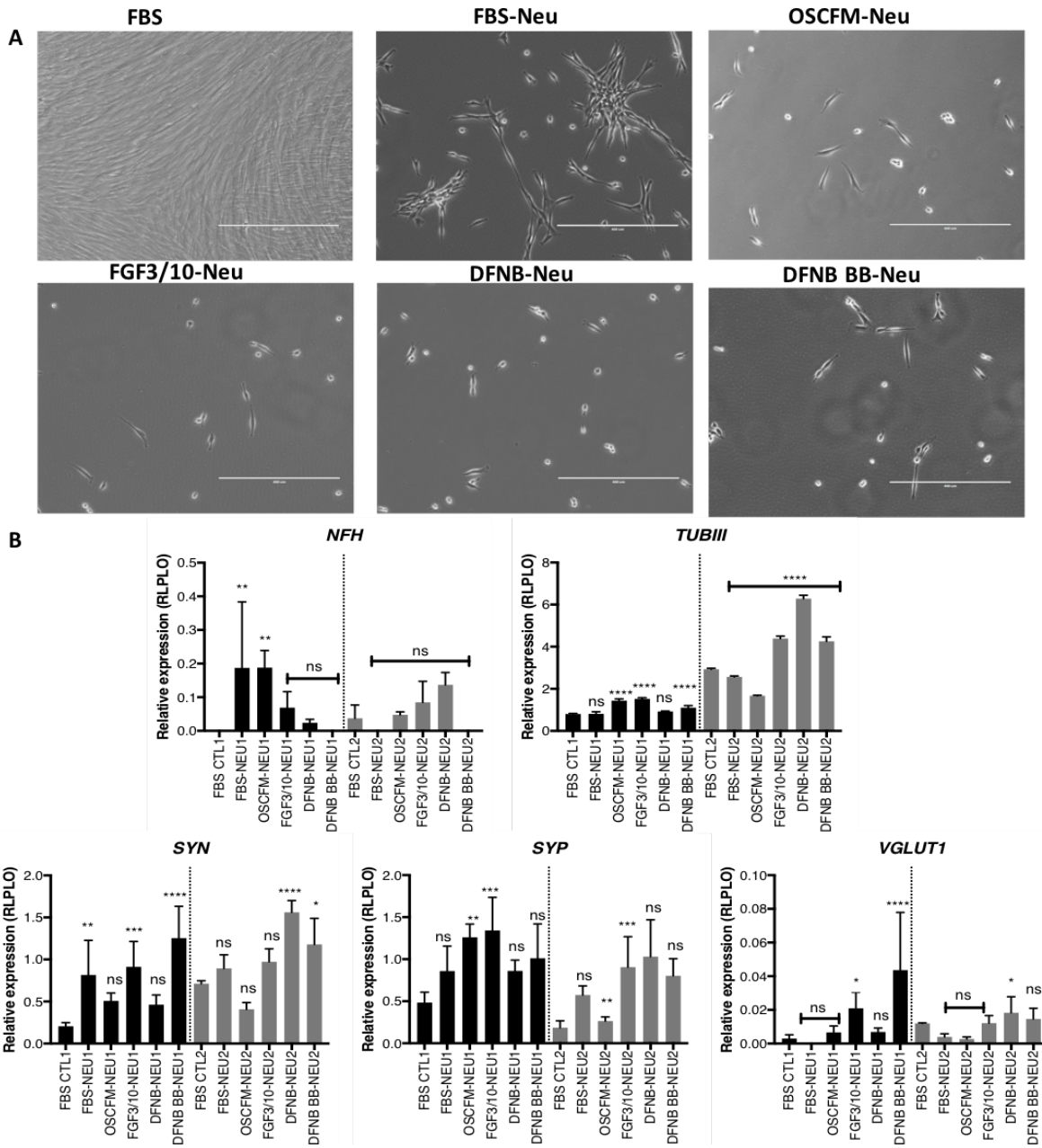


Figure 5.7. hDPC neuralisation after treatments (Phase 2). A) hDPCs originally derived in FBS medium (hDPC-FBS) were treated to generate neural progenitors and followed by neural differentiation treatment using Sonic Hedgehog induction (diagram 5.1 phase 2). Morphological changes in the treated groups were evident. B) Relative expression analysis of sensory neural related genes in two independent hDPC-FBS cultures. Values were normalised to an otic neural progenitor line. A one-way-ANOVA followed by a Tukey test for pairwise comparison was made to determine differences between the control group and the treatments. Group labelled as 1 (left bars) = hDPC FBS 4, group labelled as 2 (right bars) = hDPC FBS 16. * $p < 0.05$, ** $p < 0.01$ *** $p < 0.001$, **** $p < 0.0001$. Error bars represent technical replicates. Scale bar: 400 μ m.

| | TUJ1 | NESTIN | NF200 | NEUD | GFAP | PERIPHERIN |
|-------------|------|--------|-------|------|------|------------|
| FBS CTL | ++ | ++ | +- | +-- | -- | +- |
| FBS-NEU | ++ | ++ | ++ | +-- | -- | ++ |
| OSCFM-NEU | +- | ++ | ++ | +- | -- | ++ |
| FGF3/10-NEU | ++ | ++ | ++ | +- | -- | ++ |
| DFNB-NEU | ++ | ++ | ++ | +- | ++ | ++ |
| BB-NEU | ++ | ++ | ++ | +-- | ++ | ++ |

Table 5.2. Summary of Neuralisation of treated hDPC-FBS. The qualitative expression of neural markers was evaluated after treated hDPC-FBS were induced to neuralisation. High signal (++) , Medium signal (+-), very low signal (+--). Refer to figures 5.7 to 5.9.

hDPC FBS treatments + Neuralisation (TUJ1/NF200)

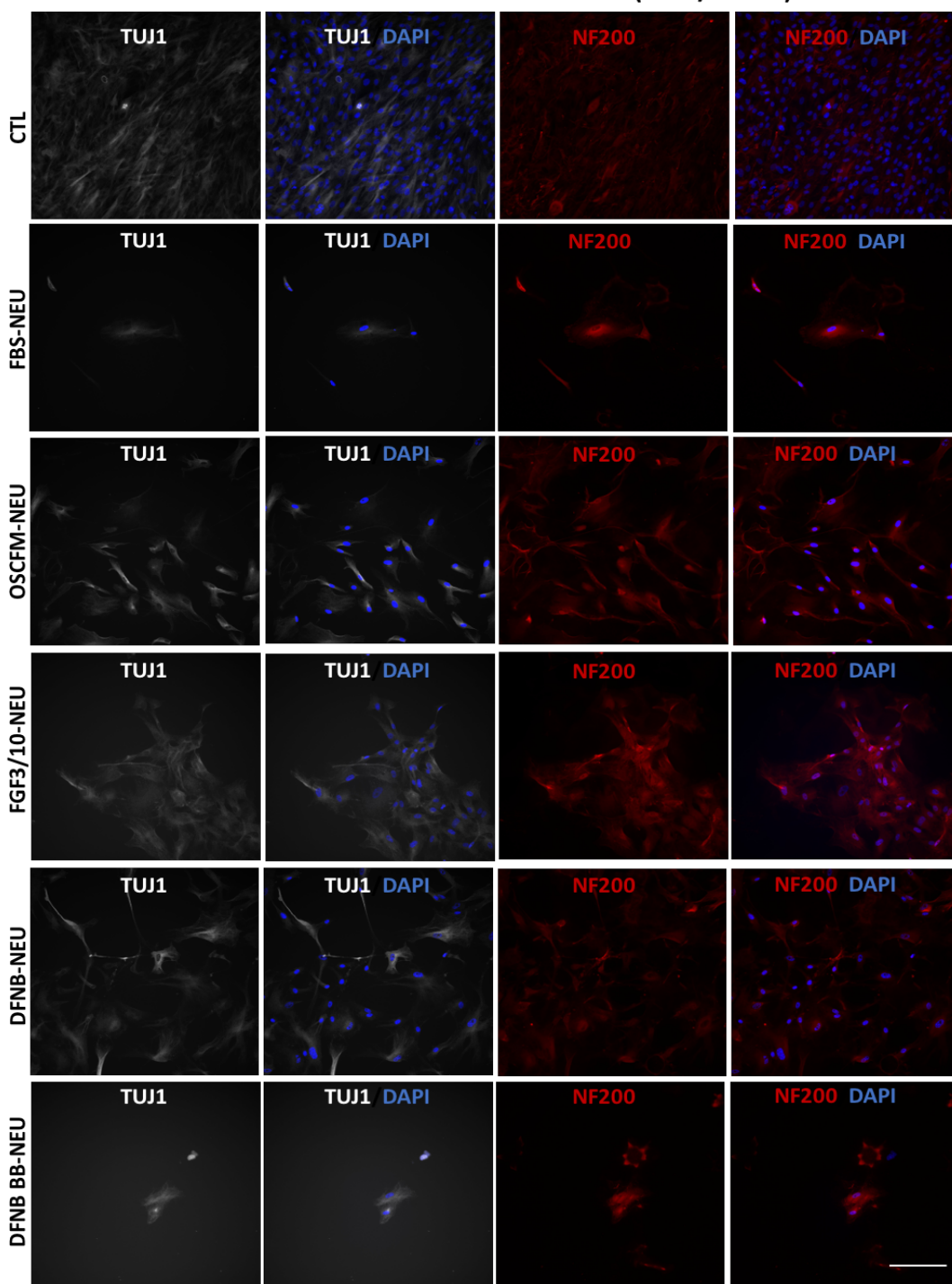


Figure 5.8 Neuralised hDPCs after treatments - Immunocytochemistry (TUJ1 and NF200). Expression of the neural markers TUJ1 and NF200 after the treated hDPCs were induced to neuralisation with Sonic hedgehog. TUJ1 and NF200 were found expressed in all experimental groups. Scale bar: 200 μ m.

hDPC FBS treatments + Neuralisation (NEUD/GFAP)

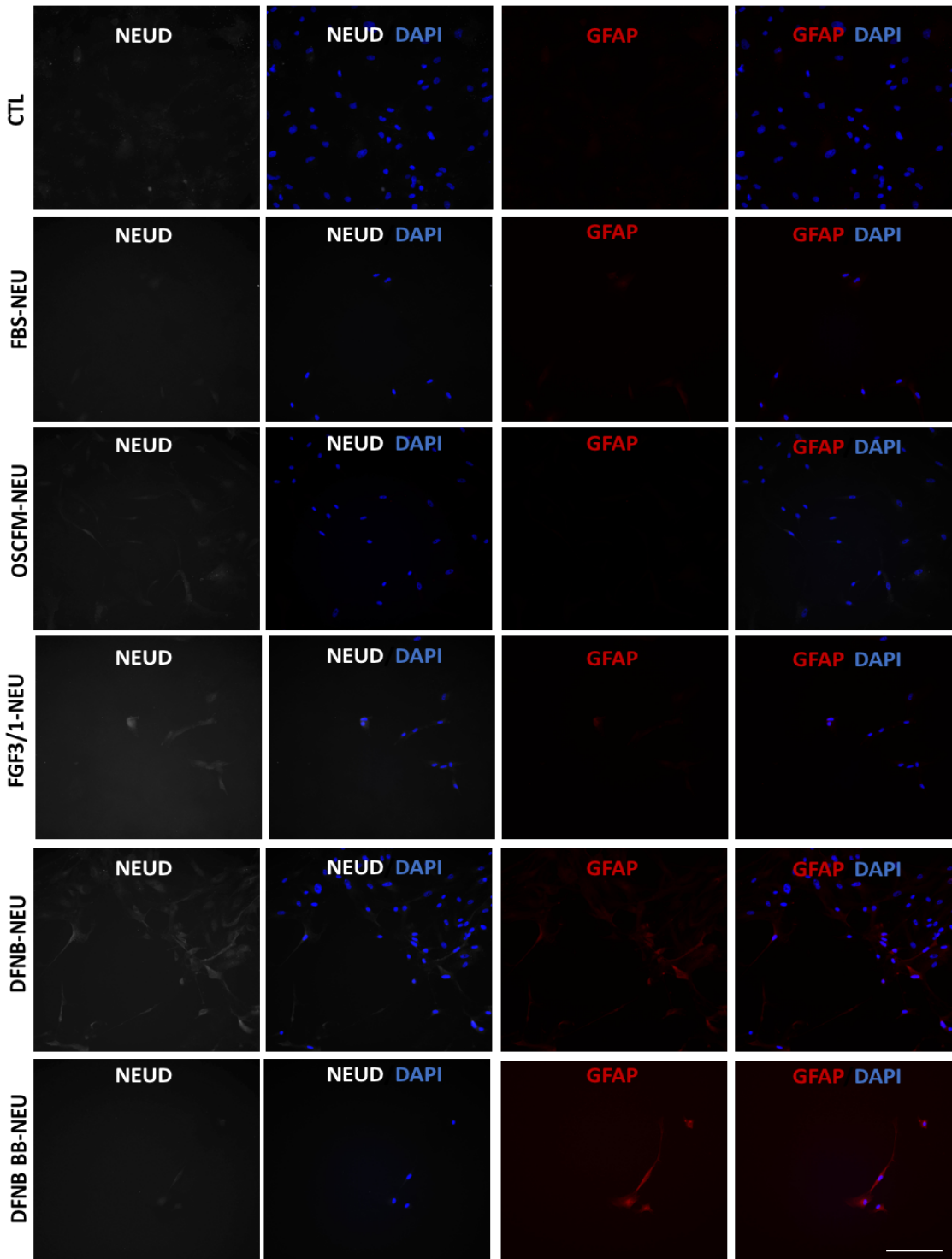


Figure 5.9. Neuralised hDPCs after treatments - Immunocytochemistry (NEUD and GFAP). Expression of the markers NEUD and GFAP after the treated hDPCs were induced to neuralisation with Sonic hedgehog. NEUD expression varies across conditions, more evident on OSCFM-Neu, FGF3/10-Neu and DFNB-Neu. GFAP is expressed only in DFNB-Neu and DFNB BB-Neu. Scale bar: 200µm.

hDPC FBS treatments + Neuralisation (NESTIN/PERIPHERIN)

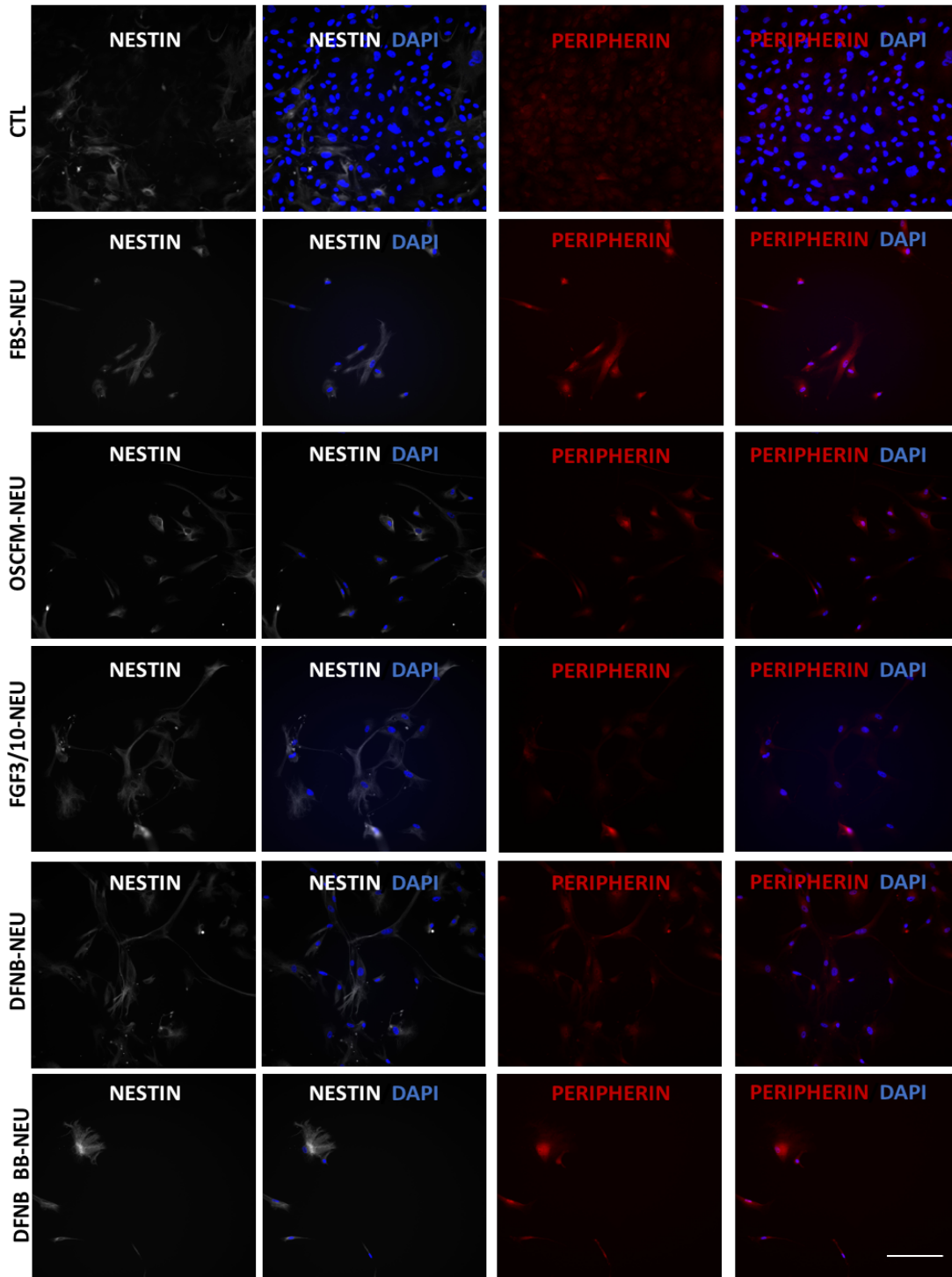


Figure 5.10. Neuralised hDPCs after treatments - Immunocytochemistry (NESTIN and PERIPHERIN). Expression of NESTIN and PERIPHERIN after the treated hDPCs were induced to neuralisation with Sonic hedgehog. NESTIN and PERIPHERIN expression is present across conditions. Scale bar: 200µm.

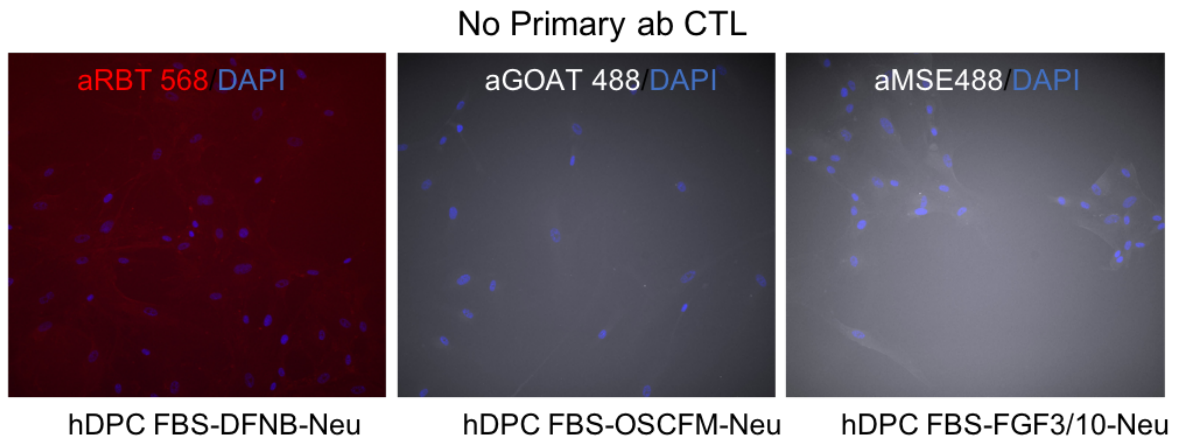


Figure 5.11 hDPC inductive Treatments + differentiation no primary antibody (ab) controls. hDPC FBS under different treatments were induced to neuralised. A control of negative staining was done by incubating the cultures without the primary antibody to detect any unspecific signal from the secondary antibody.

5.2. Evaluation of human Foetal auditory stem cells (hFASCs)-conditioned media on hDPC-FBS cultures.

Apart from using different treatments to obtain neural progenitor cells, we evaluated the effect of conditioned media (CM) from two independent human foetal auditory stem cells (hFASC) on hDPC-FBS cells. We hypothesized that the factors contained in the CM would promote the differentiation of hDPCs into otic progenitors, similar to what was observed in bone marrow mesenchymal stem cells⁴⁴. After 10-12 days in hFASC conditioned media (hFASC 033 and hFASC 035), the cultures were stained by immunocytochemistry (ICC). We included OSCFM and FGF 3/10 treatments for comparison.

To identify an otic neural progenitor (ONP) phenotype in the cultures growing in hFASC-CM, several neural, neural progenitors and WNT pathway markers were evaluated. As expected, we found TUJ1, NF200 and GLI present, as seen before in basal conditions and other treatments. β -Catenin (β -Cat), member of the canonical WNT pathway was present in the cytoplasm. NeuroD1 (NEUD) was clearly shown in cells growing with both conditioned media. The ONP markers Achaete-Scute family transcription factor 1 (ASCL1), Paired box 8 (PAX8) and Paired box 2 (PAX2) were weakly present in the FBS control group and FGF3/10, but positive in OSCFM, and conditioned media. In the case of SOX2, it appeared stronger in

both conditioned media groups. T Cell leukemia homeobox 3 (TLX3) a homeobox gene for neural fate was present in FBS cells, and mildly present in OSCFM and FGF3/10, but absent in both conditioned media groups. Brain specific homeobox protein 3 (BRN3a) was almost completely absent in all groups, only weakly present in FGF3/10 and hFASC 033. Finally, SOX10 appeared also undetectable except for a weak expression in FBS control and hFASC 035 (Table 5.3; Figures 5.10, 5.11, 5.12, 5.13, 5.14 and 5.15).

| | TUJ1 | NF200 | GLI1 | BCAT | NEUD | ASCL1 | PAX8 | PAX2 | SOX2 | TLX1 | BRN3a | SOX10 |
|--------------|------|-------|------|------|------|-------|------|------|------|------|-------|-------|
| FBS CTL | ++ | ++ | ++ | ++ | +-- | +-- | +-- | +- | +- | ++ | -- | +-- |
| OSCFM | ++ | ++ | ++ | ++ | +- | ++ | ++ | ++ | +- | +- | -- | -- |
| FGF3/10 | +- | ++ | ++ | ++ | +- | +- | -- | +- | +- | +- | +-- | -- |
| hFASC 033 | ++ | ++ | ++ | ++ | ++ | ++ | ++ | ++ | ++ | -- | +-- | -- |
| hFASC 035 | ++ | ++ | ++ | ++ | ++ | ++ | ++ | ++ | ++ | +-- | -- | +-- |

Table 5.3. Summary of hDPC-FBS after hFASC conditioned medium. The qualitative expression of neural markers was evaluated after hDPC-FBS grown with hFASC conditioned medium were induced to neuralisation (Shh protocol). High signal (++), Medium signal (+-), very low signal (+--).

In general terms, hDPC-FBS cells grown in FASCs condition media seem to express markers related to otic neural progenitors such as NEUD, ASCL1, PAX8, PAX8 and SOX2 when compared to the control, OSCFM and FGF3/10 treatments.

hDPC FBS grown in hFASC conditioned media (ASCL1/NEUD)

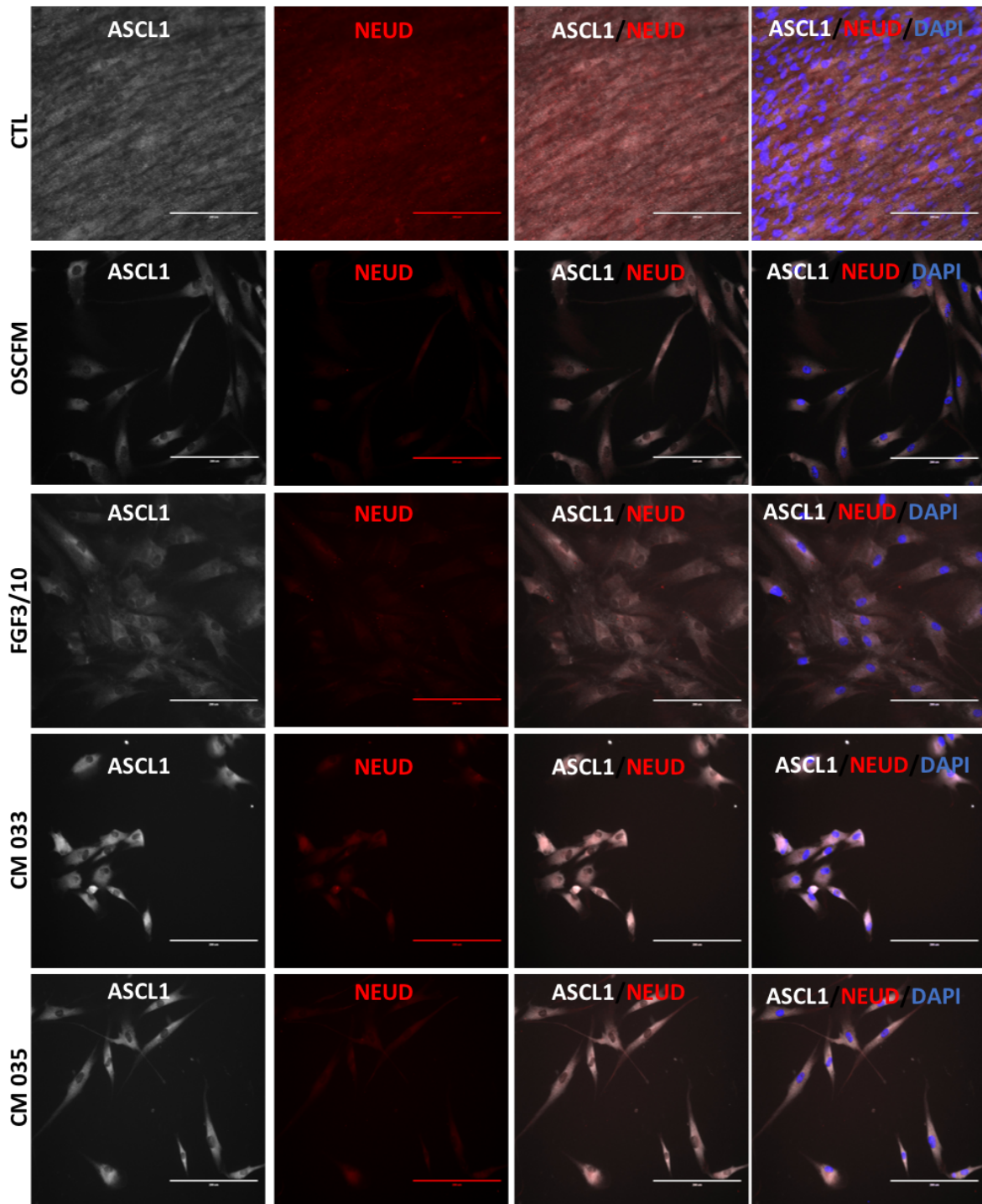


Figure 5.10. Effect of hFASC conditioned media on hDPC-FBS. Expression of the neural progenitor markers ASCL1 and NEUD after 12 days of culture with conditioned media. Both markers are clearly found in the cytoplasm. CTL: 20% FBS Medium. Scale bar: 200 μ m.

hDPC FBS grown in hFASC conditioned media (BRN3a/SOX2)

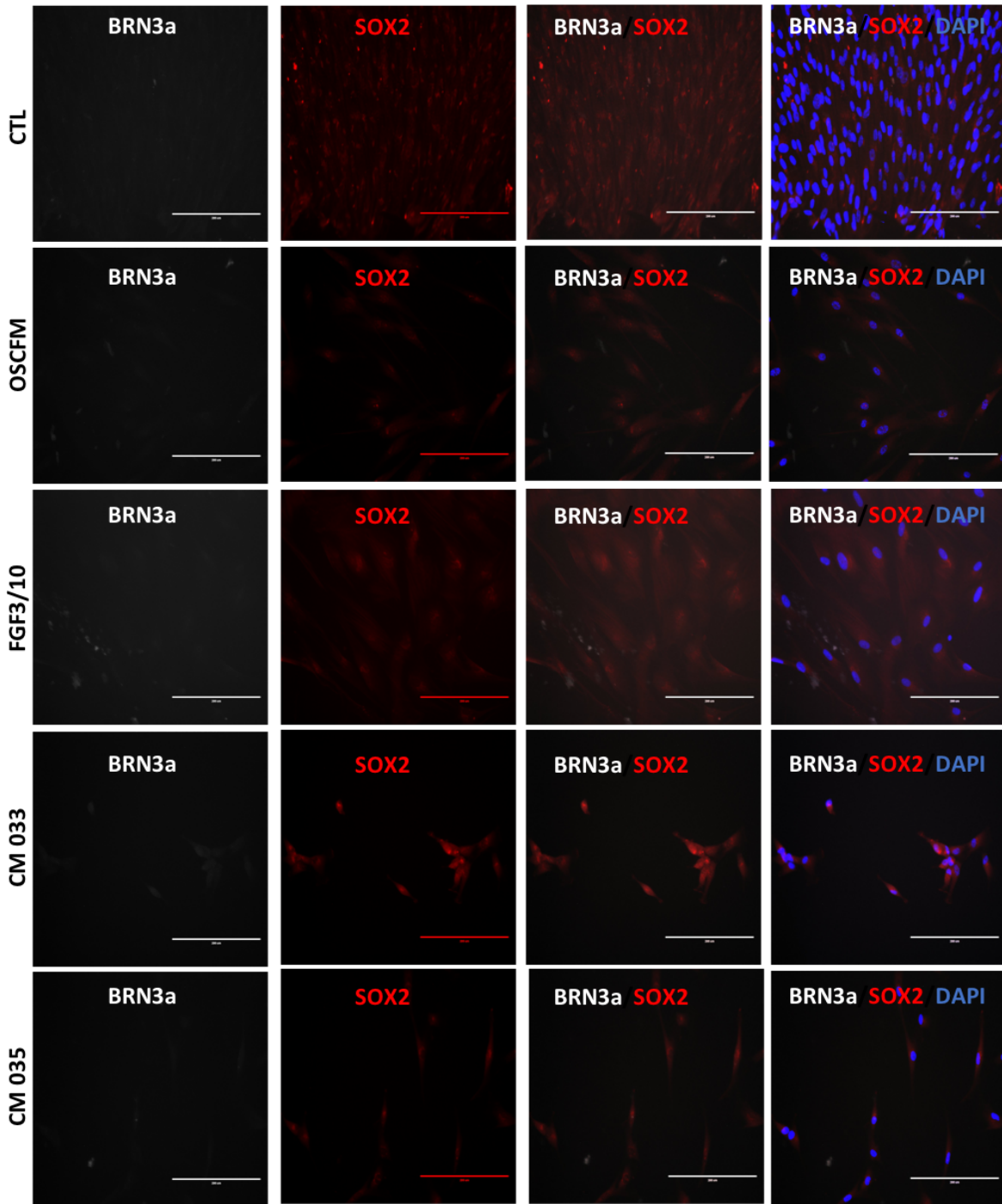


Figure 5.11. Effect of hFASC conditioned media on hDPC-FBS. Expression of the neural progenitor markers BRN3a and SOX2 after 12 days of culture with conditioned media. BRN3a is weakly expressed in FGF3/10 and CM 033 media. SOX2 is evident in all experimental groups. CTL: 20% FBS Medium. Scale bar: 200µm.

hDPC FBS grown in hFASC conditioned media (PAX2/PAX8)

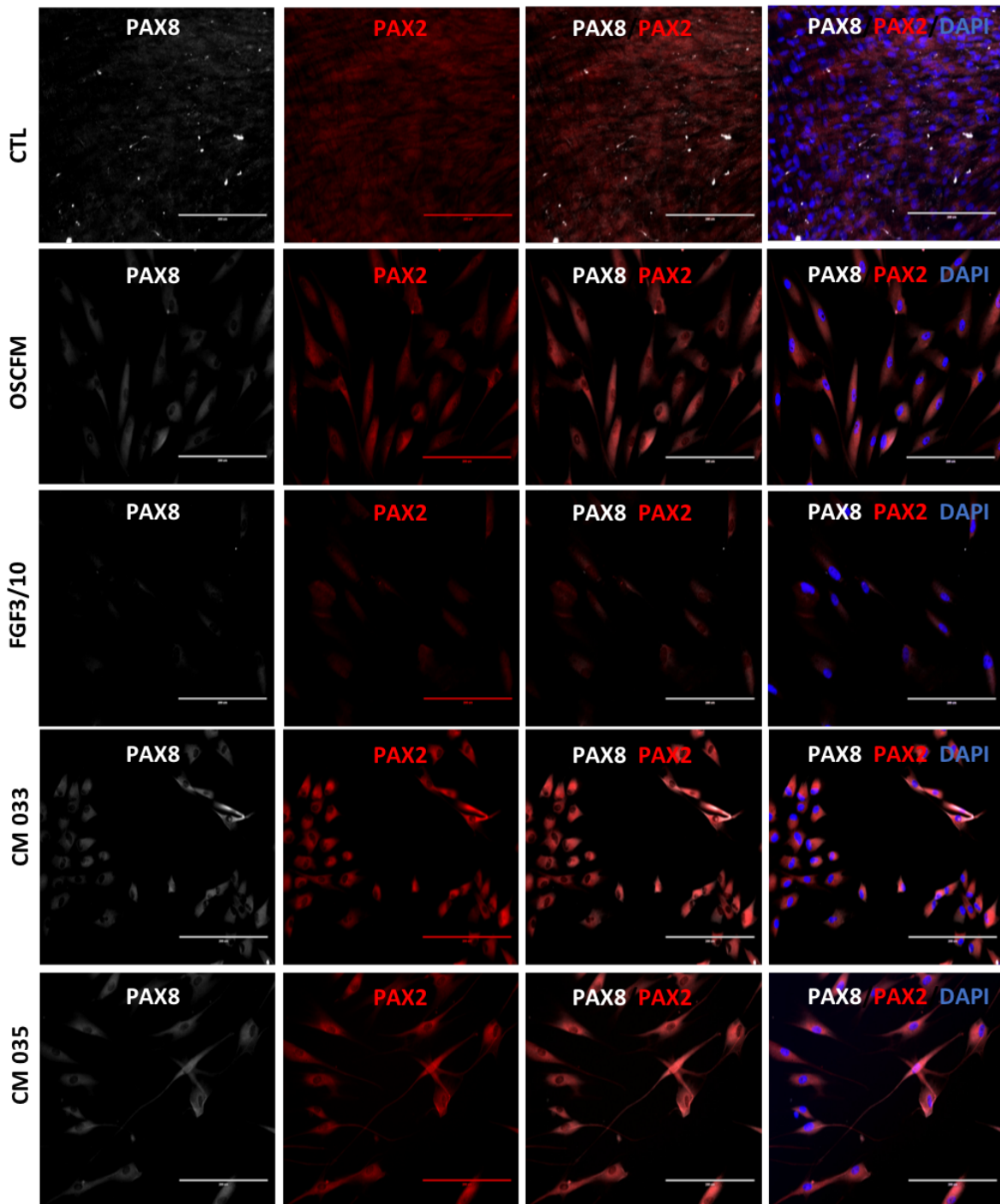


Figure 5.12. Effect of hFASC conditioned media on hDPC-FBS. Expression of the neural progenitor markers PAX8 and PAX2 after 12 days of culture with conditioned media. PAX8 signal is found in all conditions except for FGF3/10. PAX2 is evident in all conditions, weaker in FGF3/10. CTL: 20% FBS Medium. Scale bar: 200µm.

hDPC FBS grown in hFASC conditioned media (β -CAT/SOX10)

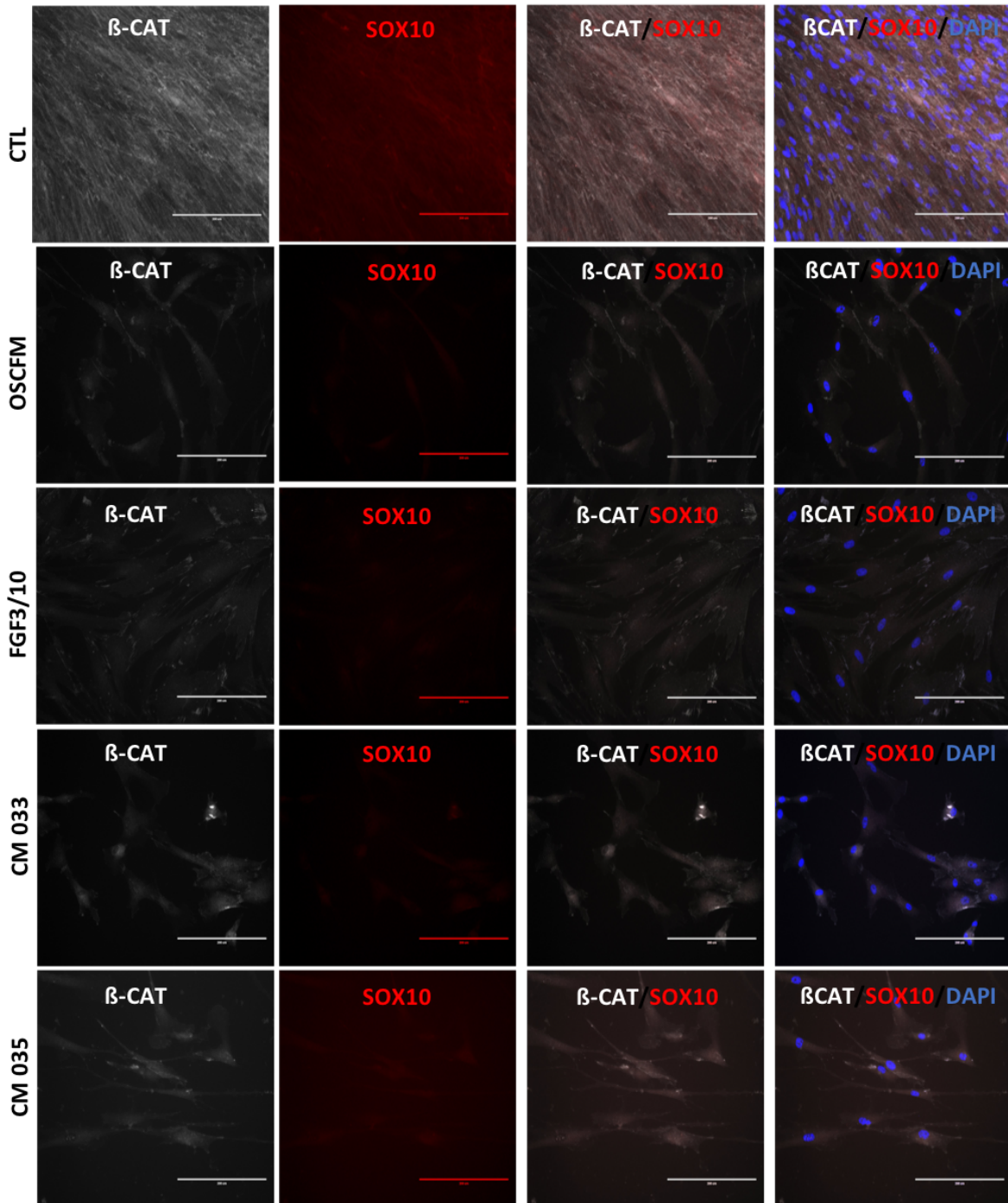


Figure 5.13. Effect of hFASC conditioned media on hDPC-FBS. Expression of the markers β -CAT and SOX10 after 12 days of culture with conditioned media. β -CAT is present in all experimental groups. SOX10 expression is weakly observed in CM 033. CTL: 20% FBS Medium. Scale bar: 200 μ m.

hDPC FBS grown in hFASC conditioned media (TLX1/GLI1)

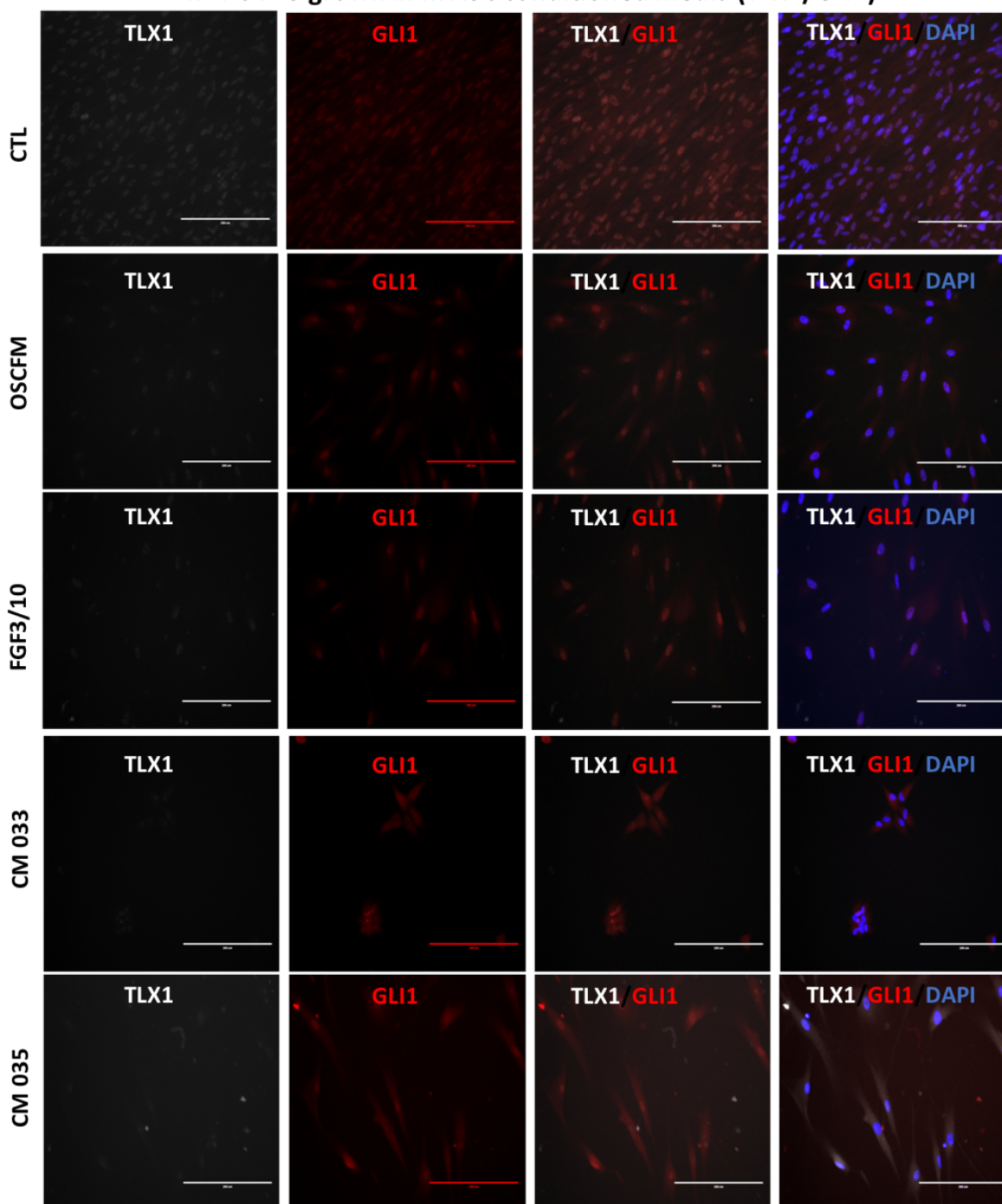


Figure 5.14. Effect of hFASC conditioned media on hDPC-FBS. Expression of the neural progenitor markers TLX1 and GLI1 after 12 days of culture with conditioned media. TLX1 expression is clear in the CTL group. GLI1 signal was found in all experimental groups. CTL: 20% FBS Medium. Scale bar: 200 μ m.

hDPC FBS grown in hFASC conditioned media (TUJ1/NF200)

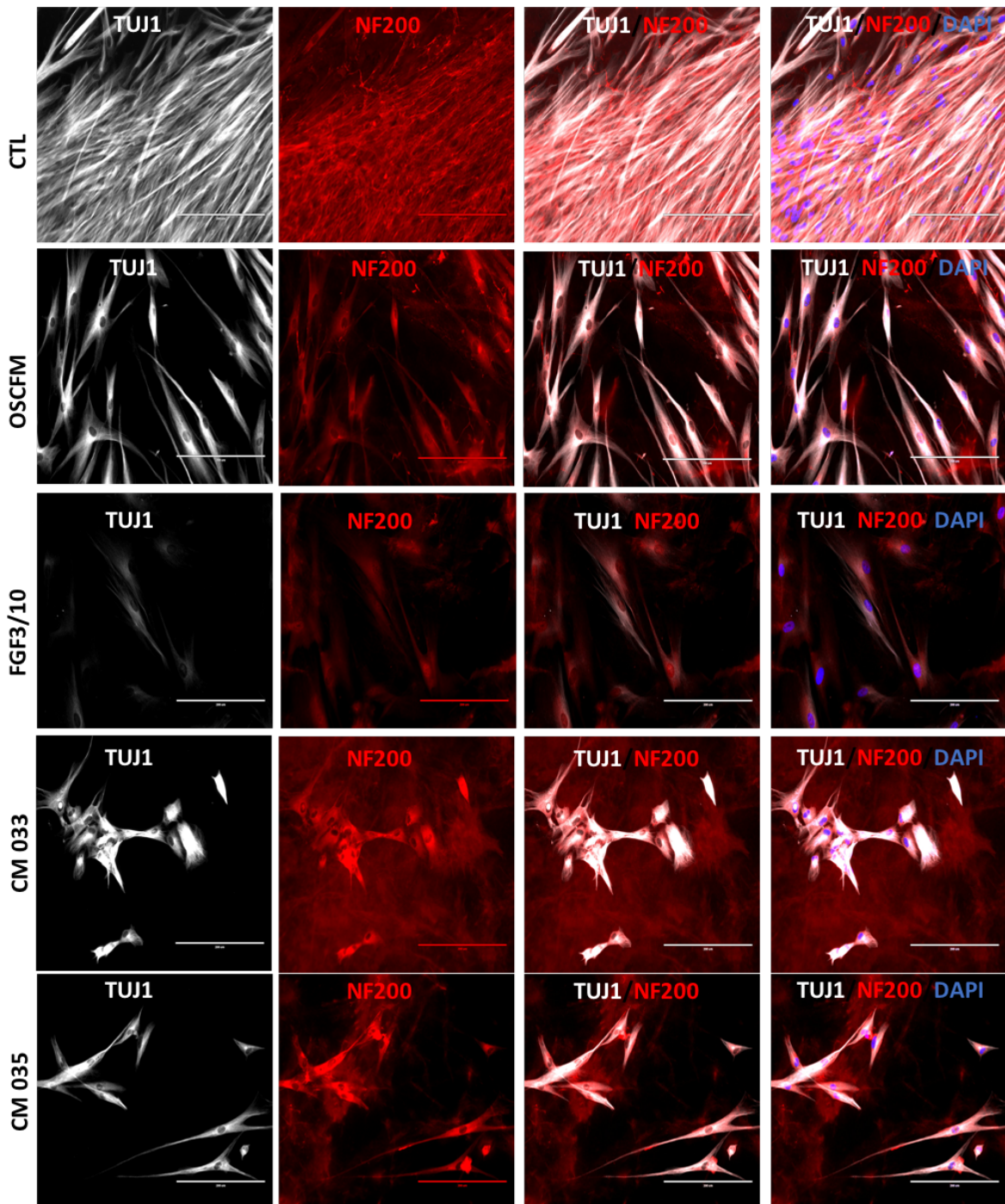


Figure 5.15. Effect of hFASC conditioned media on hDPC-FBS. Expression of the neural markers TUJ1 and NF200 after 12 days of culture with conditioned media. TUJ1 and NF200 were found expressed in all experimental groups. CTL: 20% FBS Medium. Scale bar: 200µm.

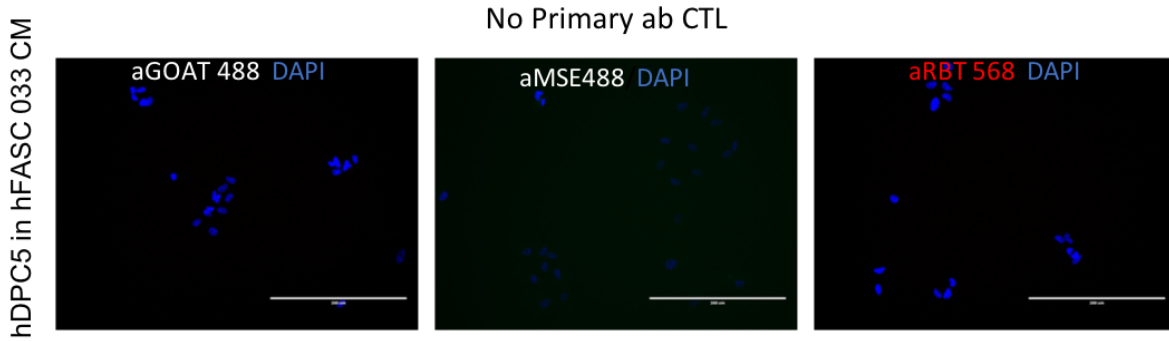


Figure 5.16. hFASC-CM no primary control. A control of negative staining was done by incubating the cultures without the primary antibody to detect any unspecific signal from the secondary antibody. Scale bar: 200 μ m.

Altogether, the different strategies attempted to obtain auditory neurons from human dental pulp cells in their basal conditions (FBS, OSCFM or BMP4) resulted unsuccessful. Similar to our results in mice, hDPC-FBSs were able to respond partially better to the neuralisation after treatment or induction with different factors (i.e. FGF3/10, hFASC-CM). Thus, our treatment conditions including hFASC-conditioned media provided evidence of the feasibility of obtaining neural progenitors, somewhat otic-like.

5.3. Evaluation of P75⁺ve FACS sorted hDPCs for auditory nerve differentiation.

The heterogeneity found in cultures, observed by the dynamic variation of STRO-1 and P75 (chapter 4, Fig. 4.11), and the generalised lack of neural induction by Sonic Hedgehog protocol (chapter 4), motivated us to study a fraction or subpopulation within hDPC cultures that could be neuralised better. P75 has been proposed as a surface marker associated to neurogenic cells in human dental pulp cells¹²². Based on the cited evidence, we selected P75 as a target for direct isolation of neurogenic cells in our hDPC-FBS cultures by fluorescent activated cell sorting (FACS).

We performed Flow cytometry analysis after live staining of hDPC -FBS cells with P75 antibody (Centre for Stem Cell Biology-CSCB in-house antibody). After the initial gating, we quantify the hDPC-P75⁺ve population from 7 independent hDPC-FBS and 3 hDPC-OSCFM

cultures (5.17A and 5.17B). In both hDPC-culture conditions, the P75⁺ fractions were small. hDPC-FBS on average contained 3.84% (± 3.40) of a P75⁺ population, varying from 0.27% the smallest to 10% the largest. In turn, hDPC-OSCFM had an average of 3.55% (± 1.96), with the smallest and largest being 1.51% and 5.44% respectively (5.17C). Following the flow cytometry analysis, we proceeded to isolate the P75⁺ fraction by fluorescence activated cell sorting (FACS). An initial conventional RT-PCR was used to identify particular differences from the P75⁺, P75⁻ fractions with unsorted cells in a single hDPC-FBS culture. In this qualitative experiment, all the groups expressed *SOX9*, *NESTIN* and *OCT4*. *SOX10* was completely absent and surprisingly, *P75* appeared only in the unsorted group (Fig. 5.17D). This result requires further validation.

Following the flow cytometry and RT-PCR analysis, we continue to investigate whether the P75⁺ population had a particular neurogenic advantage by inducing the fractions to neuralised, again using the Sonic Hedgehog protocol. After cell sorting of the hDPC FBS 5 culture, the resulting fractions were the following (Diagram 5.2):

- Unsorted cells in FBS as control (Undif-unsort),
- Unsorted cells in neural induction (Unsort-Neu),
- P75⁺ cells in neural induction (P75⁺-Neu),
- P75⁻ cells in neural induction (P75⁻-Neu).

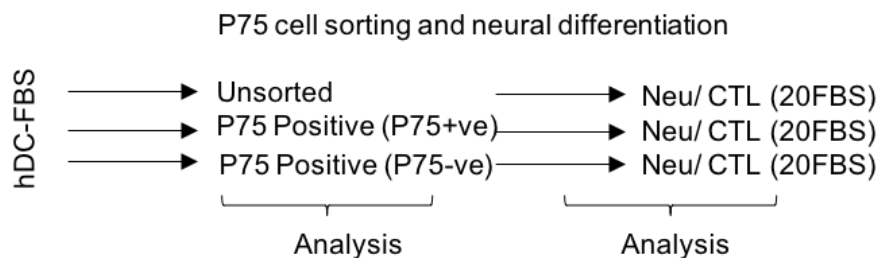


Diagram 5.2. Work flow of P75 FACS and neural induction. We obtained hDPC-FBS culture sub-populations by fluorescent activated cell sorting (FACS) of the P75 marker. We then induced the neural induction of the resulting fractions by Sonic hedgehog protocol.

Morphologically, Unsorted control cells and unsorted neuralised cells looked similar to what was observed earlier from other cell cultures (Fig. 5.18A). The P75 positive and negative fractions looked similar to neuralised hDPC cultures, but in a smaller density (Fig. 5.18A). We analysed quantitatively by RT-PCR the expression of the neural markers: *NFH*, *TUBIII*, *SYN*, *SYP* and *VGLUT1* to evaluate whether the P75 fraction was more competent for auditory neural differentiation. The results were normalised to the ESC line H14 S9. Interestingly, in every observed gene, the P75^{+ve} neuralised fraction did not present an upregulation of any of the neural markers studied. The only significant change was observed in *TUBIII*, which presented an upregulation in the P75^{-ve} neuralised fraction (Fig. 5.18B). Once again, Sonic Hedgehog neural differentiation did not induce a neural phenotype on hDPCs. Nevertheless, an interesting pattern appeared in the non-induced undifferentiated fractions. In all cases, the P75^{-ve} fraction, which was grown in FBS medium for the time of neuralisation (10-14 days), presented a significant higher relative expression of the neural genes, compared to the P75^{+ve} fraction (Fig. 5.18B).

Additionally, we included the neural progenitor markers: *FOXP1*, *NESTIN*, *NEUROD1* and *SOX2*, the epithelial marker *ECAD* and P75 to our analysis. Interestingly, *FOXP1*, *NESTIN* and *SOX2* presented a significant upregulated expression after neural induction in the P75^{-ve} population, suggesting that Shh neural induction promoted the expression of these genes in this fraction, but not in the P75^{+ve} cells (Fig 5.18B; Fig. S5). Additionally, other markers tested in a separate experiment suggested an upregulation (not statistically significant) of *NESTIN*, *GATA2* and *GATA3* in the neuralised P75^{-ve} fraction, supporting a differential response from this fraction to Shh induction (Fig. S4). On the other hand, after neural induction, *NEUROD1* appeared undetermined, and P75 presented a higher expression in the neuralised p75^{+ve} fraction in comparison to unsorted- and P75^{-ve} – neuralised fractions. In the undifferentiated controls, *NESTIN* and *NEUROD1* were found to be expressed at significantly higher levels in the P75^{-ve} fraction compared to the P75^{+ve} cells. *SOX2* appeared undetermined in all undifferentiated groups, while *FOXP1* was expressed at similar levels in the same conditions. The expression of P75 in undifferentiated groups was also evaluated, interestingly, the expression of this marker was significantly higher in the

separated fractions, compared to the unsorted cells. Furthermore, there wasn't a difference in P75 expression in the P75^{+ve} and P75^{-ve} fraction after two weeks in the standard FBS control conditions (Fig. 5.18C). Hence, the P75^{-ve} appears to be upregulating neural- and neural progenitor-related markers in comparison to the P75^{+ve} fraction, arguing against our initial hypothesis.

We then analysed by ICC if there were clear differences in relation to neural markers. The pan neural markers NFH and TUJ1 were present as before in other conditions and treatments. TAU was absent in all fractions, and SYP was clearer in the P75 positive and negative fractions. PERIPHERIN was stronger in the neuralised groups in comparison to the undifferentiated unsorted control, no difference was clearly evident between the sorted fractions with this method. SOX2 and MAP2 were absent or weakly expressed. NEUROD1 (NEUD) was present in the neuralised fractions at seemingly similar intensities. GFAP was weakly expressed in the P75 positive and negative fractions (Table 5.4; Fig. 5.19, Fig. 5.20, Fig. 5.21, Fig. 5.22 and Fig. 5.23). This experiment was repeated in an independent hDPC16-FBS culture (Sup. Fig. S6-S9).

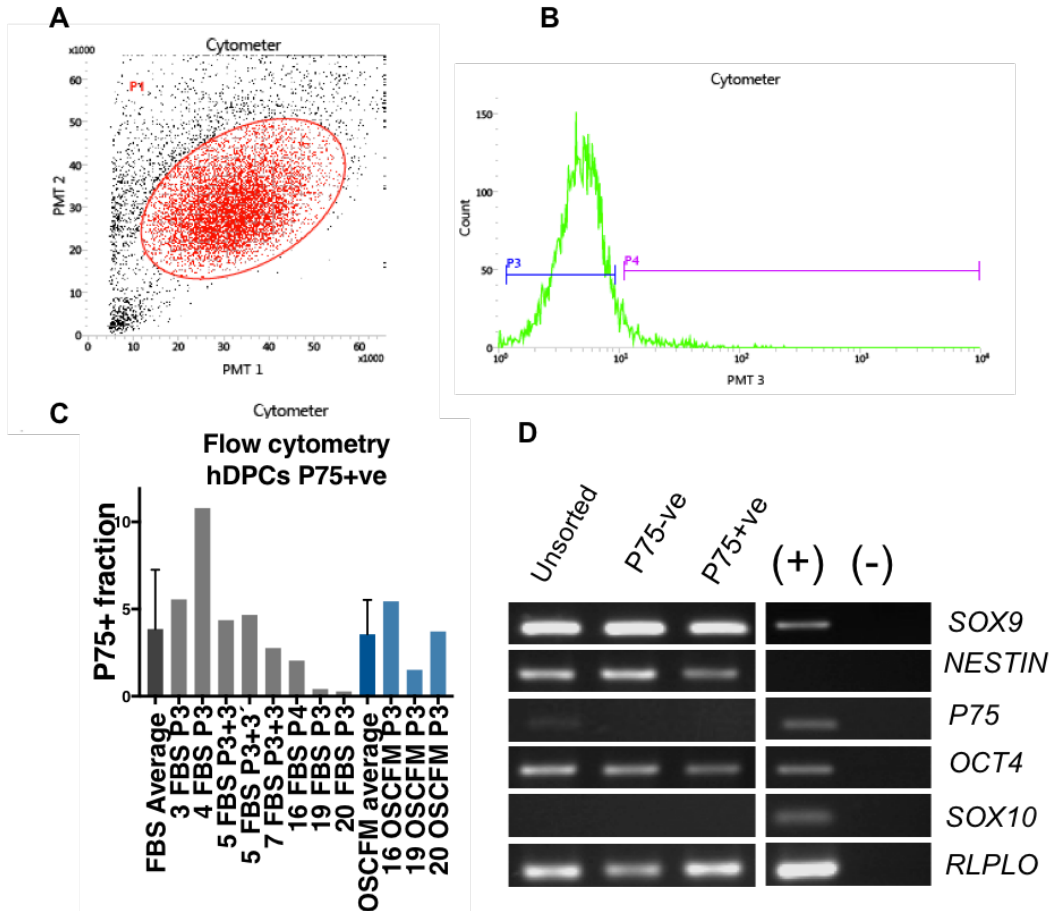


Figure 5.17 Flow cytometry analysis of P75 in hDPCs. A) Gating of viable cells: forward (PMT-1; size) and side (PMT-2; complexity-granularity) scatter. In red circle, the analysed cells included in the experiment (viable). B) Gating of fluorescence threshold: cell number (count-Y axis) and fluorescence intensity (X axis) of hDPC cells. P3 represents the base line of negative fluorescence (P75-ve). P4 represents cells with a fluorescence level above the negative threshold (P75+ve). C) Summary of P75 analysis in hDPC-FBS (grey bars) and hDPC-OSCFM (blue bars). D) Conventional PCR in agarose gel of the subpopulations after cell sorting. Positive control (+): ESC-derived neural crest cells; negative control (-): H₂O.

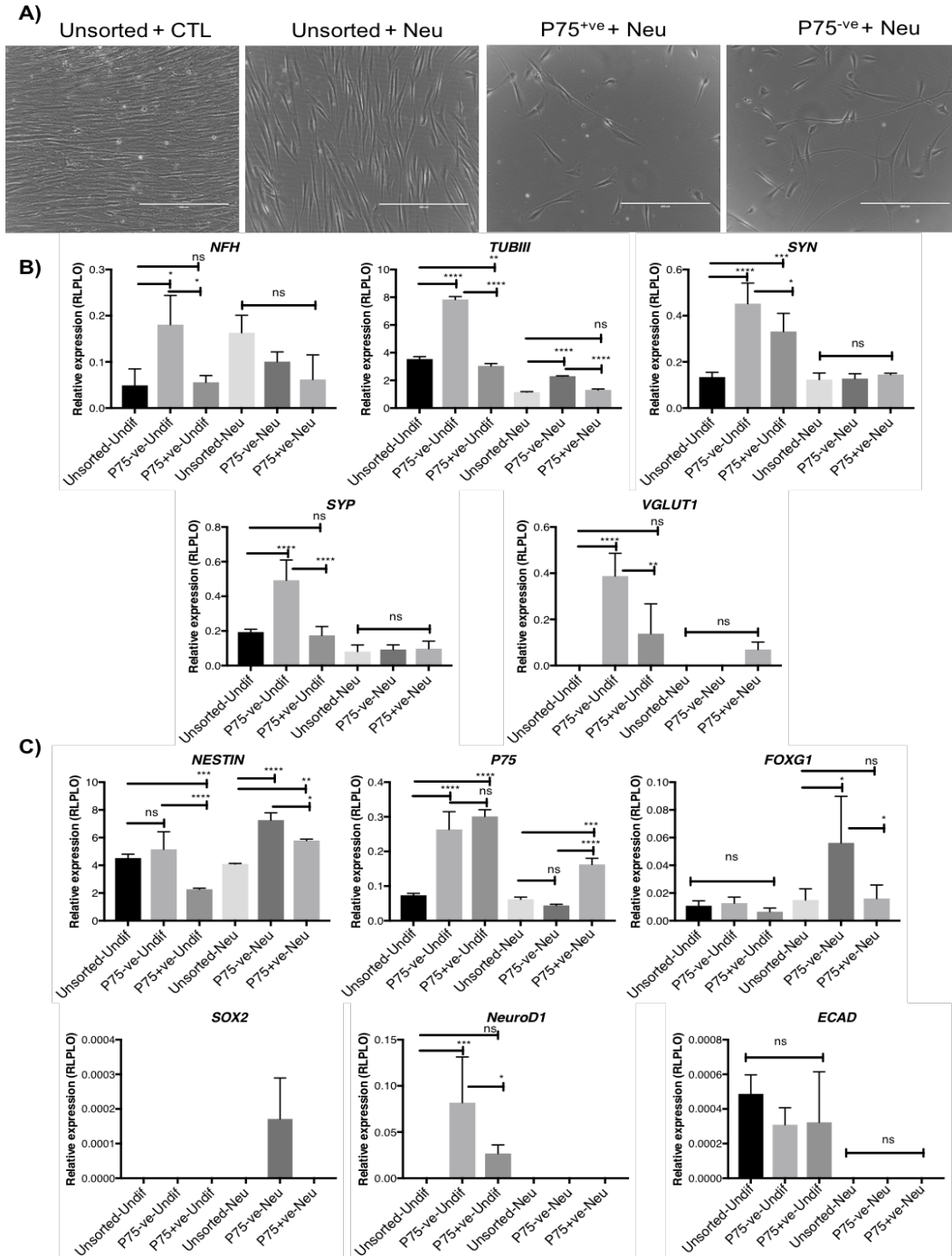


Figure 5.18. Neuralisation of hDPC-FBS sorted fractions. hDPC FBS 5 was used A) Bright field images of the sorted fractions after 2 weeks of neural induction for auditory neuron differentiation. B) Relative expression analysis of **neural markers** in the P75 fractions after neural induction. We found all evaluated markers (NFH, TUBIII, SYN, SYP and VGLUT1) to be expressed in higher levels in the P75-ve undifferentiated group. C) Relative expression analysis of **neural progenitor** markers in the P75 fractions after neuralisation. The markers NESTIN, FOXG1 and SOX2 have higher expression levels in the P75-ve fraction (after neuralisation). Expression relative to the ESC line H14 S9. Scale bar: 400 μ m. A one-way-ANOVA followed by a Tukey test for pairwise comparison was made to determine differences between groups. * $p < 0.05$, ** $p < 0.01$, *** $p < 0.001$, **** $p < 0.0001$. Error bars represent technical replicates.

| | TUJ1 | NF200 | SYP | TAU | PERIPHERIN | BRN3A | SOX2 | MAP2 | GFAP | NEUD |
|---------------------------|------|-------|-----|-----|------------|-------|------|------|------|------|
| Undif- Unsort | ++ | ++ | -- | -- | +-- | -- | -- | +- | +-- | +-- |
| Neu- Unsort | ++ | ++ | -- | -- | +- | -- | -- | ++ | +- | ++ |
| P75 ^{+ve} Neu | +- | ++ | +-- | -- | +- | -- | -- | +- | +- | ++ |
| P75 ^{-ve} Neu | ++ | ++ | +- | -- | ++ | -- | -- | ++ | +- | ++ |

Table 5.4., Summary of P75 sorting after neural induction (ICC). Qualitative expression of neural markers after neuralisation of the sorted fractions. High signal (++), Medium signal (+-), very low signal (+--). Unsorted cells in FBS as control (Undif-unsort), Unsorted cells in neural induction (Unsort-Neu), P75^{+ve} cells in neural induction (P75^{+ve}-Neu), P75^{-ve} cells in neural induction (P75^{-ve}-Neu).

Neural induction of hDPC-FBS after P75 sorting (NFH/TUJ1)

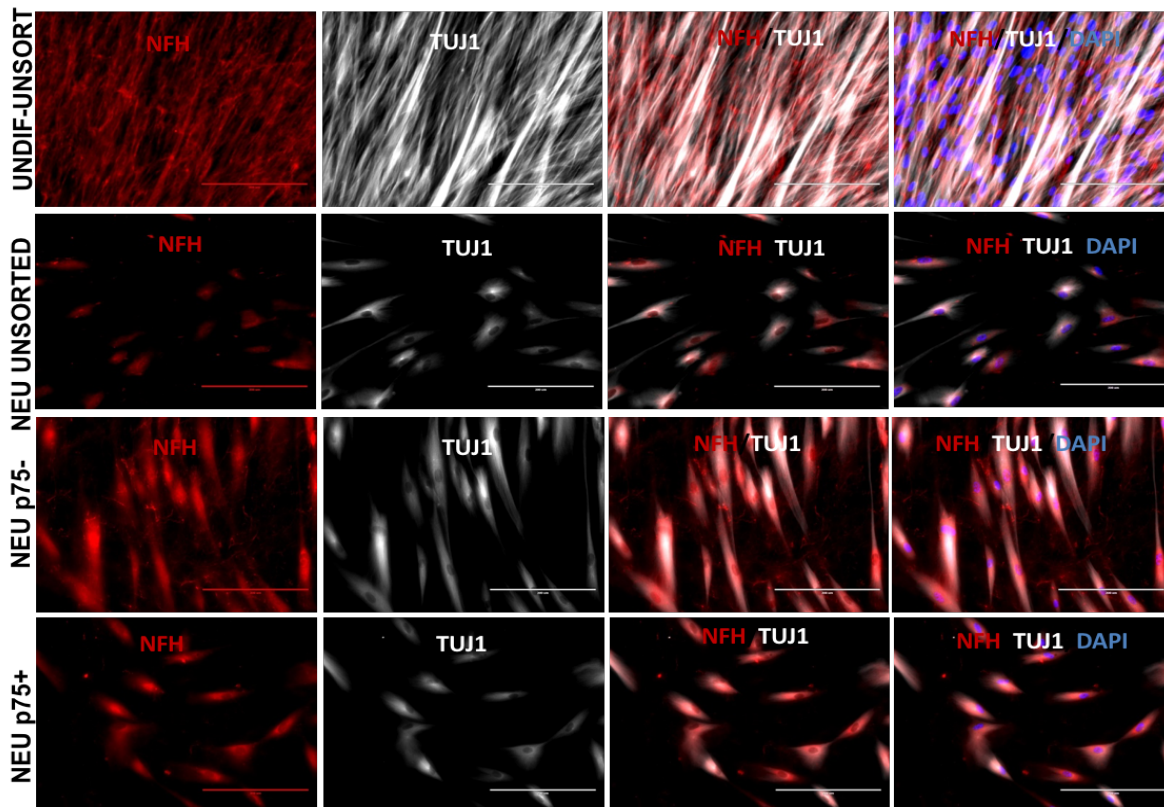


Figure 5.19. hDPC5 FBS P75 cell sorting and neuralisation. The neural markers NFH and TUJ1 present in the P75 fractions after neuralisation. Unsorted cells in FBS as control (Undif-unsort), Unsorted cells in neural induction (Unsort-Neu), P75^{+ve} cells in neural induction (P75^{+ve}-Neu), P75^{-ve} cells in neural induction (P75^{-ve}-Neu). Scale bar: 200µm. For each marker, the image was taken with the same configuration among treatments to allow comparison.

Neural induction of hDPC-FBS after P75 sorting (TAU/SYP)

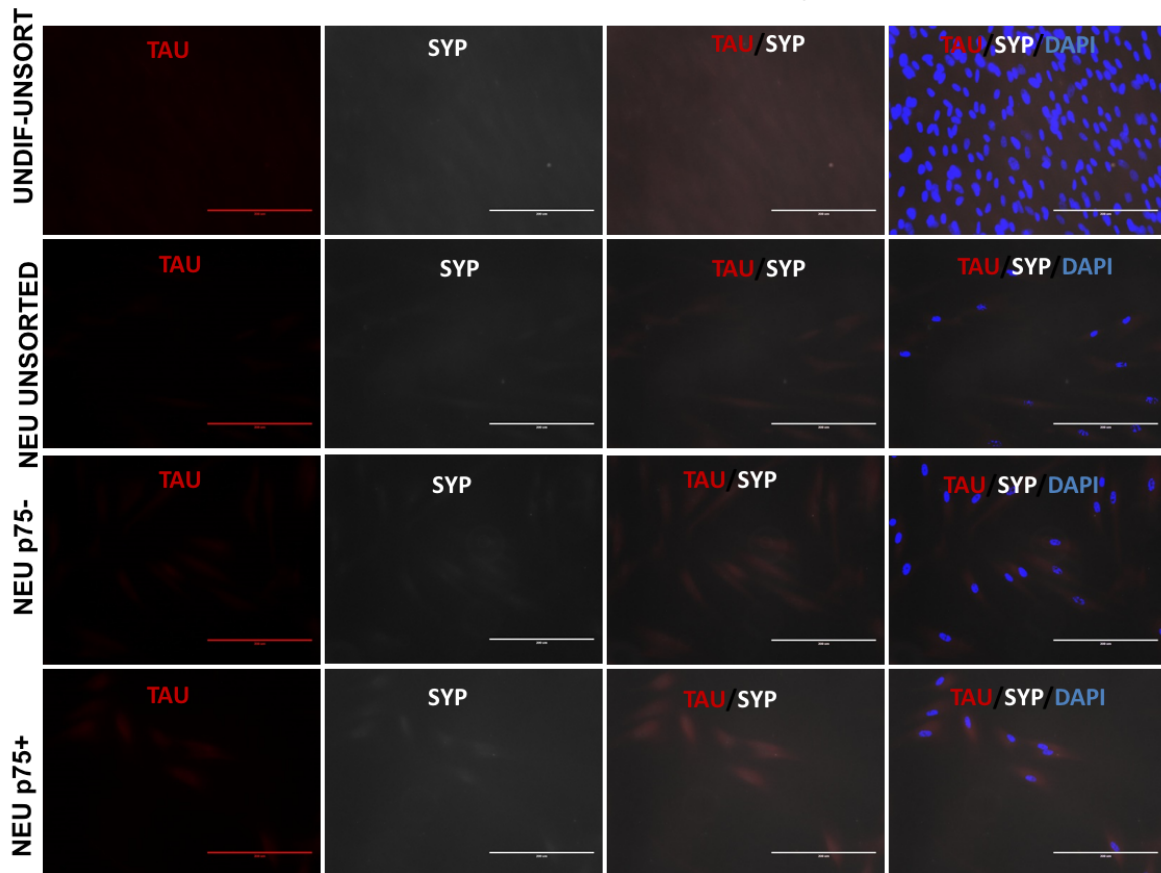


Figure 5.20. hDPC5 FBS P75 cell sorting and neuralisation. The neural markers TAU and SYP in the P75 fractions after neuralisation. TAU is not expressed in any group. Weak signal of SYP in Neu P75+ and Neu P75-. Unsorted cells in FBS as control (Undif-unsort), Unsorted cells in neural induction (Unsort-Neu), P75^{+ve} cells in neural induction (P75^{+ve}-Neu), P75^{-ve} cells in neural induction (P75^{-ve}-Neu). Scale bar: 200µm. For each marker, the image was taken with the same configuration among treatments to allow comparison.

Neural induction of hDPC-FBS after P75 sorting (PER/BRN3a)

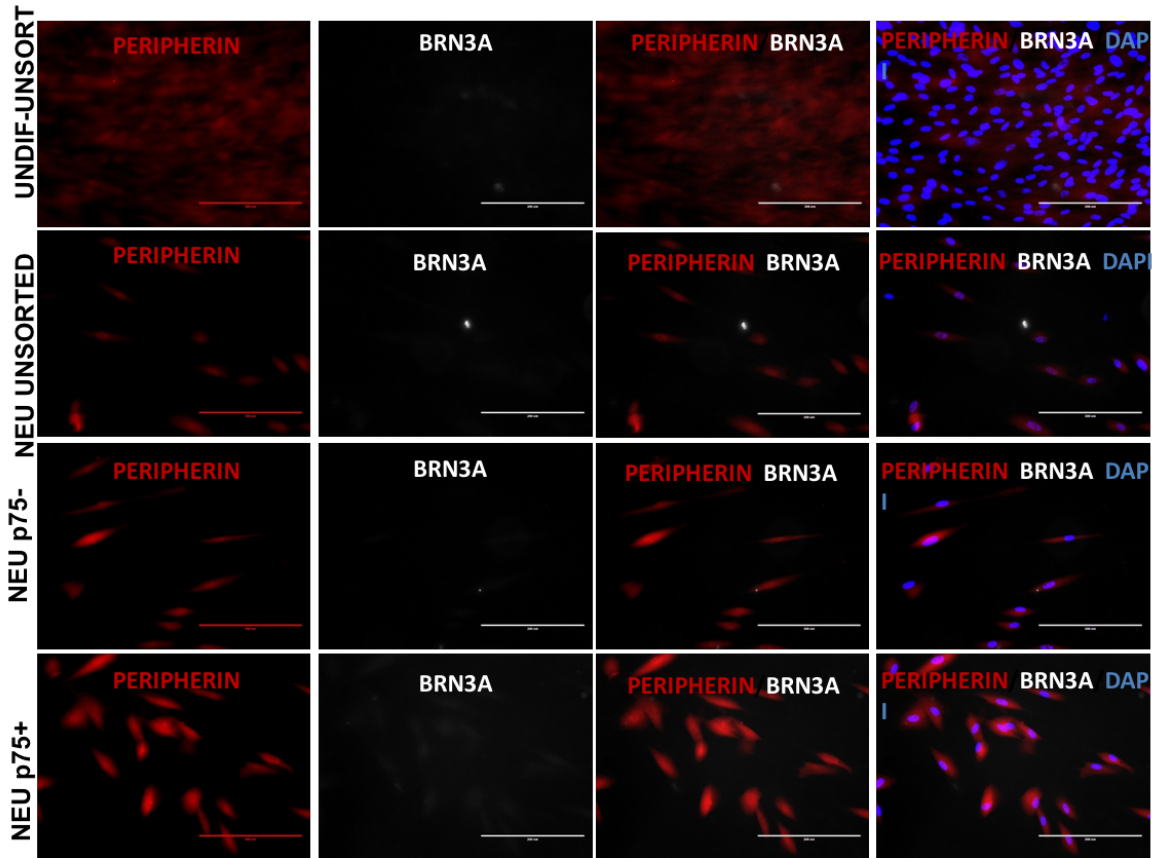


Figure 5.21. hDPC5 FBS P75 cell sorting and neuralisation. The neural markers PERIPHERIN and BRN3a in the P75 fractions after neuralisation. PERIPHERIN expression is present in all groups. Intensity seemingly stronger in both NEU P75-ve and NEU P75+ve fractions. BRN3a is absent from all groups. Unsorted cells in FBS as control (Undif-unsort), Unsorted cells in neural induction (Unsort-Neu), P75^{+ve} cells in neural induction (P75^{+ve}-Neu), P75^{-ve} cells in neural induction (P75^{-ve}-Neu). Scale bar: 200µm. For each marker, the image was taken with the same configuration among treatments to allow comparison.

Neural induction of hDPC-FBS after P75 sorting (SOX2/MAP2)

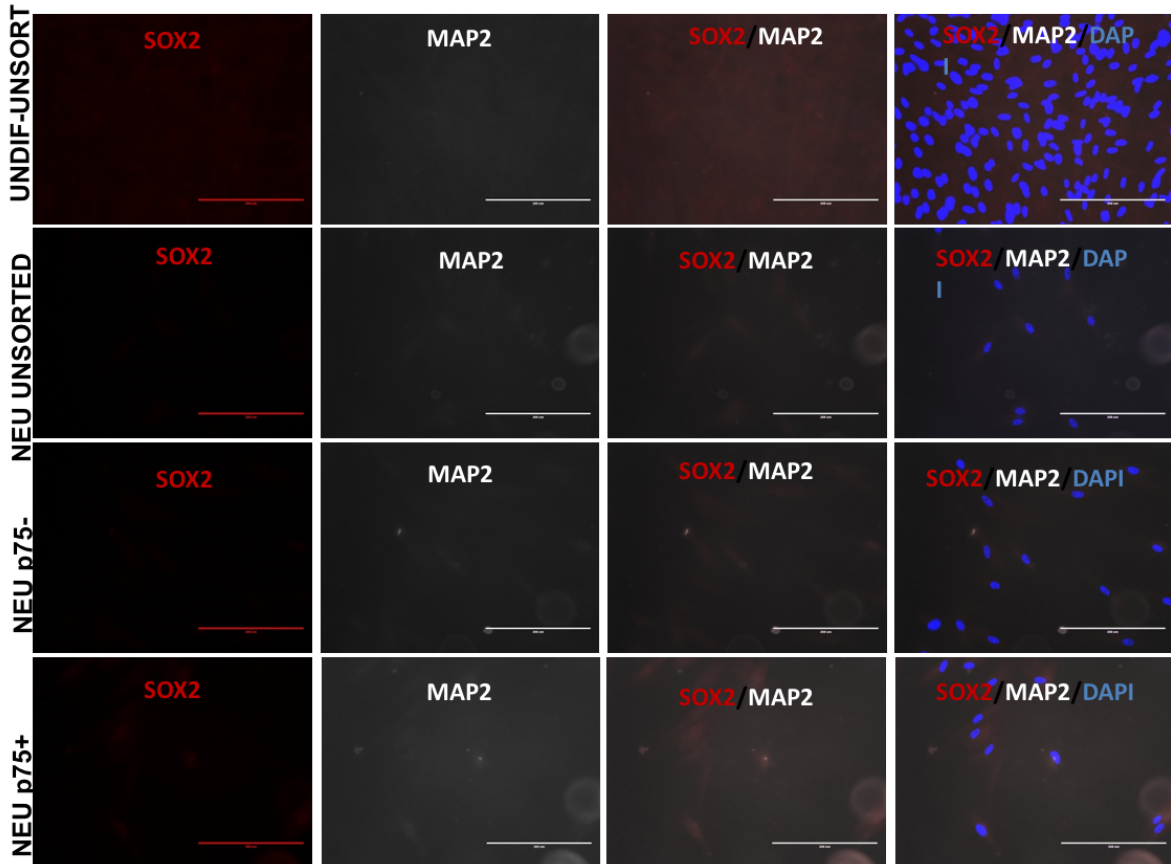
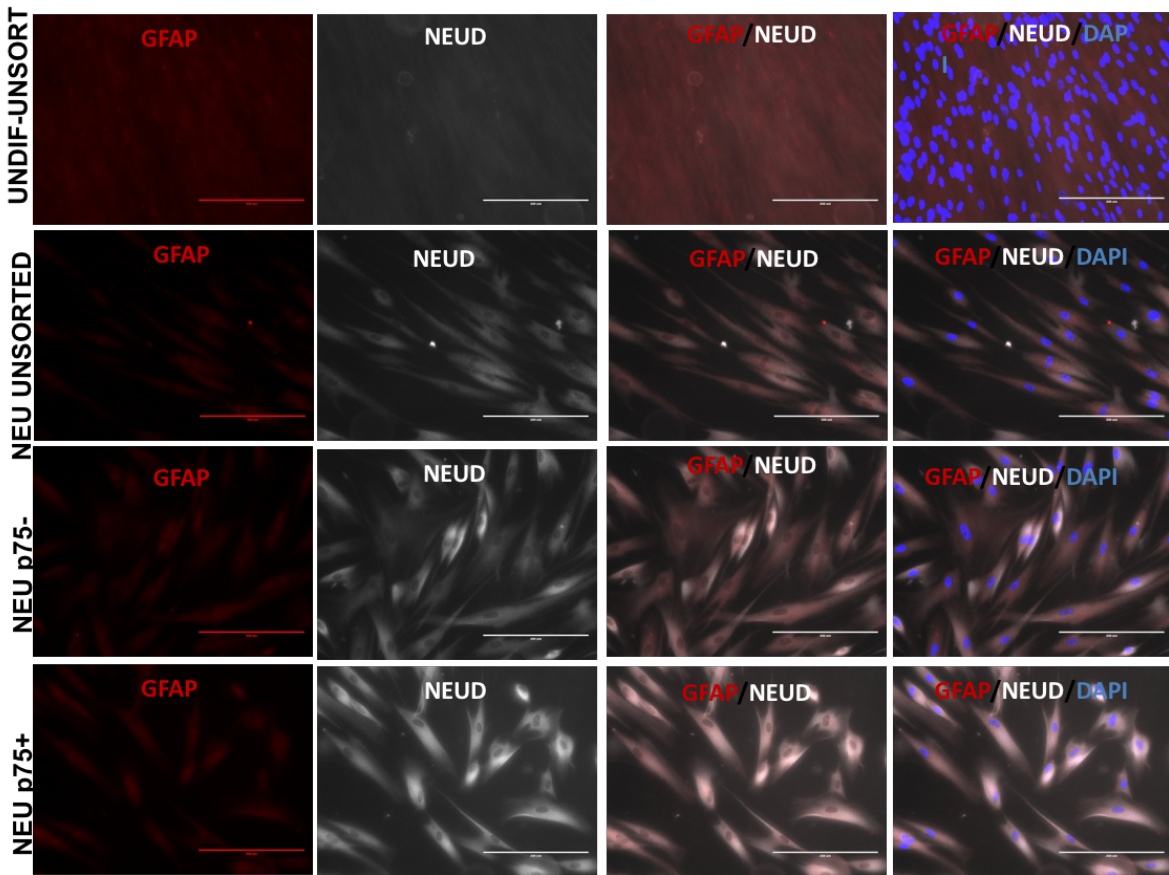


Figure 5.22. hDPC5 FBS P75 cell sorting and neuralisation. The markers SOX2 and MAP2 in the P75 fractions after neuralisation. SOX2 is not expressed in any group. MAP2 is absent or very weak. Unsorted cells in FBS as control (Undif-unsort), Unsorted cells in neural induction (Unsort-Neu), P75^{+ve} cells in neural induction (P75^{+ve}-Neu), P75^{-ve} cells in neural induction (P75^{-ve}-Neu). Scale bar: 200µm. For each marker, the image was taken with the same configuration among treatments to allow comparison.

Neural induction of hDPC-FBS after P75 sorting (GFAP/NEUD)



No primary control

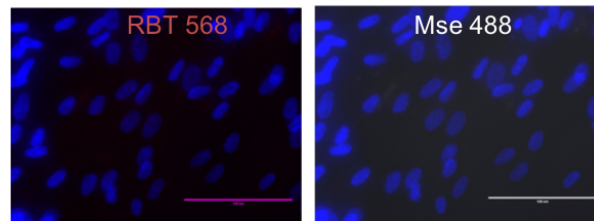


Figure 5.23. hDPC5 FBS P75 cell sorting and neuralisation. The markers GFAP and NEUD in the P75 fractions after neuralisation. GFAP and NEUD signal is seemingly stronger in the NEU P75- and NEU P75+ fractions. Unsorted cells in FBS as control (Undif-unsort), Unsorted cells in neural induction (Unsort-Neu), P75^{+ve} cells in neural induction (P75^{+ve}-Neu), P75^{-ve} cells in neural induction (P75^{-ve}-Neu). Scale bar: 200µm. For each marker, the image was taken with the same configuration among treatments to allow comparison. No primary controls for figures 5.19 to 5.23 are shown at the bottom.

In this and previous chapters, our results did not show conclusive results of hDPC-FBS differentiation into mature sensory neurons. Thus, we decided to test a different protocol for neural differentiation that has successfully been used on hDPCs, in our P75 FACS fractions. We used a neural maturation protocol described by Gervois et al., (2016) and analysed the results using ICC. We found similar results showing a lack of the sensory neural markers: BRN3a, SYP, and TAU in the neuralised fractions. However, the expression of TUJ1, NF200 and PERIPHERIN was found seemingly with a stronger signal in all neuralised groups, suggesting a general response to this neuralising condition. However, there still wasn't an apparent difference between the P75^{+ve} and P75^{-ve} fractions, which supports that the P75^{+ve} fraction lacks an advantage for neural differentiation (Table 5.5; Fig. 5.24, Fig. 5.25 and Fig. 5.26).

| | TUJ1 | NF200 | PERIPHERIN | BRN3A | SYP | TAU |
|--------------------------|------|-------|------------|-------|-----|-----|
| Undif-Unsort | ++ | ++ | +- | -- | -- | -- |
| Neu-Unsort | ++ | ++ | ++ | -- | -- | -- |
| Undif-P75 ^{-ve} | ++ | ++ | +- | -- | -- | -- |
| P75 ^{-ve} Neu | ++ | ++ | ++ | -- | -- | -- |
| Undif-P75 ^{+ve} | ++ | ++ | +- | -- | -- | -- |
| P75 ^{+ve} Neu | ++ | ++ | ++ | -- | -- | -- |

Table 5.5. Summary of alternative neural maturation of P75 fractions. Qualitative expression of neural markers after neuralisation of the sorted fractions with an alternative neuralisation protocol (dcAMP). High signal (++), Medium signal (+-), very low signal (+--). Unsorted cells in FBS as control (Undif-unsort), Unsorted cells in neural induction (Unsort-Neu), P75^{+ve} cells in neural induction (P75^{+ve}-Neu), P75^{-ve} cells in neural induction (P75^{-ve}-Neu).

In general, our results show a differential response to Shh neural induction among the fractions, but the P75^{+ve} fraction doesn't seem to be more neurogenic as the RT-PCR quantitative results suggest. Gervois' neural maturation protocol seemed to induce a neural-like phenotype, as suggested by a clearer TUJ1 and NF200 expression pattern, and a seemingly stronger signal using PERIPHERIN on the neuralised groups. However, ICC doesn't allow a more comprehensive distinction among our conditions and a quantitative analysis should follow to validate this trend.

Neural induction of hDPC-FBS after P75 sorting (NFH/TUJ1)-Gervois protocol

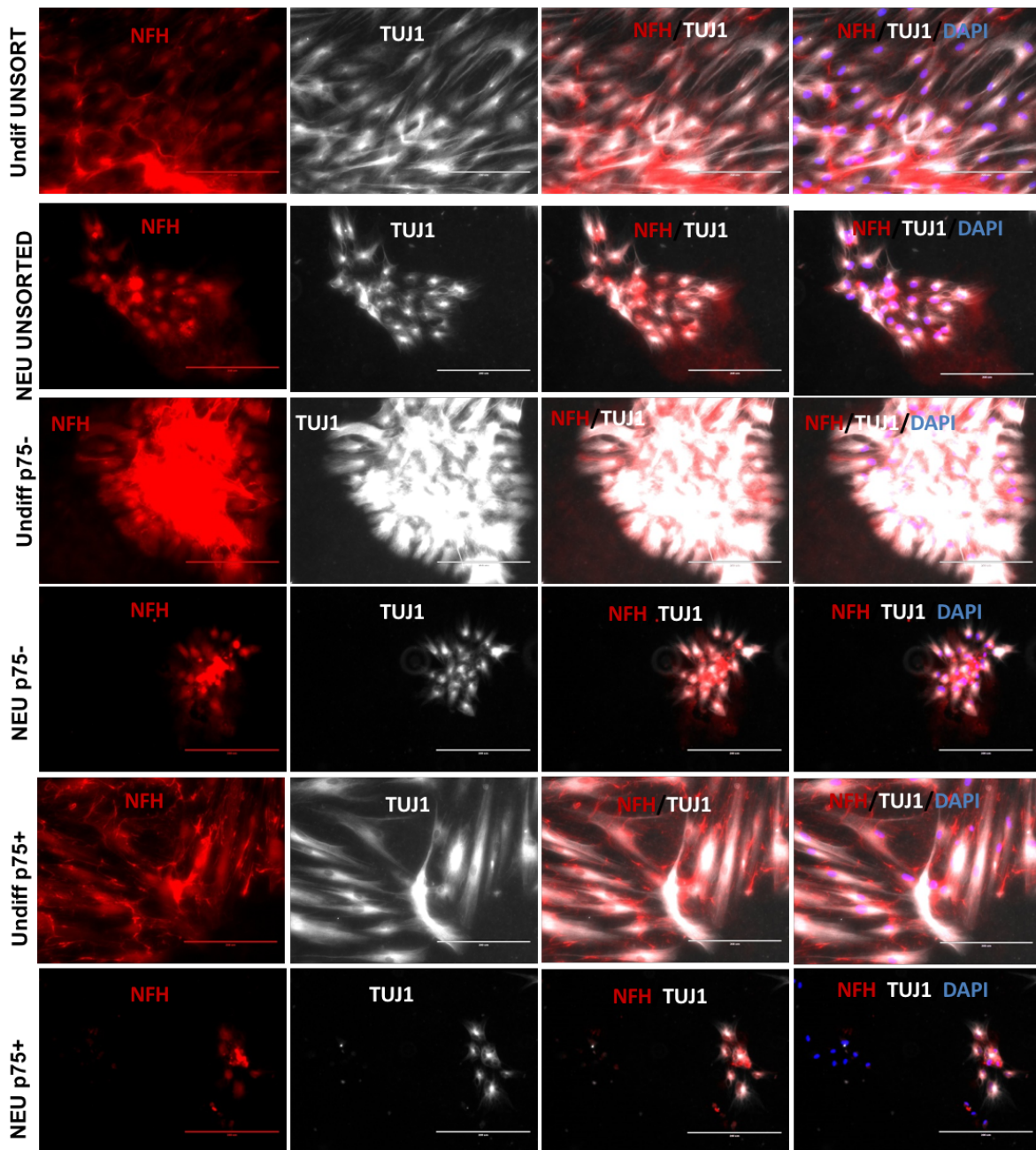


Figure 5.24. hDPC5 FBS P75 cell sorting and neuralisation with alternative protocol (dcAMP). The markers NFH and TUJ1 present in the P75 fractions after neuralisation with an alternative protocol (dcAMP). UNDIFF-Untersort: NEU Untersort: unsorted fraction induced to neuralisation; Undiff-p75-: P75^{-ve} fraction non-induced to neuralisation; NEU P75-: P75^{-ve} fraction induced to neuralisation. Undiff P75+: P75^{-ve} fraction non-induced to neuralisation; NEU P75+: P75^{+ve} fraction induced to neuralisation. Scale bar: 200µm. For each marker, the image was taken with the same configuration among treatments to allow comparison.

Neural induction of hDPC-FBS after P75 sorting (PER/BRN3A)-Gervois protocol

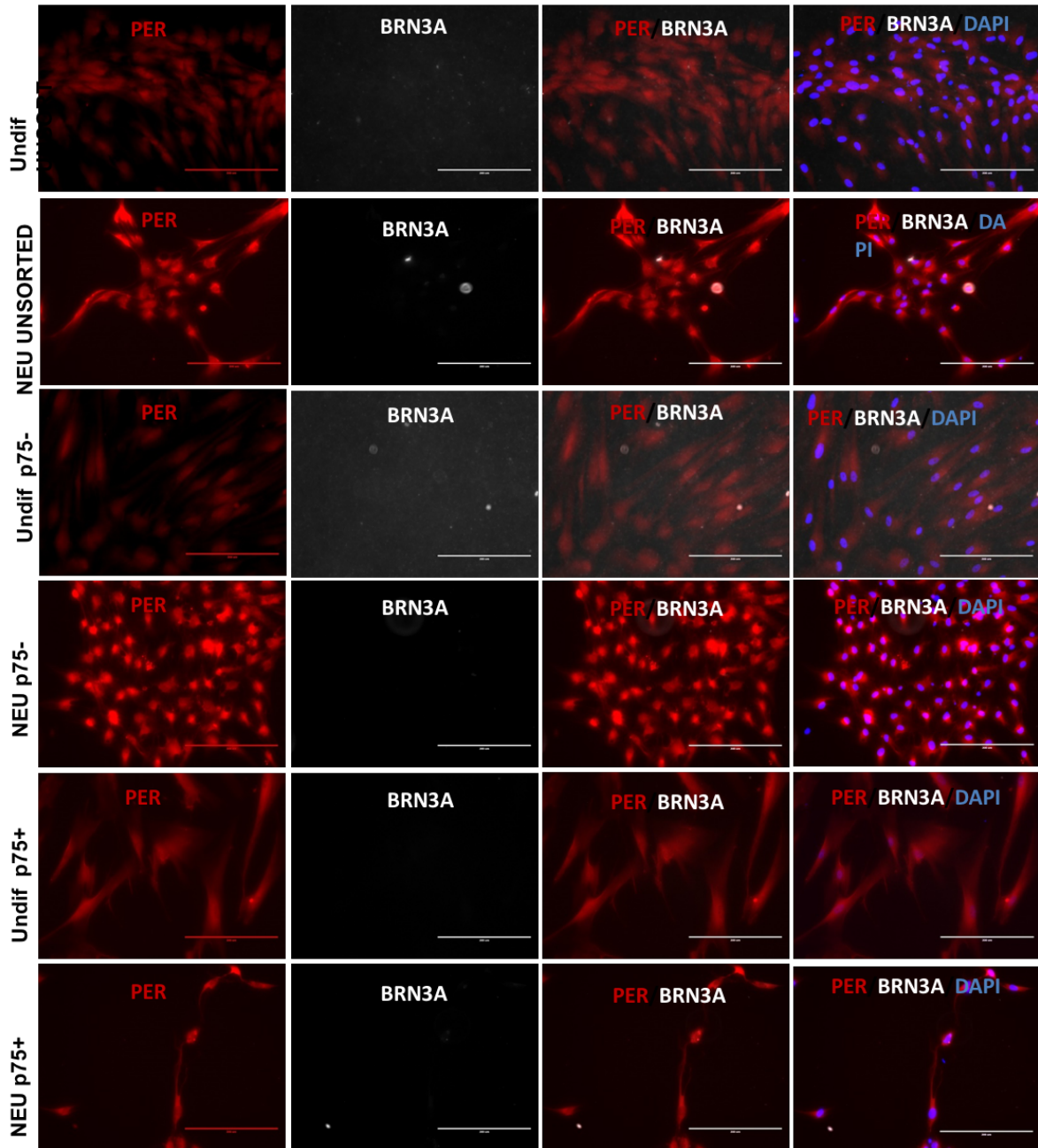
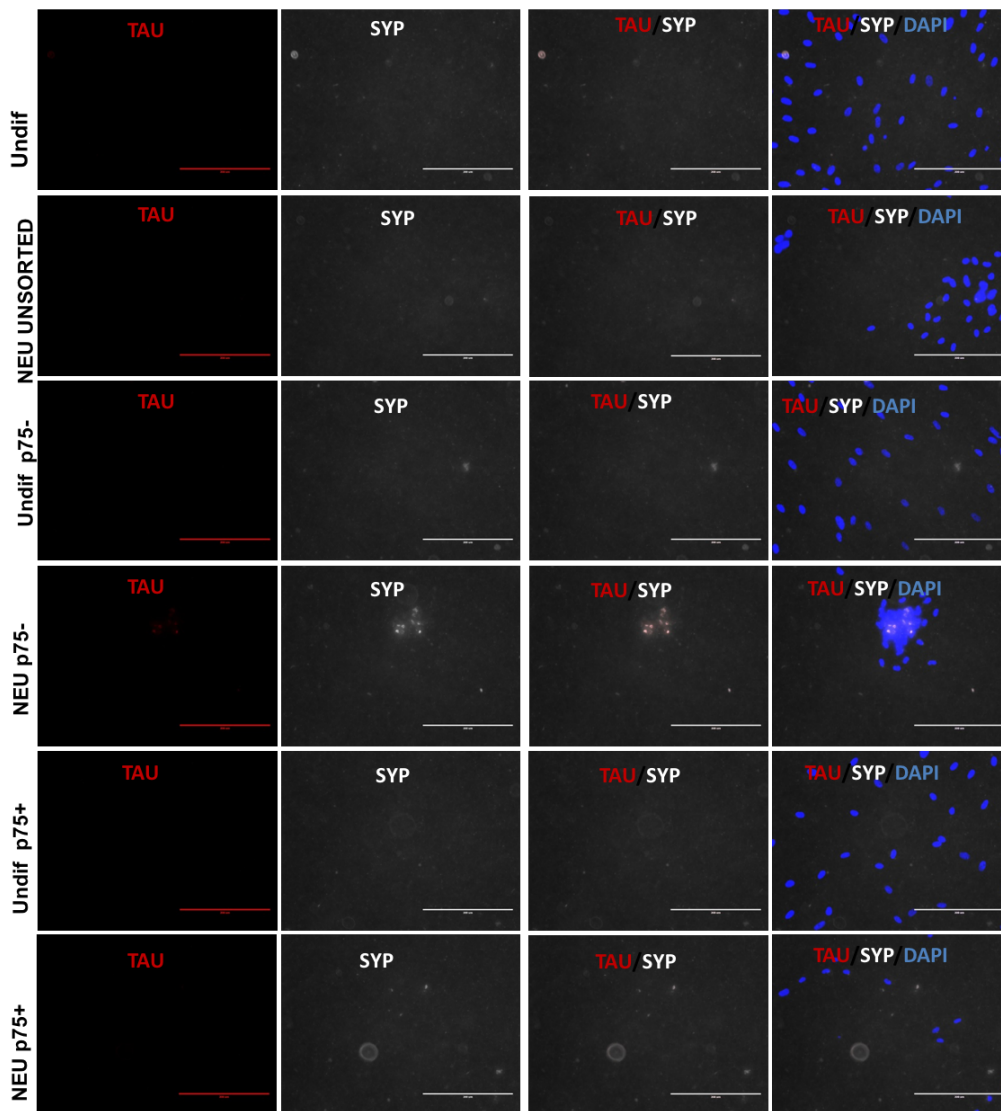


Figure 5.25. hDPC5 FBS P75 cell sorting and neuralisation with alternative protocol (dcAMP). The markers PERIPHERIN (PER) and BRN3A in the P75 fractions after neuralisation. PERIPHERIN signal is seemingly more intense in the NEU groups. BRN3a is not present. UNDIF-Ursort: Non-induced unsorted cells (CTL); NEU Unsort: unsorted fraction induced to neuralisation; Undiff-p75-: P75^{-ve} fraction non-induced to neuralisation; NEU P75-: P75^{-ve} fraction induced to neuralisation. Undiff P75+: P75^{-ve} fraction non-induced to neuralisation; NEU P75+: P75^{+ve} fraction induced to neuralisation. Scale bar: 200µm. For each marker, the image was taken with the same configuration among treatments to allow comparison.

Neural induction of hDPC-FBS after P75 sorting (TAU/SYP)-Gervois protocol



No primary control

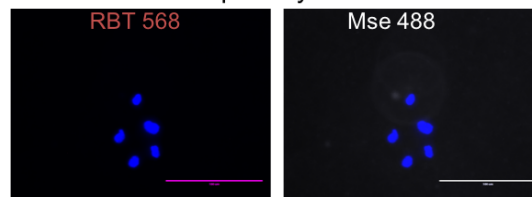
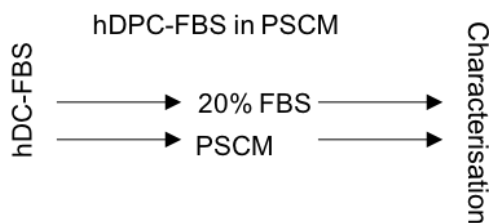


Figure 5.26. hDPC5 FBS P75 cell sorting and neuralisation with alternative protocol (dcAMP). The markers TAU and SYP in the P75 fractions after neuralisation with the alternative protocol (dcAMP). SYP is only present in the NEU P75- group. TAU is absent from all groups. UNDIF-Unsort: Non-induced unsorted cells (CTL); NEU Unsort: unsorted fraction induced to neuralisation; Undiff-p75-: P75^{-ve} fraction non-induced to neuralisation; NEU P75-: P75^{-ve} fraction induced to neuralisation. Undiff P75+: P75^{-ve} fraction non-induced to neuralisation; NEU P75+: P75^{+ve} fraction induced to neuralisation. Scale bar: 200µm. For each marker, the image was taken with the same configuration among treatments to allow comparison. No primary controls for figures 4.24 to 4.26 are shown at the bottom.

5.4. Characterisation of hDPC-FBS transferred to pluripotent stem cell medium.

As an alternative method to generate otic neural progenitors, the literature suggested a growing condition capable of yielding pluripotent-like cells from human dental pulp cell cultures⁸⁷. Because the protocols to obtain otic neural progenitors (ONP) are based on embryonic stem cells (pluripotent), our initial objective was to test if ONP derivation could be possible from hDPCs growing in pluripotent stem cell medium (PSCM). To do this, we took two previously frozen hDPC-FBS cultures and transferred and maintain them in PSCM and FBS medium in parallel (Diagram 5.3).



| Medium | Basal Conditions |
|--|--|
| <i>Fetal bovine serum (FBS)</i> ⁵ | DMEM, 1x P/S, 2mM Glutamax (GIBCO), 100µM Ascorbic Acid (Sigma), 10%, 15% or 20% foetal bovine serum (FBS; GIBCO). No coating. |
| <i>Pluripotent stem cell medium</i> ^{52,87} | 60% DMEM-Low Glucose (SIGMA), 40% MCDB-201 (Sigma), 1X Insulin-transferrin-selenium (ITS, Sigma), 1X linoleic acid-bovine serum albumin (LA-BSA; Sigma), 1nM Dexamethasone (Sigma), 100µM Ascorbic Acid, 100 I.U./mL Penicillin/100µg/mL Streptomycin, 2% FBS (HyClone, Fisher Scientific), 10ng/mL hPDGF-BB (R&D Systems), 10ng/mL EGF (R&D Systems). Coated with 100ng/mL Fibronectin (Sigma). |

Diagram 5.3. hDPC-FBS transferred to the “pluripotent stem cell medium” (PSCM) and media reminder. Cultures from hDPC-FBS were transferred to PSCM and a control group maintained in the 20FBS basal condition in parallel. The cultures were then characterized.

The morphology had slight changes from a fibroblastic shape to a spindle-like shape (Fig. 5.27A). In terms of cell growth, hDPC-PSCM presented a similar proliferation compared to hDPC-FBS (Fig. 5.26B). To characterise if the cells transferred to PSCM were in fact becoming pluripotent-like, we analysed the relative expression levels of the pluripotent genes *OCT4*, *NANOG*, *SOX2* and included *P75* from two independent hDPC-cultures from two separate occasions (Fig. 5.27C).

As seen before, the hDPC-FBS presented basal levels of pluripotent stem cell markers, including *OCT4* in these particular hDPC-FBS cultures. Nevertheless, the expression of pluripotent markers was not higher when grown in PSCM, except for one hDPC7-PSCM (Fig. 5.27C). When evaluated by ICC, there wasn't any striking difference between the cells growing in PSCM and their parental line in FBS. The expression of GFAP, GLI1, *OCT4* remained similar. In this specific line, *SOX2* appeared clearly expressed in the cell nuclei. *P75* was weakly expressed in the FBS group (Table 5.4; Fig. 5.28). Therefore, a general enhanced pluripotent signature was not apparent using this alternative condition.

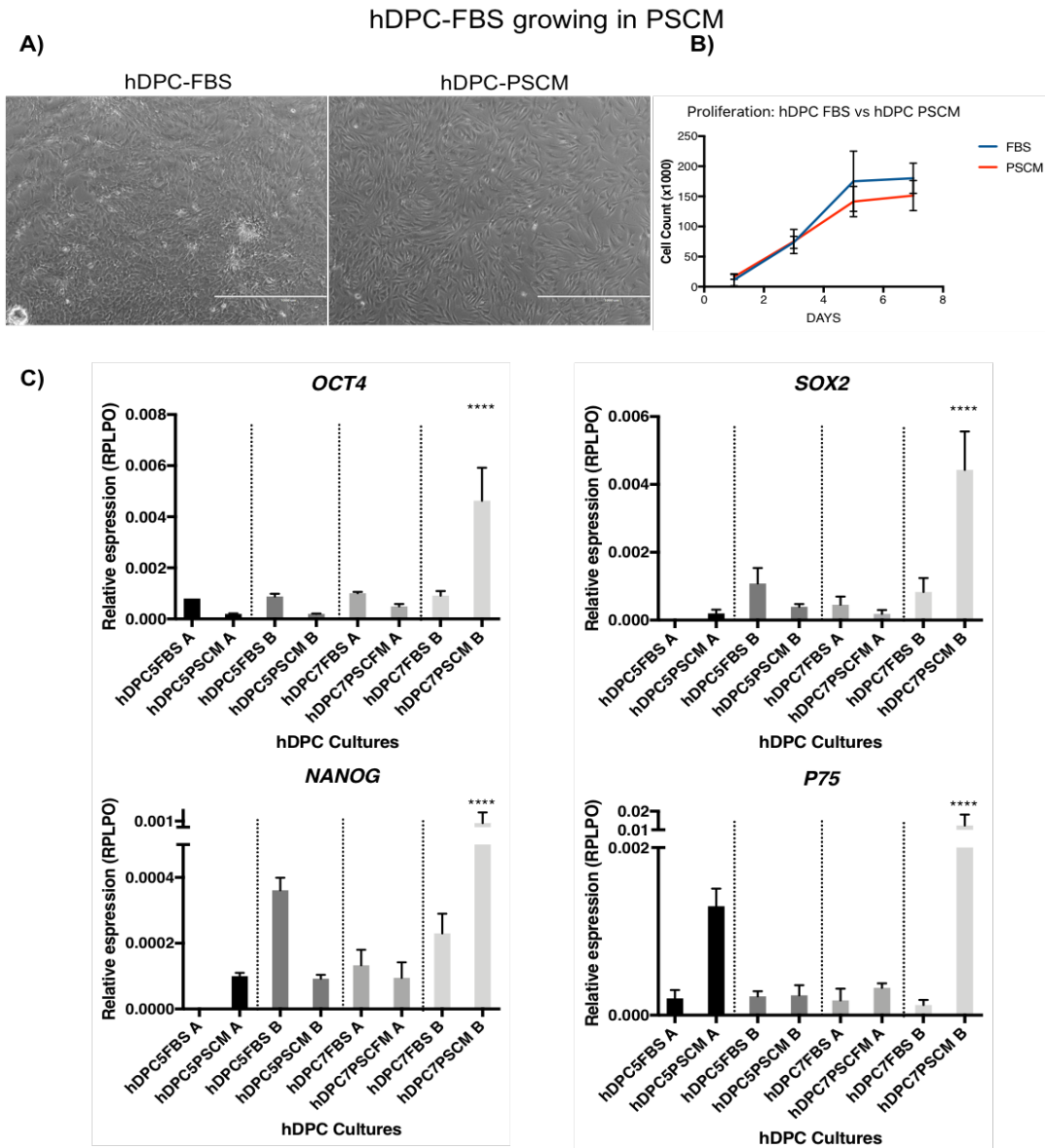


Figure 5.27. hDPC-PSCM characterisation. hDPCs were cultured in their basal FBS media and transferred to pluripotent stem cell medium (PSCM). A) hDPC transferred to PSCM did not present major differences in morphology. B) Cell proliferation curve. FBS cultures did not present a significantly different cell count after a week in culture (n=2). C) Relative expression analysis of pluripotent genes *SOX2*, *OCT4* and *NANOG*, as well as P75 normalised to an embryonic stem cells line. hDPC 5 and hDPC 7 cultures from different vessels (i.e. A, B) were used for this experiment. No significant difference was observed between the two conditions (FBS vs PSCM) except for the hDPC7 (B) culture. Scale bar: 1000µm. A one-way-ANOVA followed by a Sidak's test for pairwise comparison was made to determine statistical differences. ****p<0.001. Error bars represent technical replicates.

| | GFAP | SOX10 | GLI1 | P75 | SOX2 | OCT4 |
|-----------|------|-------|------|-----|------|------|
| hDPC-FBS | ++ | -- | ++ | +-- | ++ | +-- |
| hDPC-PSCM | ++ | -- | ++ | -- | ++ | +-- |

Table 5.4. hDPC-PSCM characterisation by ICC. Expression of relevant markers in comparison to the hDPC-FBS parental line. Qualitative analysis of hDPC-FBS cultures transferred to pluripotent stem cell medium (PSCM). High signal (++), Medium signal (+-), very low signal (+--).

hDPC7 FBS in Pluripotent Stem Cell Medium (PSCM)

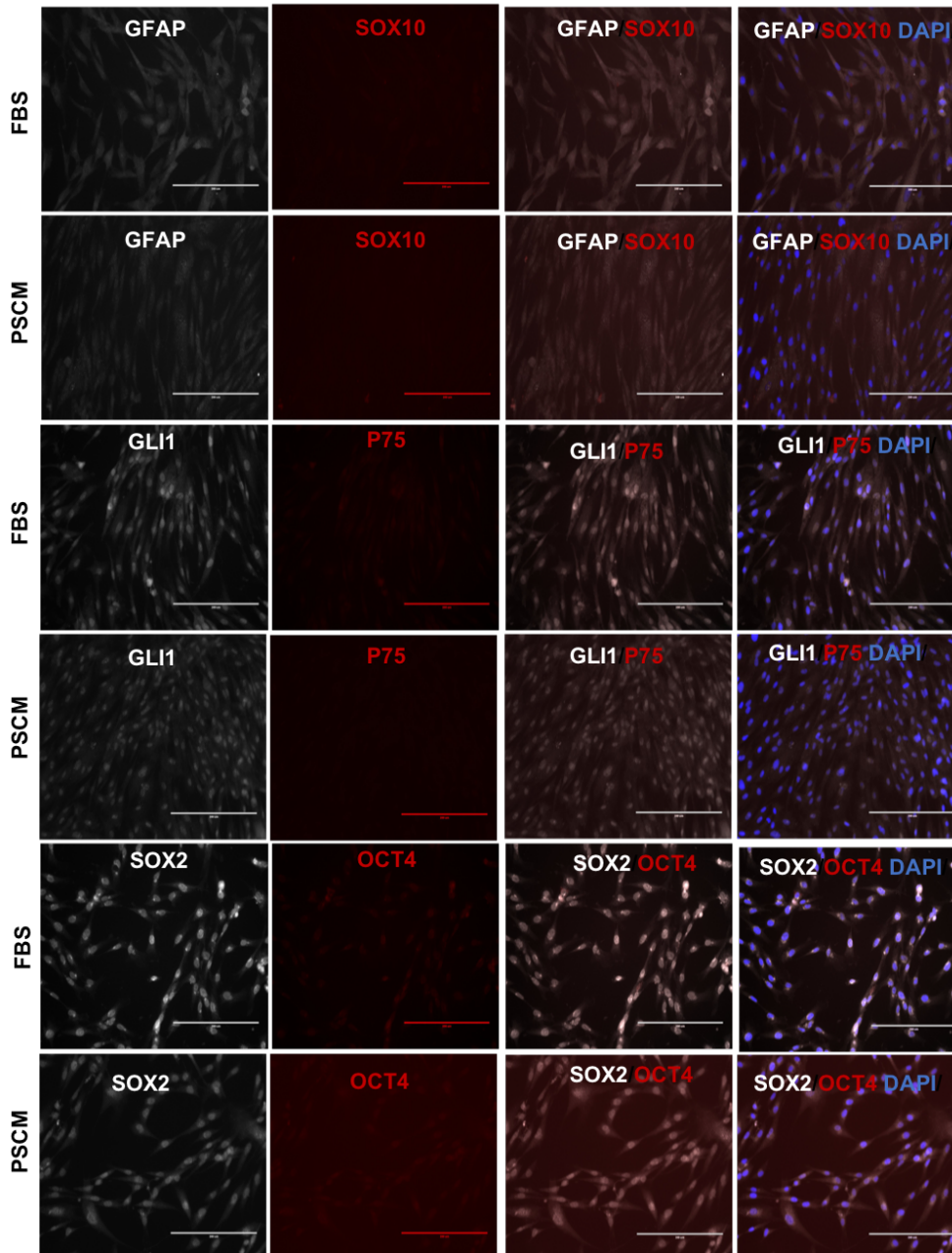


Figure 5.28. Characterisation of hDPC-PSCM. hDPCs growing in FBS and PSCM in parallel were labelled using immunocytochemistry (ICC). A similar profile is observed between the two conditions. GFAP, GLI1, SOX2 and OCT4 are present in the cultures, while P75 and SOX10 signal is absent. Scale bar: 400µm. For each marker, the image was taken with the same configuration among treatments to allow comparison.

5.5. Discussion

5.5.1. Otic neural progenitor obtainment from hDPC-FBS.

Driving otic neural progenitors from adult stem cells could bring important advantages for deafness therapies. However, pluripotent stem cells are currently the most successful in generating auditory cells for inner ear regeneration^{31,33,34}. Previously, we failed to generate auditory neurons from hDPCs by following a protocol designed for otic progenitor maturation (Chapter 4). Therefore, in this chapter we tried to generate otic neural progenitors (ONP) from hDPC-FBS cultures and evaluate their auditory neuron differentiation. To induce an ONP-like phenotype, we tried several conditions based on 1) our mouse results and 2) a established protocol designed for pluripotent stem cells. Our findings represent preliminary information about the capacity of hDPC to become otic neural progenitors. The results showed discrete qualitative differences between the treatments (FGF3/10, OSCFM BB, etc.), as observed by ICC and quantitatively by RT-qPCR. Thus, the treated cells resulted in ONP-like cultures in preliminary experiments. Furthermore, after treatments for generating ONP-like cells followed by neural differentiation, FGF3/10 and DFNB BB treatments showed a general upregulation of sensory neural markers, suggesting a better response. This result could suggests a significant improvement from Bone Marrow MSCs tested in our research group by Boddy et al. (2012⁴⁴), in which Bone marrow MSCs induced with FGF3/10 failed to acquire an ONP-like phenotype. In addition, another report from Bone Marrow MSCs described that only after transfection of the transcription factor ATOH1, the MSCs obtained an otic progenitor phenotype and further differentiate into hair-like cells⁴³. The capacity of responsiveness to our treatments by hDPCs support our hypothesis that hDPCs provide advantages for neural regeneration due to their neural crest origin. Further validation of this results should be made with other independent dental pulp cultures.

Additional to the treatments used to induce an ONP-like phenotype, we tried a method also described by Boddy et al., (2012) for Bone Marrow MSCs. In the cited report, MSCs were

only able to acquire an ONP-like signature and be further induced to a neural-like state when grown in hFASC-conditioned medium. In this chapter, we described the same protocol and found qualitatively, that hDPCs grown in hFASC-conditioned medium and FGF3/10 treatment, seemingly expressed neural progenitor markers with a stronger intensity, compared to the FBS control. In this regard, it would be necessary to evaluate these results quantitatively by RT-qPCR and also to test the auditory neural differentiation.

Altogether, the preliminary observations suggest the possibility of obtaining auditory neural progenitors from human dental pulp cells, and we propose to test their neuralisation using Sonic Hedgehog induction as well as further validation with more hDPC cultures.

5.5.2. Evaluation of P75 as a neurogenic marker in hDPC-FBS cultures.

In a separate method, P75 was evaluated as a marker of neurogenic cells or neural crest stem cells in hDPCs. P75 has been used as a marker of neural crest-derived cells in cultures from other dental-related tissues and other NCSCs^{56,68,72}. Additionally, human neural crest cells derived from embryonic stem cells are characterised by the expression of P75 and HNK-1, providing further support to the use of P75 as a neural crest marker in hDPCs^{97,160,161}. In the case of human dental pulp cells, the only available description of P75 subpopulation as a neurogenic marker was reported by Pan et al., (2016¹²²). The cited report found that P75^{+ve} cells co-expressed SOX1, SOX2 and NESTIN in a higher proportion than P75^{-ve} cells, and proposed P75 as a neurogenic marker in hDPCs. Nevertheless, P75^{+ve} cells have not been isolated and directly tested as to whether they may provide a more efficient method for acquiring a neural phenotype than an unsorted or P75^{-ve} populations. In this chapter, we reported that hDPC-FBS and hDPC-OSCFM have a similar percentage of P75^{+ve} cells in culture. Following sorting of hDPC-FBS cultures, we induced neural differentiation and characterised the resulting fractions by RT-qPCR. Interestingly, we found that after neural induction with Sonic hedgehog, all the neural markers tested presented a statistically similar relative expression (among the neuralised fractions; except *TUBIII*). Also, the undifferentiated groups presented lower levels of the neural markers in comparison to their neuralised homologs. In the same experiment, we also analysed the expression of neural progenitor genes such as *NESTIN*, *FOXG1* and *SOX2*, which all had a relative upregulation

particularly in the P75^{-ve} neuralised fraction. Interestingly, P75 has been proposed and shown to be a good candidate to identify cells with enhanced proliferation and classical mesodermal differentiation bone marrow's and dispose's tissue MSC^{162,163}. In human dental pulp however, contrasting evidence can be found. Alvarez et al., (2015)¹⁶⁴, found P75 as a single MSC marker with better properties for odontogenic/chondrogenic differentiation. Whereas Mikami et al. (2011)^{164,165}, proposed that the same marker inhibits the multilineage differentiation of hDPC-MSCs. Additionally, Alraies et al. (2017) found that P75 expressing cultures reached senescence and slow their proliferation faster¹⁶⁶. What is clear from these reports, is that the negative and positive P75 fractions present different properties among adult stem cells, but their potential for neural differentiation was not tested. Our experiments suggest that undifferentiated P75 fractions (Unsorted, P75^{+ve}, P75^{-ve}) presented differences in neural marker expression after two weeks expanding in the basal 20%FBS (control) condition. The negative fraction presented a significant upregulation of all the neural markers compared to the unsorted and positive fractions. Together, 4 important observations should be noted from the literature and our results:

- 1) P75^{-ve} cells present a significant increase in neural genes after 2 weeks of expansion in basal conditions (20%FBS),
- 2) P75^{-ve} cells upregulate neural progenitor genes after Sonic hedgehog neuralisation,
- 3) our qualitative data doesn't show an evident difference in the neural phenotype of P75 fractions using another neuralisation protocol and,
- 4) literature indicating that P75^{+ve} cells present an enhanced mesodermal differentiation^{162,163}.

Hence, we suggest that the P75^{+ve} fraction might not present advantages as a neurogenic subpopulation.

As an alternative explanation, even sub-fractions of P75^{+ve} cells could present different differentiation properties. For instance, a report suggest different multipotent potential in Bone Marrow's P75-sorted MSCs¹⁶⁷. Furthermore, hDPCs STRO⁺/c-KIT⁺/CD34⁺ cells (Expressing P75) are able to gain a neural fate, but not the STRO⁺/c-KIT⁺/CD34⁻ (No P75 expression)¹⁵⁰. This suggestion implies that under the context of the hDPC tested (20%FBS-

standard condition and Shh induction), P75 by itself is not a reliably candidate of neurogenic cells within hDPC-FBS cultures.

5.5.3. Pluripotent stem cell medium for hDPC-FBS growth

Finally, as another strategy for obtaining otic neural progenitors (ONP), we tested a pluripotent stem cell condition. The logic under this experiment, was that if ONPs have been generated from pluripotent stem cells (PSC)^{31,44} with better results than MSCs⁴⁴, then generating a pluripotent-like phenotype from hDPCs could facilitate ONP generation.

By transferring hDPC-FBS into the pluripotent medium used by Atari et al.(2012)⁸⁷, who previously provided evidence of a phenotypic change from MSC to PSC in hDPCs, we attempted to generate hDPCs with a pluripotent resemblance. However, we did not find any general significant upregulation of pluripotent markers at the mRNA level, and when found, there were considerably lower than the embryonic stem cell line used to normalise the data.

5.6. Summary

In summary, we have provided evidence that suggest that otic neural progenitors (ONPs)-like can be obtained from hDPCs-FBS cultures induced with FGF3/10 or cultured with hFASC conditioned medium, as shown by the enhanced neural-like signature and neural progenitor marker expression, respectively. We have also shown evidence of a differential behavior of P75 positive and negative fractions under basal (FBS) and Sonic Hedgehog (neuralising) conditions, suggesting that the negative fraction could present a neurogenic nature, rather than the positive fraction as was originally suggested. Finally, in our hands, generation of a pluripotent-like phenotype from hDPC-FBS cultures was not possible.

CHAPTER 6

“Derivation of neural crest-derived stem cell neurospheres from human dental pulp and their potential for auditory nerve regeneration”

6. Derivation of neural crest-derived stem cell neurospheres from human dental pulp and their potential for auditory nerve regeneration.

In the present thesis, we aimed to test the potential of human dental pulp cells for auditory regeneration. Accordingly, in the previous chapters we have described several methods for otic progenitor and auditory neural differentiation with encouraging, but not definitive results. The basal molecular signature found during our hDPC cultures characterization (FBS, OSCFM and BMP4) suggested a neural crest-like nature (Chapter 4). Thus, in this chapter we explored further the neural crest nature of human dental pulp cells. We employed neurosphere formation as a method that has been used to derive or induce a neural crest-like phenotype in other neural crest-derived tissues including the adult palate, gingiva, bulge follicle, among others^{50,72}. In addition, this chapter aimed to present a direct application to hDPCs for regenerative medicine. Thus, we aimed to investigate the neurosphere potential for nerve regeneration in a model of auditory regeneration.

6.1. Human dental pulp cells can be grown as spheres in low-attachment conditions.

It was hypothesized that growing human dental pulp cells as spheres aggregates could drive them in to a more stable or enhanced neural crest stem cell phenotype. Monolayer hDPC cultures from all conditions (FBS, OSCFM and BMP4), and ESC-otic neural progenitors (ONPs), were grown in non-adherent culture conditions (See methods; Fig 6.1A). The general workflow followed in this chapter is described in diagram 6.1. At day 4, the spheres diameter was measured and the number of spheres per well was counted for each condition. Overall, a main large sphere was evident, surrounded by smaller aggregates. The sphere number among FBS, OSCFM and BMP4 cultures remained similar to each of them. In contrast, spheres from ONPs were commonly found in larger numbers (Figure 6.1B). In terms of their size, the spheres diameter ranged from 100 μ m-300 μ m. On average, FBS and OSCFM derived-spheres were statistically significantly larger than the others and similar to each other, whereas BMP4 and ONP derived-spheres were smaller (Fig. 6.1C).

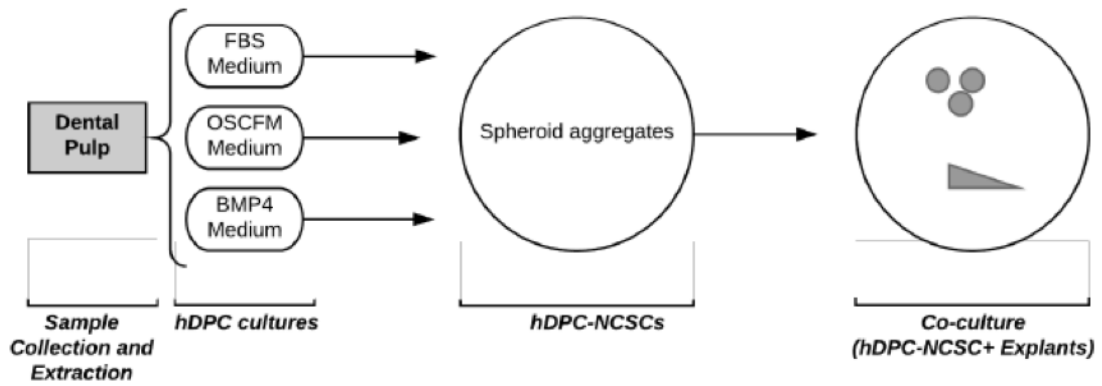


Diagram 6.1. Workflow of neurosphere formation, characterization and evaluation of hDPC cultures. After collection of hDPCs, we directly cultured hDPC in FBS, OSCFM or BMP4 media. Following expansion of hDPC cultures the cells were grown in low-attachment conditions for neurosphere or spheroid aggregation. The resulting sphere aggregates were tested in an *ex-vivo* model of auditory nerve regeneration.

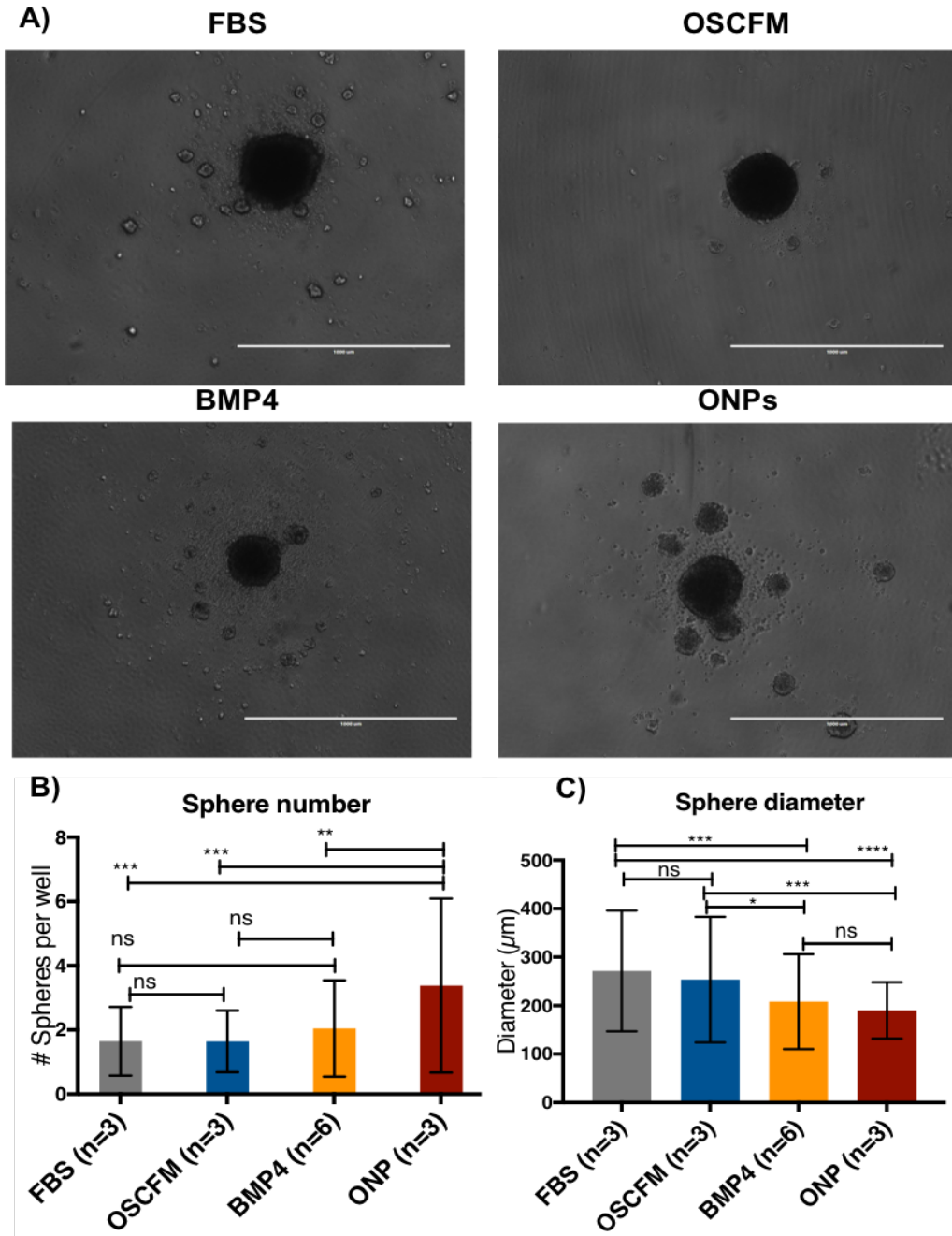


Figure 6.1. hDPCs can be grown as sphere aggregates. A) Bright field image of sphere aggregates from FBS, OSCFM, BMP4 and ONP cultures at day 4. B) Sphere number per well, average number of spheres in each well for each condition (each independent experiment consisted of at least 10 wells). C) Sphere diameter, average sphere diameter for each condition (each independent experiment consisted of at least 10 spheres). A sphere was considered for the counting if the diameter was above 100 µm. One-way ANOVA followed by a Tukey test for pair wise comparison. * $p < 0.05$, *** $p < 0.001$, **** $p < 0.0001$. Scale bar: 1000µm.

6.2. hDPC-spheres present a neural crest-derived stem cell molecular signature and differentiate into neural –like cells by chemically induced cues.

In order to establish the molecular signature of the hDPC-derived spheres, we prepared the spheres for cryosectioning and immuno-labelling to detect the neural crest related markers: Activating enhancer-binding protein 2-alpha (AP2a), SRY BOX10 (SOX10), Nerve growth factor receptor (P75), SRY BOX9 (SOX9), SRY BOX2 (SOX2), NESTIN, Snail family transcriptional receptor 2 (SLUG) and Snail family transcriptional receptor 1 (SNAIL1). The expression of the mesenchymal stem cell marker STRO-1 and epithelial cell adhesion molecule (EPCAM) was also evaluated (Fig 6.2, Fig. 6.3 and Fig. 6.4).

Multiple spheres derived from at least 2 independent FBS cultures showed colocalization of the following markers: SOX2/SLUG, and SOX9/NESTIN. SNAIL1 was also evident in two of three cultures observed, while P75 was present in 1 of three neurosphere cultures. AP2a, SOX10, EPCAM and STRO-1 were absent in FBS-derived spheres. EPCAM and STRO-1 were also absent from the neurosphere samples (Fig. 6.2).

In the case of OSCFM cultures, similar results were observed in 2-5 independent cultures. We identified SOX2/SLUG and SOX9/NESTIN double positive spheres. SNAIL1 was present in 4 of 5 independent cultured spheres and SOX10 in 2 of 4 cultures. AP2, P75 were absent, STRO-1 and EPCAM appeared positive in one of the two tested cultures (Fig. 6.3).

Multiple BMP4-derived spheres from 2-4 independent cultures were evidently different from FBS and OSCFM spheres. Besides also presenting double positive staining of SOX2/SLUG and SOX9/NESTIN, BMP-4 spheres resulted positive for SNAIL1, AP2a, P75 and SOX10 in at least 2 independent cultures, showing an enhanced or frequent neural crest signature by ICC than FBS and OSCFM-derived spheres (Fig. 6.4).

FBS-derived hDPC Spheres

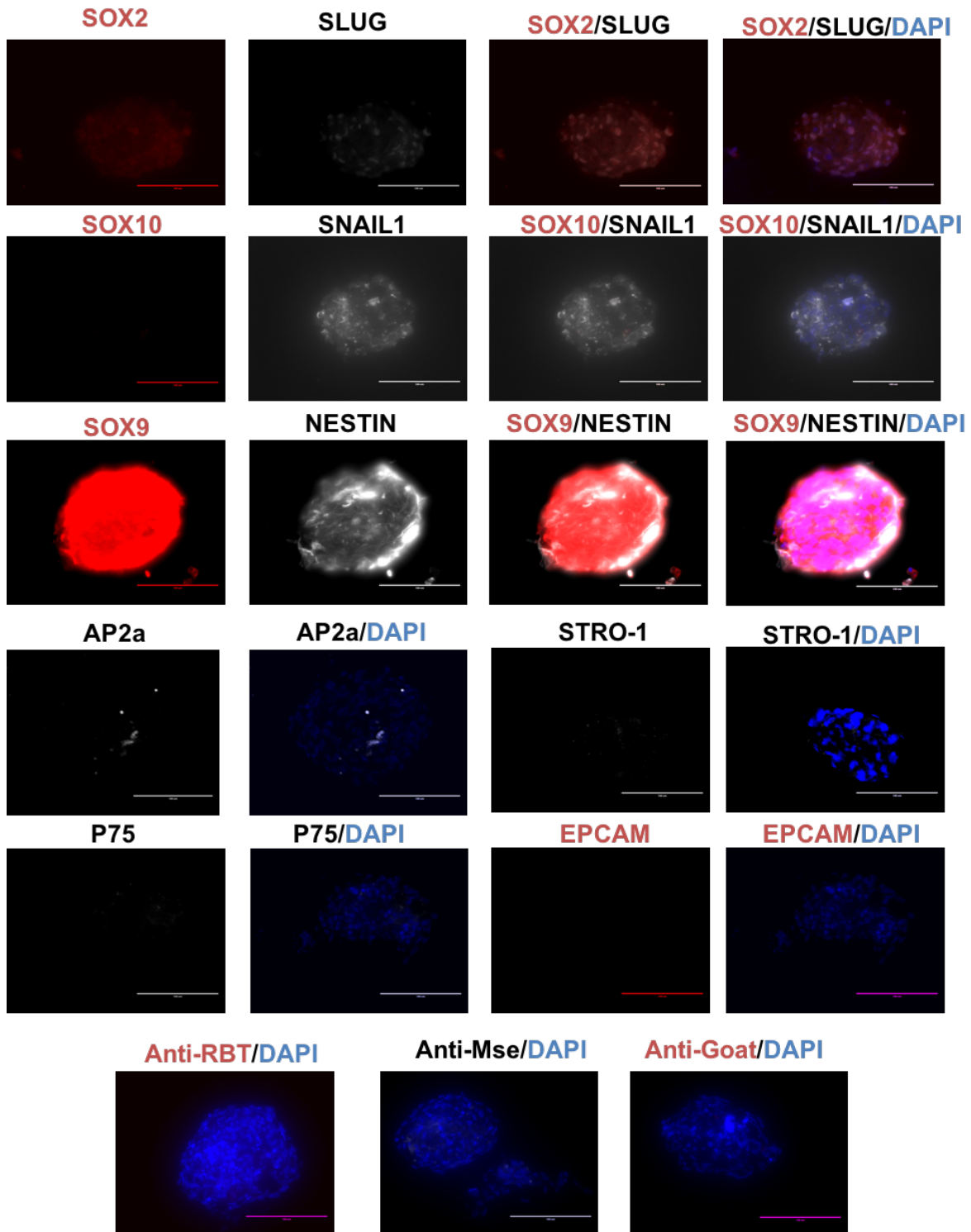


Figure 6.2. hDPC-NCSCs from FBS Cultures. Evaluation of relevant NCSC markers in hDPC-FBS grown as neurospheres for 7 days. Bottom row represents the no primary antibody control to account for any unspecific fluorescent signal from the secondary antibodies. Scale bar: 100µm.

OSCFM-derived hDPC Spheres

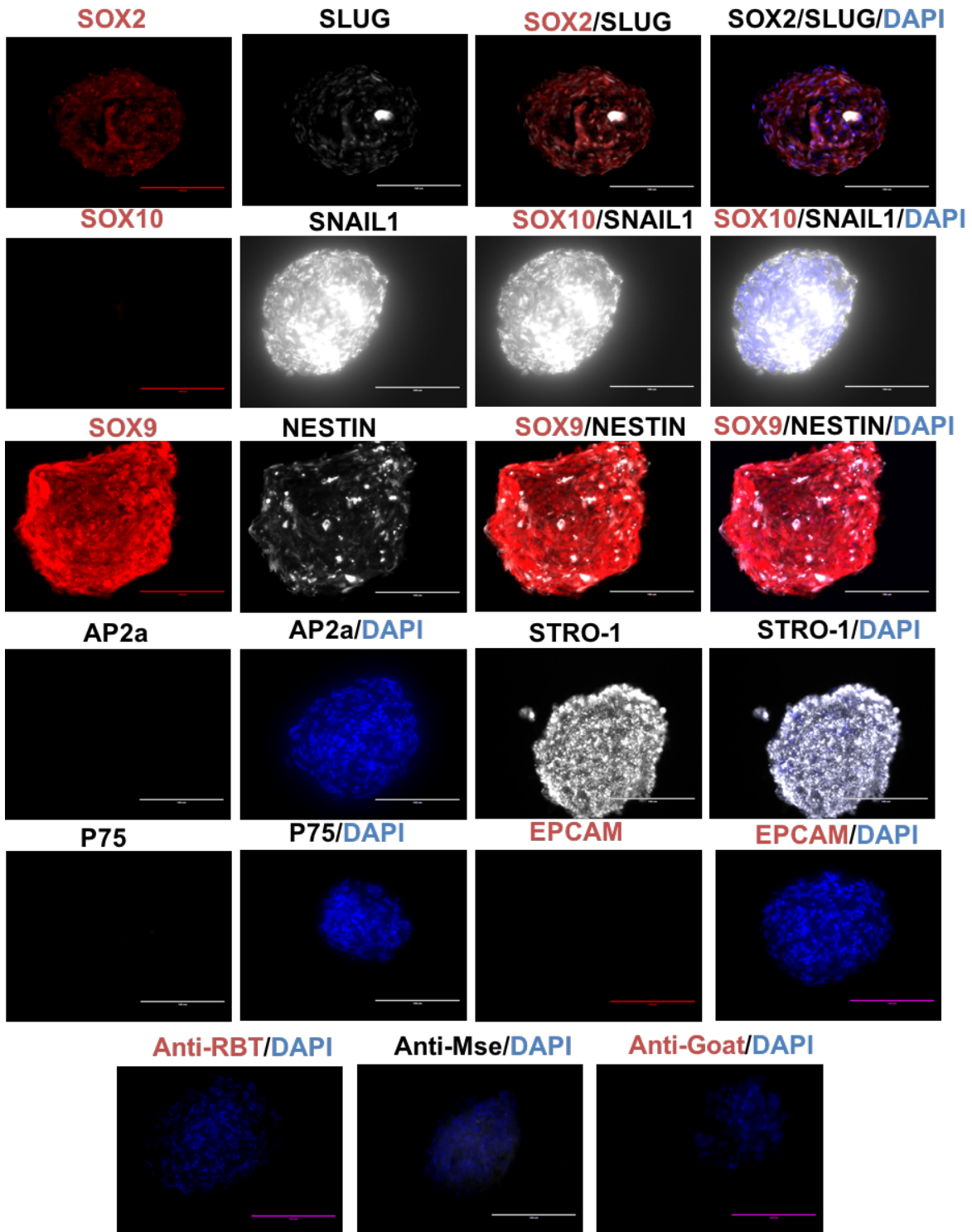


Figure 6.3. hDPC-NCSCs from OSCFM Cultures. Evaluation of relevant NCSC markers in hDPC-OSCFM grown as neurospheres for 7 days. Bottom row represents the no primary antibody control to account for any unspecific fluorescent signal from the secondary antibodies. Scale bar: 100μm.

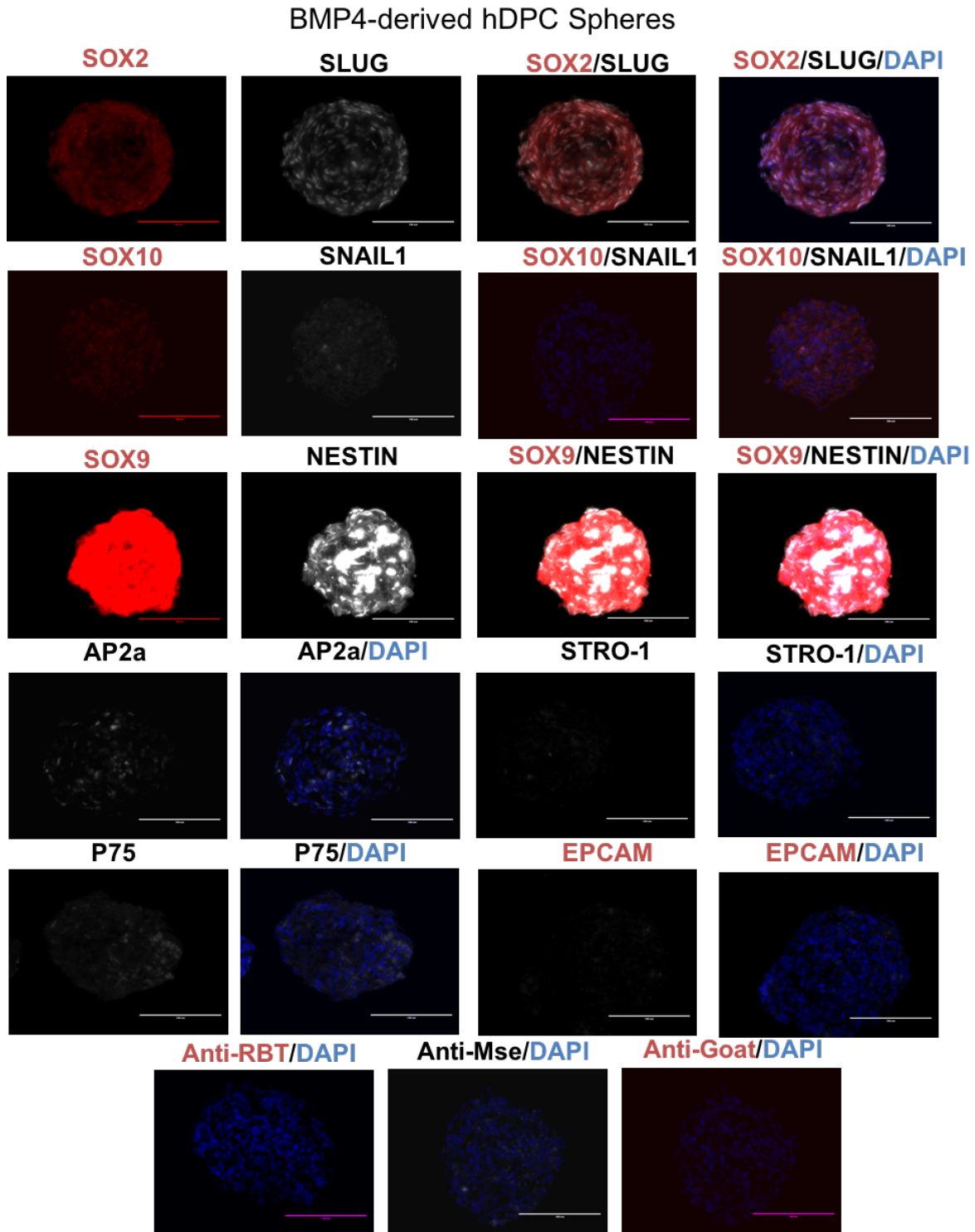


Figure 6.4. hDPC-NCSCs from BMP4 Cultures. Evaluation of relevant NCSC markers in hDPC-BMP4 grown as neurospheres for 7 days. Bottom row represents the no primary antibody control to account for any unspecific fluorescent signal from the secondary antibodies. Scale bar: 100 μ m.

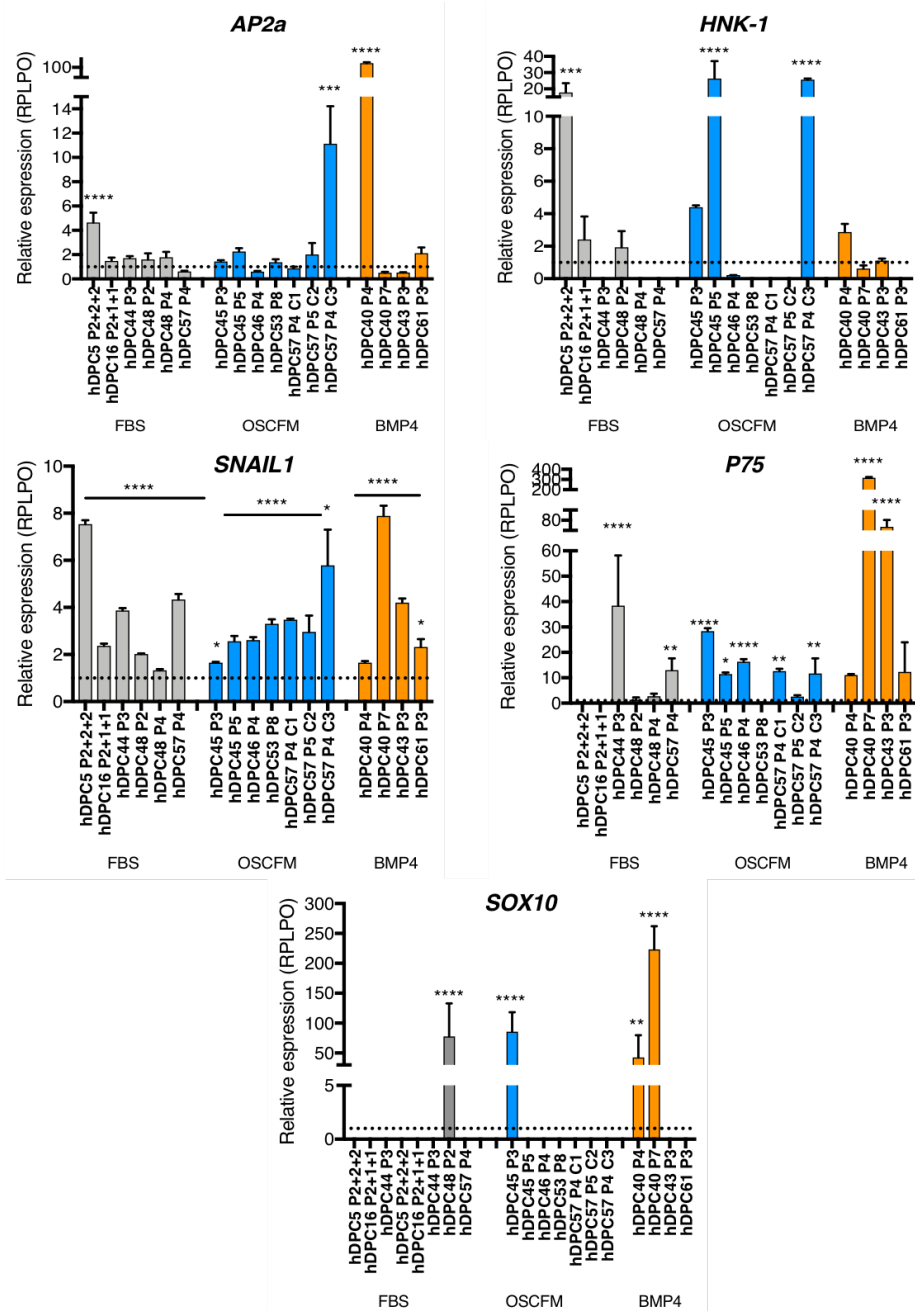


Figure 6.5. hDPC-NCSCs relative expression analysis. Sphere aggregates from all conditions (FBS-grey, OSCFM-blue and BMP4-orange) were analyzed by RT-qPCR for the expression of NCSC markers: AP2a, HNK-1, SNAIL1, P75 and SOX10. Each bar represents an independent neurosphere culture that was normalized and compared individually to their own monolayer counterpart (monolayer: dotted line). A one-way-ANOVA followed by a Sidak's test for pairwise comparison was made to determine differences between the monolayer and the spheres for each hDPC culture. * $p < 0.05$, *** $p < 0.001$, **** $p < 0.0001$. Error bars represent technical replicates.

The expression of NCSC-related markers was then studied at the mRNA level by RT-qPCR. We performed a relative expression analysis to compare each neurosphere culture with their own monolayer counterpart, we then performed a one-way ANOVA to determine if the differences observed were statistically significant. The graphs show independent neurosphere cultures represented as individual bars, and the dotted line is representing the monolayer cultures (Fig. 6.5).

AP2 α mRNA expression was found upregulated only in one sphere culture of each condition (Table 6.1; Fig. 6.5).

HNK-1 mRNA expression was upregulated in one FBS sphere culture (out of 6) and 2 OSCFM sphere cultures (out of 7). We observed a non-statistically significant upregulation for one OSCFM sphere culture and one BMP4 sphere culture (Fig. 6.5).

The only marker that, when evaluated showed a mRNA relative expression upregulation in all hDPC cultures and conditions was *SNAI1*. Overall, the spheres presented a higher *SNAI1* relative expression in comparison to their monolayer cultures (Fig. 6.5).

P75 mRNA was mainly upregulated in 2 of 6 hDPC-FBS sphere cultures and 5 of 7 OSCFM sphere cultures. In the case of BMP4-spheres, two of the analyzed cultures presented significantly higher expression of *P75*, and we observed a third one with a non-statistically significant upregulation compared to its monolayer culture (Fig. 6.5).

Finally, *SOX10* expression was detected at higher levels in one sphere culture from FBS and OSCFM spheres and 2 of 4 BMP4 sphere cultures condition. To note, detection of the *SOX10* mRNA transcript appeared undetermined for the monolayer cultures (Fig. 6.5).

In terms of particular hDPC cultures, we couldn't detect a definite clear pattern of gene expression for particular cultures. However, from the 5 markers that were analyzed, hDPC57 OSCFM P4 C3 and hDPC40 BMP4 P4 expressed 4 of the 5 markers in a statistically higher relative level. hDPC45 OSCFM at passage 3 and 5 upregulated 3 of the 5 neural crest related genes analyzed, however, not the same ones. We also observed particular differences between cultures from the same patient origin, but grown independently in different vessels (i.e. hDPC57 OSCFM C1, C2, C3) or different passage number (i.e. hDPC45 OSCFM P3 and P5/ hDPC40 BMP4 P4 and P7).

| Level | Condition | AP2a | SNAI | P75 | SOX10 |
|-------------------|-----------|------|------|------|-------|
| Protein (ICC) | FBS | 0% | 66% | 33% | 0% |
| | OSCFM | 0% | 80% | 0% | 50% |
| | BMP4 | 100% | 66% | 100% | 100% |
| mRNA (RT-qPCR) | FBS | 16% | 100% | 33% | 20% |
| | OSCFM | 14% | 100% | 71% | 20% |
| | BMP4 | 25% | 100% | 50% | 50% |

Table 6.1. Summary of NCSC characterization by immunocytochemistry and RT-qPCR. A) Percentage of independent sphere cultures that resulted positive for the NCSC markers ($n \geq 3$) by ICC. B) Percentage of independent sphere cultures that resulted in a significantly higher relative expression of NCSC markers to their monolayer counterpart by RT-qPCR, respectively.

Together, ICC and RT-qPCR results portrayed an overview of the neural crest-derived stem cell (NCSC) signature present in the hDPC-spheres. A summary of the NCSCs signature and their variation among conditions and independent cultures is depicted in table 6.1. A trend became evident in which BMP4 cultures had a higher prevalence of the neural crest markers AP2a, P75 and SOX10 by ICC. At mRNA level, a higher percentage of the tested BMP4 cultures upregulated *AP2a* and *SOX10*. Considering that monolayer cultures present an absence/low levels of SOX10 and P75 -at both Protein (by ICC) and mRNA levels (by RT-qPCR)- their re-expression or upregulation (at least partial for FBS, OSCFM and BMP4 spheres) indicate a stronger NCSC signature in spheres, hence, human dental pulp-derived neural crest cells (hDPC-NCSCs).

6.3. hDPC-NCSCs grown as spheres can differentiate into neural-like cells under chemical inductive cues.

The NCSC molecular signal shown by hDPC grown as spheres suggested a resemblance to neural crest cells, at least in appearance (marker expression). Therefore, we aimed to test their differentiation potential into a neural lineage. Neural differentiation was attempted by following a published protocol on human dental pulp cells also grown as spheres⁸⁹. This protocol induces a neural differentiation by cytokine/chemical induction with dcAMP and NT3, as described in methods. The experimental overview is depicted in diagram 6.2.

The spheres under the neural chemical induction attached to the surface and either spread

around the primary sphere body or adhered without spreading. Morphological changes were evident, with thin, long cell projections, and cells seemingly interconnected with each other, particularly on BMP4-derived NCSCs, but also found on FBS and OSCFM-derived NCSCs (Fig. 6.6). The cells were left under differentiation conditions for up to 2 weeks, but changes in BMP4 cultures were evident as early as in day 6.

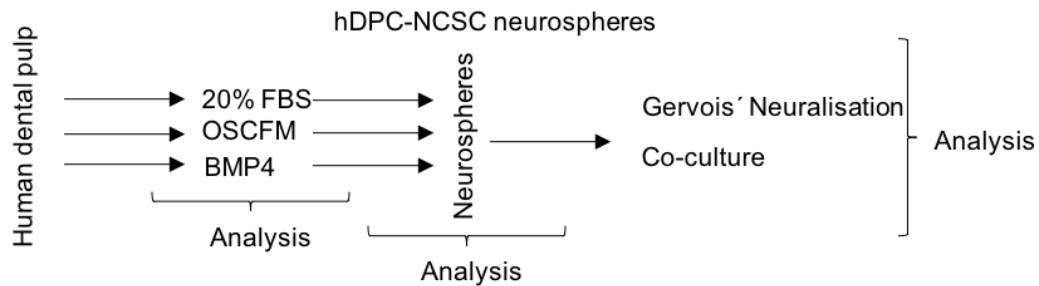


Diagram 6.2. Workflow of hDPC neurospheres for auditory neural differentiation. After the initial establishment and characterization of hDPC-cultures we grew the cultures as neurospheres. We tested the neuralisation of hDPC-neurospheres *in vitro* and *ex-vivo*.

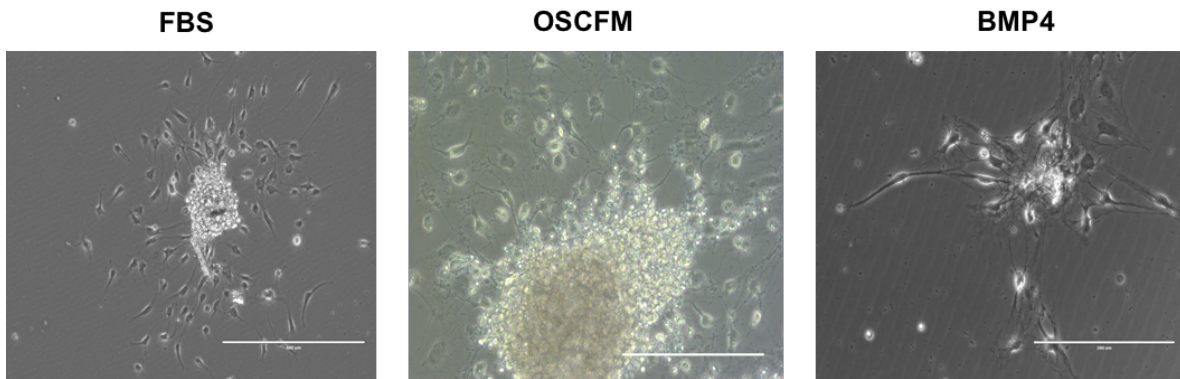


Figure 6.6. Bright field images of neuralised hDPC-NCSCs. Neural morphology after induction by chemical cues (dcAMP/NT3) of hDPC-NCSCs from FBS, OSCFM and BMP4 cultures. Cells with neural-like morphology defined by long, thin cell projections and cell networking in the case of BMP4-derived neural-like cells. Scale bar: 200 μm .

We then performed an ICC experiment to determine qualitatively if the neuralised hDPC-NCSCs were in fact showing signals of a neural phenotype by chemical induced differentiation. After neural induction in at least 3 independent experiments, we performed double labelling of the pan-neural and sensory neural markers TAU/Synaptophysin (SYP), β -

III Tubulin (TUJ1)/ Neurofilament heavy chain (NF200), Brain-specific homeobox-POU (BRN3a)/PERIPHERIN (PER) and C-terminal binding protein 2 (RIBEYE also CTBP2)/ Forkhead box G1 protein (FOXG1). The neural-induced spheres were compared to a control condition without the chemical inducing factors dcAMP and NT3.

hDPC-FBS derived NCSCs after chemical neuralisation showed in some cases a neural morphology. We also found TUJ1 and NF200 co-expressing in the neuralised condition, and with an apparent higher fluorescent intensity than the control. PER was also observed with a higher apparent signal in comparison to the control. We did not observe a clear pattern of SYP, TAU or BRN3a expression in the neuralised or in the control condition. In one experiment, RIBEYE and FOXG1 expression was observed in both control and neuralised groups. The expression of this markers was seemingly stronger in the neuralised group (Fig. 6.7).

In turn, we observed that hDPC-NCSCs from OSCFM cultures also presented a dual positive expression of TUJ1 and NF200, with a seemingly stronger fluorescent signal in the chemical neuralising condition. PER signal was again more intense in appearance in the neuralised group than in the control group. SYP, BRN3a and TAU did not show a clear pattern of expression in the neuralised or control group. RIBEYE/FOXG1 were again present in both groups in one experiment, being the neural condition the one with a seemingly stronger signal (Fig. 6.8).

Finally, for BMP4-derived NCSC spheres, we found drastic and fast morphological changes when induced to chemical neuralisation. In agreement with the neural morphology, we detected a clear pattern of TUJ1 and NF200 dual positive cells in the neuralised group, but not in the control. Similar to hDPC-FBS and hDPC-OSCFM NCSCs, BMP4-derived spheres showed PER expression in a more intense fashion than the non-neuralised control. Importantly, we also detect the expression of TAU and BRN3a in the neuralised group, and not in the control. Results from one experiment showed the presence of RIBEYE and FOXG1 in both conditions (Fig. 6.9).

Chemical induction of hDPC-FBS into sensory neurons

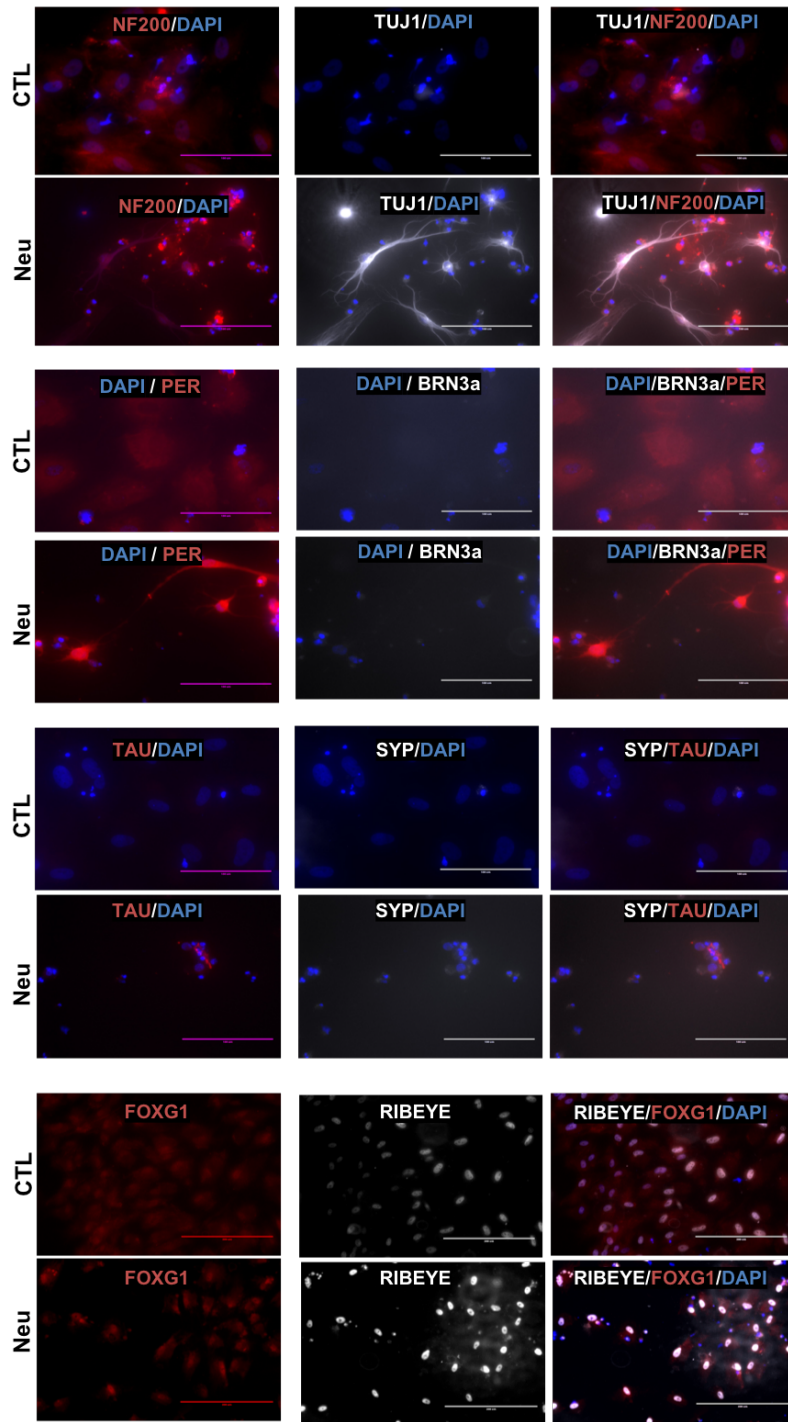


Figure 6.7. FBS-derived neural-like cells, immunocytochemistry (ICC). hDPC-NCSCs after 2 weeks of differentiation. Representative images of 3 independent experiments stained for the neural markers: SYP, TAU, TUJ1, NF200, BRN3a and PER. Results from one experiment are shown for RIBEYE and FOXG1. The Neural induced neurospheres present a Neural-like morphology and a higher fluorescence intensity compared to the control group. CTL: Control group (undifferentiated), Neu: Neuralised group. Scale bar: 200µm. For each marker, the image was taken with the same configuration among treatments to allow comparison.

Overall, hDPC-NCSCs had a different response to the chemical neural inductive cues between the culture conditions (FBS, OSCFM and BMP4) in terms of morphology and neural marker expression. The pan-neural markers TUJ1 and NF200 were constantly present in neuralised cells from all conditions and seemingly co-localised better than the control cultures. Whereas PER, RIBEYE and FOXG1 were present in neural-like cells derived from all conditions. The BMP4-derived NCSCs were the only ones that yielded neuron-like cell morphology with more discernible differences from their control group. hDPC-BMP4 NCSCs also presented a higher TAU and PER expression, and a clear and strong TUJ1/NF200 dual labelled cells in contrast to their control. SYP and BRN3a were absent in the neural induced cultures from all conditions.

Chemical induction of hDPC-OSCFM into sensory neurons

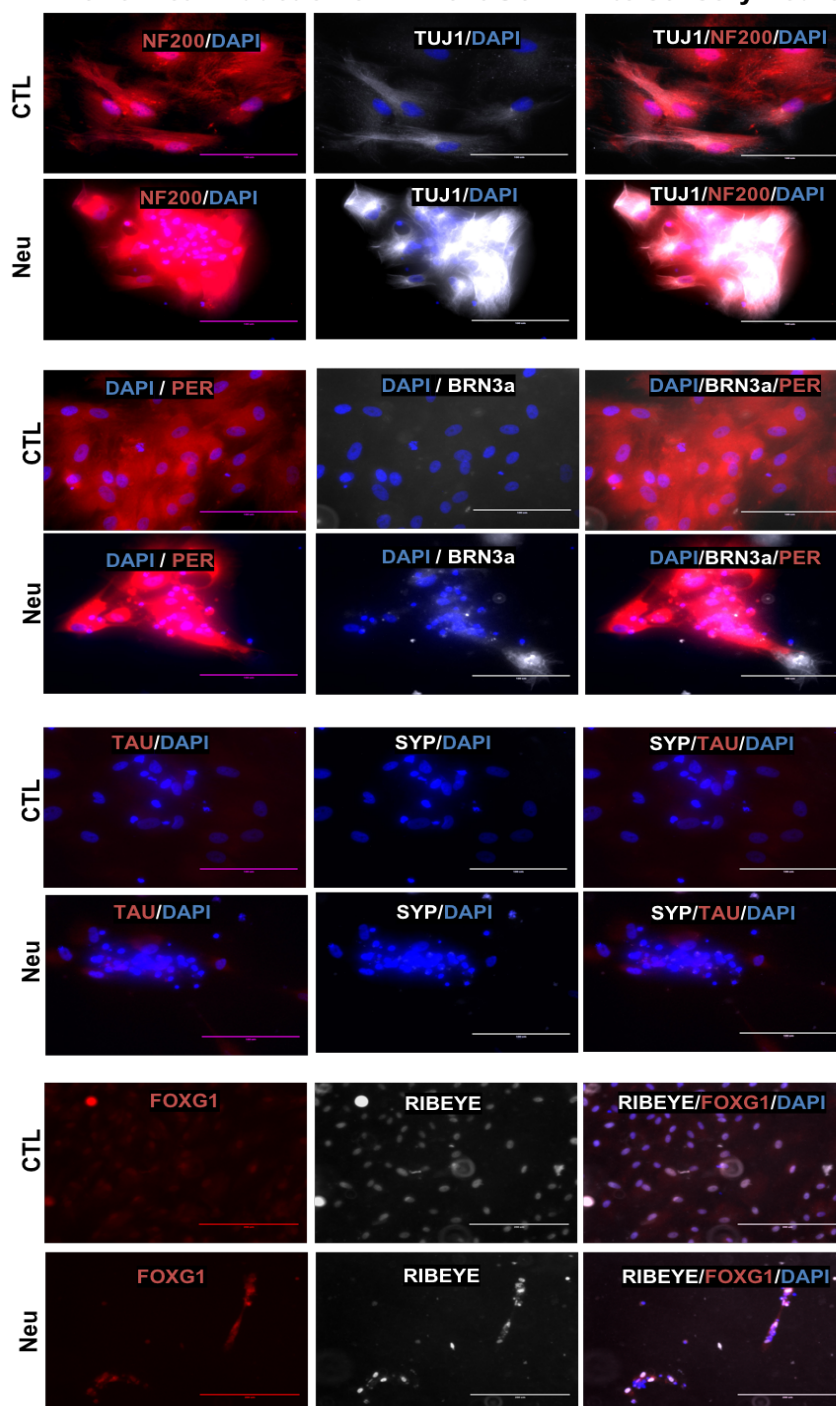


Figure 6.8. OSCFM-derived Neural-like cells, immunocytochemistry (ICC). hDPC-NCSCs after 2 weeks of differentiation. Representative images of 3 independent experiments stained for the neural markers: SYP, TAU, TUJ1, NF200, BRN3a and PER. Results from one experiment are shown for RIBEYE and FOXG1. A Neural-like morphology wasn't always evident in neuralised OSCFM-NCSCs, but they presented a higher fluorescence intensity in the neuralised condition. CTL: Control group (undifferentiated), Neu: Neuralised group. Scale bar: 200 μ m. For each marker, the image was taken with the same configuration among treatments to allow comparison.

Chemical induction of hDPC-BMP4 into sensory neurons

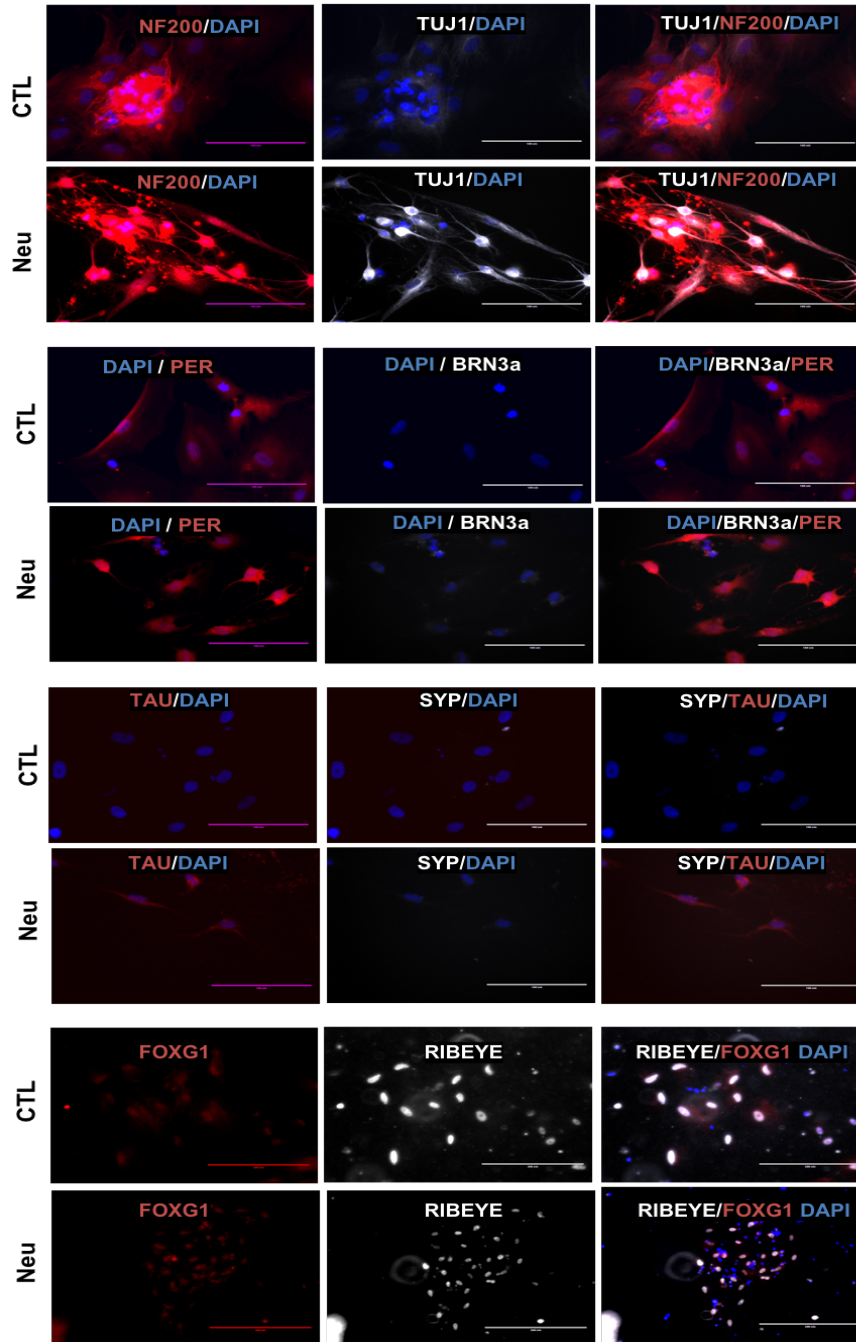


Figure 6.9. BMP4-derived Neural-like cells, immunocytochemistry (ICC). hDPC-NCSCs after 6-14 days of differentiation. Representative images of 4 independent experiments stained for the neural markers: SYP, TAU, TUJ1, NF200, BRN3a and PER. Results from one experiment are shown for RIBEYE and FOXG1. The Neural induced neurospheres present a Neural-like morphology and a higher fluorescence intensity in comparison to the control group. CTL: Control group (undifferentiated), Neu: Neuralised group. Scale bar: 200 μ m. For each marker, the image was taken with the same configuration among treatments to allow comparison.

6.4. hDPC-NCSCs can differentiate into neural-like cells in a model of auditory nerve regeneration.

After characterising the molecular NCSC signature and the differentiation potential of hDPC-NCSCs into neuron-like cells, we then aimed to evaluate their differentiation potential in a specific model of nerve regeneration. We cultured cochlear explants dissected from early postnatal gerbils (P4-P10) with hDPC-NCSCs from the three different expansion conditions (FBS, OSCFM and BMP4). After 7 to 10 days in co-cultures we determined if the hDPC-NCSC differentiated in this *ex-vivo* system by ICC. For this assay, ESC-derived otic neural progenitors (ONPs) were also tested as a positive control of a specific cell type with sensory-neuron differentiation potential.

After 24h-48h the explants and hDPC-spheres started to show outgrowth and adhere to the surface. By day 7-10, the hDPC- sphere cells were hard to distinguish from the proliferating explant cells under the microscope (Fig. 6.10A). As a method to specifically label the human cells and be able to perform live visualisation, we used the Boron-dipyrromethene (BODIPY) staining as described in methods. Human dental pulp cells also outgrew from the spheres and in cases acquire a neural-like morphology. We also used BODIPY staining to evaluate possible interactions between labelled human cells and the explant before fixation (Fig 6.10B).

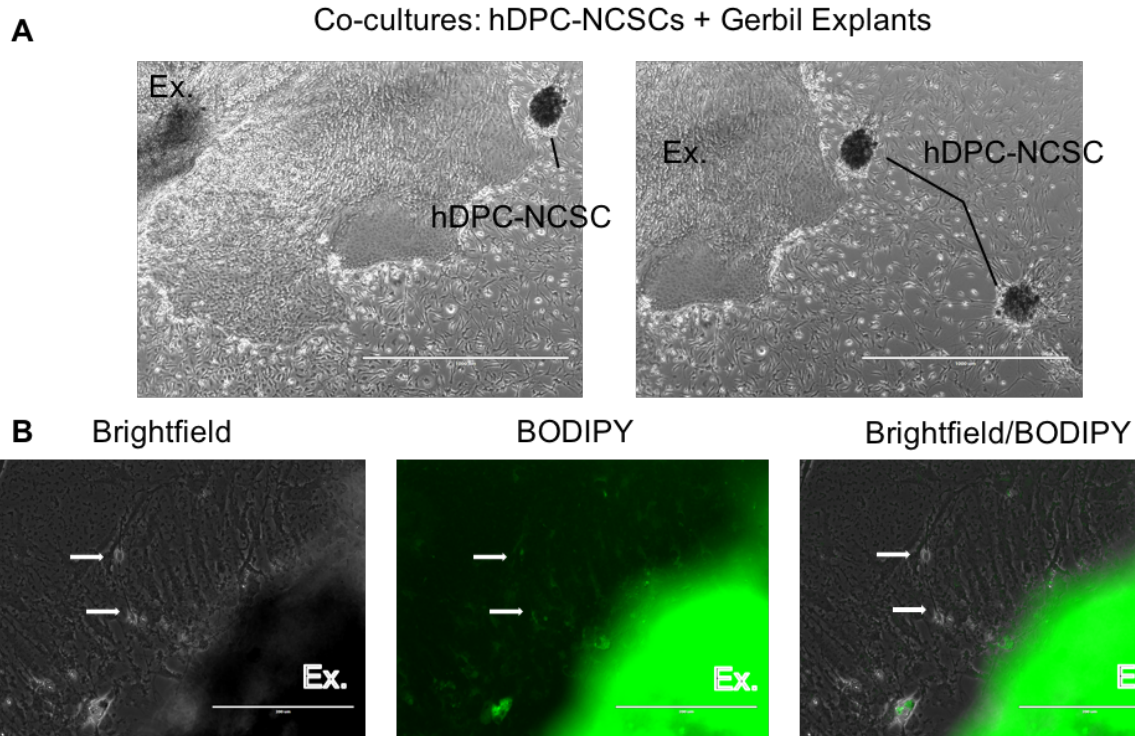


Figure 6.10. hDPC-NCSCs and cochlear explants co-cultures. A) Bright field image of hDPC-derived spheres and cochlear explants (Ex) after 7-10 days. B) BODIPY-labelled hDPCs close to the explant (Ex) have a neural-like morphology. Scale bar: A) 1000 μ m, B) 200 μ m.

To observe in more detail the proposed interaction of hDPC-NCSCs with the explants, ICC and confocal imaging was performed on fixed samples. Human cells were distinguished from the gerbil explant cells by means of the human specific antibodies: Human mitochondria antibody (hMIT) and the proteolytic component, tetradecameric peptidase (CLPP). We also looked for neural markers in order to identify signs of neural differentiation in the hDPC-NCSCs. The pan neural markers TUJ1, NF200 and SYP were used for this purpose together with a more specific auditory neuron marker: Sodium-Potassium ATPase subunit 3 (NKAA3). Additionally, we labelled the explant's sensory hair cells (inner ear mechanoreceptors) with Myosin 7a (MYO7a) and used Glutamate receptor 2 (GLUTR2) to observe whether we could find evidence of synapse formation and therefore signs of re-innervation.

FBS-derived NCSCs (labelled by hMIT) co-cultured with gerbil explants showed the growth of long cell projections in direction of the gerbil explants and triple labeling of hMIT, NF200

and NKAa3, suggesting neural differentiation in direction of the explant (Fig. 6.11). We observed multiple cell projections from hDPC-FBS cells in contact with the explant (Fig. 6.11B). A separate neural marker, SYP, was also present in hDPCs-FBS in the co-culture system, as identified by the human specific CLPP marker (Fig. 6.11C).

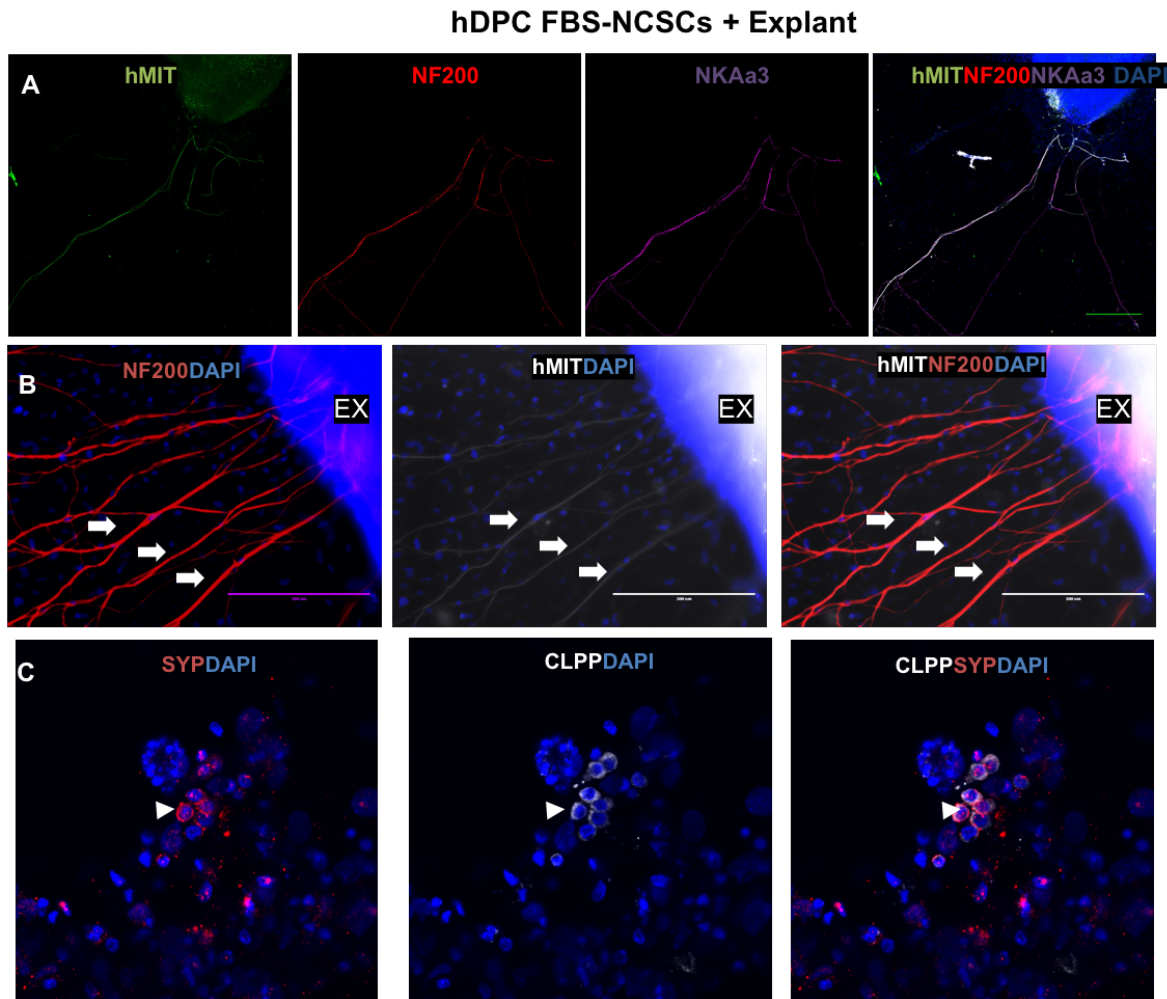


Figure 6.11. Cochlear explants and FBS-derived spheres. Postnatal cochlear explants (Ex) were co-cultured with hDPC-NCSCs (FBS), recognized by the human specific antibodies hMIT and CLPP. A) confocal microscopy of hMIT positive cells co-expressing the neural marker NF200 and the specific auditory nerve marker NKAa3. B) Fluorescent microscopy of co-labelled hMIT positive cells and NF200 nerve fibers in contact with the explant (Arrows). C) Confocal microscopy of CLPP positive cells and the sensory-neural marker SYP (Arrowhead). Scale bar: A) 250 μ m, B) 200 μ m.

OSCFM-derived NCSCs labelled by hMIT also showed thin, long projections, together with the clear ganglionic morphology and NF200 expression (Fig. 6.12). Thus, the results suggest that hDPC-OSCFM cells were undergoing neural differentiation. Moreover, the hMIT neural-like fibers were found growing in direction to the sensory hair cells of the cochlear explant, identified by MYO7a (6.12B). A detailed analysis of the confocal images revealed that human neural projections dual labelled with hMIT and NKAA3 could be found directly in contact with the sensory hair cells labelled with MYO7a (Figure 6.12C, D and B'). Thus, similar to hDPC FBS-NCSC, OSCFM-derived spheres also showed signs of spiral ganglion neuron-like differentiation.

hDPC OSCFM-NCSCs + Explant

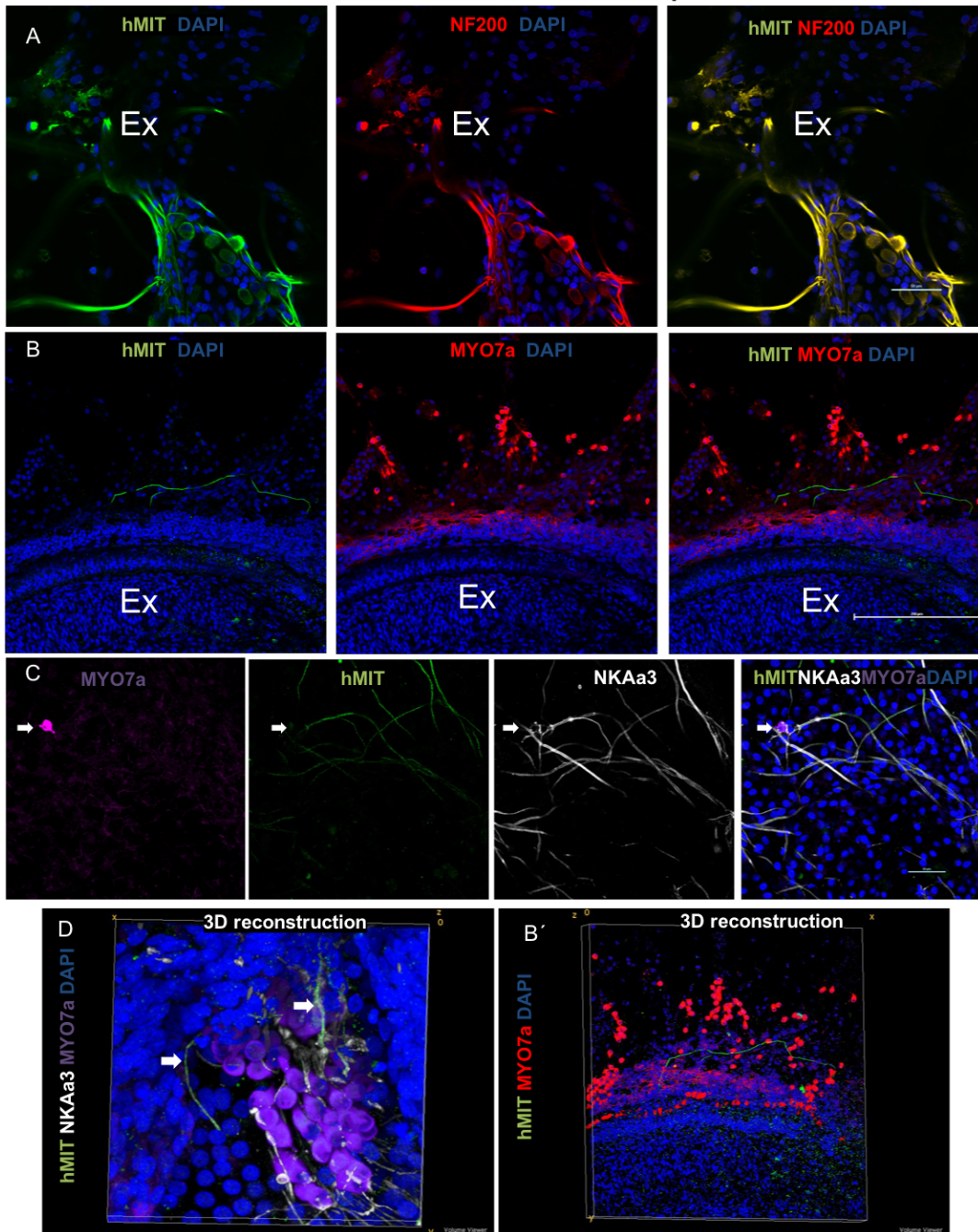


Figure 6.12. Cochlear explants and OSCFM-derived spheres. Postnatal cochlear explants (Ex) were co-cultured with hDPC-NCSCs (OSCFM), recognized by the human specific antibody hMIT A) Confocal microscopy of an OSCFM hDPC-NCSC cluster (hMIT) with ganglionic morphology and NF200 positive cell projections in contact with the explant B) Confocal microscopy of hMIT positive cells in close proximity with the explant's hair cells (MYO7a; arrows). C) OSCFM hDPC-NCSCs (hMIT) co-expressing the auditory neuron marker NKAA3 are in direct contact to a sensory hair cell labelled with MYO7a. D) A 3d reconstruction of a sensory hair cell cluster (MYO7a) being directly reached by OSCFM hDPC-NCSCs co-expressing NKAA3 (arrows). B') 3D reconstruction of an hMIT positive cell fiber extending toward the explant (MYO7a). Scale Bar: A, C) 50µm, B) 250µm.

Finally, as seen in FBS- and OSCFM-derived NCSC cultures, hDPC-NCSCs derived from BMP4 cultures showed a similar NF200-hMIT co-expression and directionality towards the explant (Fig. 6.13A). The BMP4 hDPC-NCSCs were observed close to regions with MYO7a sensory hair cells and NKAA3 positive fibers. (Fig. 6.13B). We also identified BMP4-NCSCs dual labelled with hMIT and NKAA3 in direct contact with hair cells positive for GLUTR2 (Fig 6.13C and C'). Additionally, we identify BMP4 NCSCs with the human marker CLPP co-expressing NKAA3, providing further evidence of spiral ganglion-like differentiation of the human derived BMP-NCSCs. RIBEYE was also present in the co-cultures, but was not indicative of synaptic activity in the particular sample observed (Fig. 5.13D and D').

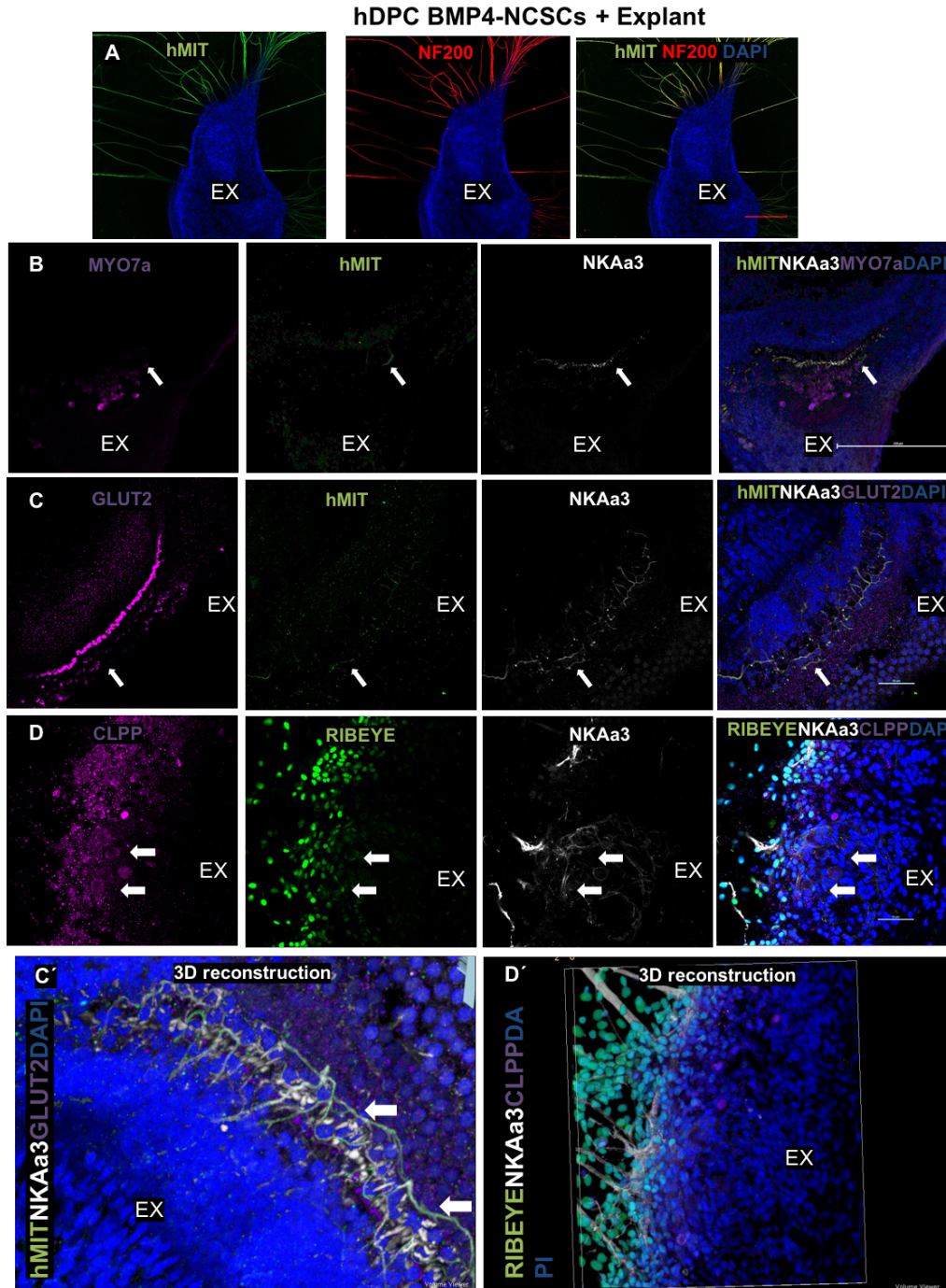


Figure 6.13. Cochlear explants and BMP4-derived spheres. Postnatal cochlear explants (Ex) were co-cultured with hDPC-NCSCs (BMP4), recognized by the human specific antibody hMIT and CLPP. A) Gerbil explants being reached by BMP4 hDPC-NCSCs (hMIT) co-expressing the neural marker NF200. B, C) BMP4 hDPC-NCSCs (hMIT) co-expressing the auditory neuron marker NKAa3 are in direct contact to a sensory hair cell labelled with MYO7a (B) and GLUTR2 (C). D) Confocal microscopy of an BMP4 hDPC-NCSC cluster labelled by another human specific marker: CLPP and co-expressing NKAa3. RIBEYE is expressed in the nuclei of cells in the explant. C') A 3D reconstruction of a sensory hair cell cluster (GLUTR2) being directly reached by OSCFM hDPC-NCSCs co-expressing NKAa3 (arrows). D') 3D reconstruction of CLPP positive human cell fibers expressing NKAa3. Scale Bar: A, B) 250µm, C, D) 50µm.

We also observed the behavior of *bona fide* otic neural progenitor (ONP) in the same circumstance. Spheres derived from ONPs in co-culture with cochlear explants also showed long, thin cells projections in contact with sensory hair cells. ONP cells also expressed NKAA3, suggesting auditory neuron differentiation (Fig. 5.14A). A very distinctive ganglionic morphology was observed in neuralised cells from ONPs (Fig. 5.14B).

These results provided evidence of a similar responsiveness to the *ex-vivo* system seen in hDPC-NCSCs, also in ONPs. Therefore, the acquisition of neural-like morphology and expression of the neural markers NF200, NKAA3 and SYP and their putative connections to sensory hair cells support the potential of hDPC-NCSCs to differentiate in a specific model of auditory nerve differentiation.

ONP (Spheres)+ Explant

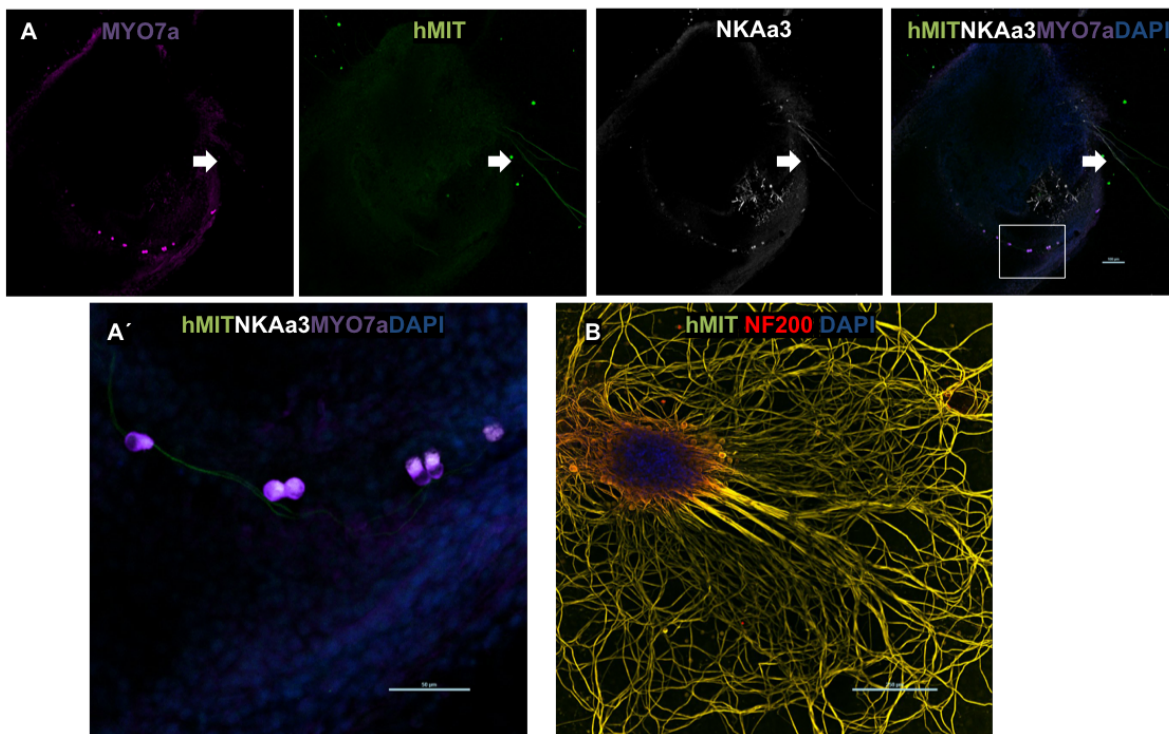


Figure 6.14. Cochlear explants and ONPs. Postnatal cochlear explants were co-cultured with ONPs, recognized by the human specific antibody hMIT. A) ONP-derived spheres (hMIT) co-expressing the auditory neuron marker NKAA3 are in direct contact to a sensory hair cell labelled with MYO7a. A') Higher magnification of hMIT/NKAA3 dual positive cells with MYO7a positive sensory hair cells (Box in A). B) ONP spheres in the co-culture resulted in a neural-like morphology and long cell projections positive for the neural marker NF200. Scale bar: A, A': 50µm, B) 205µm.

6.5. Schwann cell differentiation of hDPC-NCSC spheres

The molecular signature of hDPC-NCSCs and their ability to differentiate into neural-like cells suggested their functional resemblance to Neural Crest Cells. To further investigate a functional trait, human dental pulp cells grown as sphere aggregates and described as NCSCs were subjected to two different protocols of Schwann cell differentiation as per done in monolayer cultures.

Unfortunately, the fluorescent microscopy was highly affected by background noise and unspecific staining in all conditions. Nevertheless, cultures labelled with the alexa-568 (RED) secondary antibodies raised in Rabbit and Goat were less affected and allowed observation, although still presenting background staining.

Overall, none of the hDPC-NCSCs resulted in a particular clear difference after differentiation. In terms of the protocols used, S100 calcium binding protein (S100 β) appeared more nuclear in the Studer's protocol for all hDPC-NCSCs (FBS, OSCFM and BMP4). Whereas in the control condition and Dezawa's protocol, S100 β appeared more cytoplasmic, but seemingly stronger in the latter group. Glial fibrillary associated protein (GFAP) expression wasn't identified in any of the groups from any of the hDPC-NCSCs. Similarly, P75 wasn't detected in any instance. In the case of SOX10, it seemingly appeared clearer under the Dezawa's protocol in comparison to the control and Studer's groups in FBS, OSCFM and BMP4-derived spheres. These differences although discrete, should be validated further (Fig. 6.15, Fig. 6.16 and Fig. 6.17).

Schwann cell differentiation of hDPC-NCSCs (FBS)

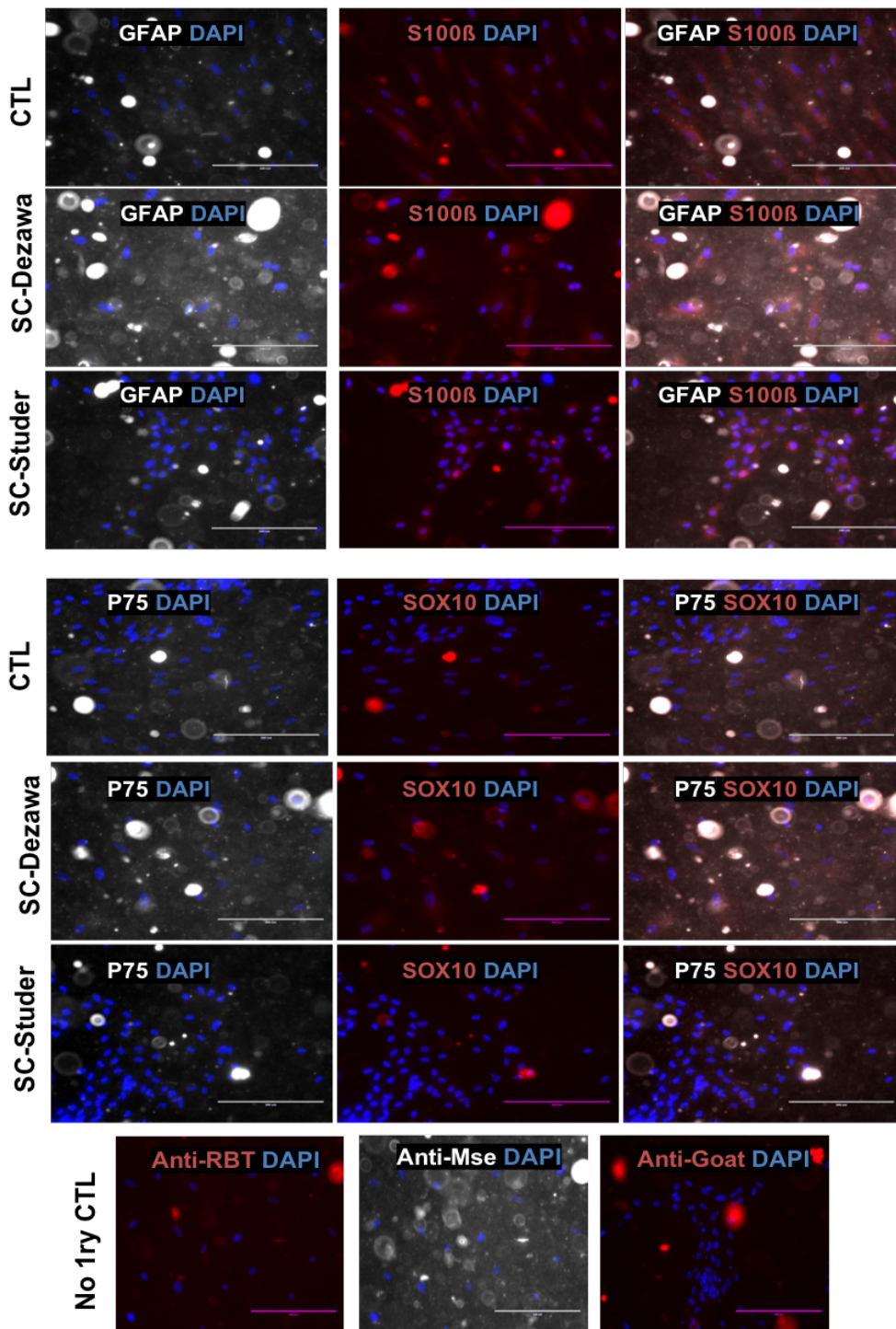


Figure 6.15. Schwann cell differentiation of hDPC-NCSCs from FBS cultures. FBS-derived spheres after 2 weeks of Schwann cell differentiation using two separate protocols (Dezawa and Studers) and an undifferentiated control group (CTL). Representative images of at least 2 independent experiments. Expression of GFAP/S100β and P75/SOX10 was evaluated by immunocytochemistry. High background noise and light artefacts affected the fluorescent imaging as seen in the no primary antibody controls for secondary antibodies). Scale bar: 200μm.

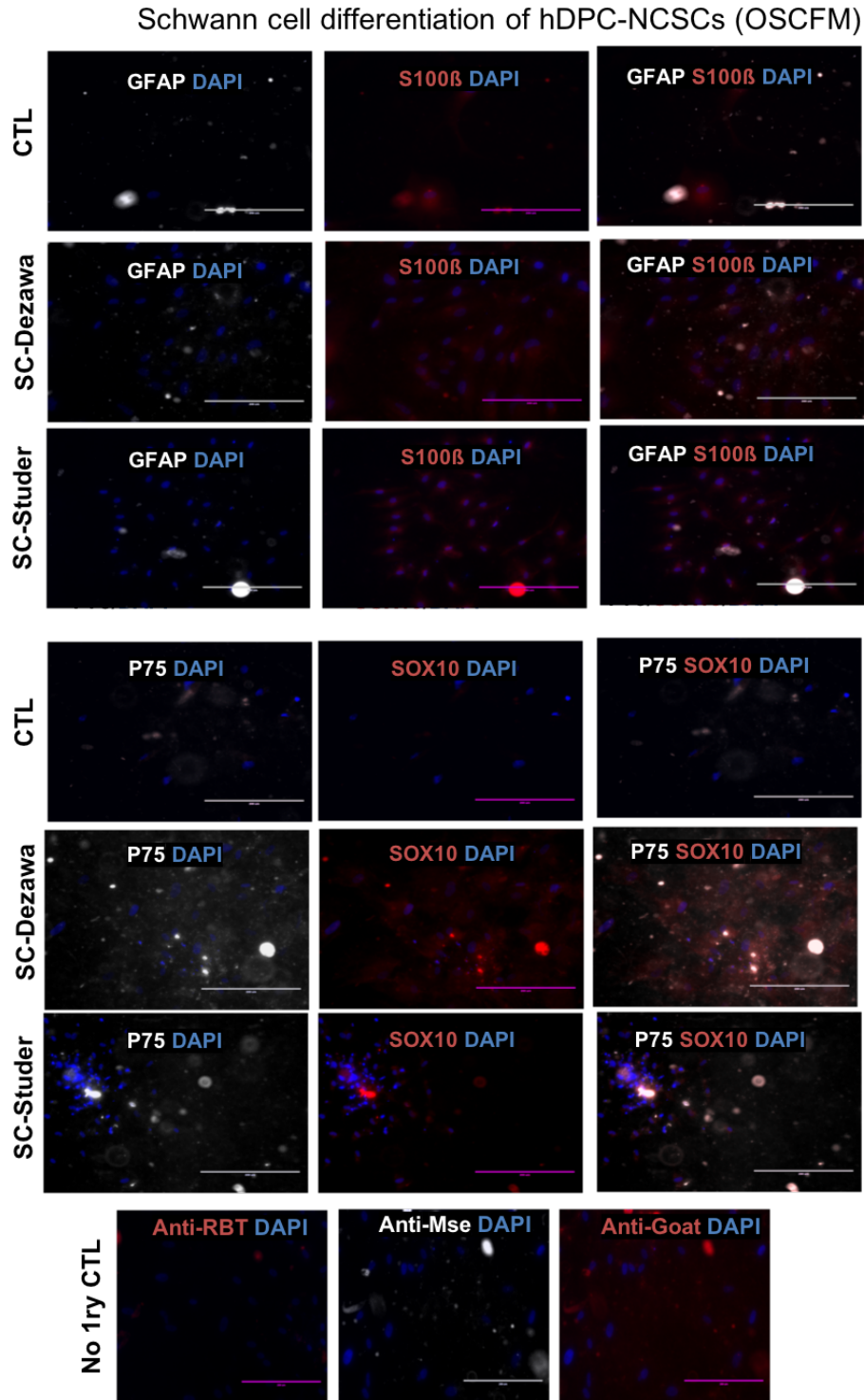


Figure 6.16. Schwann cell differentiation of hDPC-NCSCs from OSCFM cultures. OSCFM-derived spheres after 2 weeks of Schwann cell differentiation using two separate protocols (Dezawa and Studers) and an undifferentiated control group (CTL). Representative images of at least 2 independent experiments. Expression of GFAP/S100β and P75/SOX10 was evaluated by immunocytochemistry. High background noise and light artefacts affected the fluorescent imaging as seen in the no primary antibody controls for secondary antibodies). Scale bar: 200μm.

Schwann cell differentiation of hDPC-NCSCs (BMP4)

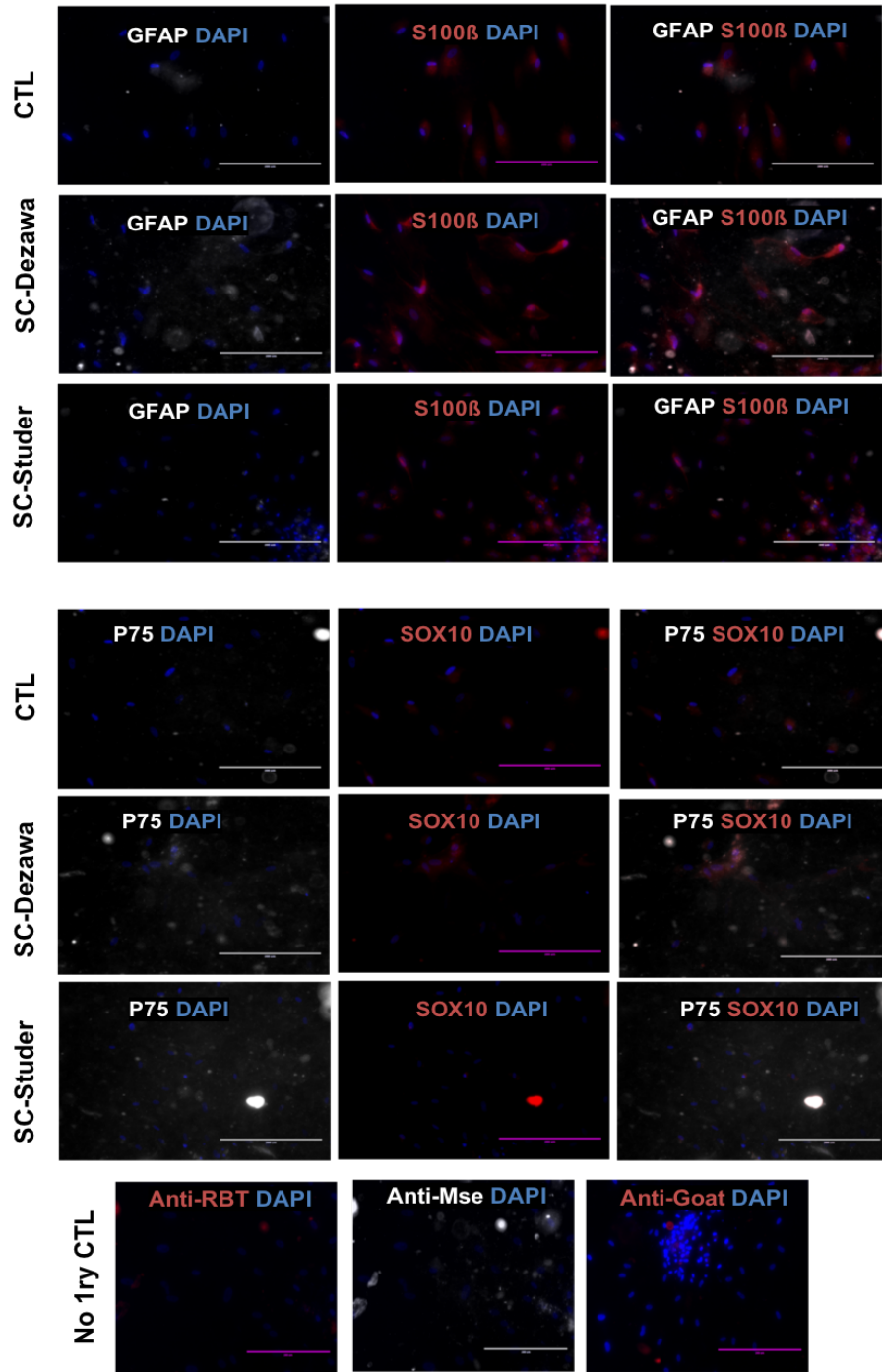


Figure 6.17. Schwann cell differentiation of hDPC-NCSCs from BMP4 cultures. BMP4-derived spheres after 2 weeks of Schwann cell differentiation using two separate protocols (Dezawa and Studers) and an undifferentiated control group (CTL). Representative images of at least 2 independent experiments. Expression of GFAP/S100 β and P75/SOX10 was evaluated by immunocytochemistry. High background noise and light artefacts were evident, but in a lower scale than in FBS and OSCFM cultures. BMP4-NCSCs induced to differentiate into Schwann cells did not show any immediate difference in marker expression or intensity in relation to the undifferentiated control (CTL). Scale bar: 200 μ m.

6.6. Characterisation of hDPC in a Neural Crest Stem Cell medium (NCSCm).

Lastly, as another alternative condition to grow human dental pulp cell cultures, we tested a medium recently shown to induce a neural crest-like phenotype in periodontal ligament stem cells and deciduous teeth stem cells^{69,70}.

At least three independent hDPC-FBS cultures were left to grow in the neural crest stem cell medium (NCSCm) for 5 days (diagram 6.3). The culture aspect had a clear change, with small tight colonies of epithelial resemblance (Fig. 6.18A). We then analysed the relative expression of neural crest-related markers by qPCR in comparison to their basal state growing in FBS. In two of the hDPC-FBS cultures tested, we included the previously characterised hDPC-spheres for comparison. Interestingly, *AP2α*, *HNK-1* and *SNAIL1* showed a clear upregulation in relation to their control groups. The first two with higher levels than their sphere counterparts. On the other hand, *SOX10* and *P75* appeared to be null expressed or significantly downregulated, respectively (Fig. 6.18B).

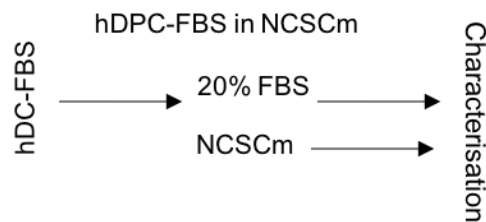


Diagram 6.3. Workflow of hDPC-FBS transferred to Neural crest stem cell medium (NCSCm). hDPC-FBS were cultured in parallel in 20% FBS medium and the reported NCSCm^{69,70} for characterization.

At the protein level, an ICC assay of the hDPC7-FBS in NCSCm, revealed the cytoplasmic presence of SOX10 and SOX2, as well as the presence of AP2a, SLUG, GLI1 and STRO-1. A weak to null expression of P75 was also detected. Overall, the NCSC, resulted in the upregulation of neural crest related genes at the RNA level and further supported by their presence at the protein level. The exceptions to the previously stated are P75 and SOX10, that remained undetermined at the RNA level and weakly expressed by ICC (Fig. 6.19).

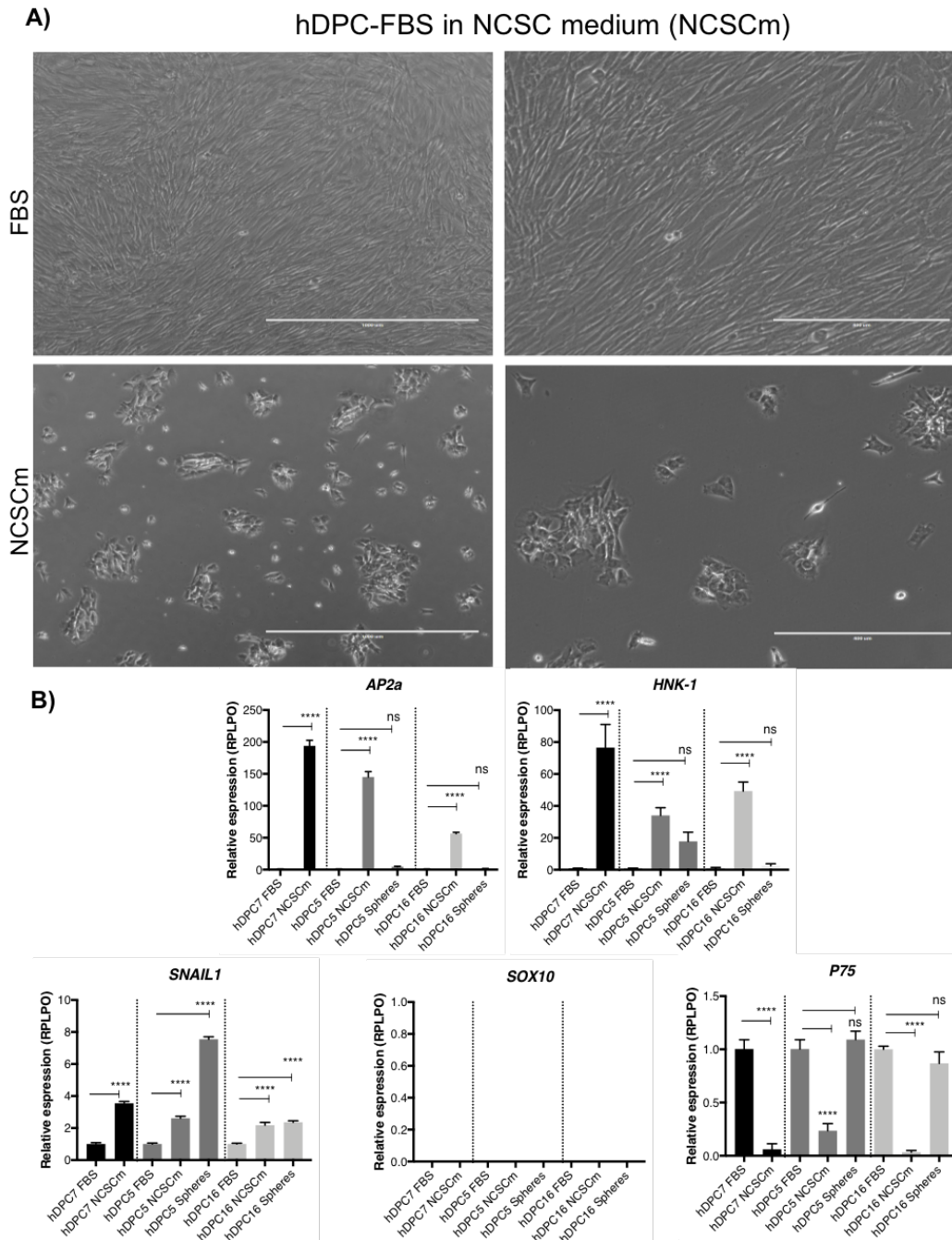


Figure 6.18. hDPC7 FBS in NCSCm. A) Bright field images of hDPC-FBS (Top) and in neural crest stem cell medium (NCSCm) at day 5 (Bottom) in two magnifications (Left lower, right higher magnification). Cultures in NCSCm presented an epithelial, polygonal morphology and cells arranged in small colonies. B) Relative Expression of Neural Crest related genes in hDPC-FBS growing in NCSCm and spheres normalised to their basal condition (FBS). NCSCm from 3 independent cultures expressed upregulated *AP2a*, *HNK-1* and *SNAIL1* in relation to the FBS control. *SOX10* and *P75* were found in lower levels in NCSCm in relation to the control. Neurosphere cultures from the FBS-hDPC tested presented an upregulation only for *SNAIL1* in comparison to the control and the NCSCm groups. Scale bar: 1000µm (Left), 400µm (right). ****p<0.0001.

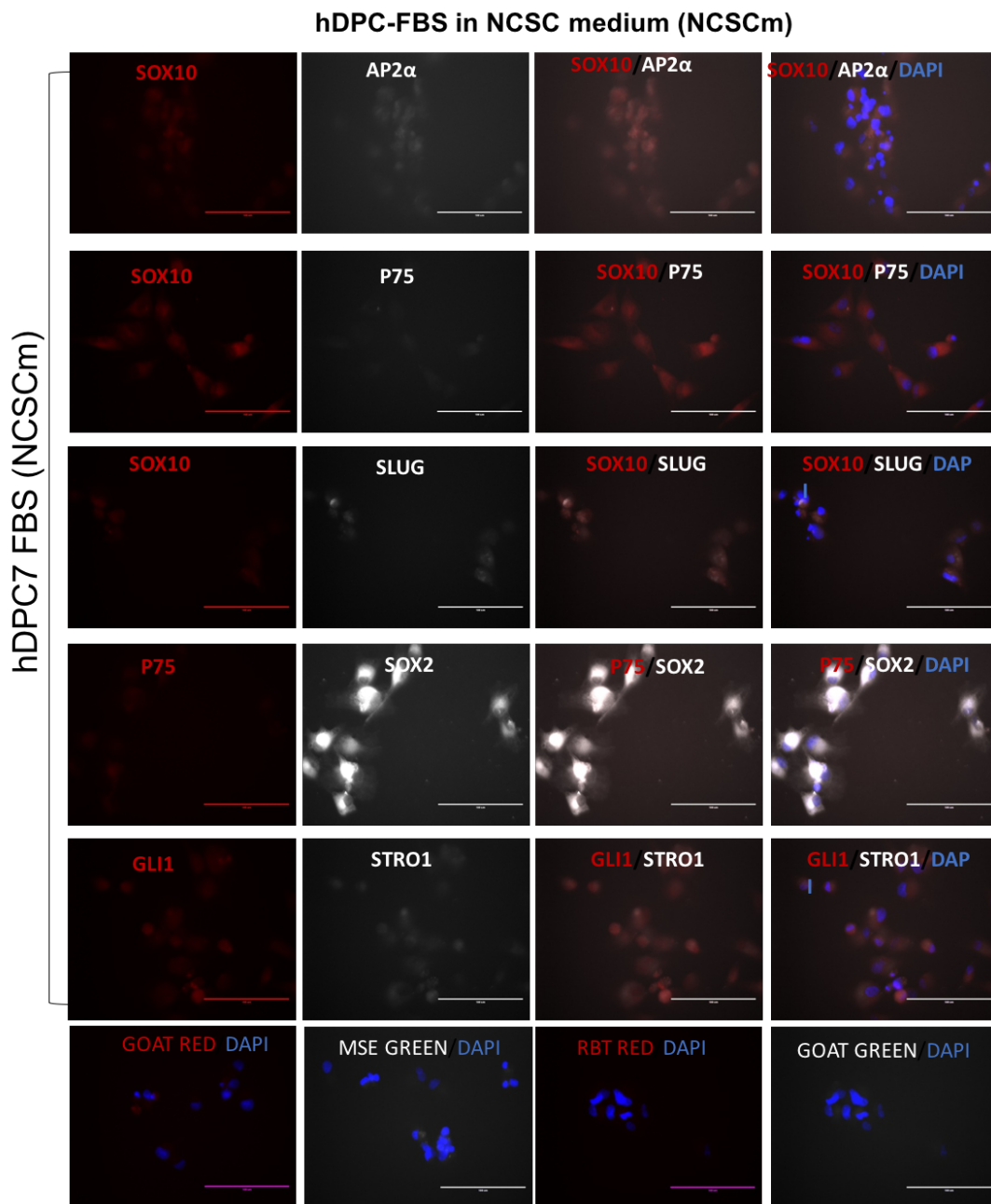


Figure 6.19. hDPC7 FBS in NCSCm, immunocytochemistry (ICC). The expression of SOX10, GLI1, STRO-1, SOX2, P75, SLUG and AP2a was evaluated by ICC. Bottom row: No primary antibody controls. Scale bar: 100 μ m.

6.7. Discussion

6.7.1. Sphere aggregation as a method to obtain NCSCs

The hDPCs developmental origin and basal expression of ectodermal and neural genes support an advantage from bone marrow's MSCs to be used for neural-related conditions¹⁶⁸. Nevertheless, our observations in mDPCs and hDPCs, together with the literature, suggested that full neural differentiation was possible only after reprogramming, or pre-treatments before neural maturation, as discussed earlier. Hence, the inherited ectomesenchymal trait is insufficient to develop a true neural phenotype. For this reason, we and others, have proposed that a particular neurogenic or neural crest-like population could be isolated from dental pulp cell cultures^{74,122}. Evidence from other adult stem cells with neural crest origin grown *in vitro*, has shown that we can obtain a neural crest-like trait defined by multipotency and a NCSC molecular signature^{54,56,58,117}. As neural and glial differentiation are lineages derived from neural crest cells, our aim was to evaluate if a neural crest-like population could be obtained from human dental pulp cells and if hDPCs-NCSCs could be used in auditory nerve regeneration.

We evaluated driving the hDPCs from our three different conditions (FBS, OSCFM and BMP4) into sphere aggregates. Sphere aggregation has been shown to induce or select a NCSC phenotype from bone marrow, hair follicle bulge, nasal tissue, Schwann cells, palatal tissue, gingiva and deciduous teeth^{50,54,56,58,64,72,169}. Also, it has been recently reported that hDPC spheres express higher levels of NANOG, CD44, TP63 and GBL1L2 (stem cell markers) and differentiate spontaneously into somewhat neural and osteogenic phenotypes¹⁴¹.

In our results, we have shown that the cell number and diameter did not change significantly between hDPC spheres from FBS, OSCFM and BMP4. Nevertheless, the molecular signature that the spheres presented did show variations. Initially, we couldn't detect major quantitative differences among the monolayer cultures (Chapter 4). We selected the markers for analysis based on published studies on embryonic human neural crest cultures and tissue. For instance, the expression of *SNAI2 (SLUG)*, *SOX9*, *SOX10* and *P75* mRNA in cultured human migratory neural crest also coincided with the expression in other amniotes¹⁷⁰. Furthermore, a separate study found that in human tissue, embryonic

pre-migratory neural crest expressed PAX7, SOX9 and SOX10 while migratory neural crest cells are reported to express SOX9, SOX10, AP2a, P75 and HNK-1¹⁷¹. In the case of reports from *in vitro*-derived neural crest cells from embryonic stem cells, use the expression of Ap2a, P75, HNK-1 and SOX10 to describe a neural crest phenotype^{97,172}. We selected the markers reported above, to test the hypothesis that direct culturing into a neurogenic media (such as OSCFM and BMP4) allows a NCSCs phenotype when driven to sphere aggregates (diagram 6.1). After analyzing the spheres aggregates by ICC, positive expression of SLUG, SOX9 and NESTIN was present independently of the initial condition (FBS, OSCFM or BMP4), whereas AP2a, SOX10 and P75 appeared only in some hDPC-derived NCSC, particularly hDPC-BMP4. In this regard, positive expression of AP2a, SOX10 and P75 appeared frequently in BMP4-NCSCs. During development in amphibians, it is known that BMP factors are key in inducing the expression of the early marker AP2a¹⁷³, therefore a possible explanation of AP2a appearing at protein level is by a direct effect from BMP4. This result provided initial support of differences related to the original medium conditions in the cultures. Our mentioned ICC results, together with the mRNA upregulation in several hDPC-NCSCs of mainly *P75*, *SOX10* and *SNAIL1* suggest an enhanced neural signature compared with that observed in monolayer cultured hDPCs. Additionally, in support of our discussion on culture heterogeneity (chapter 4), we detected constant variations between cultures from the same conditions and importantly, from the same donor sample at different passage or from independently grown vessels. The latter refers to cultures that early in culture establishment or passage were split into separate vessels in low densities and grown independently. As discussed broadly on chapter 4, differences between clones and passage number even within cultures of similar origin have been observed before, and represent a major consideration for future applications and reproducibility.

6.7.2. Neural differentiation of hDPC-NCSCs

The enhanced NCSC signature observed in neurospheres, motivated us to test their proposed neural crest behavior in neural and glial differentiation. From the literature, it is known that NCSCs from adult tissues can acquire a neural phenotype. For instance, human inferior turbinate (nasal) stem cells (ITSC), grown as spheres and characterised as NCSCs,

were able to differentiate *in vitro* into dopaminergic neurons, and showed signs of functional recovery in parkinsonian rats¹⁷⁴. On the other hand, the potential of a dental-related human-NCSCs for a particular neurodegenerative disorder, is commonly only implied and is usually left untested (Table 1.1)^{64,68-70,72}. In fact, only one report from human gingival derived NCSC addressed a functional model of peripheral nerve regeneration⁶⁵. It must be clarified that we are referring to cultures described as NCSCs from dental tissues and tested in relevant models of disease, rather than just the chemical differentiation *in vitro*⁸⁸⁻⁹⁰. In this chapter, we first tested a protocol reported by Gervois et al., (2015) to derive functional neurons from hDPCs. This protocol required the generation of neurospheres before the induction to mature neurons as an intermediate step⁸⁹. Therefore, although not characterised nor implied by the authors in the original report⁸⁹, we suggested that a NCSC phenotype was required for neural maturation (thus, the need of neurosphere formation). We stopped neuralisation at week 1 or 2 based on the observation that BMP4 cultures started presenting a neural-like morphology after a shorter incubation period (6 days to 2 weeks). Although we have no evidence of functional neural maturation, we propose that the response and changes observed in BMP4 cultures are related to their enhanced NCSC phenotype. In support of this, BMP4 factor has been identified as a key regulator of neural crest development, and also as an important element for sensory neural differentiation in NCSCs^{108,118,121,160}. In this regard, BMP4 has previously been identified by others as a key regulator to drive sensory neuron differentiation, impeding NCSCs from dorsal root ganglion from committing to progenitors of the central nervous system¹⁰⁸. Additionally, MSCs have been reported to differentiate into spiral ganglion-like neurons when BMP4 was used in the media¹⁷⁵. Furthermore, derivation of neural crest cells from ESCs has been successfully described by using BMP4¹⁷⁶. Our data further supports the importance of growing the cells in the presence of BMP4 from the beginning, showing the rapid response of cells grown in BMP4 compared to FBS and OSCFM conditions. However, we do not rule out the possibility that NCSC-FBS and NCSC-OSCFM cultures could present a stronger neural-like phenotype than the one observed if left for a longer period.

6.7.3. hDPCs-NCSCs in a model of auditory nerve regeneration

To further explore hDPC-NCSCs applications in regenerative medicine and to advance from current implications to experimental evidence, we tested hDPC-NCSCs capacity to respond to neural induction *ex vivo*, in a model of auditory nerve regeneration^{177,178}.

Co-culturing the hDPC-NCSCs spheres from the three conditions (FBS, OSCFM and BMP4) with cochlear explants indicate that hDPC-NCSCs can differentiate into neural-like cells expressing SYP, NF200, NKAa3 and TUJ1 in proximity to the explants. Similar results have been shown from auditory nerve and ESC-derived neural progenitors in similar models, capable of re-innervating and re-establishing synapses with early postnatal (P3-P6) cochlea explants after 10 days of *ex-vivo* co-culture. For instance, Tong et al. (2013)¹⁷⁷ co-cultured explants with auditory nerves, and found that the nerves were able to re-establish synaptic connections with the hair cells. ESC- and iPSC-derived neural progenitors have also been shown to re-innervate cochlear explants, providing proof of concept of the use of pluripotent stem cells for auditory nerve regeneration and supporting further transplantation studies^{178,179}. In our results, we observed a disorganized neurite growth towards the explant, also an odd hair cell organization and/or low hair cell number resulting from *ex-vivo* outgrowth after 10 days in co-culture, which agrees with the finding reported by Gunewardene et al. (2016)¹⁷⁹. Recently, NCSCs from hair follicle bulge were used in a similar model of mouse cochlear explants, the authors showed the expression of the neural marker TUBIII and migration of the human cells towards the explant⁶⁰. In this thesis, we also observed the expression of neural markers in hDPC-NCSC co-cultures. Furthermore, we provided clearer evidence of neural differentiation into spiral ganglion-like cells. Spiral ganglion-like differentiation is supported not only by morphological changes, but also by expression of a more specific auditory neuron marker: NKAa3¹⁸⁰ and evidence of direct contact between hDPCs and sensory hair cells within the explant. Thus, our results support the use of neural crest-derived stem cells for auditory regeneration. Our observations provide proof of concept of a direct application from an adult source of NCSCs in an auditory nerve regeneration model. Furthermore, to the best of our knowledge, is the first described application for neural differentiation from a human oral-derived source, described as NCSC.

6.7.4. Glial differentiation of hDPC-NCSCs

In relation to their glial differentiation potential, we followed the same protocols used before on the monolayer cultures (Chapter 4). Similar to our previous observations, sphere aggregates resulted in discrete changes in the observed markers S100 β , SOX10, P75 and GFAP by ICC. The potential of neural crest cells to acquire a glial cell fate, is described not only for embryonic neural crest cells, but also from embryonic stem cell-derived neural crest cells^{97,160}. The fact that none of the protocols used here provided clear evidence of a Schwann cell phenotype (protocols for mesenchymal and Neural Crest glial differentiation). Hence, our results suggest that hDPCs sphere aggregates could be bias towards a neural fate or that the glial differentiation protocol needs optimization for hDPCs. We can propose a neural fate bias in hDPCs, which is supported by Lee et al. (2007), who proposed that neural acquisition precedes glial differentiation, and also, glial competence depends on temporal changes in development. Therefore, neural differentiation would occur more easily, until glial competence is acquired. This hypothesis was based on their observations that ESC-derived neural crest cells were able to differentiate into Schwann cells only after a period of time *in vitro*, instead of immediately after NCSC formation⁹⁷. Thus, hDPC-NCSCs could require temporal adaptation (i.e. culture proliferation, passaging as spheres) to be capable of glial differentiation.

6.7.5. Effect of neural crest stem cell medium on hDPC-FBS

Finally, we tested a recent published protocol to obtain NCSC by culturing hDPCs in a medium containing a WNT activator and a TGF β inhibitor. The author tested WNT and TGF β pathway modification on periodontal ligament stem cells (PDLSC) and dental pulp from deciduous teeth (SHEDS^{69,70}) and observed a significant increase of P75 and HNK-1 positive population. Additionally, the authors strongly suggest that the neural crest resemblance could correlate to an epithelial trait, meaning that WNT activation and TGF β inhibition could induce mesenchymal to epithelial transition. Furthermore, the neural crest phenotype in the cited reports was inhibited by addition of serum to the growing conditions, promoting a mesenchymal trait^{69,70}. WNT and TGF β pathway regulatory factors have also been used on ESCs to derive neural crest cells, as shown elsewhere¹⁷². In our results, we also found

differences between the basal conditions and cells transferred to the “neural crest stem cell medium” (NCSCm), in which we observed a significant and consistent upregulation of *AP2a*, *SNAIL1* and *HNK1* (also compared to sphere aggregates-NCSCs). However, the expression of *SOX10* remained un-determined and *P75* in NCSCm appeared downregulated in comparison to the basal FBS condition. At protein level observed by ICC, *SOX10* appeared cytoplasmic while *P75* expression was weak. Discrepancies between our results and those of Garcia-Ramirez and Gazarian, can be related to the fact that we used cultures from permanent teeth rather than deciduous teeth or periodontal ligament, as they did^{69,70}. We do not have evidence of epithelial or mesenchymal markers to correlate with our results. Nevertheless, the possibility of a switch in the role of *P75* from children to adult teeth would be interesting to investigate, as differences have been reported before from teeth at different ages^{164,165}. In contrast to *P75* and *SOX10*, our cells transferred to NCSCm presented an upregulation of the neural crest markers *AP2a*, *HNK-1* and *SNAIL1* when compared to the basal condition FBS. The NCSC expression pattern observed in our hDPC-FBS growing in NCSCm is not determinant, but could be attributed to a different state or transition of neural crest cells (i.e. pre-migratory, migratory or post-migratory neural crest cells)¹⁷⁶ or even an incomplete acquisition of the neural crest phenotype (lack of *SOX10* and *P75*). It would be necessary to test cells obtained from NCSCm in neural and glial differentiation protocols, and in specific models of nerve regeneration to evaluate their potential.

6.8. Summary

Overall, we have provided evidence of obtaining a neural crest-derived stem cell (NCSC) phenotype from hDPC cultures grown as neurospheres. hDPC BMP4-derived neurospheres seem to present an enhanced NCSCs signature in comparison to FBS and OSCFM spheres. Nevertheless, all hDPC-derived neurospheres were successful to generate spiral ganglion-like neurons in an *ex-vivo* model of auditory nerve regeneration, providing proof of concept of their regenerative potential for deafness treatments.

CHAPTER 7

“General discussion and future directions”

7. General discussion and future directions.

In the present work, we have expanded the evidence of establishing human dental pulp cultures. By providing detailed information for each sample used, we are able to present a broad picture of sample suitability. The importance of this, falls into the common questions relating dental pulp cells: are cells viable in older patients, can caries affect therapeutic potential, is any tooth suitable for stem cell extraction? Here, we have been able to support previous work suggesting that cultures can be established from a range of samples, including carious teeth and patients up to 60-years-old as described by others^{87,130,131,181}. We support the use of carious teeth as a source of viable hDPCs, samples of patients up to 37-years-old, and the use not only from third molars, but also from incisors (1, 5, 6). Together, we have shown the availability and accessibility of the samples in different situations, which resemble possible scenarios in proposed clinical settings, posing hDPCs as ideal for autologous cell therapies.

In the past, the ability of human dental pulp cells to differentiate into a variety of cell types including osteoblast, chondrocytes, adipocytes, neurons and Schwann cells has been shown^{5,89,91,143,182}. Furthermore, the neural crest origin of hDPCs has been cited as an advantageous trait for neurodegenerative disorders compared to other MSC sources¹²², and efforts to obtain neural crest-derived stem cells have gained importance in several adult stem cells sources that developed from the neural crest^{56,58,59}. In particular for hDPC, the observation that an intermediate population from the standard FBS condition is required for neural maturation^{88,90,154}, together with increasing reports obtaining NCSCs from other dental-derived stem cells^{64,69,70,72}, suggested that a neural crest or neurogenic population could be induced or enriched from human dental pulp cells from permanent teeth. We focused in obtaining such a subpopulation from the initial extraction and establishment of hDPC cultures. Importantly, we have been able to establish hDPC cultures in serum-free, neurogenic conditions as a method with increasing interest for translational research^{141,183}. Also, we established hDPC cultures in neurogenic media (OSCFM and BMP4) as a method to induce a neural progenitor or neural crest phenotype^{94,175}. Importantly, BMP4 has been shown to promote not only a neural crest phenotype, but also facilitate sensory neural

differentiation and spiral ganglion differentiation^{108,118,121,160,184}. Our results suggest an enhanced NCSCs phenotype from hDPC-OSCFM and hDPC-BMP4 cultures, but neuralisation seemed more evident in cultures from the latter. It must be considered that hDPC-BMP4 cultures had lowest culture establishment efficiency and also was the condition with the slowest growth. Hence, it is proposed that cultures grown on OSCFM under serum-free conditions could be supplemented with BMP4 before or during sphere aggregate formation in future experiments. In this way, hDPC cultures could be grown in a medium easily replaced with cGMP compliance and with an enhanced potential for sensory neural differentiation. Thus, we provide further evidence of the growth of human dental pulp cells under serum-free conditions, and propose their ability to grow under future cGMP conditions.

Regarding the feasibility of obtaining otic fates from human dental pulp cells, we attempted several ways to establish a neurogenic condition to favor the specific differentiation to auditory nerve cells from hDPC-FBS. The evidence presented in this thesis, suggests that Sonic Hedgehog is not the best inducer for neural differentiation in hDPCs. However, the several treatments used here (i.e. FGF3/10, BIO + BMP4, hFASC-CM, etc.) provided hints of hDPCs responsiveness to acquire an otic progenitor-like phenotype. This responsiveness should be tested further with other protocols capable of driving neural maturation, such as a recently reported protocol to obtain spiral ganglion neurons from hDPC¹⁵⁴. Furthermore, highly sensitive quantitative methods (i.e. Taqman PCR) should be used to allow discerning between the initial basal expression of neural related markers and the neural differentiated cells. The evidence presented in this thesis support for the the use of hDPCs for otic neural progenitor obtainment, and support the proposition that hDPCs hold a better potential than other non-neural crest-derived MSCs for this purpose^{43,44}.

Furthermore, our results suggest that the proposed neurogenic marker P75 might not be a good candidate for sensory neural differentiation, but rather it may support the differentiation towards other mesodermal cell fates, as suggested elsewhere^{163,164,167}. We have provided further evidence of the small percentage of P75^{+ve} subpopulation¹²², and

propose the contrasting hypothesis that the P75^{+ve} population under standard conditions is not neurogenic.

In terms of a neural crest-derived stem cell phenotype described in this thesis (hDPC-NCSCs), there are a small, but increasing number of reports describing hDPC-NCSCs from permanent teeth. One of these reports provided evidence of the feasibility of growing monolayer cultures in a similar medium conditions to our OSCFM medium (containing EGF and bFGF⁷⁴) and a recently published work describing the proliferation of hDPC-spheres expressing P75 and SOX10 markers¹⁸⁵. However, our results described here present a more comprehensive characterization of neural crest-derived stem cell markers in hDPCs. Additionally, we have also shown that monolayer cultures, although suitable for expansion, still result in heterogeneity and loss of NC markers with passage. In our work, driving sphere aggregation induced an overall enhanced NCSC signature in comparison to monolayer cultures. Hence, we report a suitable technique for obtaining NCSCs from human dental pulp cells from permanent teeth. Noteworthy, recent reports support the advantages of growing hDPC as sphere aggregates, describing advantages in comparison to monolayer cultures and enhanced multilineage differentiation. Together with our results, it is supported that 3D cultures, such as neurospheres, can provide more complexity and a better microenvironment in comparison to monolayer cultures¹⁸⁵⁻¹⁸⁷.

It would be important to further validate and compare our hDPC-NCSCs with other dental related NCSCs and importantly with *bona fide* neural crest cells (i.e. ESC-derived NCSCs) to contextualize the level of resemblance.

We have provided evidence of the ability of hDPCs to obtain a NCSCs phenotype and differentiate into neural-like cells. In this regard, many other authors have found similar results, even providing functional evidence^{88,90,131,154}. Nevertheless, the so-called potential for particular neurodegenerative disorders remain largely untested for hDPCs described and characterized as NCSCs. So far, the only example of a direct application of hDPC-NCSCs was described in an *in vivo* model for Parkinson disease⁹². The results obtained in this thesis

present the second example of a direct application for hDPC-NCSCs, providing proof of concept of their use for auditory nerve regeneration. To the best of our knowledge this is the first time that a human-derived, dental-related source described and characterised as NCSCs, has been used in a specific model of nerve regeneration: in this case the auditory nerve. We cannot leave behind the ground-breaking efforts of previous authors obtaining NCSC and mature neural cells from other neural crest-derived sources (including hDPCs), but it would be important to include evidence of their use in therapeutic models, that could in turn provide evidence and accelerate their translation to clinic^{186,188}.

CHAPTER 8

“Conclusions”

8. Conclusions

Based on our results we can conclude that:

- 1) Mouse dental pulp cells are neurogenic and heterogeneous. We did not detect any particular advantage of growing them in the pluripotent stem cell medium.
- 2) Human dental pulp tissue presents a putative perivascular stem cell niche labelled by STRO-1 and also express other markers such as GLI1, SOX10 and CELSR1, but no attributable feature to these markers can be implied.
- 3) Human dental pulp cell cultures can be established efficiently under standard conditions in the presence of serum, and also in serum-free conditions such as those used in OSCFM and BMP4. These should facilitate the translation to GMP quality standards. However, none of the conditions allowed homogeneous, stable cultures.
- 4) Teeth in different conditions can be used for culture establishment, supporting their use for autologous cell therapies.
- 5) Human dental pulp cells derived under the three main conditions explored in this Thesis (FBS, OSCFM and BMP4) were unable to neuralise when cultured with the auditory nerve maturation protocol, including Sonic Hedgehog and neurotrophins.
- 6) Human dental pulp cells acquired an incomplete Schwann cell differentiation with two differentiation protocols, but it is proposed that their basal state could be sufficient for neural trophic support.
- 7) Human dental pulp cells can become neural progenitor-like cells following treatment with FGF3/10 and by growing them in hFASC conditioned medium.
- 8) The P75 population from hDPCs doesn't reflect a neurogenic population, it is proposed that it is not sufficient as a single marker for a neurogenic population.
- 9) An enhanced neural crest-derived phenotype is observed by driving the cells to sphere aggregates. The hDPC-OSCFM and hDPC-BMP4 sphere cultures showed a better NCSC signature compared to hDPC-FBS sphere cultures.
- 10) hDPC-NCSC have been shown to obtain a neural-like phenotype and seemingly respond to cochlear explants in a relevant model of auditory nerve regeneration.
- 11) hDPC-NCSC spheres do not show evident signals of Schwann cell differentiation.

Overall, we have shown that human dental pulp cells could be used for auditory nerve regeneration under serum-free conditions when induced to a NCSCs phenotype (neurospheres). Our results invite us to propose the ability of these cells to be cultured under cGMP compliance and be used in clinical settings for the cure of deafness and other neurodegenerative disorders.

9. References

- 1 Rivolta, M. N. New strategies for the restoration of hearing loss: challenges and opportunities. *Br. Med. Bull.* **105**, 69-84, doi:10.1093/bmb/lds035 (2013).
- 2 Raphael, Y. Cochlear pathology, sensory cell death and regeneration. *Br. Med. Bull.* **63**, 25-38 (2002).
- 3 Okano, T. & Kelley, M. W. Stem Cell Therapy for the Inner Ear: Recent Advances and Future Directions. *Trends Amplif.* **16**, 4-18, doi:10.1177/1084713812440336 (2012).
- 4 Rivolta, M. N. Vol. 15 283-286 (2010).
- 5 Gronthos, S., Mankani, M., Brahimi, J., Robey, P. G. & Shi, S. Postnatal human dental pulp stem cells (DPSCs) in vitro and in vivo. *Proceedings of the National Academy of Sciences of the United States of America* **97**, 13625 (2000).
- 6 Karamzadeh, R. & Eslaminejad, B. (Regenerative medicine and tissue engineering, 2013).
- 7 Hudspeth, A. How the Ear's Works Work. *Nature* **341**, 397-397 (1989).
- 8 Stuart Ira, F. & Fox, S. I. *Human physiology*. 13th ed. edn, (New York : McGraw-Hill Higher Education ; London : McGraw-Hill distributor, 2013, 2013).
- 9 Dallos, P. THE ACTIVE COCHLEA. *J. Neurosci.* **12**, 4575-4585 (1992).
- 10 Fettiplace, R. & Carole, H. M. Vol. 7 19-29 (Nature, Nature Reviews Neuroscience, 2006).
- 11 Mathieu, M., Yann, N., Jérôme, S., Olivier, S. & Alexis Bozorg, G. Design, Kinematic Optimization, and Evaluation of a Teleoperated System for Middle Ear Microsurgery. *The Scientific World Journal* **2012**, doi:10.1100/2012/907372 (2012).
- 12 Scott, F. G. a. & Gilbert, S. F. *Developmental biology*. 10th edition. edn, (Sunderland, Massachusetts : Sinauer Associates, 2014, 2014).
- 13 Steventon, B., Mayor, R. & Streit, A. Neural crest and placode interaction during the development of the cranial sensory system. *Developmental Biology* **389**, 28-38, doi:10.1016/j.ydbio.2014.01.021 (2014).
- 14 Groves, A. K. & LaBonne, C. Setting appropriate boundaries: Fate, patterning and competence at the neural plate border. *Developmental Biology* **389**, 2-12, doi:10.1016/j.ydbio.2013.11.027 (2014).
- 15 Alvarez, Y. *et al.* Requirements for FGF3 and FGF10 during inner ear formation. *Development* **130**, 6329-6338, doi:10.1242/dev.00881 (2003).
- 16 Wright, T. J. & Mansour, S. L. Fgf3 and Fgf10 are required for mouse otic placode induction. *Development* **130**, 3379-3390, doi:10.1242/dev.00555 (2003).
- 17 Freter, S., Muta, Y., Mak, S.-S., Ladher, R. K. & Rinkwitz, S. Progressive restriction of otic fate: The role of FGF and Wnt in resolving inner ear potential. *Development* **135**, 3415-3424, doi:10.1242/dev.026674 (2008).
- 18 Bok, J., Bronner-Fraser, M. & Wu, D. K. Role of the hindbrain in dorsoventral but not anteroposterior axial specification of the inner ear. *Development (Cambridge, England)* **132**, 2115, doi:10.1242/dev.01796 (2005).

- 19 Riccomagno, M. M., Martinu, L., Mulheisen, M., Wu, D. K. & Epstein, D. J. Specification of the mammalian cochlea is dependent on Sonic hedgehog. *Genes & development* **16**, 2365, doi:10.1101/gad.1013302 (2002).
- 20 Ma, Q., Chen, Z., Barrantes, I. D. B., Luis de La Pompa, J. & Anderson, D. J. neurogenin1 is Essential for the Determination of Neuronal Precursors for Proximal Cranial Sensory Ganglia. *Neuron* **20**, 469-482, doi:10.1016/S0896-6273(00)80988-5 (1998).
- 21 Ma, Q., Anderson, D. J. & Fritsch, B. Neurogenin 1 Null Mutant Ears Develop Fewer, Morphologically Normal Hair Cells in Smaller Sensory Epithelia Devoid of Innervation. *Journal of the Association for Research in Otolaryngology* **1**, 129-143, doi:10.1007/s101620010017 (2000).
- 22 Chen, J. & Streit, A. Induction of the inner ear: Stepwise specification of otic fate from multipotent progenitors. *Hearing Research* **297**, doi:10.1016/j.heares.2012.11.018 (2012).
- 23 Strauer, B. E. & Kornowski, R. Stem cell therapy in perspective. *Circulation* **107**, 929 (2003).
- 24 Tannishtha, R., Sean, J. M., Michael, F. C. & Irving, L. W. Stem cells, cancer, and cancer stem cells. *Nature* **414**, 105, doi:10.1038/35102167 (2001).
- 25 Pera, M. F., Reubinoff, B. & Trounson, A. Human embryonic stem cells. *Journal of Cell Science* **113**, 5-10 (2000).
- 26 Trounson, A. & Pera, M. Vol. 76 660-661 (2001).
- 27 Keisuke, O. *et al.* A more efficient method to generate integration-free human iPS cells. *Nature Methods* **8**, 409, doi:10.1038/nmeth.1591 (2011).
- 28 Takahashi, K. & Yamanaka, S. Induction of Pluripotent Stem Cells from Mouse Embryonic and Adult Fibroblast Cultures by Defined Factors. *Cell* **126**, 663-676, doi:10.1016/j.cell.2006.07.024 (2006).
- 29 Yamanaka, S. Induced Pluripotent Stem Cells: Past, Present, and Future. *Cell Stem Cell*, doi:10.1016/j.stem.2012.05.005.
- 30 Oshima, K. *et al.* Mechanosensitive Hair Cell-like Cells from Embryonic and Induced Pluripotent Stem Cells. *Cell* **141**, 704-716, doi:10.1016/j.cell.2010.03.035 (2010).
- 31 Chen, W. *et al.* Restoration of auditory evoked responses by human ES-cell-derived otic progenitors. *Nature* **490**, 278-282, doi:10.1038/nature11415 (2012).
- 32 Chen, W. *et al.* Human Fetal Auditory Stem Cells Can Be Expanded In Vitro and Differentiate Into Functional Auditory Neurons and Hair Cell-Like Cells. *Stem Cells* **27**, 1196-1204, doi:10.1002/stem.62 (2009).
- 33 Koehler, K. R. *et al.* Generation of inner ear organoids with functional hair cells from human pluripotent stem cells. *Nature biotechnology* **35**, doi:10.1038/nbt.3840 (2017).
- 34 DeJonge, R. E. *et al.* Modulation of Wnt Signaling Enhances Inner Ear Organoid Development in 3D Culture. *PLoS ONE*, doi:10.1371/journal.pone.0162508 (2016).
- 35 Dominici, M. *et al.* Minimal criteria for defining multipotent mesenchymal stromal cells. The International Society for Cellular Therapy position statement. *Cytotherapy*, 2006, Vol.8(4), p.315-317 **8**, 315-317, doi:10.1080/14653240600855905 (2006).

- 36 Horwitz, E. *et al.* Clarification of the nomenclature for MSC: The International Society for Cellular Therapy position statement. *Cytotherapy*, 2005, Vol.7(5), p.393-395 **7**, 393-395, doi:10.1080/14653240500319234 (2005).
- 37 Cho, H.-H., Jang, S., Cho, Y.-B., Park, J.-S. & Jeong, H.-S. Functional neural differentiation of human adipose tissue- derived stem cells using bFGF and forskolin. *BMC Cell Biology* **11**, 25, doi:10.1186/1471-2121-11-25 (2010).
- 38 Dezawa, M., Takahashi, I., Esaki, M., Takano, M. & Sawada, H. Sciatic nerve regeneration in rats induced by transplantation of in vitro differentiated bone-marrow stromal cells. *European Journal of Neuroscience* **14**, 1771-1776, doi:10.1046/j.0953-816x.2001.01814.x (2001).
- 39 Koide, Y. *et al.* Two distinct stem cell lineages in murine bone marrow. *Stem Cells* **25**, 1213-1221, doi:10.1634/stemcells.2006-0325 (2007).
- 40 Pittenger, M. F. *et al.* Multilineage potential of adult human mesenchymal stem cells. *Science* **284**, 143-147 (1999).
- 41 Kaewkhaw, R., Scutt, A. M. & Haycock, J. W. Anatomical Site Influences the Differentiation of Adipose- Derived Stem Cells for Schwann- Cell Phenotype and Function. *Glia* **59**, 734-749, doi:10.1002/glia.21145 (2011).
- 42 Lindner, U., Kramer, J., Rohwedel, J. & Schlenke, P. in *Transfus. Med. Hemother.* Vol. 37 75-83 (2010).
- 43 Jeon, S.-J., Oshima, K., Heller, S. & Edge, A. S. B. Bone marrow mesenchymal stem cells are progenitors in vitro for inner ear hair cells. *Molecular and Cellular Neuroscience* **34**, 59-68, doi:10.1016/j.mcn.2006.10.003 (2007).
- 44 Boddy, L. S. *et al.* Vol. 7 1-11 (Regen. Med., 2012).
- 45 Jang, S. *et al.* Neural- Induced Human Mesenchymal Stem Cells Promote Cochlear Cell Regeneration in Deaf Guinea Pigs. *Clin. Exp. Otorhinolaryngol.* **8**, 83-91, doi:10.3342/ceo.2015.8.2.83 (2015).
- 46 Fu, Y. *et al.* Trophic Effects of Mesenchymal Stem Cells in Tissue Regeneration. *Tissue Engineering Part B: Reviews* **23**, 515-528, doi:10.1089/ten.teb.2016.0365 (2017).
- 47 Fetoni, A. R. *et al.* Grafting and Early Expression of Growth Factors from Adipose-Derived Stem Cells Transplanted into the Cochlea, in a Guinea Pig Model of Acoustic Trauma. *Frontiers in Cellular Neuroscience* **8**, doi:10.3389/fncel.2014.00334 (2014).
- 48 Jang, S. *et al.* Transplantation of human adipose tissue- derived stem cells for repair of injured spiral ganglion neurons in deaf guinea pigs. *Neural Regeneration Research* **11**, 994-1000, doi:10.4103/1673-5374.184503 (2016).
- 49 Crane, J. F. & Trainor, P. A. Neural Crest Stem and Progenitor Cells. **22**, 267-286, doi:10.1146/annurev.cellbio.22.010305.103814 (2006).
- 50 Nagoshi, N. *et al.* Ontogeny and Multipotency of Neural Crest-Derived Stem Cells in Mouse Bone Marrow, Dorsal Root Ganglia, and Whisker Pad. *Cell Stem Cell* **2**, 392-403, doi:10.1016/j.stem.2008.03.005 (2008).
- 51 Kikuchi, M. *et al.* Neural crest- derived multipotent cells in the adult mouse iris stroma. *Genes to Cells* **16**, 273-281, doi:10.1111/j.1365-2443.2011.01485.x (2011).
- 52 Janebodin, K. *et al.* Isolation and Characterization of Neural Crest- Derived Stem Cells from Dental Pulp of Neonatal Mice. *PLoS One* **6**, doi:10.1371/journal.pone.0027526 (2011).

- 53 Locher, H. *et al.* Hair follicle bulge cultures yield class III β - tubulin- positive melanogial cells. *Histochem Cell Biol* **144**, 87-91, doi:10.1007/s00418-015-1312-8 (2015).
- 54 Widera, D. *et al.* Schwann cells can be reprogrammed to multipotency by culture. *Stem Cells and Development* **20**, 2053-2064, doi:10.1089/scd.2010.0525 (2011).
- 55 Bressan, R. B. *et al.* EGF– FGF2 stimulates the proliferation and improves the neuronal commitment of mouse epidermal neural crest stem cells (EPI-NCSCs). *Experimental Cell Research* **327**, 37-47, doi:10.1016/j.yexcr.2014.05.020 (2014).
- 56 Widera, D. *et al.* Adult Palatum as a Novel Source of Neural Crest-Related Stem Cells. *STEM CELLS* **27**, 1899-1910, doi:10.1002/stem.104 (2009).
- 57 Kaku, M. *et al.* Identification and characterization of neural crest- derived cells in adult periodontal ligament of mice. *Archives of Oral Biology* **57**, 1668-1675, doi:10.1016/j.archoralbio.2012.04.022 (2012).
- 58 Hauser, S. *et al.* Isolation of Novel Multipotent Neural Crest- Derived Stem Cells from Adult Human Inferior Turbinate. *Stem Cells and Development* **21**, 742-756, doi:10.1089/scd.2011.0419 (2012).
- 59 Clewes, O. *et al.* Human Epidermal Neural Crest Stem Cells (hEPI-NCSC)— Characterization and Directed Differentiation into Osteocytes and Melanocytes. *Stem Cell Rev and Rep* **7**, 799-814, doi:10.1007/s12015-011-9255-5 (2011).
- 60 Timo, S. *et al.* Neuronal differentiation of hair- follicle-bulge-derived stem cells co-cultured with mouse cochlear modiolus explants. *PLoS ONE* **12**, e0187183, doi:10.1371/journal.pone.0187183.
- 61 Fawzy El-Sayed, K. M. & Dörfer, C. E. Gingival Mesenchymal Stem/ Progenitor Cells: A Unique Tissue Engineering Gem. *Stem Cells International* **2016**, doi:10.1155/2016/7154327 (2016).
- 62 Zhang, Q. *et al.* Mesenchymal stem cells derived from human gingiva are capable of immunomodulatory functions and ameliorate inflammation- related tissue destruction in experimental colitis. *Journal of immunology (Baltimore, Md. : 1950)* **183**, 7787, doi:10.4049/jimmunol.0902318 (2009).
- 63 Tomar, G. B. *et al.* Human gingiva- derived mesenchymal stem cells are superior to bone marrow- derived mesenchymal stem cells for cell therapy in regenerative medicine. *Biochemical and Biophysical Research Communications* **393**, 377-383, doi:10.1016/j.bbrc.2010.01.126 (2010).
- 64 Fournier, B. P. *et al.* Characterisation of human gingival neural crest-derived stem cells in monolayer and neurosphere cultures. *European Cells and Materials* **31**, 40-58 (2016).
- 65 Zhang, Q. *et al.* Neural Crest Stem- Like Cells Non-genetically Induced from Human Gingiva-Derived Mesenchymal Stem Cells Promote Facial Nerve Regeneration in Rats. *Molecular Neurobiology*, 1-19, doi:10.1007/s12035-018-0913-3 (2018).
- 66 Seo, B.-M. *et al.* Investigation of multipotent postnatal stem cells from human periodontal ligament. *The Lancet* **364**, 149-155, doi:10.1016/S0140-6736(04)16627-0 (2004).

- 67 Coura, G. S. *et al.* Human periodontal ligament: a niche of neural crest stem cells. *Journal of Periodontal Research* **43**, 531-536, doi:10.1111/j.1600-0765.2007.01065.x (2008).
- 68 Pelaez, D., Huang, C.-Y. C. & Cheung, H. S. Isolation of pluripotent neural crest-derived stem cells from adult human tissues by connexin-43 enrichment. *Stem cells and development* **22**, 2906, doi:10.1089/scd.2013.0090 (2013).
- 69 Ramírez-García, L., Cevallos, R. & Gazarian, K. Unveiling and initial characterization of neural crest- like cells in mesenchymal populations from the human periodontal ligament. *Journal of Periodontal Research* **52**, 609-616, doi:10.1111/jre.12429 (2017).
- 70 Karlen, G. G. & Luis, R. R.-G. Human Deciduous Teeth Stem Cells (SHED) Display Neural Crest Signature Characters. *PLoS ONE* **12**, e0170321, doi:10.1371/journal.pone.0170321.
- 71 Degistirici, Ö. *et al.* Defining properties of neural crest- derived progenitor cells from the apex of human developing tooth. *Tissue Engineering - Part A*. **14**, 317-330, doi:10.1089/tea.2007.0221 (2008).
- 72 Abe, S., Hamada, K., Miura, M. & Yamaguchi, S. Neural crest stem cell property of apical pulp cells derived from human developing tooth. *Cell Biology International* **36**, 927-936, doi:10.1042/CBI20110506 (2012).
- 73 Shi, S. & Gronthos, S. Perivascular niche of postnatal mesenchymal stem cells in human bone marrow and dental pulp. *Journal of Bone and Mineral Research* **18**, 696-704 (2003).
- 74 Al-Zer, H. *et al.* Enrichment and Schwann Cell Differentiation of Neural Crest-derived Dental Pulp Stem Cells. *In Vivo* **29**, 319-326 (2015).
- 75 Thesleff, I. & Hurmerinta, K. Vol. 18 75-88 (Oxford, UK, 1981).
- 76 Ruch, J. V., Lesot, H. & Begue-Kirn, C. Odontoblast differentiation. *International Journal of Developmental Biology* **39**, 51-68 (1995).
- 77 Koussoulakou, D., Margaritis, L. & Koussoulakos, S. A Curriculum Vitae of Teeth: Evolution, Generation, Regeneration. *International Journal of Biological Sciences* **5**, 226-243 (2009).
- 78 Catón, J. & Tucker, A. S. Vol. 214 502-515 (2009).
- 79 Koussoulakou, D. S., Margaritis, L. H. & Koussoulakos, S. L. Vol. 5 226-243 (2009).
- 80 Tucker, A. & Sharpe, P. Vol. 5 499 (Nature reviews genetics, 2004).
- 81 Keranen, S. V. E., Kettunen, P., Aberg, T., Thesleff, I. & Jernvall, J. Gene expression patterns associated with suppression of odontogenesis in mouse and vole diastema regions. *Dev. Genes Evol.* **209**, 495-506 (1999).
- 82 Bei, M. & Maas, R. FGFs and BMP4 induce both Msx1- independent and Msx1- dependent signaling pathways in early tooth development. *Development* **125**, 4325-4333 (1998).
- 83 Maas, R. & Bei, M. Vol. 8 4-39 (1997).
- 84 Ohazama, A., Tucker, A. & Sharpe, P. T. Organized tooth- specific cellular differentiation stimulated by BMP4. *J. Dent. Res.* **84**, 603-606 (2005).
- 85 Antonio, N. & Nanci, A. *Ten Cate's oral histology : development, structure, and function*. 8th ed. / Antonio Nanci. edn, (St. Louis, Mo. : Elsevier, c2013, 2013).

- 86 Masako, M. *et al.* SHED: Stem cells from human exfoliated deciduous teeth. *Proceedings of the National Academy of Sciences of the United States of America* **100**, 5807, doi:10.1073/pnas.0937635100 (2003).
- 87 Atari, M. *et al.* Dental pulp of the third molar: a new source of pluripotent-like stem cells. *J. Cell Sci.* **125**, 3343-3356, doi:10.1242/jcs.096537 (2012).
- 88 Király, M. *et al.* Simultaneous PKC and cAMP activation induces differentiation of human dental pulp stem cells into functionally active neurons. *Neurochemistry International* **55**, 323-332, doi:10.1016/j.neuint.2009.03.017 (2009).
- 89 Gervois, P. *et al.* Neurogenic Maturation of Human Dental Pulp Stem Cells Following Neurosphere Generation Induces Morphological and Electrophysiological Characteristics of Functional Neurons. *Stem Cells and Development* **24**, 296-311, doi:10.1089/scd.2014.0117 (2015).
- 90 Arthur, A., Rychkov, G., Shi, S., Koblar, S. A. & Gronthos, S. Adult human dental pulp stem cells differentiate toward functionally active neurons under appropriate environmental cues. *Stem Cells* **26**, 1787-1795, doi:10.1634/stemcells.2007-0979 (2008).
- 91 Martens, W. *et al.* Human dental pulp stem cells can differentiate into Schwann cells and promote and guide neurite outgrowth in an aligned tissue- engineered collagen construct in vitro. *FASEB journal : official publication of the Federation of American Societies for Experimental Biology* **28**, 1634, doi:10.1096/fj.13-243980 (2014).
- 92 Fujii, H. *et al.* Dopaminergic differentiation of stem cells from human deciduous teeth and their therapeutic benefits for Parkinsonian rats. *Brain Research* **1613**, 59-72, doi:10.1016/j.brainres.2015.04.001 (2015).
- 93 Ferro, F., Spelat, R., Beltrami, A. P., Cesselli, D. & Curcio, F. Isolation and Characterization of Human Dental Pulp Derived Stem Cells by Using Media Containing Low Human Serum Percentage as Clinical Grade Substitutes for Bovine Serum (HS and FBS Media and Adult Stem Cells). **7**, e48945, doi:10.1371/journal.pone.0048945 (2012).
- 94 Jung, J., Kim, J.-W., Moon, H.-J., Hong, J. Y. & Hyun, J. K. Characterization of Neurogenic Potential of Dental Pulp Stem Cells Cultured in Xeno/ Serum- Free Condition: and Assessment. *Stem Cells International* **2016**, doi:10.1155/2016/6921097 (2016).
- 95 Bakopoulou, A. *et al.* Isolation and prolonged expansion of oral mesenchymal stem cells under clinical- grade, GMP- compliant conditions differentially affects "stemness" properties. *Stem cell research & therapy* **8**, 247, doi:10.1186/s13287-017-0705-0 (2017).
- 96 Anitua, E., Troya, M. & Zalduendo, M. Progress in the use of dental pulp stem cells in regenerative medicine. *Cytotherapy*, doi:10.1016/j.jcyt.2017.12.011 (2018).
- 97 Gabsang, L. *et al.* Isolation and directed differentiation of neural crest stem cells derived from human embryonic stem cells. *Nature Biotechnology* **25**, doi:10.1038/nbt1365 (2007).
- 98 Parker, M., Brugeaud, A. & Edge, A. Primary Culture and Plasmid Electroporation of the Murine Organ of Corti. *Journal of Visualized Experiments: JoVE* (2010).

- 99 Feng, J., Mantesso, A., De Bari, C., Nishiyama, A. & Sharpe, P. Dual origin of mesenchymal stem cells contributing to organ growth and repair. *Proc. Natl. Acad. Sci. U. S. A.* **108**, 6503-6508, doi:10.1073/pnas.1015449108 (2011).
- 100 Kaukua, N. *et al.* Glial origin of mesenchymal stem cells in a tooth model system. *Nature* **513**, 551+, doi:10.1038/nature13536 (2014).
- 101 Sharpe, P. in *Development* Vol. 143 2273-2280 (2016).
- 102 Zhao, H. *et al.* Secretion of Shh by a Neurovascular Bundle Niche Supports Mesenchymal Stem Cell Homeostasis in the Adult Mouse Incisor. *Cell Stem Cell* **14**, 160-173, doi:10.1016/j.stem.2013.12.013 (2014).
- 103 Nakatsuka, R. *et al.* 5-Aza-2'-deoxycytidine treatment induces skeletal myogenic differentiation of mouse dental pulp stem cells. *Archives of Oral Biology* **55**, 350-357, doi:10.1016/j.archoralbio.2010.03.003 (2010).
- 104 Murdoch, B., DelConte, C. & García-Castro, M. I. Pax7 Lineage Contributions to the Mammalian Neural Crest (The Pax7 Lineage in the Neural Crest). *PLoS ONE* **7**, e41089, doi:10.1371/journal.pone.0041089 (2012).
- 105 Sambasivan, R. *et al.* Distinct Regulatory Cascades Govern Extraocular and Pharyngeal Arch Muscle Progenitor Cell Fates. *Developmental Cell* **16**, 810-821, doi:10.1016/j.devcel.2009.05.008 (2009).
- 106 Wang, L., Liu, Y., Li, S., Long, Z. & Wu, Y. Wnt signaling pathway participates in valproic acid-induced neuronal differentiation of neural stem cells. *Int. J. Clin. Exp. Pathol.* **8**, 578-585 (2015).
- 107 Lange, C. *et al.* Small molecule GSK-3 inhibitors increase neurogenesis of human neural progenitor cells. *Neuroscience Letters* **488**, 36-40, doi:10.1016/j.neulet.2010.10.076 (2011).
- 108 Weber, M. *et al.* Alternative Generation of CNS Neural Stem Cells and PNS Derivatives from Neural Crest-Derived Peripheral Stem Cells. *STEM CELLS* **33**, 574-588, doi:10.1002/stem.1880 (2015).
- 109 Nakatsuka, R. *et al.* 5-Aza-2'-deoxycytidine treatment induces skeletal myogenic differentiation of mouse dental pulp stem cells. *Arch. Oral Biol.* **55**, 350-357, doi:10.1016/j.archoralbio.2010.03.003 (2010).
- 110 Brian, E. G., Purudappa, P. P. & Yun-Feng, L. Multilineage Differentiation of Dental Pulp Stem Cells from Green Fluorescent Protein Transgenic Mice. *International Journal of Oral Science* **2**, 21, doi:10.4248/IJOS10015 (2010).
- 111 Ellis, K. M., Carroll, D. C., Lewis, M. D., Rychkov, G. Y. & Koblar, S. A. Neurogenic potential of dental pulp stem cells isolated from murine incisors. *Acta Veterinaria Scandinavica*, 30, doi:10.1186/scrt419 (2014).
- 112 Balic, A., Aguila, H. L., Caimano, M. J., Francone, V. P. & Mina, M. Characterization of stem and progenitor cells in the dental pulp of erupted and unerupted murine molars. *Bone* **46**, 1639-1651, doi:10.1016/j.bone.2010.02.019 (2010).
- 113 Breyer, A. *et al.* Multipotent adult progenitor cell isolation and culture procedures. *Experimental Hematology* **34**, 1596-1601, doi:10.1016/j.exphem.2006.07.013 (2006).
- 114 Nosrat, I. V., Widenfalk, J., Olson, L. & Nosrat, C. A. Dental Pulp Cells Produce Neurotrophic Factors, Interact with Trigeminal Neurons in Vitro, and Rescue

- Motoneurons after Spinal Cord Injury. *Developmental Biology* **238**, 120-132, doi:10.1006/dbio.2001.0400 (2001).
- 115 Nosrat, I., Seiger, A., Olson, L. & Nosrat, C. A. Expression patterns of neurotrophic factor mRNAs in developing human teeth. *Cell Tissue Res.* **310**, 177-187, doi:10.1007/s00441-002-0618-8 (2002).
- 116 Young, F. I. *et al.* Clonal Heterogeneity in the Neuronal and Glial Differentiation of Dental Pulp Stem/ Progenitor Cells. *Stem Cells International* **2016**, doi:10.1155/2016/1290561 (2016).
- 117 Kikuchi, M. *et al.* Neural crest- derived multipotent cells in the adult mouse iris stroma. *Genes to cells : devoted to molecular & cellular mechanisms* **16**, 273, doi:10.1111/j.1365-2443.2011.01485.x (2011).
- 118 Shi, F., Corrales, C. E., Liberman, M. C. & Edge, A. BMP4 induction of sensory neurons from human embryonic stem cells and reinnervation of sensory epithelium. *Eur. J. Neurosci.* **26**, 3016-3023, doi:10.1111/j.1460-9568.2007.05909.x (2007).
- 119 Luo, L. H. *et al.* in *Stem Cells Int.* Vol. 2018 (2018).
- 120 Sugimura, R. *et al.* Noncanonical Wnt Signaling Maintains Hematopoietic Stem Cells in the Niche. *Cell* **150**, 351-365, doi:10.1016/j.cell.2012.05.041 (2012).
- 121 Mimura, S. *et al.* Bone morphogenetic protein 4 promotes craniofacial neural crest induction from human pluripotent stem cells. *International journal of developmental biology* **60**, 21-28, doi:10.1387/ijdb.160040mk (2016).
- 122 Pan, W. *et al.* Characterization of p75 neurotrophin receptor expression in human dental pulp stem cells. *International Journal of Developmental Neuroscience* **53**, 90-98, doi:10.1016/j.ijdevneu.2016.07.007 (2016).
- 123 Yu, J. H. *et al.* Differentiation potential of STRO- 1(+) dental pulp stem cells changes during cell passaging. *BMC CELL BIOLOGY* **11**, doi:10.1186/1471-2121-11-32 (2010).
- 124 Nishimura, K., Weichert, R. M., Liu, W., Davis, R. L. & Dabdoub, A. Generation of induced neurons by direct reprogramming in the mammalian cochlea. *Neuroscience* **275**, 125-135, doi:10.1016/j.neuroscience.2014.05.067 (2014).
- 125 Thomas, V. *et al.* Direct conversion of fibroblasts to functional neurons by defined factors. *Nature* **463**, 1035, doi:10.1038/nature08797 (2010).
- 126 Perry, B. *et al.* Collection, Cryopreservation, and Characterization of Human Dental Pulp- Derived Mesenchymal Stem Cells for Banking and Clinical Use. *Tissue Engineering Part C: Methods* **14**, 149-156, doi:10.1089/ten.tec.2008.0031 (2008).
- 127 Ji-Hyun, J. *et al.* In vitro characterization of human dental pulp stem cells isolated by three different methods. *Restorative Dentistry & Endodontics* **41**, 283-295, doi:10.5395/rde.2016.41.4.283 (2016).
- 128 Kanafi, M. M., Pal, R. & Gupta, P. K. Phenotypic and functional comparison of optimum culture conditions for upscaling of dental pulp stem cells. *Cell Biology International* **37**, 126-136, doi:10.1002/cbin.10021 (2013).
- 129 Magnucki, G. *et al.* Expression of the IGF- 1, IGFBP- 3 and IGF- 1 receptors in dental pulp stem cells and impacted third molars. *Journal of oral science* **55**, 319, doi:10.2334/josnusd.55.319 (2013).
- 130 Werle, S. *et al.* Carious deciduous teeth are a potential source for dental pulp stem cells. *Clinical Oral Investigations* **20**, 75-81, doi:10.1007/s00784-015-1477-5 (2016).

- 131 Gnanasegaran, N., Govindasamy, V. & Abu Kasim, N. H. Differentiation of stem cells derived from carious teeth into dopaminergic- like cells. *International Endodontic Journal* **49**, 937-949, doi:10.1111/iej.12545 (2016).
- 132 Shi, Y. *et al.* Comparative Analysis of Proliferation and Differentiation Potentials of Stem Cells from Inflamed Pulp of Deciduous Teeth and Stem Cells from Exfoliated Deciduous Teeth. *BioMed Research International* **2014**, doi:10.1155/2014/930907 (2014).
- 133 Martens, W. *et al.* Expression Pattern of Basal Markers in Human Dental Pulp Stem Cells and Tissue. *Cells Tissues Organs* **196**, 490-500, doi:10.1159/000338654 (2012).
- 134 Lizier, N. F. *et al.* Scaling- Up of Dental Pulp Stem Cells Isolated from Multiple Niches (Scaling- Up of Dental Pulp Stem Cells). *PLoS ONE* **7**, e39885, doi:10.1371/journal.pone.0039885 (2012).
- 135 Feng, J. *et al.* BMP signaling orchestrates a transcriptional network to control the fate of mesenchymal stem cells in mice. *Development (Cambridge, England)* **144**, 2560, doi:10.1242/dev.150136 (2017).
- 136 Yoshiba, N. *et al.* Immunohistochemical analysis of two stem cell markers of α -smooth muscle actin and STRO- 1 during wound healing of human dental pulp. *Histochemistry and Cell Biology* **138**, 583-592, doi:10.1007/s00418-012-0978-4 (2012).
- 137 Huang, G., Sonoyama, W., Chen, J. & Park, S. In vitro characterization of human dental pulp cells: various isolation methods and culturing environments. *Cell and Tissue Research* **324**, 225-236, doi:10.1007/s00441-005-0117-9 (2006).
- 138 Woods, E. J. *et al.* Optimized cryopreservation method for human dental pulp-derived stem cells and their tissues of origin for banking and clinical use. *Cryobiology* **59**, 150-157, doi:10.1016/j.cryobiol.2009.06.005 (2009).
- 139 Ducret, M. *et al.* Production of human dental pulp cells for cellularized biomaterials with a GMP approach. *Eur. Cells Mater.* **30**, 10-10 (2015).
- 140 Brigittealliot, L., Virginiebonnamain, Pascalhuet, Géraldinebienvenu & Jean, C. Human dental pulp stem cells cultured in serum- free supplemented medium. *Frontiers in Physiology* **4**, doi:10.3389/fphys.2013.00357 (2013).
- 141 Xiao, J., Yang, D., Li, Q., Tian, W. & Guo, W. The establishment of a chemically defined serum-free culture system for human dental pulp stem cells. *Stem Cell Research & Therapy* **9 (191)** (2018).
- 142 Mochizuki, M. & Nakahara, T. Establishment of xenogeneic serum- free culture methods for handling human dental pulp stem cells using clinically oriented in-vitro and in-vivo conditions. *Stem Cell Research and Therapy* **9**, <xocs:firstpage xmlns:xocs=""/>, doi:10.1186/s13287-017-0761-5 (2018).
- 143 Huang, A. H. C., Chen, Y. K., Lin, L. M., Shieh, T. Y. & Chan, A. W. S. Isolation and characterization of dental pulp stem cells from a supernumerary tooth. *Journal of Oral Pathology & Medicine* **37**, 571-574, doi:10.1111/j.1600-0714.2008.00654.x (2008).
- 144 Trubiani, O. *et al.* Expression Profile of the Embryonic Markers Nanog, OCT- 4, SSEA- 1, SSEA- 4, and Frizzled- 9 Receptor in Human Periodontal Ligament Mesenchymal Stem Cells. *J. Cell. Physiol.* **225**, 123-131, doi:10.1002/jcp.22203 (2010).

- 145 Ma, D. *et al.* Stathmin inhibits proliferation and differentiation of dental pulp stem cells via sonic hedgehog/ Gli. *Journal of cellular and molecular medicine*, doi:10.1111/jcmm.13621 (2018).
- 146 Majumdar, D., Kanafi, M., Bhonde, R., Gupta, P. & Datta, I. Differential Neuronal Plasticity of Dental Pulp Stem Cells From Exfoliated Deciduous and Permanent Teeth Towards Dopaminergic Neurons. *Journal of Cellular Physiology* **231**, 2048-2063, doi:10.1002/jcp.25314 (2016).
- 147 Vanesa, E.-E., Çağla, E. & Carlos, E.-A. IGF- I: A key growth factor that regulates neurogenesis and synaptogenesis from embryonic to adult stages of the brain. *Frontiers in Neuroscience* **10**, doi:10.3389/fnins.2016.00052 (2016).
- 148 Lv, T. *et al.* Insulin- like growth factor 1 promotes the proliferation and committed differentiation of human dental pulp stem cells through MAPK pathways. *Archives of Oral Biology* **72**, 116-123, doi:10.1016/j.archoralbio.2016.08.011 (2016).
- 149 Liu, P. *et al.* Effects of SOX2 on Proliferation, Migration and Adhesion of Human Dental Pulp Stem Cells: e0141346. *PLoS ONE* **10**, doi:10.1371/journal.pone.0141346 (2015).
- 150 Pisciotta, A. *et al.* Human Dental pulp stem cells (hDPSCs): isolation, enrichment and comparative differentiation of two sub-populations. *BMC Developmental Biology* **15**, doi:10.1186/s12861-015-0065-x (2015).
- 151 Zhang, W. B., Walboomers, X. F., Shi, S. T., Fan, M. W. & Jansen, J. A. Multilineage differentiation potential of stem cells derived from human dental pulp after cryopreservation. *Tissue Eng.* **12**, 2813-2823 (2006).
- 152 Diomedea, F. *et al.* Stemness Maintenance Properties in Human Oral Stem Cells after Long- Term Passage. *Stem Cells International* **2017**, doi:10.1155/2017/5651287 (2017).
- 153 Ma, M.-S., Boddeke, E. & Copray, S. (Stem Cell Rev. and Rep., 2014).
- 154 Gonmanee, T., Thonabulsombat, C., Vongsavan, K. & Sritanaudomchai, H. Differentiation of stem cells from human deciduous and permanent teeth into spiral ganglion neuron- like cells. *Archives of Oral Biology* **88**, 34-41, doi:10.1016/j.archoralbio.2018.01.011 (2018).
- 155 Yuanchao, X. *et al.* Sequential regulatory loops as key gatekeepers for neuronal reprogramming in human cells. *Nature Neuroscience* **19**, doi:10.1038/nn.4297 (2016).
- 156 Sanen, K. *et al.* Engineered neural tissue with Schwann cell differentiated human dental pulp stem cells: potential for peripheral nerve repair? *Journal of Tissue Engineering and Regenerative Medicine* (2017).
- 157 Dai, L.-G., Huang, G.-S. & Hsu, S.-H. Sciatic Nerve Regeneration by Cocultured Schwann Cells and Stem Cells on Microporous Nerve Conduits. *Cell Transplantation* **22**, 2029-2039, doi:10.3727/096368912X658953 (2013).
- 158 Nosrat, I. V., Widenfalk, J., Olson, L. & Nosrat, C. A. Dental pulp cells produce neurotrophic factors, interact with trigeminal neurons in vitro, and rescue motoneurons after spinal cord injury. *Dev. Biol.* **238**, 120-132 (2001).
- 159 Kolar, M. *et al.* The neurotrophic effects of different human dental mesenchymal stem cells. *Sci Rep* **7**, 12605-12605, doi:10.1038/s41598-017-12969-1 (2017).

- 160 Hackland, J. O. S. *et al.* Top-Down Inhibition of BMP Signaling Enables Robust
Induction of hPSCs Into Neural Crest in Fully Defined, Xeno-free Conditions. (2017).
- 161 Mimura, S. *et al.* Bone morphogenetic protein 4 promotes craniofacial neural crest
induction from human pluripotent stem cells. *Int. J. Dev. Biol.* **60**, 21-28,
doi:10.1387/ijdb.160040mk (2016).
- 162 Ewa, L., Danuta, J. & Marcin, M. Advantage of mesenchymal stem cells (MSC)
expansion directly from purified bone marrow CD105+ and CD271+ cells. *Folia
Histochemica et Cytobiologica* **46**, 307-314, doi:10.5603/4412 (2008).
- 163 Calabrese, G. *et al.* Potential Effect of CD271 on Human Mesenchymal Stromal Cell
Proliferation and Differentiation. *International Journal of Molecular Sciences* **16**,
15609-15624, doi:10.3390/ijms160715609 (2015).
- 164 Alvarez, R., Lee, H. L., Hong, C. & Wang, C. Y. Single CD271 marker isolates
mesenchymal stem cells from human dental pulp. *International journal of oral
science* **7**, 205-212, doi:10.1038/ijos.2015.29 (2015).
- 165 Mikami, Y. *et al.* CD271/ p75NTR Inhibits the Differentiation of Mesenchymal Stem
Cells into Osteogenic, Adipogenic, Chondrogenic, and Myogenic Lineages. *Stem Cells
and Development* **20**, 91-913, doi:10.1089/scd.2010.0299 (2011).
- 166 Alraies, A., Alaidaroos, N., Waddington, R., Moseley, R. & Sloan, A. Variation in
human dental pulp stem cell ageing profiles reflect contrasting proliferative and
regenerative capabilities. *BMC Cell Biology* **18**, doi:10.1186/s12860-017-0128-x
(2017).
- 167 Battula, V. L. *et al.* Isolation of functionally distinct mesenchymal stem cell subsets
using antibodies against CD56, CD271, and mesenchymal stem cell antigen- 1.
Haematologica **94**, 173, doi:10.3324/haematol.13740 (2009).
- 168 Govindasamy, V. *et al.* Inherent Differential Propensity of Dental Pulp Stem Cells
Derived from Human Deciduous and Permanent Teeth. *Journal of Endodontics* **36**,
1504-1515, doi:10.1016/j.joen.2010.05.006 (2010).
- 169 Martin, I. *et al.* Generation of Schwann Cell- Derived Multipotent Neurospheres
Isolated from Intact Sciatic Nerve. *Stem Cell Rev. Rep.* **8**, 1178-1187,
doi:10.1007/s12015-012-9387-2 (2012).
- 170 Thomas, S. *et al.* Human neural crest cells display molecular and phenotypic
hallmarks of stem cells. *Human Molecular Genetics* **17**, 3411-3425,
doi:10.1093/hmg/ddn235 (2008).
- 171 Betters, E., Liu, Y., Kjaeldgaard, A., Sundström, E. & García-Castro, M. I. Analysis of
early human neural crest development. *Developmental Biology* **344**, 578-592,
doi:10.1016/j.ydbio.2010.05.012 (2010).
- 172 Laura, M., Tatiana, A. Y., Parker, B. A. & Stephen, D. Wnt signaling and a Smad
pathway blockade direct the differentiation of human pluripotent stem cells to
multipotent neural crest cells. *Proceedings of the National Academy of Sciences* **108**,
19240, doi:10.1073/pnas.1113746108 (2011).
- 173 Ting, L., Young-Hoon, L., Jean-Pierre, S.-J. & Thomas, D. S. Induction of neural crest
in *Xenopus* by transcription factor AP2 α . *Proceedings of the National Academy of
Sciences of the United States of America* **100**, 532, doi:10.1073/pnas.0237226100
(2003).

- 174 Müller, J. *et al.* Intrastratial Transplantation of Adult Human Neural Crest- Derived Stem Cells Improves Functional Outcome in Parkinsonian Rats. *STEM CELLS Translational Medicine* **4**, 31-43, doi:10.5966/sctm.2014-0078 (2015).
- 175 Peng T *et al.* BMP4: a Possible Key Factor in Differentiation of Auditory Neuron-Like Cells from Bone-Derived Mesenchymal Stromal Cells. *Clin Lab* **61(9)**, 1171-1178 (2015).
- 176 Noisa, P. *et al.* Notch signaling regulates the differentiation of neural crest from human pluripotent stem cells. *Journal of cell science* **127**, 2083, doi:10.1242/jcs.145755 (2014).
- 177 Tong, M., Brugeaud, A. & Edge, A. Regenerated Synapses Between Postnatal Hair Cells and Auditory Neurons. *Journal of the Association for Research in Otolaryngology* **14**, 321-329, doi:10.1007/s10162-013-0374-3 (2013).
- 178 Nayagam, B. A. *et al.* An In Vitro Model of Developmental Synaptogenesis Using Cocultures of Human Neural Progenitors and Cochlear Explants. *Stem Cells and Development* **22**, 91-912, doi:10.1089/scd.2012.0082 (2013).
- 179 Gunewardene, N., Crombie, D., Dottori, M. & Nayagam, B. A. Innervation of Cochlear Hair Cells by Human Induced Pluripotent Stem Cell- Derived Neurons. *Stem Cells International* **2016**, doi:10.1155/2016/1781202 (2016).
- 180 McLean, W., Smith, K., Glowatzki, E. & Pyott, S. Distribution of the Na, K- ATPase α Subunit in the Rat Spiral Ganglion and Organ of Corti. *Journal of the Association for Research in Otolaryngology* **10**, 37-49, doi:10.1007/s10162-008-0152-9 (2009).
- 181 Kellner, M. *et al.* Differences of isolated dental stem cells dependent on donor age and consequences for autologous tooth replacement. *Archives of Oral Biology* **59**, 559-567, doi:10.1016/j.archoralbio.2014.02.014 (2014).
- 182 Osathanon, T., Sawangmake, C., Nowwarote, N. & Pavasant, P. Neurogenic differentiation of human dental pulp stem cells using different induction protocols. *Oral Diseases* **20**, 352-358, doi:10.1111/odi.12119 (2014).
- 183 Pisciotta , A. *et al.* Establishment of xenogeneic serum-free culture methods for handling human dental pulp stem cells using clinically oriented in-vitro and in-vivo conditions. *Front. Physiol.* **9** (2018).
- 184 Gooyit, M. *et al.* A Chemical Biological Strategy to Facilitate Diabetic Wound Healing. *ACS Chemical Biology*, 130926121023004, doi:10.1021/cb4005468 (2013).
- 185 Pisciotta, A. *et al.* Use of a 3D Floating Sphere Culture System to Maintain the Neural Crest- Related Properties of Human Dental Pulp Stem Cells. *Front. Physiol.* **9**, doi:10.3389/fphys.2018.00547 (2018).
- 186 Li, X., Ide, R., Saiki, C., Kumazawa, Y. & Okamura, H. Human Dental Pulp Cells Differentiate toward Neuronal Cells and Promote Neuroregeneration in Adult Organotypic Hippocampal Slices In Vitro. *International Journal of Molecular Sciences* **18**, 1745, doi:10.3390/ijms18081745 (2017).
- 187 Xiao, L. & Tsutsui, T. Characterization of human dental pulp cells- derived spheroids in serum- free medium: Stem cells in the core. *Journal of Cellular Biochemistry* **114**, 2624-2636, doi:10.1002/jcb.24610 (2013).
- 188 Kabatas, S., CSCivelek, E & Yilmaz, I. K., A Yilmaz, C Akyuva, Y Karaoz, E. Neuronal regeneration in injured rat spinal cord after human

dental pulp derived neural crest stem cell transplantation. *Bratisl Med* **119** (2018).

10. Supplementary information.

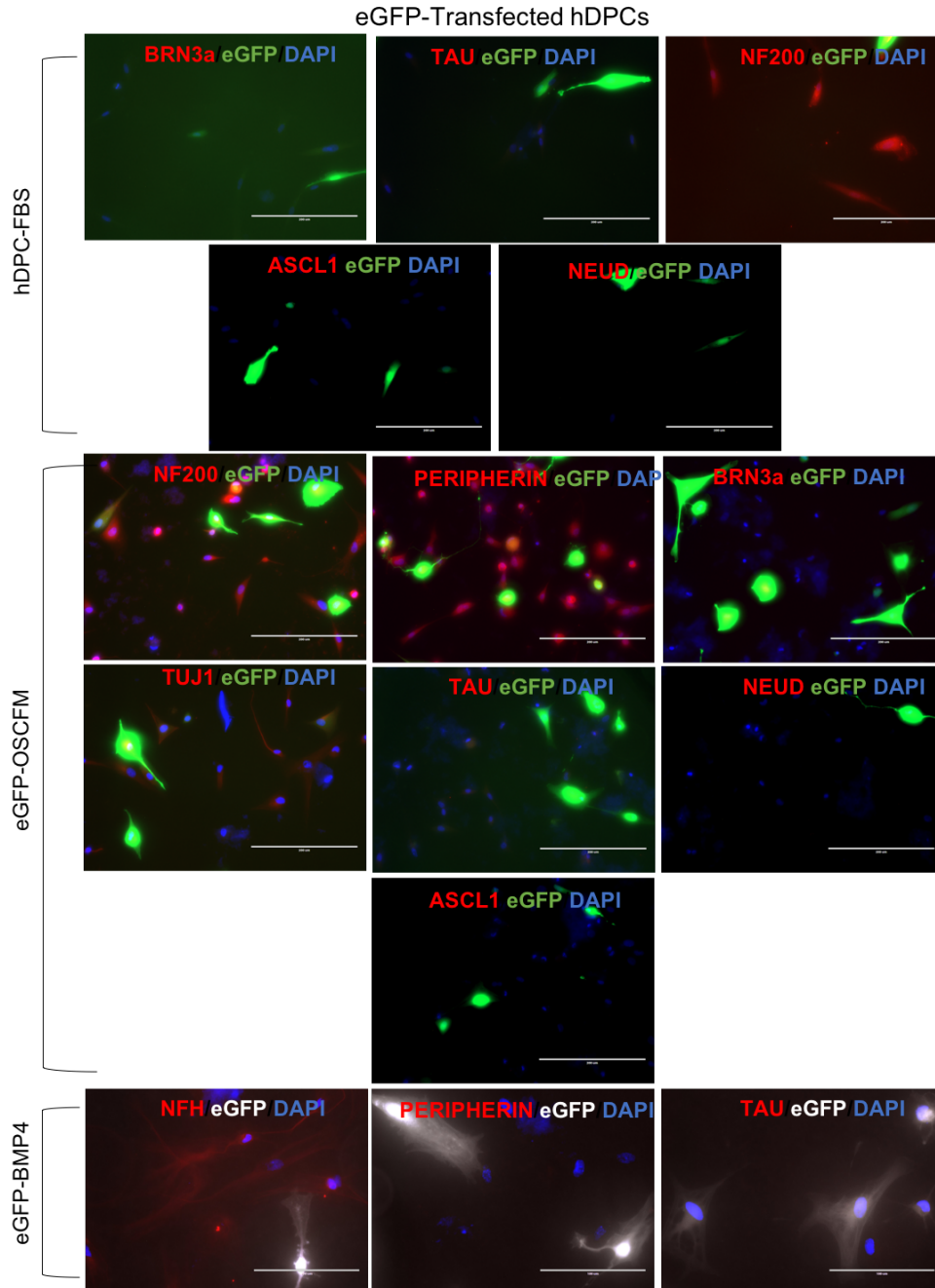


Figure S1. Transfection of eGFP plasmid: Negative control of neuralisation. hDPCs were transfected with the eGFP plasmid (TET-0-FUW-EGFP, addgene) and the expression of neural-related markers was evaluated by immunocytochemistry in cultures from our three different conditions (FBS, OSCFM and BMP4). Transfected cells present green fluorescence signal (green in hDPC-FBS and hDPC-OSCFM and grey in hDPC-BMP4) and spindle-like shape. No expression of the neural markers: BRN3a, ASCL1, NEUD and TAU. NF200 and

PERIPHERIN can be seen, but not co-labelled with the eGFP signal, suggesting that their expression is independent of the eGFP plasmid. eGFP-FBS and eGFP-OSCFM: Scale bar: 200µm. eGFP-BMP4: 100µm.

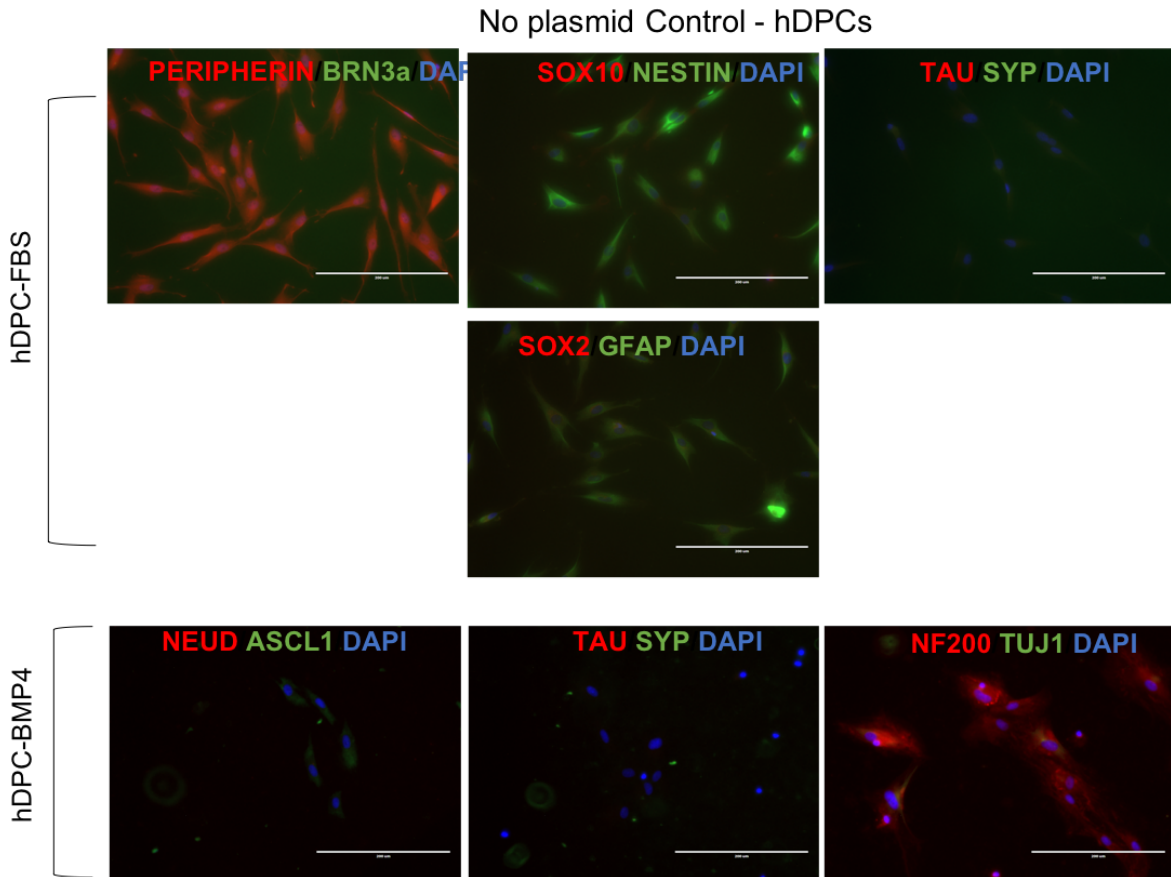


Figure S2. No plasmid controls. hDPC cultures (FBS and BMP4) were electroporated in the absence of a plasmid. The expression of PERIPHERIN, NESTIN, GFAP (in hDPC-FBS) and NF200 (in hDPC-BMP4) was observed. No expression of TAU and NEUD was observed. The cell morphology does not resemble neural-like cells. Scale bar: 200µm.

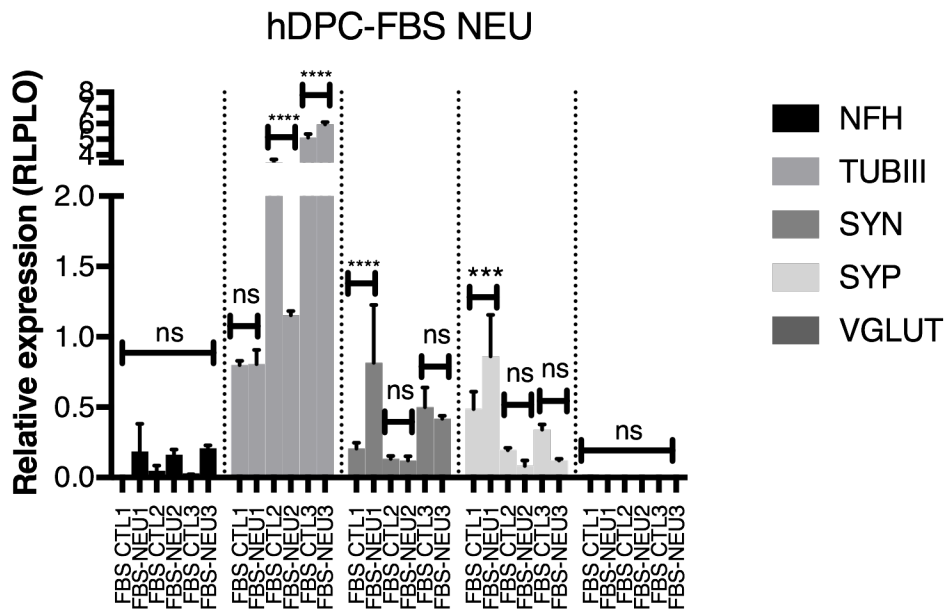


Figure S3. Neuralisation of hDPC-FBS cultures. 3 independent hDPC growing in FBS medium were treated with the Sonic hedgehog neural induction protocol for 2 weeks. A relative expression analysis was performed, the data was normalised to a ESC-derived otic neural progenitor cell line. A one-way-ANOVA followed by a Tukey test was performed to evaluate significant differences. * $P < 0.05$, **** $P < 0.0001$.

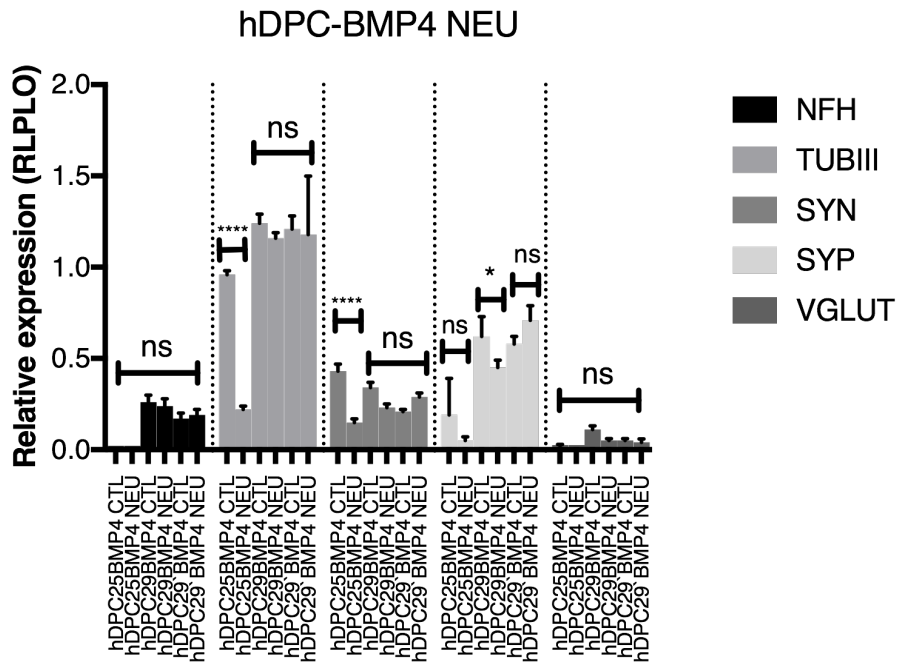


Figure S4. Neuralisation of hDPC-BMP4 cultures. 3 independent hDPC growing in BMP4 medium were treated with the Sonic hedgehog neural induction protocol for 2 weeks. A relative expression analysis was performed, the data was normalised to a ESC-derived otic neural progenitor cell line. A one-way-ANOVA followed by a Tukey test was performed to evaluate significant differences. *P<0.05, ****P<0.0001.

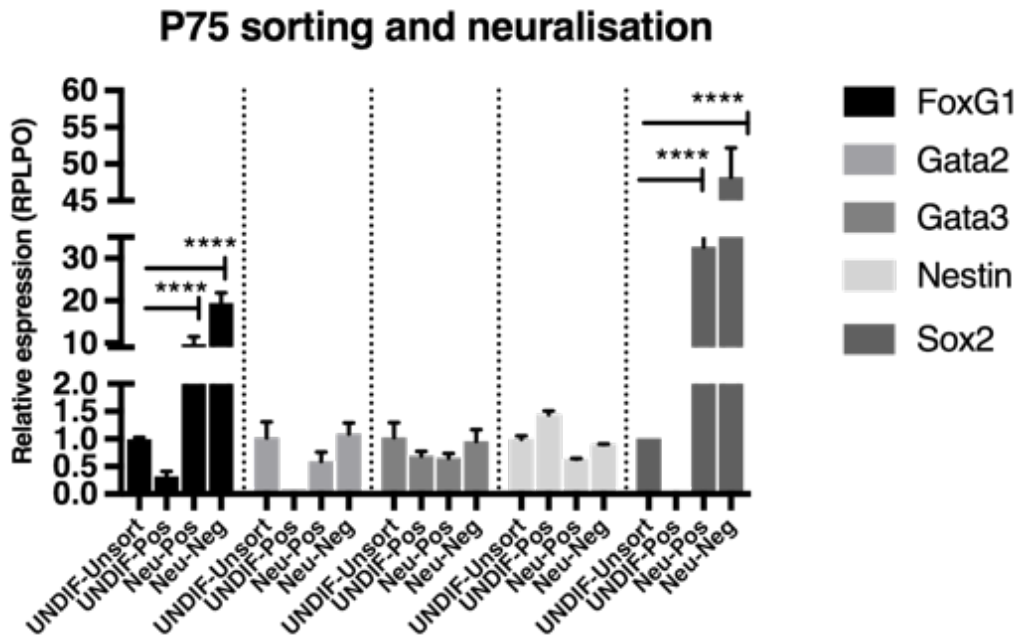


Figure S5. Neuralisation of hDPC after P75 sorting. Second independent experiment.

Neural induction of hDPC-FBS after P75 sorting (NFH/TUJ1)

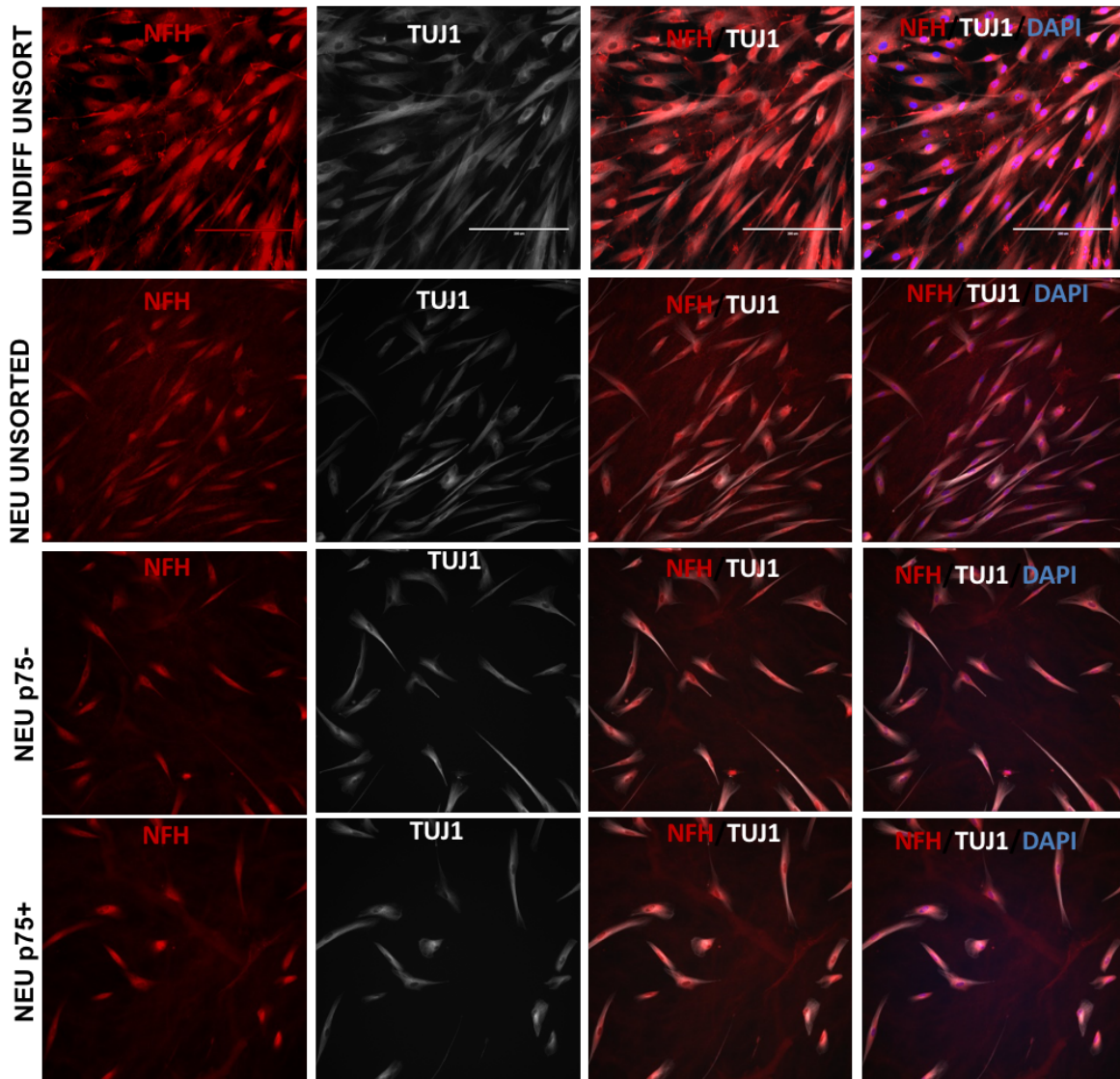


Figure S6 hDPC16 FBS P75 cell sorting and neuralisation. The neural markers NFH and TUJ1 present in the P75 fractions after neuralisation.

Neural induction of hDPC-FBS after P75 sorting (BRN3a/NEUD)

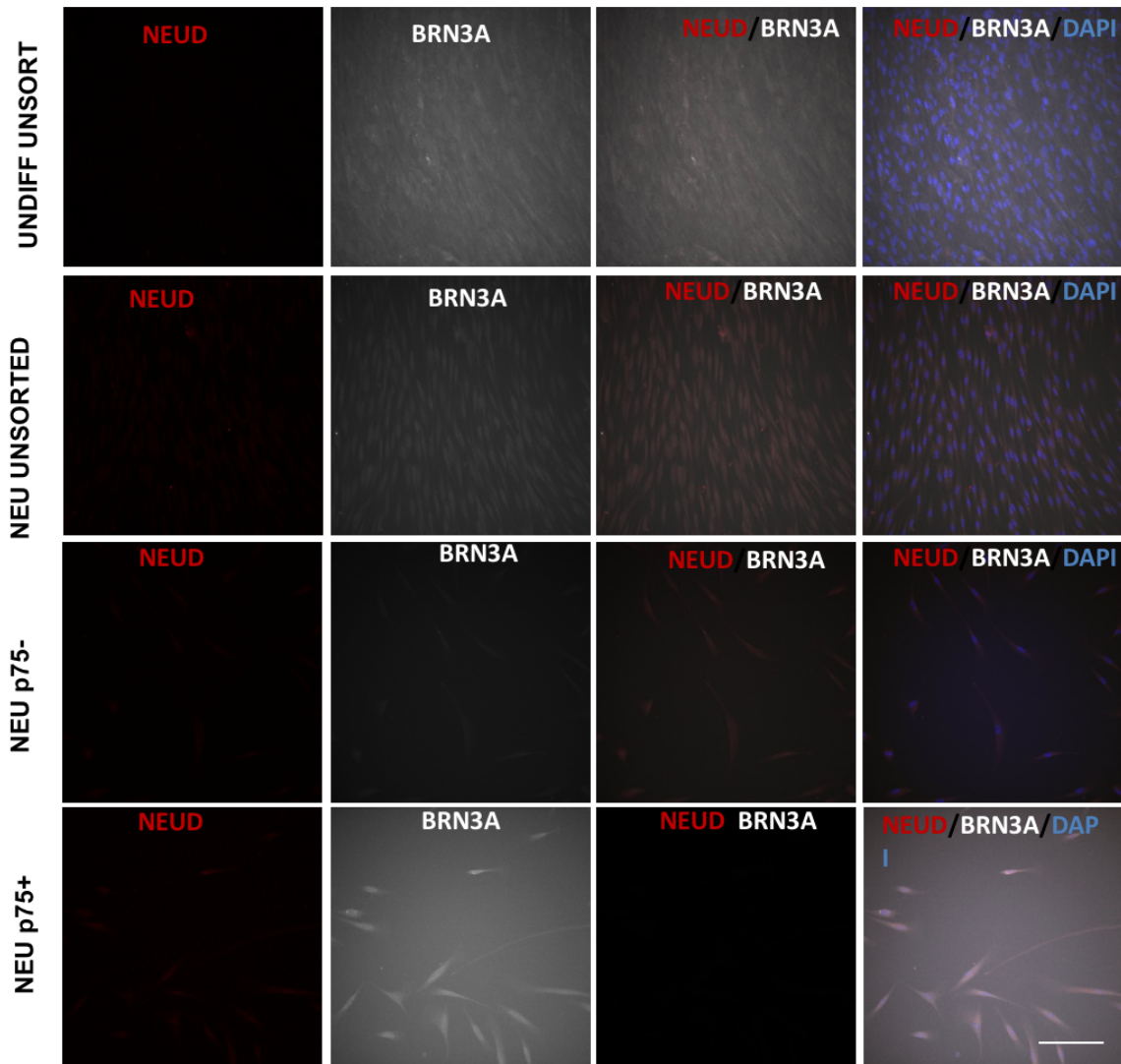


Figure S7. hDPC16 FBS P75 cell sorting and neuralisation. The neural markers NEUD and BRN3A present in the P75 fractions after neuralisation.

Neural induction of hDPC-FBS after P75 sorting (SOX10/P75)

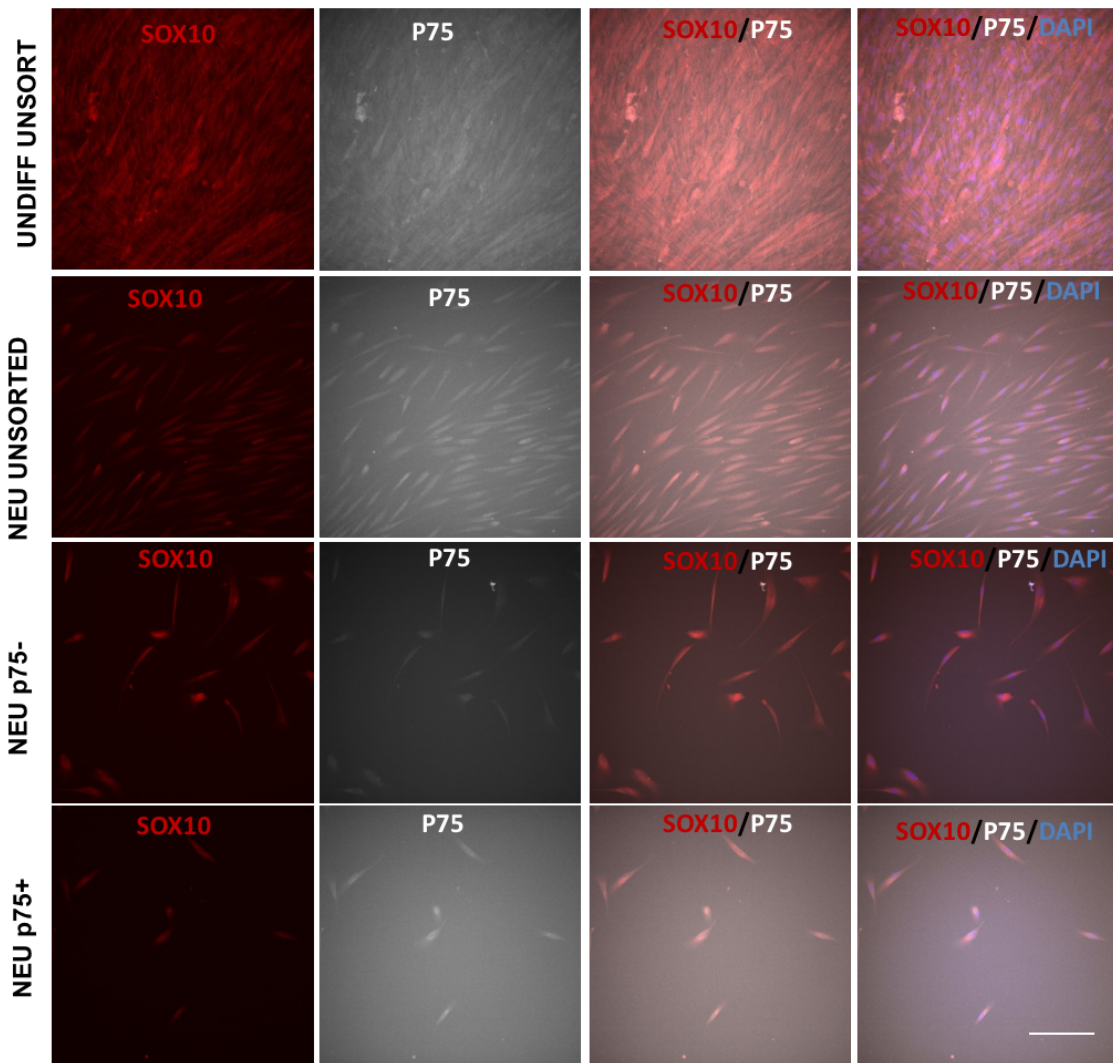
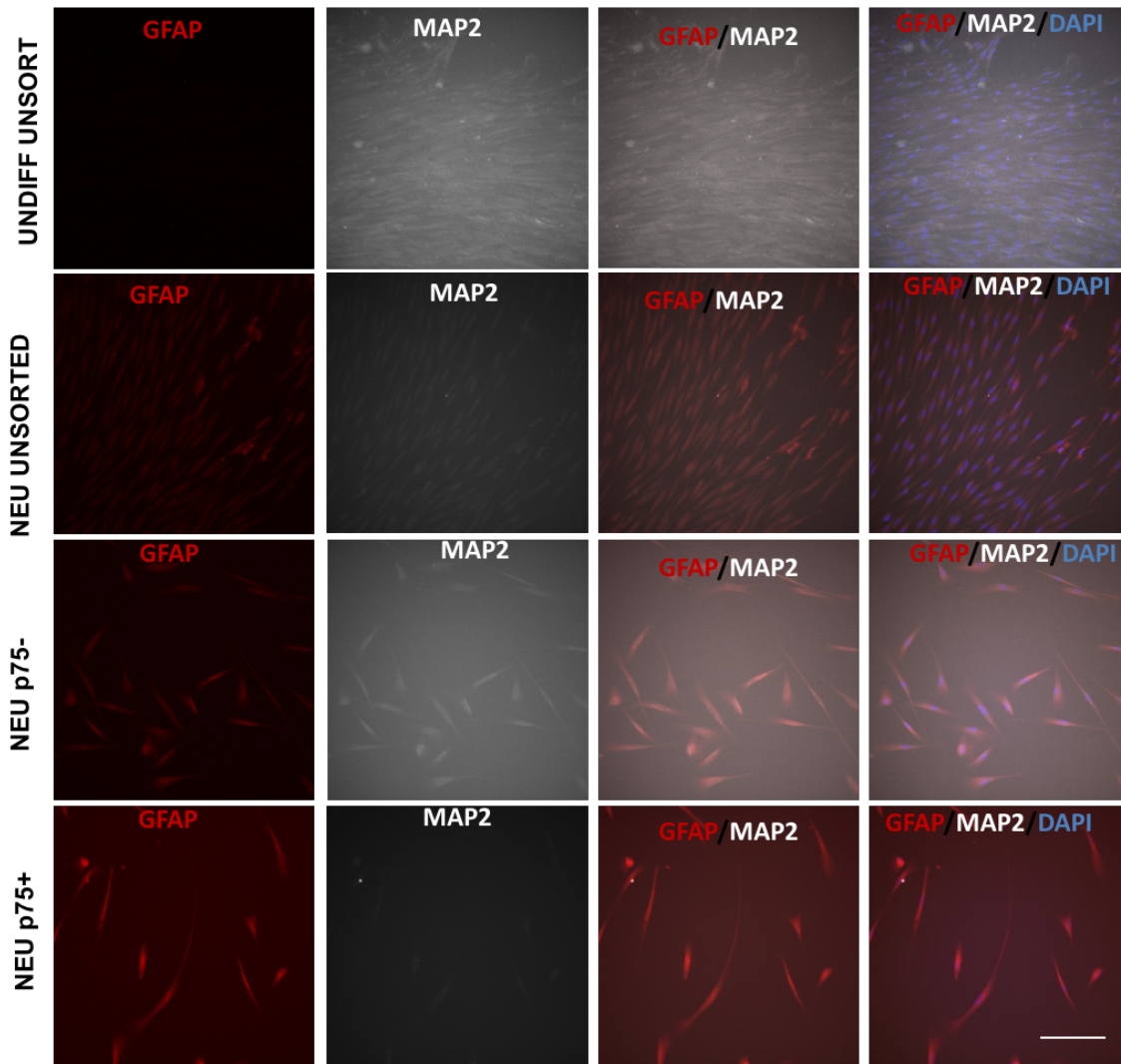


Figure S8. hDPC16 FBS P75 cell sorting and neuralisation. The neural markers SOX10 and P75 present in the P75 fractions after neuralisation.

Neural induction of hDPC-FBS after P75 sorting (GFAP/MAP2)



No primary antibody controls

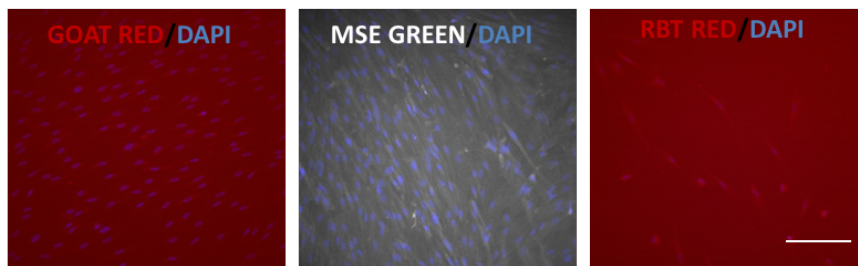


Figure S9. hDPC16 FBS P75 cell sorting and neuralisation. The markers GFAP and MAP2 present in the P75 fractions after neuralisation. Bottom row represents the negative controls corresponding to all groups in the experiment (Fig. S3 to Fig. S6).

